Sarah Firouzianbandpey

Reliability-Based Design of Wind Turbine Foundations:

Geotechnical Site Assessment

Revised Version

PhD Thesis defended at Aalborg University,
Department of Civil Engineering

River Publishers

Reliability-Based Design of Wind Turbine Foundations:

Geotechnical Site Assessment

Reliability-Based Design of Wind Turbine Foundations:

Geotechnical Site Assessment

Revised Version

PhD Thesis
Defended in public at Aalborg University
3 May 2016

Sarah Firouzianbandpey

Department of Civil Engineering,
The Faculty of Engineering and Science,
Aalborg University, Aalborg, Denmark

River Publishers

ISBN 978-87-93379-94-7 (e-book)

Published, sold and distributed by:
River Publishers
Alsbjergvej 10
9260 Gistrup
Denmark

River Publishers
Lange Geer 44
2611 PW Delft
The Netherlands

Tel.: +45369953197
www.riverpublishers.com

PREFACE

The present PhD thesis, titled "Reliability-based design of wind turbine foundations—Geotechnical site assessment", is submitted as a partial fulfilment of the requirements for the Danish PhD degree. The work has been carried out in the period October 2011 to September 2014 at the Department of Civil Engineering, Aalborg University, Denmark, under the supervision of Prof Lars Bo Ibsen and Dr Lars Vabbersgaard Andersen. Also there was an extensive collaboration with Prof D. Vaughan Griffiths in the Department of Civil Engineering, Colorado School of Mines, USA.

The PhD thesis consists of two parts:

- **Part I** deals with applications of CPTu / SCPT in-situ testing methods in subsurface investigations and uncertainty regarding different models to predict the soil type from cone data. Different empirical charts have been investigated and verified as a case study in different soil types.
- **Part II** deals with the effects of soil variability on estimating of design parameters and final cost for wind turbine foundations. The spatial correlation length of cone data was estimated and employed the identification of soil parameters at unsampled locations.

The thesis is based on the following scientific papers with a collaboration of other authors.

- Firouzianbandpey, S., Ibsen, L.B., Andersen, L.V. (2012). CPTu-based Geotechnical Site Assessment for Offshore Wind Turbines—a Case Study from the Aarhus Site in Denmark. In *Twenty-second International Offshore and Polar Engineering Conference*, Rhodes, Greece, pp. 151-158.
- Firouzianbandpey, S., Nielsen, B.N., Andersen, L.V., Ibsen, L.B. (2013). Geotechnical Site Assessment by Seismic Piezocone Test in the North of Denmark. *Seventh International Conference on Case Histories in Geotechnical Engineering, Wheeling, IL.* Missouri University of Science and Technology, 2013. Paper no. 2.34.
- Firouzianbandpey, S., Ibsen, L.B., Andersen, L.V. (2014). Estimation of soil type behavior based on shear wave velocity and normalized cone data in the north of Denmark. 3rd International Symposium on Cone Penetration Testing, Las Vegas, Nevada, USA. Pp. 621-628.
- Firouzianbandpey, S., Griffiths, D. V., Ibsen, Lars Bo., Andersen, and L. V. (2014). Spatial correlation length of normalized cone data in sand: case study in the north of Denmark. *Canadian Geotechnical Journal*, Vol. 51, No. 8, pp. 844-857.
- Firouzianbandpey, S., Ibsen, L.B., Griffiths, D.V., Vahdatirad, M. J., Andersen, L.V., Sørensen, J. D. (2014). Effect of spatial correlation length on the interpretation of normalized CPT data using a Kriging approach. *Journal of Geotechnical and Geoenvironmental Engineering (ASCE).*

Copies of all publications are enclosed in the thesis.

I would like to thank my supervisor Professor Lars Bo Ibsen for giving me the opportunity to work on this PhD thesis and for his counselling and support during the experiments and studies.
I am especially thankful to Dr Lars Vabbersgaard Andersen. If he had not served as my co-advisor and had not encouraged me throughout this dissertation process, this dissertation could not have been completed. I thank him for providing me with the opportunity to pursue this research.

I would also like to warmly acknowledge Prof D. Vaughan Griffiths for providing guidance and suggestions for me to improve this dissertation.

Among many peoples who have been helpful in the compilation of this dissertation, I would like to extend a hearty thanks to the technical staff at the Laboratories at the Department of Civil Engineering, Aalborg University for their assistance with the experimental work related to Part I.

Finally, I express my great appreciation to my family for their faith and encouragement. They deserve special mention for their inseparable support and prayers. Words fail me to express my appreciation to my husband, Javad, for his unconditional love, assistance and patience during the last three years.

Sarah Firouzianbandpey
Aalborg, December 2014

SUMMARY IN ENGLISH

With industrialization taking off in the 18th century, a dramatic increase of carbon dioxide emission began due to burning of fossil fuels. The heat-trapping nature of carbon dioxide causes global warming resulting in major concern about climate change as well as in an increased demand for more reliable, affordable, clean and renewable energy. Wind turbines have gained popularity among other renewable energy generators by having both technically and economically efficient features and by offering competitive production prices compared to other renewable energy sources. Therefore, it is a key green energy technology in breaking the fossil fuel dependency. The costs of foundations for offshore wind turbines typically amount to 20–30% of the total wind turbine budget. Thus, an optimized design of these foundations will improve the cost effectiveness by matching a suitable target reliability level.

The overall aim of the present PhD thesis is to facilitate a low-cost foundation design for future offshore wind farms by focusing on the geotechnical site assessment. First, a number of well-established techniques for soil classification based on cone penetration test (CPT) data have been investigated for a local case in order to estimate the inherent uncertainties in these models. For the purpose of verification and prediction of the best method for the region, a comparison was made with laboratory test results on samples retrieved from boreholes at the site.

In addition to this, several seismic CPTs were performed in sand and clay in order to estimate the small-strain shear modulus of the soil as a key parameter in analysis and design of foundations, and the soil type of the region was estimated based on this value. Furthermore, the shear moduli obtained from the seismic tests were compared with moduli estimated from cone data using different empirical relations.
The later part of the thesis concerns the assessment of the spatial correlation lengths of CPTu data in a sand layer. Results from two different sites in northern Denmark indicated quite strong anisotropy with significantly shorter spatial correlation lengths in the vertical direction as a result of the depositional process. The normalized cone resistance is a better estimator of spatial trends compared to the normalized friction ratio.

In geotechnical engineering analysis and design, practitioners ideally would like to know the soil properties at many locations, but achieving this goal can be unrealistic and expensive. Therefore, developing ways to determine these parameters using statistical approaches is of great interest. This research employs a random field model to deal with uncertainty in soil properties due to spatial variability by analysing CPTu data from a sandy site in northern Denmark. Applying a Kriging interpolation approach gave a best estimate of properties between observation points in the random field, and the influence of spatial correlation length on the results was investigated. Results show that a longer correlation length reduces the estimator error and results in more variation in the estimated values between the interpolated points.

RESUMÉ

Med industrialiseringens start i det 18. århundrede begyndte en dramatisk forøgelse af carbondioxid-emission forårsaget af afbrænding af fossile brændstoffer. Carbondioxids varmefangende karakter forårsager global opvarmning, hvilket resulterer i stor bekymring for klimaforandring såvel som øget efterspørgsel på mere pålidelig, prisbillig og ren vedvarende energi. Vindmøller er blevet populære blandt de andre vedvarende energigeneratorer ved både at have teknisk og økonomisk ydeevne og ved at tilbyde konkurrencedygtige produktionspriser sammenlignet med andre vedvarende energikilder. Derfor er det en vigtig grøn-energi-teknologi, der kan tilendebringe afhængigheden af fossile brændstoffer. Omkostningerne ved fundamenter til havvindmøller ligger typisk omkring 20-30% af det totale budget for vindmøller. Af denne årsag vil et optimeret design af fundamenterne forbedre omkostningseffektiviteten ved at matche et passende pålidelighedsniveau.

Det overordnede mål for denne ph.d.-afhandling er at facilitere et billigt fundamentdesign for fremtidens havbaserede vindmølleparker ved at fokusere på den geotekniske bedømmelse af området. Først er en række veletablerede teknikker til klassifikation af jord baseret på CPT (cone penetration test) data undersøgt for en lokalitet i Nordjylland. Formålet er at estimere de iboende usikkerheder i klassifikationsmetoderne. En sammenligning blev lavet med laboratorietestresultater på prøver, der er taget fra boringer ved stedet, for herigennem at kunne identificere og verificere den bedste metode for lokaliteten.

Desuden er adskillige seismiske CPT-forsøg blevet udført i sand og ler til estimering af aflejringernes forskydningsmodul ved lavt tøjningsniveau. Denne modul er en vigtig parameter i analysen og designet af fundamenter, og typen af aflejringer på lokaliteten blev estimeret på baggrund af denne værdi. Ydermere blev forskydningsmoduler fundet ud fra de seismiske test sammenlignet med modulerne estimeret ud fra CPT data ved anvendelse af forskellige empiriske relationer.

Den sidste del af afhandlingen omhandler bedømmelsen af de stedslige korrelationslængder af CPT-data i et sandlag. Resultaterne fra to forskellige steder i det nordlige Danmark indikerede en ret kraftig anisotropi med betydelig kortere korrelationslængder i den vertikale retning som et resultat af aflejringsprocessen. Den normaliserede spidsmodstand giver et bedre mål for de stedslige variation sammenlignet med den normaliserede friktionsratio. I geoteknisk analyse og design vil den udførende part ideelt set gerne kende jordens egenskaber så mange steder som muligt, men opnåelse af et sådant kendskab kan være urealistisk og bekosteligt. Derfor er udviklingen af statistiske metoder til fastlæggelse af disse parametre af stor interesse. Denne forskning benytter en stokastisk-felt-model til at behandle usikkerheder i jordens egenskaber grundet stedslig variation ved at analysere CPT data fra en sandforekomst i det nordlige Danmark. Brug af Kriging, en avanceret interpolationsmetode, har givet det bedste estimat af egenskaberne mellem observationspunkterne i det stokastiske felt, og indflydelsen på resultaterne af den stedslige korrelationslængde blev undersøgt. Resultaterne viser, at en større korrelationslængde reducerer fejlen på estimatet og resulterer i mere variation af de estimerede værdier mellem de interpolationspunkter.

List of Publications for PhD

Firouzianbandpey, S., Ibsen, L.B., Andersen, L.V. (2012). CPTu-based Geotechnical Site Assessment for Offshore Wind Turbines—a Case Study from the Aarhus Site in Denmark. In *Twenty-second International Offshore and Polar Engineering Conference*, Rhodes, Greece, pp. 151-158.

Firouzianbandpey, S., Nielsen, B.N., Andersen, L.V., Ibsen, L.B. (2013). Geotechnical Site Assessment by Seismic Piezocone Test in the North of Denmark.*Seventh International Conference on Case Histories in Geotechnical Engineering, Wheeling, IL.*Missouri University of Science and Technology, 2013. Paper no. 2.34.

Firouzianbandpey, S., Ibsen, L.B., Andersen, L.V. (2014).Estimation of soil type behavior based on shear wave velocity and normalized cone data in the north of Denmark. 3rd International Symposium on Cone Penetration Testing, Las Vegas, Nevada, USA. pp. 621-628. Paper no. 2-35.

Firouzianbandpey, S., Griffiths, D. V., Ibsen, Lars Bo., Andersen, and L. V. (2014). Spatial correlation length of normalized cone data in sand: case study in the north of Denmark. Canadian Geotechnical Journal, Vol. 51, No. 8, pp. 844-857.

Firouzianbandpey, S., Ibsen, L.B., Griffiths, D.V., Vahdatirad, M. J., Andersen, L.V., Sørensen, J. D. (2014). Effect of spatial correlation length on the interpretation of normalized CPT data using a Kriging approach.Journal of Geotechnical and Geoenvironmental Engineering (ASCE).

TABLE OF CONTENTS

CHAPTER 1: INTRODUCTION

As the fastest growing source of electricity generation in the world, wind power offers many benefits in the way of reducing consumption of fossil fuels. Even though the offshore wind turbine has fulfilled many commitments in the industry, many political, economic and technical challenges are still against this technology. In this regard, the soil-foundation part plays an important role. In this chapter, a brief overview of the geotechnical aspects of site investigations and degree of reliability in design of wind turbine foundations is presented with providing the challenges and motivations in this field.

1.1 Overview

The world is now concerned about climate change due to the dependence on coal, oil and gas. This increases the demand for more domestic, sustainable and largely untapped energy resources as an alternative to fossil fuels. Today, the modern offshore wind turbine is the most interesting source for generating renewable energy and a key technology in achieving the green energy and climate goals in the future. Europe is the world leader in offshore wind power, with the first offshore wind farm being installed in Vindeby, Denmark in 1991. So as a pioneer in offshore wind power, Danish energy policy attempts to support the development of the offshore wind industry by 2050 including a huge investment plan to supply 50% of electricity consumption by wind power up to 2020.

Investment in EU wind farms was between €13 billion (bn) and €18 bn. Onshore wind farms attracted around €8 bn to €12 bn, while offshore wind farms accounted for €4.6 bn to €6.4 bn. Indeed, lower installation cost causes that a great amount of wind turbines are located onshore.

As indicated in Figure 1-1, in terms of annual installations Germany was the largest market in 2013, installing 3,238 MW of new capacity, 240 MW (7%) of which was offshore. The UK came in second with 1,883 MW, 733 MW (39%) of which was offshore, followed by Poland with 894 MW, Sweden (724 MW), Romania (695 MW), Denmark (657 MW), France (631 MW) and Italy (444 MW). This high growth in the installed capacity of offshore wind turbines by the EU committee brings many challenges in the field of engineering and science.

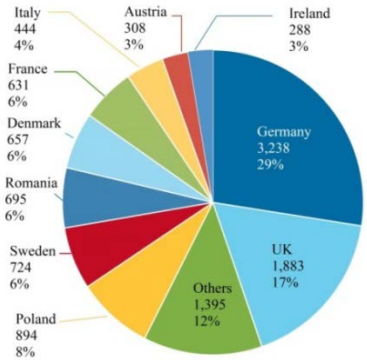

Figure 1-1. EU member state market shares for new capacity of wind power installed during 2013 in MW. Total 11,159 MW. EWEA (2013)

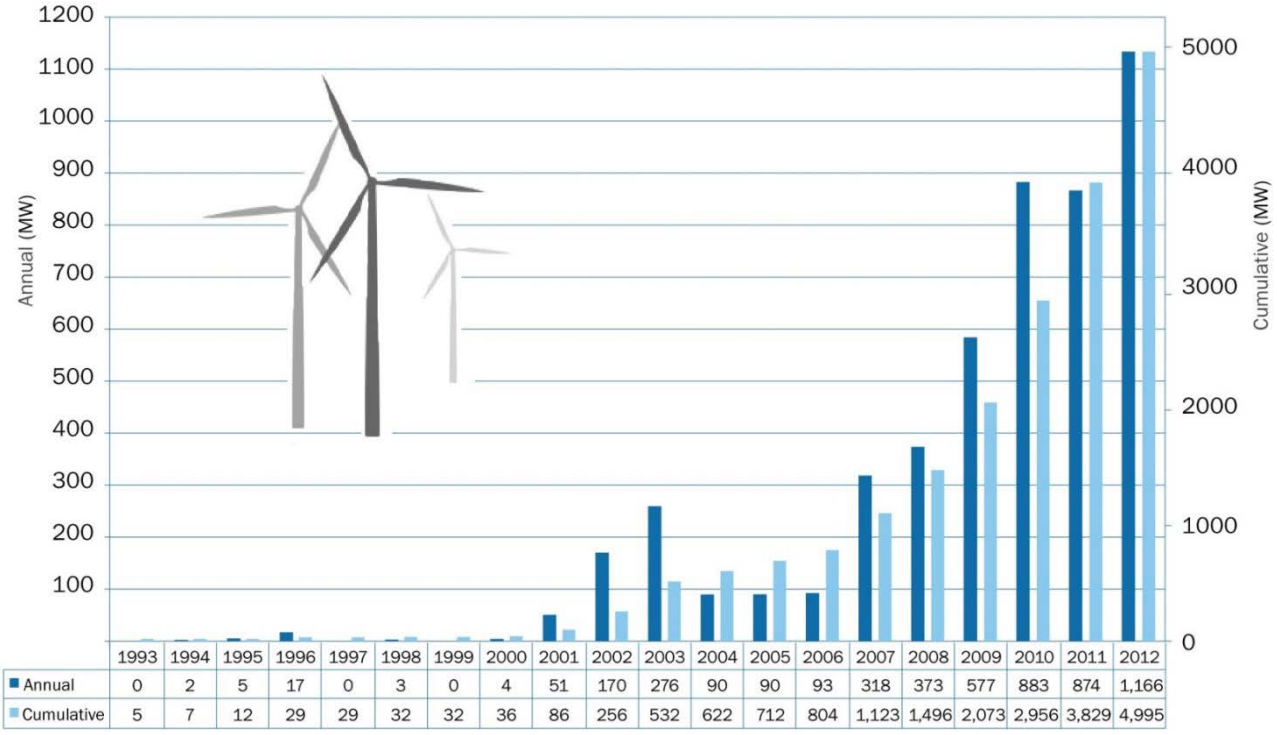

	1993	1994	1995	1996	1997	1998	1999	2000	2001	2002	2003	2004	2005	2006	2007	2008	2009	2010	2011	2012
Annual	0	2	5	17	0	3	0	4	51	170	276	90	90	93	318	373	577	883	874	1,166
Cumulative	5	7	12	29	29	32	32	36	86	256	532	622	712	804	1,123	1,496	2,073	2,956	3,829	4,995

Figure 1-2. Annual and cumulative offshore wind installations in Europe. After EWEA (2013).

Also as illustrated in Figure 1-2, the annual and cumulative offshore wind installations have increased in the last few years. This increased rate in the installed capacity of offshore wind turbines brings many challenges in civil and geotechnical engineering. Particularly, an inevitable factor against this way is the cost of wind turbines and in particular their foundations which account for around one third of the total cost of a wind farm.

1.2 Geotechnical site assessment

The nature of the ground has an inevitable influence on the construction procedure. Long term geological processes and weathering sculpt the terrain and reduce rock to sand, clay and other types of soils. These geological processes erode the higher ground and others leave complex, deposited layers of sand and clay. Together the types of rock and landform shaping processes determine the nature, strength and physical shape of the ground. Therefore, subsoil evaluation and site characterization is important for the planning and erection of wind turbines. Foundation work makes up a relatively large part of the overall cost of a wind farm. Detailed information about a site may have a significant influence on the optimization of the foundation design and can reduce the development costs. State-of-the-art spatial geophysical field methods (e.g. magnetics, side scan, echo-sounding and seismic) are combined with direct and indirect in-situ exploring methods (e.g. drillings and Cone Penetration Tests (CPT)) and the results are used to obtain material properties to be applied in computational models (e.g. finite element method).

1.3 Cone Penetration Test

The Cone Penetration Test (CPT) and its enhanced versions (piezocone-CPTu and seismic-SCPT) are in-situ testing methods with various applications in a wide range of soils. During the test, a cone mounted on a series of rods is pushed into the ground at a constant rate and continuously measures the resistance to penetration of the cone and of a surface sleeve surrounding the lower end of rod. Among other in-situ testing methods the CPTu has the advantages of fast and continuous profiling, being economical, repeatable and providing reliable data (not operator-dependent) and having a strong theoretical basis for interpretation of the geotechnical engineering properties of soils and delineating soil stratigraphy.

Figure 1-3 shows a schematic view of a cone penetrometer. The total force acting on the cone, Q_c, divided by the projected area of the cone, A_c, produces the cone resistance, q_c. The total force acting on the friction sleeve, F_s, divided by the surface area of the friction sleeve, A_s, is the sleeve friction, f_s. A piezocone also measures pore water pressure, usually just behind the cone in the location u_2. Figure 1-4 indicates a typical result of a sounding profile during the test.

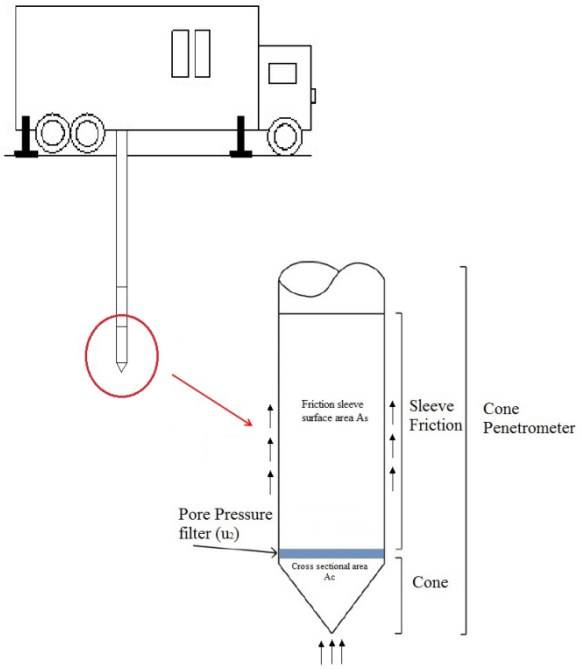

Figure 1-3. A schematic view of truck and cone penetrometers

1.3.1 Seismic Piezocone Test

Seismic piezocone penetration test (SCPTU) is a development of CPT by integrating a geophone in the cone. The geophone measures the acceleration generated by a hammer impact on a steel plate on the ground surface. A polarized shear wave is generated on the ground surface and the travel time is measured for the shear wave

for a known distance to the geophone down in the borehole. This can be regarded as a down-hole test and provides shear wave velocity measurements simultaneously with measurements of tip resistance (q_c), sleeve friction (f_s) and pore pressure (u). Determination of shear wave velocity (v_s) can be used in obtaining the soil properties. Figure 1-5 illustrates the typical layout for a downhole seismic cone test.

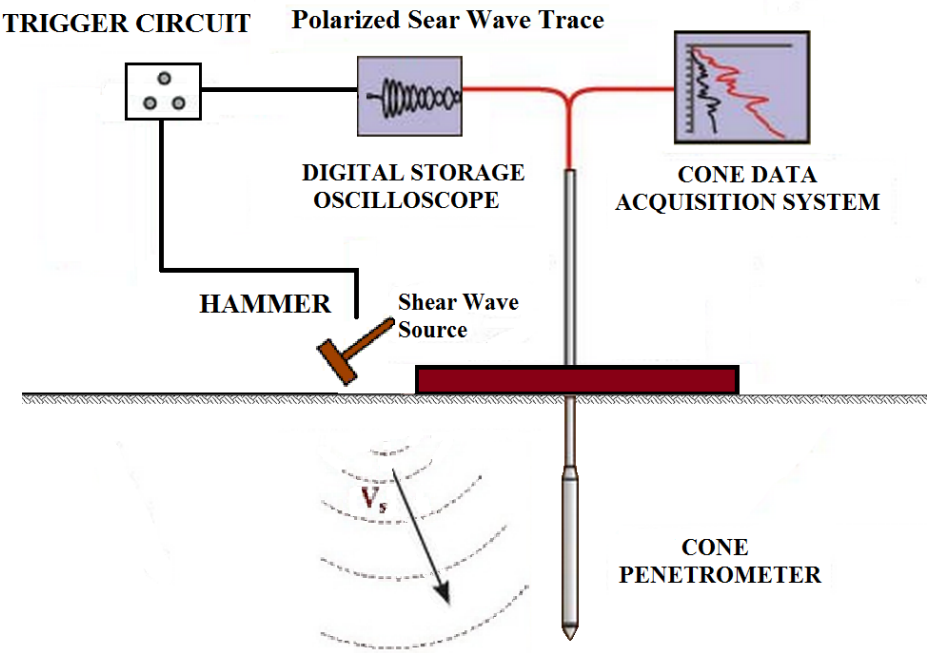

Figure 1-5. A schematic view of downhole seismic cone system

1.4 Statistical analysis of spatial variability of soils

In situ soils are heterogeneous materials created by natural environmental, geologic and physical-chemical processes, which have an influence on the design parameters of the foundation in any soil structure. Actually, the properties of soils undergo changes over both space and time. In other words, measured soil parameters can show considerable spatial variation even within relatively homogeneous layers with the same soil type. The application of statistical analysis provides the spatial variability of a data set more accurately than otherwise determined.

In order to characterize the inherent spatial variability of soils, stochastic methods may be used to incorporate the effects of spatial variability into reliability-based geotechnical design approaches. Furthermore, stochastic methods help geotechnical engineers to estimate soil properties at unsampled locations and handle uncertainties related to soil properties in a more rational manner. The inherent spatial variability of soil properties is induced by the process of soil formation and depends on type of the soil.

In general, statistical analysis can be divided into two parts as descriptive and inferential in nature. In the descriptive analysis, the aim is to best describe a particular data set by interpolating within the data set. This commonly happens when soil parameters are obtained at a field for which a construction is destined. The regression, using an appropriate polynomial function that demonstrates most of the variability, or best linear unbiased estimation (BLUE) are examples of descriptive techniques (see e.g. Fenton and Griffiths, 2008). Regression is most often geometry and observation based, whereas BLUE also incorporates the covariance structure of data.

Inference analysis occur when soil property is estimated at any unobserved location. Hence, the word inference convey this meaning that the estimation of stochastic model parameters is based on making probabilistic statements about an entire field for which data are not available or very limited. This is essential in primary designs or when a large site is to be characterized on the basis of a small number of tests in the region.

1.5 Motivation for research

In geotechnical engineering practice, soil properties at a specific site can be determined from laboratory tests based on a limited number of field specimens as well as in-situ tests performed in the field. As the budget of any construction project is limited, the ability to acquire data is constrained and the exact spatial variability of soil parameters remains largely unknown. Traditionally, geotechnical design is associated with a deterministic methodology based on representative soil properties regardless of the spatial variability within each soil layer. The simplified estimates of soil properties do not sufficiently supply valuable information for performing reliability analysis in geotechnical practice. Therefore, the statistical characteristics of spatial variability should be more closely examined based on stochastic methods.

Designers are now demanding full reliability studies, requiring more advanced models, so that engineers are becoming interested in reasonable soil correlation structures. When uncertainties related to soil properties are presented by means of stochastic methods, the influence of spatial variability of various soil properties on structure behaviour may be assessed more accurately. This can be achieved through the use of spatial correlation structures and trend analyses. These methods provide better estimates for unsampled locations and offer valuable information regarding the uncertainty of soil properties in reliability analyses.

Furthermore, the simplification due to application of partial safety factors and quantile values lead to uncertainties in current design methods. Therefore, the reliability level remains largely unknown and the design may be over-conservative. So, many initiatives are needed to reduce the expenses related to this part of the design.

Before any design and analysis, geotechnical site investigations are carried out at the location of each wind turbine, commonly as cone penetration tests (CPTu) and borehole tests. The soil properties estimated from cone

data as a quantile value and used in the deterministic design of each foundation are accompanied with large statistical uncertainties. Also soil properties vary spatially from one location to another within the field and the soil properties at locations without CPTu tests cannot be estimated at various depths with high confidence. This motivates a methodology to clearly identify the soil strata and reduce the uncertainties in prediction of design properties, paving the way for a more cost-effective geotechnical design.

1.6 Overview of the thesis

Following the introduction, the structure of the thesis is given as below.

- **Chapter 2** presents a review of the methods proposed in the literature for estimation of the soil type behavior from in-situ test results. It also gives a short introduction on different techniques available in the literature to estimate the correlation structure of the field.
- **Chapter 3** describes the scope of the thesis and introduces the aspects in the project overview.
- **Chapter4** gives a summary of the included international conference and journal papers.
- **Chapter 5** concludes the thesis with a summary and discussion of the methodology and assumptions employed in the thesis. Furthermore, the main results and recommendations for future studies are presented.
- **Appendix A** contains the enclosed conference paper titled “CPTu-based geotechnical site assessment for offshore wind turbines—a case study from the Aarhus site in Denmark”.
- **Appendix B** contains the enclosed conference paper titled “Geotechnical site assessment by Seismic Piezocone Test in the North of Denmark”.
- **Appendix C** contains the enclosed conference paper titled “Estimation of soil type behavior based on shear wave velocity and normalized cone data in the north of Denmark”.
- **Appendix D** contains the enclosed journal paper titled “Spatial correlation length of normalized cone data in sand: A case study in the North of Denmark”.
- **Appendix E** contains the enclosed journal paper titled “Effect of spatial correlation length on the interpretation of normalized CPT data using a Kriging approach”.

CHAPTER 2: STATE OF THE ART

2.1 Overview

The field of offshore wind energy is engaged with many problems and different methodologies within civil and geotechnical engineering. Many challenges are related to the estimation of the soil properties within a site for the purpose of design and analysis of the foundations. In recent decades, there has been a shift in favor of utilizing in-situ testing methods for subsurface investigation and evaluating the engineering soil parameters as an alternative to the conventional laboratory testing; but still the identification of soil stratification at locations with no direct measurement is accompanied with many uncertainties due to variability of soil. In this chapter, a brief discussion of different methods in the field of site investigations is presented. Also different methodologies to estimate soil parameters from field measurements are reviewed. This chapter also presents different methodologies for estimation of soil variation presented in the literature.

2.2 CPTu and SCPTu data for soil profile interpretation and strength parameters

Soil stratification is essential in geotechnical site characterization and structural design (Houlsby and Houlsby, 2013; Wang et al., 2014). Recent studies have reported the significant effect of soil stratification on the design of foundations, tunneling, and pipelines (Burd and Frydman, 1997; Padrón et al., 2008; Huang and Griffiths, 2010; Zhang et al., 2012; Lee et al., 2013; White et al., 2014). The identification of soil stratification includes determining soil types, the number of soil layers, the thickness of each layer and soil properties. The standardized cone penetration test (CPT) and piezocone (CPTU) have been widely used to infer the soil type by directly interpreting measured CPT/CPTU parameters (e.g. Schmertmann, 1978; Douglas and Olsen, 1981; Robertson and Campanella, 1983; Robertson, 1990; Jefferies and Davies, 1993; Olsen and Mitchell, 1995; Eslami and Fellenius, 1997; Lunne et al., 1997; Schneider et al., 2008).

Several classification charts were proposed in the literature to classify the subsurface soil from the CPT data. These charts were developed based on comparison/correlation between CPT/PCPT data profiles and soil type data bases collected and evaluated from extensive soil borings. The first soil classification chart based on cone resistance (q_c) and sleeve friction (f_s) was pioneered by Begemann (1965). Douglas and Olsen (1981) employed the electrical cone penetrometer in their soil profiling chart, including trends for liquidity index and earth pressure coefficient, as well as sensitive soils and “metastable sands”. Jones and Rust (1982) proposed a chart based on the piezocone using the measured total cone resistance and the measured excess pore water pressure mobilized during cone advancement. Due to increasing parameters like cone resistance and friction ratio with depth, the chart has the deficiency of classifying soil in a different group but it is interesting because it identifies the consistency of fine-grained soils and the density (compactness condition) of coarse-grained soils. Robertson et al. (1986) and Campanella and Robertson (1988) were the first that corrected cone resistance for pore pressure at the shoulder [$q_t = q_c + u(1-a)$], where q_t is the cone resistance corrected for pore water

pressure on shoulder, q_c is the measured cone resistance, u_2 is the pore pressure measured at cone shoulder, a is the ratio between shoulder area (cone base) unaffected by the pore water pressure to total shoulder area. As a refinement of the Robertson et al. (1986) method, Robertson (1990) considered the normalization for overburden stress in the profiling chart to compensate for the cone resistance dependency on the overburden stress. Zhang and Tumay (1996) performed some investigations on overlaps of different soil types due to uncertainty in CPT classification systems. Their work was based on the statistical and fuzzy subset approaches. Eslami and Fellenius (2004) developed a new method for soil profiling by plotting effective cone resistance (q_E) versus sleeve friction with a compiled database from 20 sites in 5 countries.

Based on data from the corrected tip resistance (q_t) and penetration pore-water pressure at the shoulder (u_2), Ramsey (2002) evolved a model for classifying soil with a simple criterion. Based on this conservative criterion, whenever the charts predict different zones, then the zone with the lower numerical value should be chosen. The soil classification charts proposed by Schneider (2008) were based on normalized piezocone parameters using parametric studies of analytical solutions, field data, and judgment based on the previous discussions. The three models proposed in the method are exactly the same but have been plotted in different formats. The soil types, essentially drained sand and transitional soils, can also be described in these models. Using probabilistic methodology, considering the inherent uncertainties, Cetin and Ozan (2009) proposed a cone penetration test (CPT) soil classification. The resulting database was probabilistically assessed through Bayesian updating methodology allowing full and consistent representation of relevant uncertainties, including model imperfection, statistical uncertainty and inherent variability.

2.2.1 Data normalization

CPT measurements should be normalized for vertical stress because it has a significant influence on CPT data and lead to an incorrect assessment of soil strength parameters. Studies show that if overburden stress effects are not properly taken into account, raw cone penetration test (CPT) measurements can be misleading. Low overburden stresses, found at shallow soil depths, will result in a small measured tip and sleeve resistance, whereas large resistances are generally encountered at greater soil depths. According to Moss et al. (2006), a logarithmic increase is recorded with depth in homogeneous soils.

The bulk of the research on CPT normalization was conducted to account for the effects of overburden stress. Robertson and Wride (1998) proposed the following technique for normalizing cone tip resistance measurements:

$$q_{c1N} = \left(\frac{q_c}{P_a}\right) C_Q \ , \qquad C_Q = \left(\frac{P_a}{\sigma'_{v0}}\right)^n \tag{1}$$

where q_{c1N} is the dimensionless cone resistance normalized due to the weight of soil on top of the cone, q_c is the measured cone tip resistance, and C_Q is a correction factor for overburden stress. The exponent *n* takes the

values 0.5, 1 .0 and 0.7 for cohesionless, cohesive and intermediate soils respectively, whereas σ'_{v0} is the effective vertical stress and P_a is the reference pressure (atmospheric pressure) in the same units as σ'_{v0} and q_c, respectively.

Also, the normalized friction ratio is calculated using the equation proposed by Wroth (1984):

$$F_R = 100\% \frac{f_s}{q_c - \sigma_{v0}} \tag{2}$$

where f_s is the measured sleeve friction and σ_{v0} is the total vertical stress. The values of q_c, σ_{v0} and f_s are all in the same units.

2.2.2 Seismic CPT and small-strain modulus

The seismic piezocone penetration test (SCPTu), as a novel development of CPTu, provides shear wave velocity (V_s) measurements during the sounding and provides more direct information in estimation of geotechnical parameters like deriving small strain shear modulus (Lunne et al., 1997; Mayne and Campanella, 2005; Liu et al., 2008; Cai et al., 2009). In the absence of direct shear wave velocity measurements, many empirical correlations have been proposed between shear wave velocity and measured cone resistance and sleeve friction (e.g. Baldi et al., 1986; Mayne and Rix, 1995; Hegazy and Mayne, 1995; Mayne, 2006).

Also the low-strain shear modulus ($G_{\max}$ or G_0) can be found using the shear wave velocity measurements obtained by assessment of SCPTu, since elasticity theory relates the shear modulus, soil density (ρ) and the shear wave velocity as $G_{\max} = \rho V_s^2$. To obtain the low-strain shear modulus, a sm all rugged velocity seismometer has been incorporated into the cone penetrometer (Robertson et al., 1986). Figure 2-1 illustrates a schematic layout of the standard downhole technique. A suitable seismic signal source should generate large amplitude shear waves with little or no c ompressional wave component. Usually an excellent seismic shear wave source consists of a rigid beam, steel jacketed and weighted to the ground.

Many correlations for determining $G_{\max}$ based on cone resistance have been recommended for a large variety of soils, either granular (Baldi et al., 1989) or cohesive (Mayne and Rix, 1993) or both soils (Hegazy and Mayne, 1995). As examples, Rix and Stokoe (1992) proposed a correlation for sands and Mayne and Rix (1993) showed that for a wide range of clays the small strain shear modulus is a function of in situ void ratio (e_0) and cone resistance (q_t) (Cai, 2010).

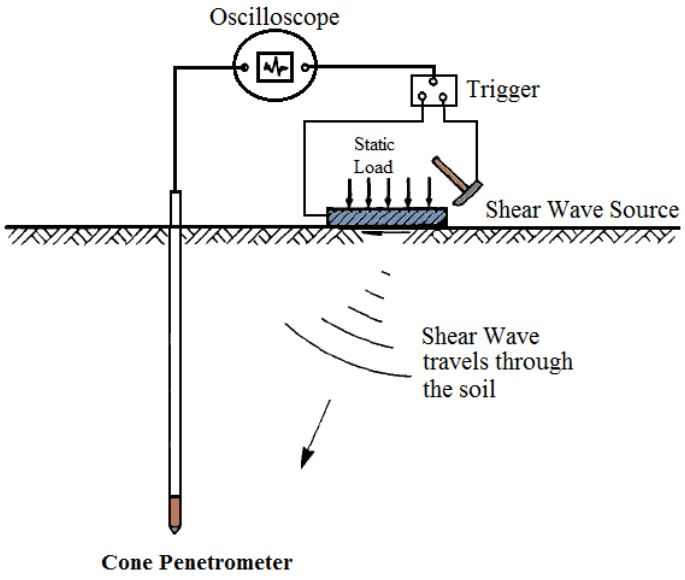

Figure 2-1. Schematic layout of downhole seismic cone penetration test

Robertson et al. (1995) proposed a soil classification chart based on normalized cone resistance (Q_t) and the ratio of small strain shear modulus (G_0) to cone resistance (G_0 / q_t), and a variety of soils such as highly compressive sands, cemented and aged soils and clays with either a high or low void ratio can be identified through the chart (Lunne et al. 1997). It should be noted that all classification charts are global in nature and provide only a guide to soil behaviour type.

2.3 Estimation of random field and variability of soil properties using cone data

Knowledge about the soil variability in the design and analysis of foundations is a key factor in verification of new design codes and therefore is of great interest in geotechnical engineering. Limited available information results in more conservative geotechnical designs (e.g. Baecher, 1986). As examples, Alonso and Krizek (1975), Tang (1979), Nadim (1986), Campanella et al. (1987), Wu et al. (1987), Reyna and Chameau (1991), Kulhawy et al. (1992), Fenton (1999), Phoon et al. (2003) and Elkateb et al. (2003a, 2003b) have performed some study to assess the inherent variability of soil using cone penetration tests (CPT). But only a few numbers have used stress-normalized CPT data (Uzielli, 2005). Fenton and Vanmarcke (1990) proposed the local average subdivision (LAS) method for modeling the inherent variability of a soil property as a random field. The method requires probability density functions (pdf). Input parameters are described by the mean μ and standard deviation σ of the property at each point in space, and a spatial correlation length δ.

Vanmarcke (1977) reported spatial correlation functions and spatial correlation lengths using common functions such as exponential, exponential oscillatory, quadratic exponential oscillatory and bilinear.

In geotechnical investigations, developing new ways to determine soil properties using statistical approaches are important. Probabilistic methods have been proposed in geotechnical engineering for estimating uncertainties in geotechnical predictions (e.g. Zhang et al., 2011), and the application of geostatistics to large geotechnical projects has been approved as a powerful tool in analysis and design (e.g. Ryti, 1993; Rautman and Cromer, 1994; Wild and Rouhani, 1995; Rouhani, 1996). The Kriging method, based on D. G. Krige's empirical work for assessing mineral resources (Krige, 1951), and later formulated by Matheron (1962) into a statistical approach in geostatistics can be used to stablish a spatial interpolation between known data. Kriging generates a best, linear unbiased estimate of a random field between known data by having the ability of estimating the mean trend (see e.g. Fenton and Griffiths, 2008). In environmental and geotechnical engineering, Kriging is commonly applied to the mapping of soil parameters and piezometric surfaces (e.g. Journel and Huijbegts, 1978; Delhomme, 1978; ASCE, 1990).

2.4 Characterization of spatial variability

A realization of the soil variability for the purpose of analysis and design of foundation is a basis for calibration of new design codes. Due to limited site data and natural variability of soil parameters, foundation design is usually accompanied with significant uncertainty. In the case of limited available information, geotechnical design is inevitably more conservative, cf. e.g. (Baecher, 1986). Similar to the mean and standard deviation of soil parameters, the spatial correlation length has a great influence on determining the probabilistic outcomes.

2.4.1 Identification of statistically homogeneous soil layers

The identity of the soil type can only be obtained at the location at which a CPT is conducted. If the soil type at nearby locations is required during a design or construction process, the results at the existing location generally cannot be used directly due to the significant variability of natural soils (Lloret-Cabolt et al., 2014). The stratification of natural soil may change greatly within a small horizontal distance of say 5 m (Das, 2010). The evaluation of soil stratification at unsampled locations with no available data remains an unsolved problem. The interpolation technique can give a rough estimation of a certain soil parameter at unsampled locations based on existing CPT data (Beacher and Christian, 2003; Lacasse and Nadim, 1996). This estimation will inevitably vary in a wide range due to the considerable variability of CPT measurements as well as the uncertainties associated with soil classification methods (e.g. Zhang and Tumay, 1999; Kurup and Griffin, 2006; Jung et al., 2008; Cetin and Ozan, 2009; Wang et al., 2013). Therefore, clear determination of soil stratification from a scattered and obscured estimation of soil parameters is difficult (Houlsby and Houlsby, 2013).

If statistical characteristics of soil properties are independent from spatial location, they are called statistically homogeneous. The first step to characterize the inherent spatial variability of soil properties is to identify statistically homogeneous sub-layers with the same characteristics by interpreting the available data. When the results of soil classifications performed on samples retrieved from bore-holes are available, identifying layers with similar soil types is straightforward. For in situ tests such as the cone penetration test (CPT) where no

specimens are obtained, the identification of layers with the same soil type must be based on indirect methods as explained in detail in previous sections.

2.5 Correlation structure of the field

Depicting of how rapidly the field varies in space enables us to characterize a random field. This is achieved by the second moment of the field's joint distribution, which is defined as the covariance function,

$$C(t', t^*) = Cov[X(t'), X(t^*)] = E[X(t')X(t^*)] - \mu_X(t')\mu_X(t^*) \quad (3)$$

where $\mu_X(t)$ is the mean of X at the position t. A more meaningful measure about the degree of linear dependence between $X(t')$ and $X(t^*)$ is the correlation function,

$$\rho(t', t^*) = \frac{C(t', t^*)}{\sigma_X(t')\sigma_X(t^*)} \quad (4)$$

where $\sigma_X(t)$ is the standard deviation of X at the position t.

A commonly applied model of the correlation function in geostatistics is a single exponential curve, proposed by a great number of related research and mathematical simplicity, cf. e.g. (DeGroot, 1996; DNV, 2010).

2.5.1 Spatial correlation length

The spatial correlation length, also known as the scale of fluctuation, is the distance for which points are highly correlated and reflects the variability of a strongly correlated domain.

The correlation length for a one dimensional real valued field is defined as the area under the correlation function (Vanmarcke, 1984):

$$\delta = 2\int_0^\infty \rho(\tau)\, d\tau \quad (5)$$

There are different techniques available in the literature for the estimation of the spatial correlation length. Vanmarcke (1977) approximated correlation functions and the scales of fluctuation of residuals by use of such common models in Table 1. For example, DeGroot and Baecher (1993) employed the exponential model to estimate the horizontal scale of fluctuation of undrained shear strength in a soft marine clay layer as 46 m and using the squared exponential model, Tang (1979) estimated the horizontal scale of fluctuation of cone resistance of CPT data in a marine clay layer as 60 m.

Several common admissible models for correlation functions proposed within the geotechnical and geohydrological literature are presented in Table 2-1. Most studies in geotechnical site investigations illustrate higher correlation length in the horizontal direction rather than vertical due to the horizontal formation of soil strata, in which soil properties are more correlated. As an example and from the reported experimental data in

literature (JCSS-C1. 2006), the horizontal correlation length for the tip resistance in sea clay is around 40 m, whereas it is 2 m in vertical direction (Chiasson and Wang, 2006).

Table 2-1. Autocorrelation models and the corresponding spatial correlation length (after Vanmarcke, 1977) (JCSS probabilistic model code)

Type	Normalized autocorrelation function	Spatial correlation length δ
1. Exponential	$\exp(-\frac{r}{D})$	$\delta = 2D$
2. Exponential, oscillatory	$\exp(-\frac{r}{D})\cos(br)$	$\delta = \frac{2D}{1+b^2D^2}$
3. Quadratic exponential (Gaussian)	$\exp(-\left(\frac{r}{D}\right)^2)$	$\delta = D\sqrt{\pi}$
4. Quadratic exponential oscillatory	$\exp(-\left(\frac{r}{D}\right)^2)J_0(br)$	$\delta = D\sqrt{\pi}\exp(-\frac{1}{8}b^2D^2)I_0(\frac{1}{8}b^2D^2)$
5. Bilinear note: applicability restricted to 1-D fields	$(1-\frac{\lvert r\rvert}{D})$ for $\lvert r\rvert \le D$ 0 for $\lvert r\rvert > D$	$\delta = D$
Remarks: $J_0(.)$ and I_0 are Bessel functions of first kind and order zero respectively. D and b are model parameters, and r is the distance argument of the autocorrelation function.		

2.6 Modeling spatial variability of the site using Kriging

Since its introduction in the 1960s, Kriging has been widely applied to many areas of engineering and science, including geostatistics. In environmental and geotechnical engineering, Kriging is commonly applied to the mapping of soil parameters and piezometric surfaces (e.g. Journel and Huijbegts, 1978; Delhomme, 1978; ASCE, 1990).

Principally Kriging is a best, linear unbiased estimation with the added capability to estimate the mean trend. The main application of Kriging is to provide a best estimate of the random field at unsampled locations and is modelled as a weighted linear combination of the observations.

Assume that X_1 , X_2, …, X_k are observations of the random field $X(x)$ at the points x_1, x_2, . . , x_k, that is, $X_k = X(x_k)$. A Kriging estimator is said to be linear because the predicted value $\hat{X}$ is a linear combination that is written as:

$$\hat{X} = \sum_{k=1}^{n} \beta_k X_k \tag{6}$$

where the n unknown weights β_k are solutions of a system of linear equations which is obtained by assuming that $\hat{X}$ is a sample-path of a random process X. The hat in $\hat{X}$ shows that it is an estimation. Naturally, when the

point X_j is close to one of the observation points, the corresponding weight β_j should be high. In contrary, when the random field $X(x)$ and X_j are in different (uncorrelated) soil layers, probably β_j is small. The error of prediction of the method

$$\varepsilon = X - \sum_{k=1}^{n} \beta_k X_k \tag{7}$$

is to be minimized. The Kriging assumption is that the mean and the covariance of X is known and then, the Kriging predictor is the one that minimizes the variance of the prediction error.

Kriging has some merit compared to other common interpolation techniques. For example, it can generate site-specific interpolation layout by directly integrating a model of the spatial variability of the data (Rouhani, 1996). Stochastic dependency in geotechnics can be due to the geological processes acted over a large domains across geological period (e.g. sedimentation in large basins) or in fairly small areas for only a short time (e.g. turbiditic sedimentation, glacio-fluviatile sedimentation).

2.6.1 Random field generation

Modelling of the soil as a random field requires a numerical stochastic analysis. The first step in such analysis is performing a random field simulation. Different methods proposed in geotechnical practices to generate multi-dimensional random fields. The most common algorithms are:

- Correlation Matrix Decomposition or Cholesky decomposition method.
- Turning Bands Method (TBM).
- Moving Average (MA) methods.
- Fast Fourier Transform (FFT) method.
- Local Average Subdivision (LAS) method.
- Discrete Fourier Transform (DFT) method.

All methods use the same procedure by generating a set of spatially correlated random field from a set of uncorrelated standard Gaussian (zero mean and unit standard deviation) distributed random seeds. The correlation is introduced via a correlation function. Transforming from the Gaussian distributed field to the desired field (e.g. log-normally distributed) with the specified mean and standard deviation is carried out afterwards. The correlation matrix decomposition method is the direct method of generating random field with the specified correlation matrix (Fraleigh and Beauregard, 1990). Turning bands method was originally proposed by (Matheron, 1973) for second-order stationary fields and is a fast method when dealing with a big two- or three-dimensional random field.

The correlation matrix decomposition method was used in the verification part of this study due to simplicity and speed of generation.

2.6.1.1 Correlation Matrix Decomposition Method

In correlation matrix decomposition method, the random field is generated directly using a specified correlation function for the field, $\boldsymbol{\rho}$. If $\boldsymbol{\rho}$ is a positive definite matrix, then a factorization of $\boldsymbol{\rho}$ can be produced as Eq. (7) (Fraleigh and Beauregard, 1990):

$$\boldsymbol{L}\boldsymbol{L}^{T} = \boldsymbol{\rho} \tag{8}$$

where $\boldsymbol{L}$ is a lower triangular matrix. Eq. (8) is typically solved using Cholesky decomposition and matrix $\boldsymbol{L}$ is used for correlating a set of uncorrelated standard Gaussian random seeds.

Below, steps for generating a random field using matrix decomposition method are given.

1. Generate a set (vector) of standard Gaussian distributed seeds, $\boldsymbol{U}_{n\times 1}$, where n is the number of samples or locations,
2. Construct the correlation matrix, $\boldsymbol{\rho}_{n\times n}$, using the specified correlation function for the field,
3. Decompose the correlation matrix by solving Eq. (8) and find the lower triangular matrix, $\boldsymbol{L}_{n\times n}$,
4. Multiply matrix $\boldsymbol{L}_{n\times n}$ to vector $\boldsymbol{U}_{n\times 1}$ in order to generate a vector of correlated random samples, $\boldsymbol{Y}_{n\times 1}$ as $\boldsymbol{Y}_{n\times 1} = \boldsymbol{L}_{n\times n}\boldsymbol{U}_{n\times 1}$,
5. Transfer the correlated random field, $\boldsymbol{Y}_{n\times 1}$, to the field $\boldsymbol{X}_{n\times 1}$ having considered the cumulative distribution function (CDF), F :

$$F\left(x_i\right) = \Phi\left(y_i\right) \Rightarrow x_i = F^{-1}\left(\Phi\left(y_i\right)\right) \tag{9}$$

where x_i and y_i are the ith entry of $\boldsymbol{X}_{n\times 1}$ and $\boldsymbol{Y}_{n\times 1}$, respectively. Further, $\Phi(.)$ is the standard Gaussian CDF.

As an example, a two-dimensional (2D) random field for the cone resistance of soil is shown in Figure 2-2.

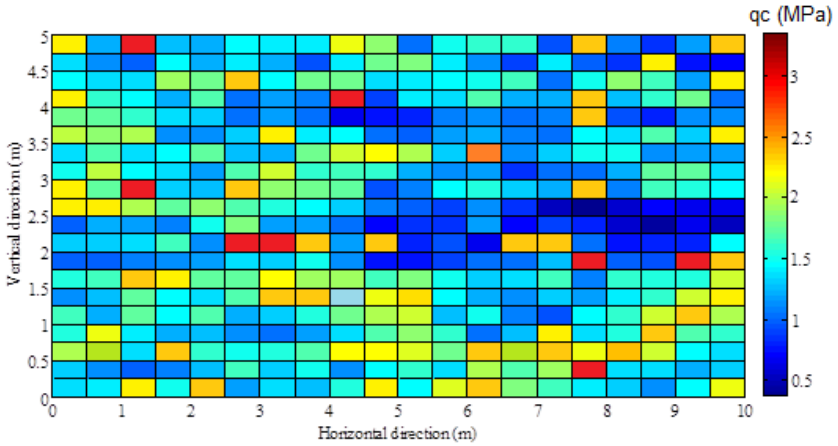

Figure 2-2. An illustration of the lognormal 2D random field for cone resistance using the matrix decomposition method. Mean value =1.50 MPa, *COV*=0.4 , horizontal correlation length = 5 m and vertical correlation length = 1 m.

CHAPTER 3: SCOPE OF THE THESIS

As mentioned in the previous chapter, several empirical correlations have been proposed in the literature for estimating the soil behavior type and strength parameters from in-site testing methods. Nevertheless, compatibility of these methods should be considered in a local case. Also due to inherent variability of the soil layers, those estimations are accompanied with many uncertainties and should be taken into consideration. This chapter explains the overall aim of the current PhD thesis. Also the main objectives of the project as well as its novelty are pointed out.

3.1 Main findings of state-of-the-art

Site characterization is a unique problem in geotechnical engineering that utilizes both prior information (including engineering judgment) and project-specific information from test borings, in-situ testing, and/or laboratory testing. The problem is further complicated by inherent spatial variability of geo-materials and the fact that only a small portion of geo-materials are examined during site characterization.

Some research is conducted about reliability based design of wind turbine foundations. However, limited research has been carried out regarding the spatial co-variation of soil parameters over a large field. The conventional method for determining a soil type is by laboratory classification of samples retrieved from a borehole. If a continuous, or nearly continuous, subsurface profile is desired, the cone penetration test (CPT) provides time and cost savings over traditional methods of sampling and testing. CPT results are typically used to infer soil types and soil properties. Specifically, CPT are used for determining soil classification, obtaining the drained and undrained shear strength parameters of sand and clay deposits, and estimating the deformation modulus for designs of geotechnical structures.

The aim of the project is to formulate a method for probabilistic site description based on cone penetration tests and establish a probabilistic method that enables a reliable foundation design for offshore wind farms, which requires fewer tests than present methods.

3.2 Objectives

- Considering the aspects introduced in the project overview, the objectives of the present study can be categorized as following:
- Conducting several cone penetration tests in different sites and estimating the soil type of the region using various soil classification charts by considering an inherent uncertainty for the model and method-verification using laboratory classification test results on samples retrieved from bore-holes. The sites chosen for analysis, even if they are on land, are representative for the soil conditions that can be expected in an offshore wind farm.

- Comparing the results for the purpose of choosing the best method compatible with the soil type of the region as a case study. This help engineers to find the best compatible classification method for the soil in high cost projects (e.g. site investigation phase for the offshore wind turbine foundation analysis).
- Performing several seismic cone penetration tests in both sand and clay and analyzing data based on different correlations presented in the literature to estimate shear wave velocity and shear moduli of the soil based on cone data. Two seismic analysis methods are employed to estimate the shear wave velocities from time acceleration data to see which one is more reliable in estimation of shear wave velocity. The results are further compared and verified with the measurements of shear wave velocity achieved from SCPTu tests. The seismic tests are carried out because the elastic properties of the soil must be found with high accuracy since the serviceability limit state has been found to be the design driver in many cases. Such studies decrease the uncertainty regarding the choosing method for estimation of soil parameters in analysis of offshore wind turbine foundations.
- Shear wave velocity measurements obtained from SCPTu tests are used in the classification chart based on small strain shear modulus and normalized cone resistance. The results are further compared and verified with the classification test results of samples retrieved from boreholes on the site.
- Performing a reliable estimation of soil properties of the field, as well as the knowledge about variation of soil parameters and soil inhomogeneties in both vertical and horizontal direction. The main topic of this part is spatial analysis of the measurements from the CPTu tests performed in the field. This study seeks to estimate anisotropic spatial correlation length of two sandy sites in northern Denmark, using statistical trends and correlations, and to interpolate soil properties at unsampled locations of cone data.
- Creating random field models to deal with uncertainty in soil properties due to the spatial variability. This is achieved by analysing some in-situ cone penetration test (CPT) data from a sandy site in the region. In order to provide a best estimate of properties between observation points in the random field, a Kriging interpolation approach has been applied to interpolate between known borehole data. Studies such as this can reduce the cost of site investigation by providing more reliable interpolated information for design and analysis of offshore wind turbine foundations.

3.3 Overview of publications

The current PhD thesis has been divided into three research parts and concluded in 5 scientific papers, cf. Figure 3-1. Part I focusses on the estimation of soil stratigraphy using CPT in-situ testing method and classification methods. Part II presents interpretation of seismic cone penetration tests in sand and clay and its application to estimate the shear moduli of the soil using seismic analysis. Also estimation of the soil type by having the values of small strain shear modulus is presented in this section.

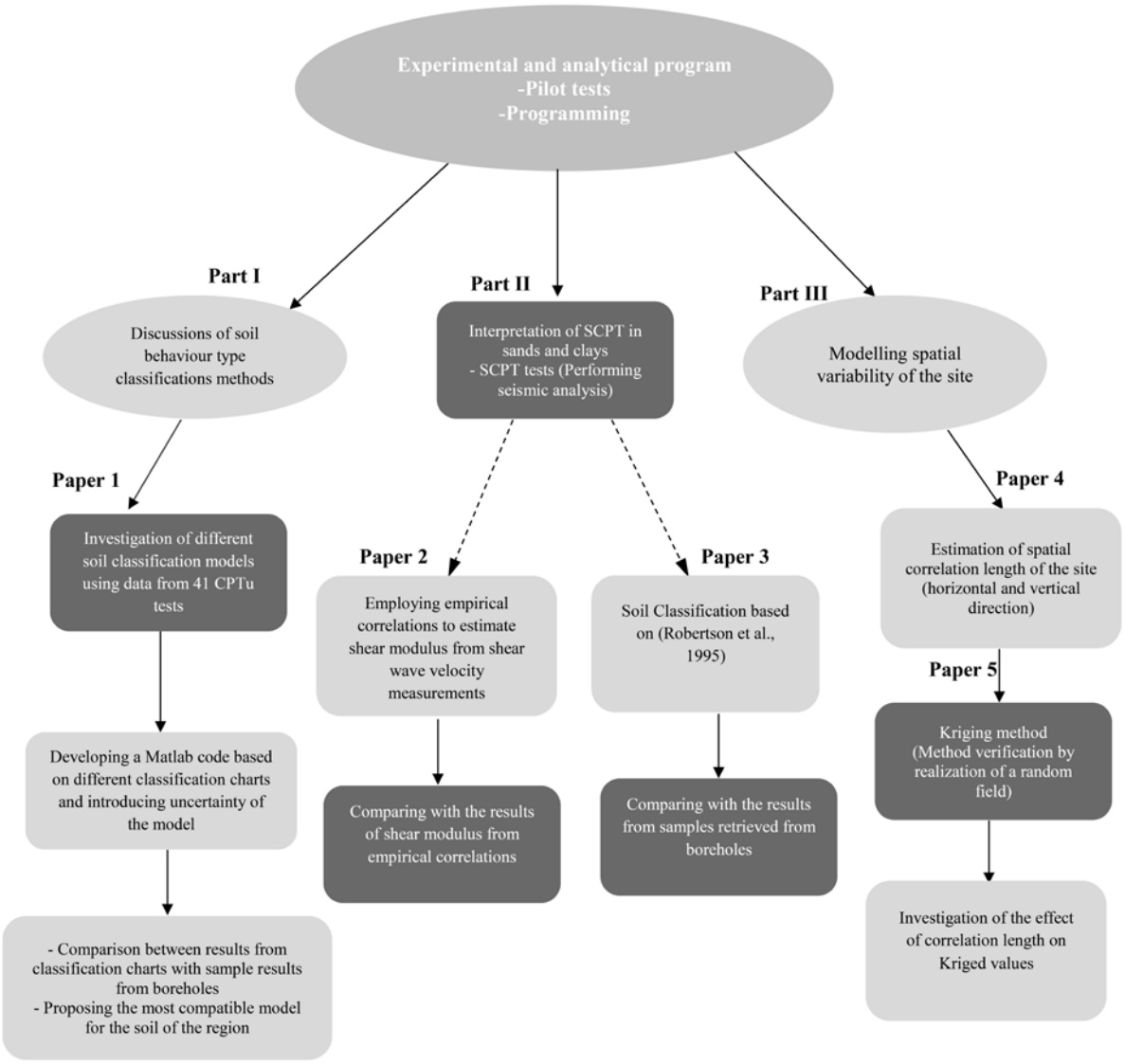

Figure 3-1. Overview of the research topics and papers

Part III concerns the modelling of spatial variability at the site by introducing the spatial correlation length of cone data. Also this part presents a probabilistic method to predict cone data at unsampled locations by realization of a random field and applying the Kriging estimation method.

CHAPTER 4: SUMMARY OF INCLUDED PAPERS

The current PhD project is disseminated via five scientific papers, including three conference paper and two journal papers which can be found in the enclosed appendices. The papers come along with the objectives of the research project during the PhD program. In the following chapter, the significant outcome of the papers is given including assumptions, methodology and results.

4.1 Paper 1

Published in Twenty-second International Offshore and Polar Engineering Conference, Rhodes, Greece, pp. 151-158.

The paper title is "CPTu-based geotechnical site assessment for offshore wind turbines—a case study from the Aarhus site in Denmark".

This study presents a thorough site investigation of a wind farm at Aarhus, using different CPTu-based soil classification methods. These include methods by Robertson et al., (1986), Robertson (1990), Ramsey (2002), Eslami and Fellenius (2004) and Schneider (2008). The data from 41 CPTu tests and five bore-hole tests have been used. The raw cone penetration measurements are scrutinized and removed further for data connected with physical or mechanical errors. The corrected data were then used for classifying soil by the above mentioned charts and uncertainties related to each method estimated by presenting a model preference to show how certain the method is about the soil type of each data point. For this purpose, the classification diagram is digitalized (in this case a resolution of about 2000 × 2000 pixels is used) and a window is defined around a given data point. The size of the window is a heuristic choice meaning that a larger window implies more candidates for the soil type proposed by the classification method.

Main results

The main findings from Paper 1 are:

- Even though the cone penetration test is a standard method of assessing soil properties, errors related to measuring can still occur during the test. Here measurements with considerable peaks are removed. These peaks are basically due to stiff thinly interbedded materials within the soil deposits and are not representative of the soil type in that location. This is basically based on engineering judgment, and is very important as this removal has effects on the classification results. In Figure 4-1, an example of this error filtering is illustrated for a representative borehole by red circles marking the suspected measurement.
- All CPT classification methods are based on the idea that combinations of CPT parameters falling within a "zone" in the classification chart are classified as a particular soil type. However, the lines separating the "zones" are not resulting from theoretical solutions and subject to uncertainty in the sense that the engineer has to decide whether a given data point is in one or another "zone".

- The certainty introduced in the soil classification chart is a probability meaning that it is always between 0 and 1.Figure 4-2 shows that for measurements which are close to the borders this value is small (close to 0) and for those which are far from border lines it is close to 1.

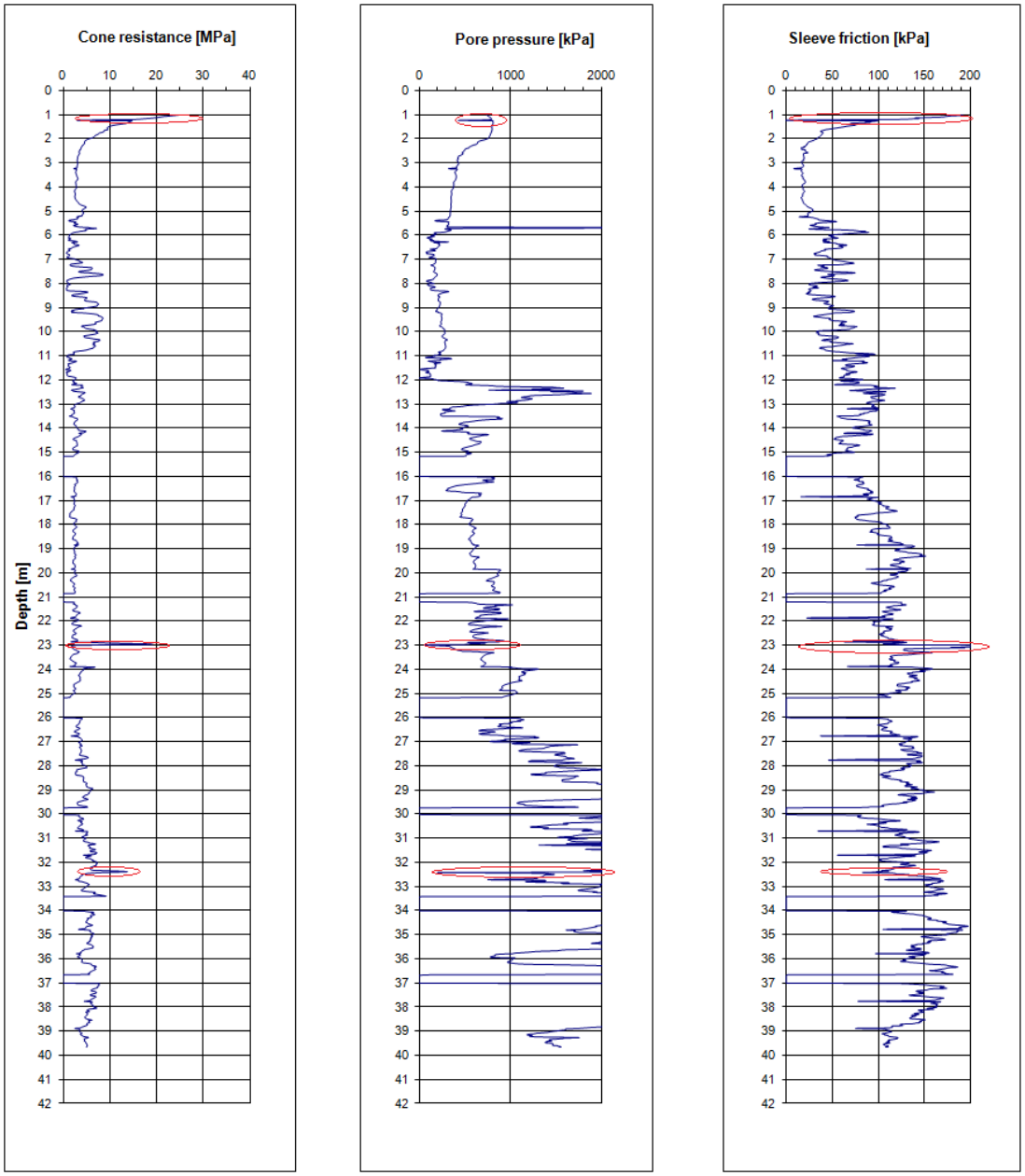

Figure 4-1. Example of error filtering in sounding 08. Red circles show measurements with considerable peaks that should be removed.

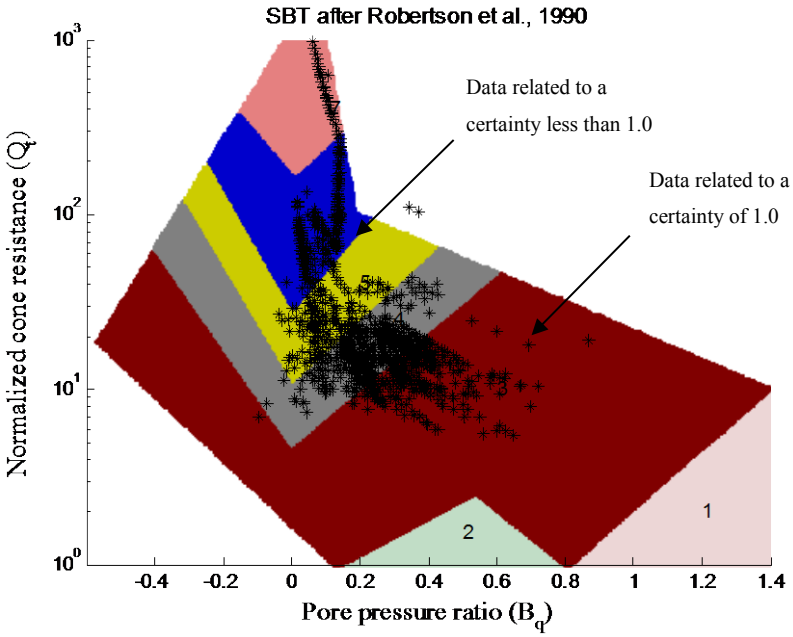

Figure 4-2. CPTu data plotted on the chart proposed by Robertson et al. (1990). The soil types corresponding to zones 1 to 7 are: 1. Sensitive, fine-grained soils; 2. Organic soils and peat; 3. Clays, clay to silty clay; 4. Silt mixtures, silty clay to clayey silt; 5. Sand mixtures, sandy silt to silty sand; 6. Sands, silty sand to clean sand; 7. Sand to gravelly sand;

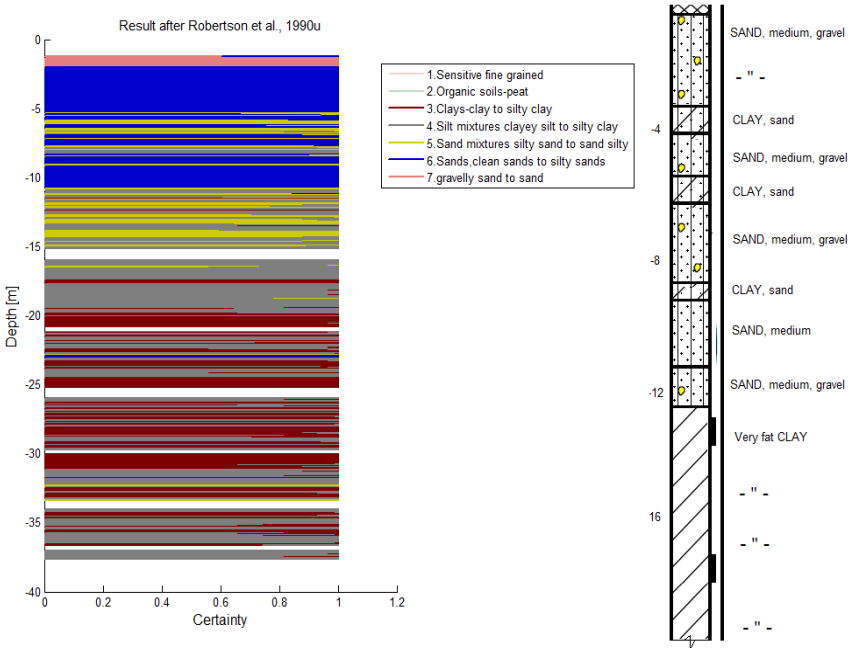

Figure 4-3. Different values of certainties versus depth from Robertson et al. (1990) and soil profiling from a borehole in the region.

- The results from comparison with bore-hole data showed that most of CPT classification methods, in general, are acceptable for classifying the soil, but some of them are more confident with higher certainties in some specific soils. This emphasizes that different methods have different capabilities in

identifying correctly various soil behavior. This is possibly related to the differences in the development processes behind the charts, due to different background data.

- The comparisons between different classification methods and verifications with bore-hole results provide guidance for soil of the region to be assessed in the future with fewer tests, which results in saving time and expenses.

Discussion and concluding remarks

Error filtering is an initial and important part of the evaluation of CPT data. Main errors are due to either local soil inhomogeneity or big halts during the sounding. Peaks occur when the cone reaches a thin layer of stiff material such as lenses of stiff silt or sand or small stones or boulders within the layer. These peaks should be carefully removed as they lead to a considerable error in predicting the real parameters of the entire layer. The errors due to halts often happen when a new rod should be attached to reach further depth. These errors appear as large drops in the cone resistance and big change in drained conditions.

The size of the window for estimating the soil type reflects the uncertainty related to a visual interpretation of the printed diagram. A smaller window implies that the soil types assigned to measurements near zone boundaries are classified with more confidence.

In future analysis basis on visual interpretation of the diagram, it is advised to employ different size of the windows and perform a sensitivity analysis to find the best size for the window.

4.2 Paper 2

Published in Seventh International Conference on Case Histories in Geotechnical Engineering, Wheeling, IL. Missouri University of Science and Technology, 2013. Paper no. 2.34.

The paper title is “Geotechnical site assessment by seismic piezocone test in the north of Denmark”.

There are different correlation methods reported to predict shear modulus from CPTu data, but their validity still needs to be verified for a local case. So the paper presents a description of performed SCPTu and shear wave types in both sand and clay as a case study along with two different methods of finding S-wave velocities in order to analyse and compare with the values obtained from empirical correlations presented in the literature. The measurements of shear wave velocity achieved from SCPTu tests are further compared and verified with the results.

Main results

The main findings from Paper 2 are:

- Several seismic cone penetration tests were performed in two sites (one with mostly clayey soil and the other with mostly sand) in the north of Denmark with generating two pulses on the ground surface (Figure 4.4). All SCPT readings were taken with intervals of 1 m. Two analysis methods, "Reverse

polarity" and "Cross-correlation", were employed to calculate shear wave velocities from signal traces of seismic data, and the results were compared to each other to investigate which method is more compatible in the region. Figure 4-5 illustrates an example of time series in each analysis method.

- Since only one strike (left or right) is enough in the cross-correlation method to estimate the shear wave velocity, the interval time that sounding is halted is shorter compare to the reverse polarity method in which two strikes are needed. This can be counted as a disadvantage of the reverse polarity method. Also the point at which two strikes are superimposed should be chosen by the analyst, which increases the uncertainty of the procedure. Because by introducing a different cross-point, the value of shear wave velocity changes while in cross correlation method the shear wave velocity is estimated by mathematical analysis. The Cross-correlation method removes human bias and gives realistic error estimates.

(a) (b)

Figure. 4-4. Truck and drilling rig (left), L plate and sledge hammer for S-wave generation (right)

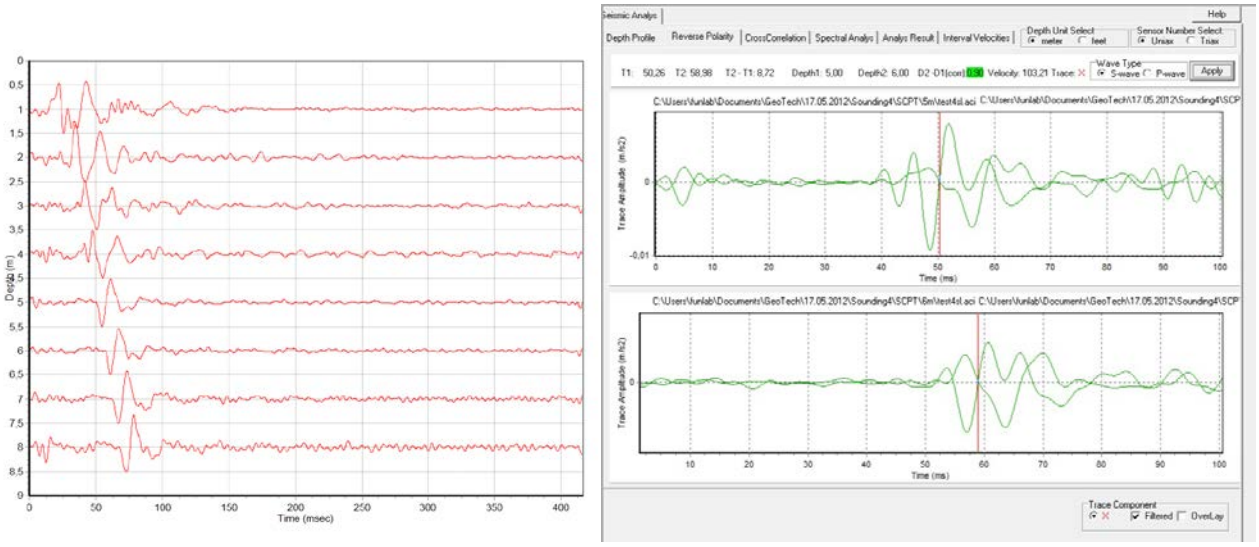

(a) (b)

Figure 4-5. SCPT analysis methods (a) Cross correlation, (b) Reverse polarity between depth 5- 6 m

- Comparison of the shear moduli calculated from CPTu data using empirical correlations with the SCPTu field test results show that the empirical methods over estimated the modulus. This is shown in Figure 4-6 by comparing shear modulus values obtained by empirical methods and from field data.

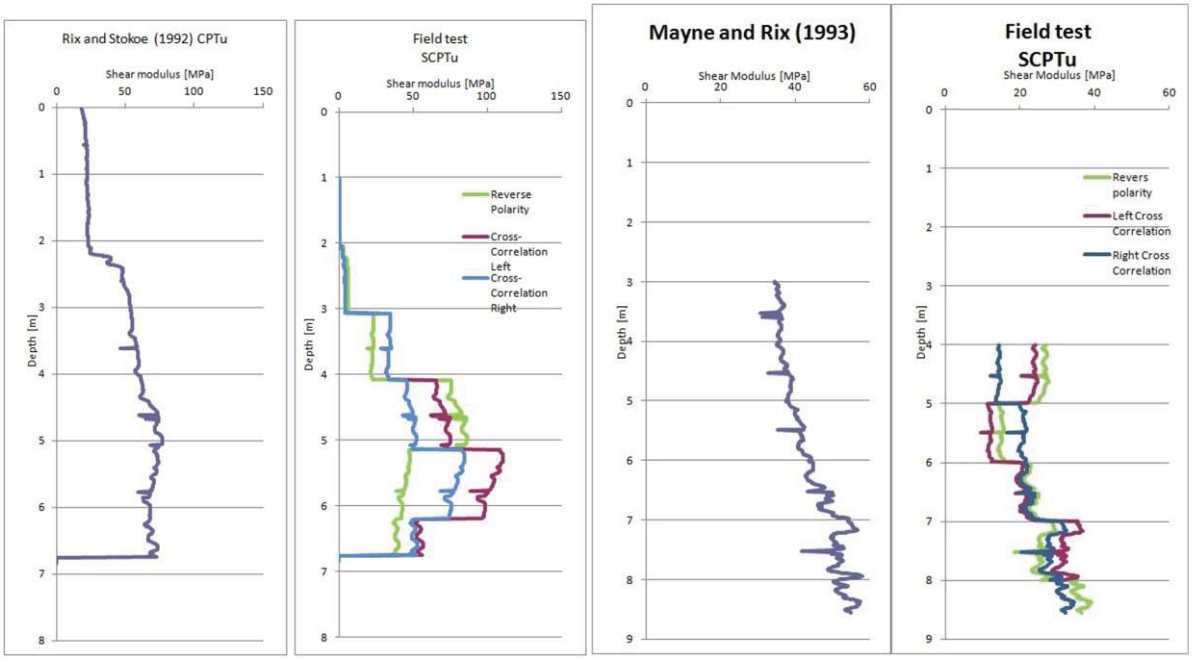

(a) (b)

Figure 4-6. Shear modulus results obtained from empirical methods and field data: (a) Sand; (b) Clay

Discussion and concluding remarks

Even though the seismic cone penetration test has some merits, many considerations should be taken into account during the manipulation and data analysis. As shown in Figure 4-7, the difference between field tests and empirical methods is considerable. Many factors could be involved in the final results of the study. The first and the most possible factor is the existence of the background noise in the area. This noise is visible from the first and/or last part of the signal, before/after the passage of the wave produced by the hammer. Vibrations from sources such as traffic can disturb the main signal produced by the hammer, leading to erroneous predictions of the wave speed In addition, when the tests are carried out at depths with a difference of one meter, the velocities are not directly representative for the soil deposits that are determined based on the standard CPT assessment and borehole logging. Instead, the velocities are mean values for the 1 m deep layers present between adjacent measurement positions.

The big difference between three analysis methods in the field test diagrams could be due to not providing similar conditions to produce the left and right strike. Also the important effect of choosing the intersection point in reverse polarity analysis method should not be ignored (Fig. 4-8).

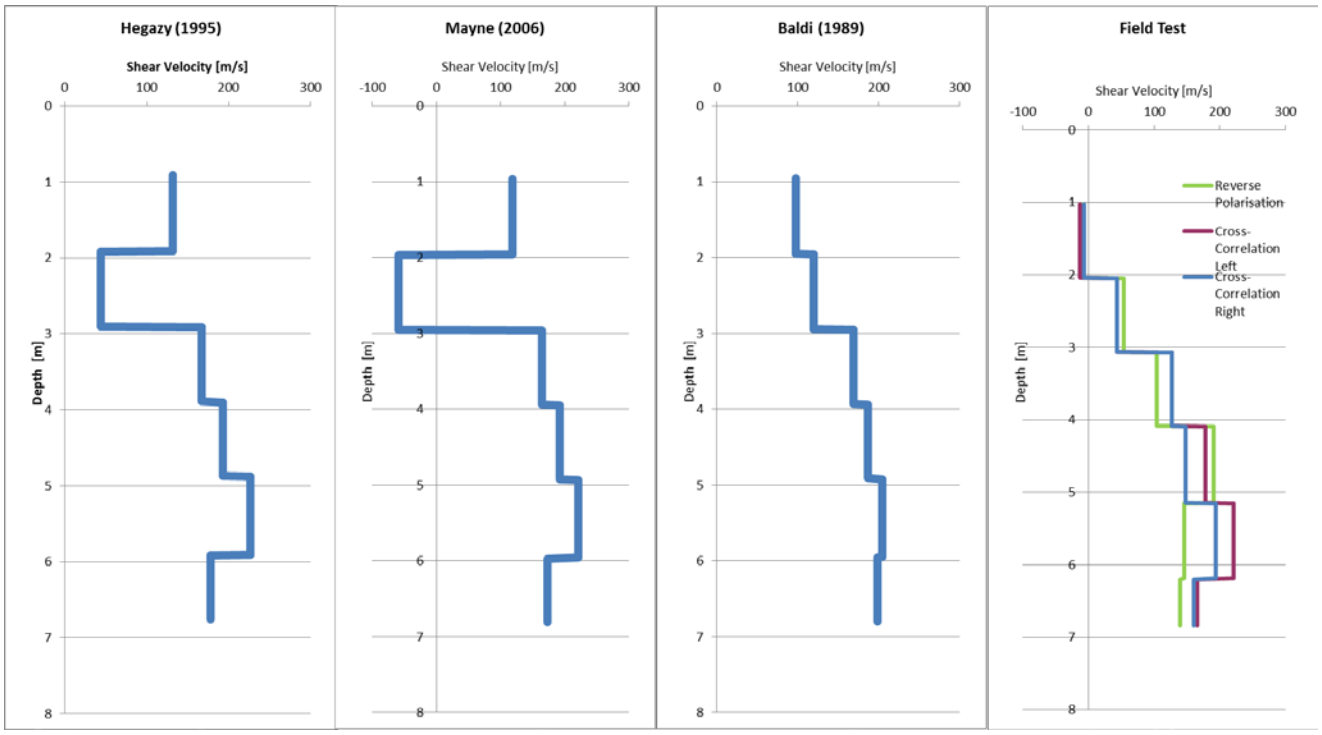

(a) Sand - CPT 3

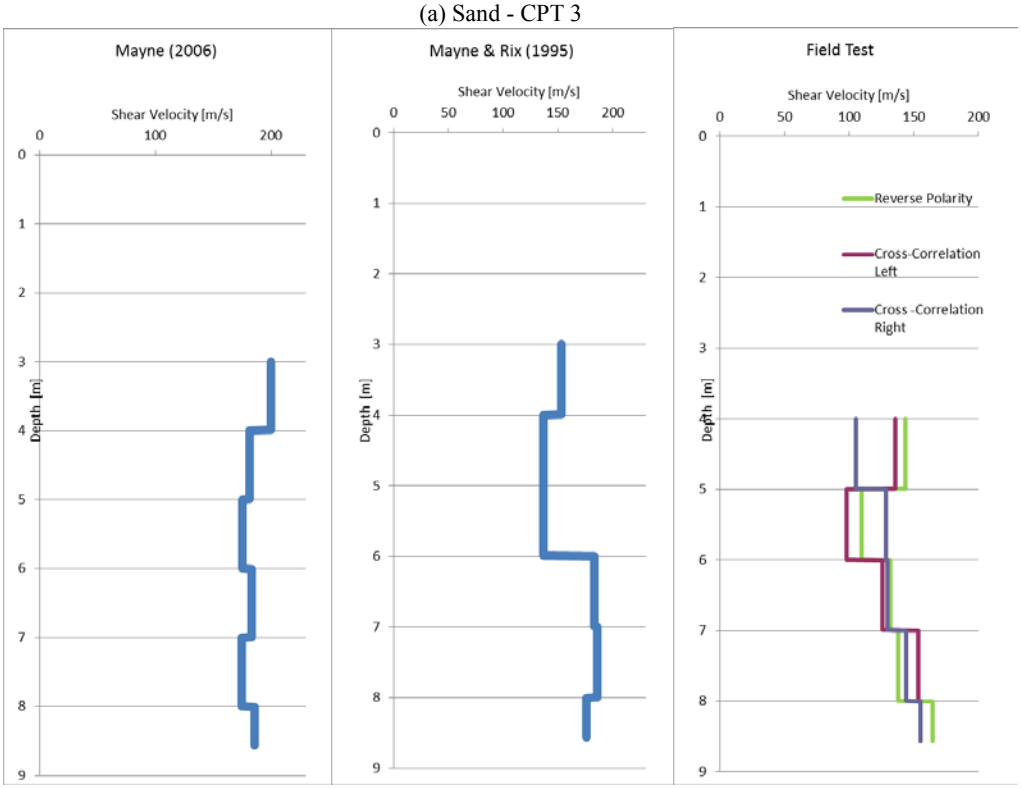

(b) Clay - CPT 5

Figure 4-7. Average shear velocities obtained from empirical methods and field test results.

As a historical note, the reverse polarity method was invented in a time when the recorded signals were analogue. Today the recordings are digital so that users have much more stronger capabilities to do something more significant than pick of a single point where two wavelets are superimposed.

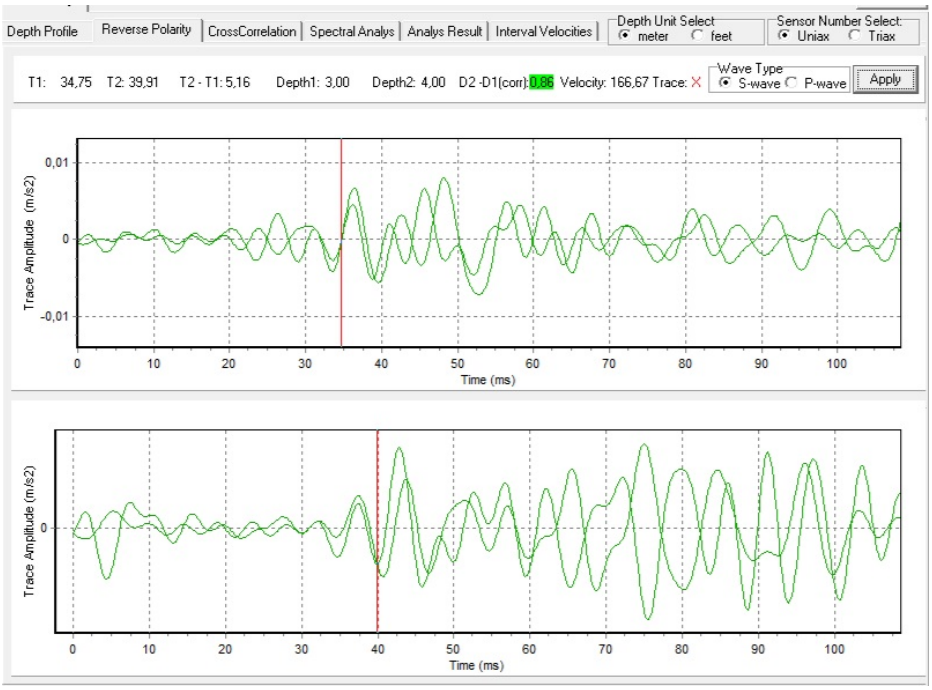

Figure 4-8. An example of a wrong analysis conducted in th revers polarity method

Figure 4-8 shows an example of wrong analysis based on two strikes. In such cases that the results are too sensitive and the reversal signals are overall not good, it might be recommended to use a first arrival (or first peak) method or cross-correlation analysis based on only one-direction single signal (Campanella 1986).

In the paper published in 7ICCHGE, shear velocities obtained from empirical correlations are plotted for each 2 cm in Fig. 10. However, it can be argued that this is subject to come uncertainty because these values are based on relative densities estimated from CPT measurements. In future analysis, it is advised to find densities from intact samples at the site and compare with the results.

4.3 Paper 3

Published in 3rd International Symposium on Cone Penetration Testing, Las Vegas, Nevada, USA. Pp. 621-628. The paper title is “Estimation of soil type behaviour based on shear wave velocity and normalized cone data in the north of Denmark”.

In this paper, the chart by Robertson et al. 1995 based on small strain shear modulus and normalized cone resistance was employed to classify the soil using SCPTu data from a sandy site. Using two different analysis methods, the values of shear wave velocity and subsequently small strain shear modulus have been obtained and applied in the chart to estimate the soil type of the region. The results are further verified and compared with the soil classification test results on the samples retrieved from boreholes.

Main results

The main findings from Paper 3 are:

- After correction of measured data from the CPT and normalizing the cone resistance for the effect of overburden pressure, the data were used in the chart proposed by Robertson et al. (1995) based on shear wave velocity measurements. Results are illustrated in Figures 4-7 and 4-8 for a representative SCPTu sounding profile.

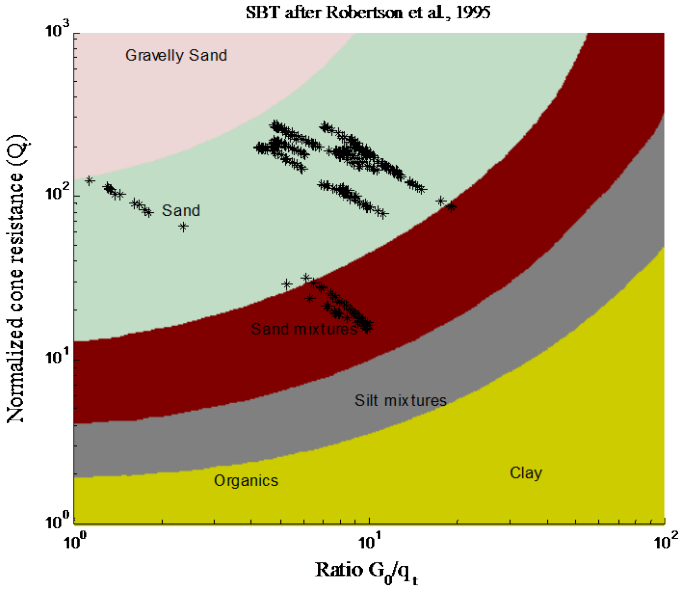

Figure 4-7. Results from the data in the soil classification chart after Robertson et al., 1995- Sounding No. 3 (Sandy site)

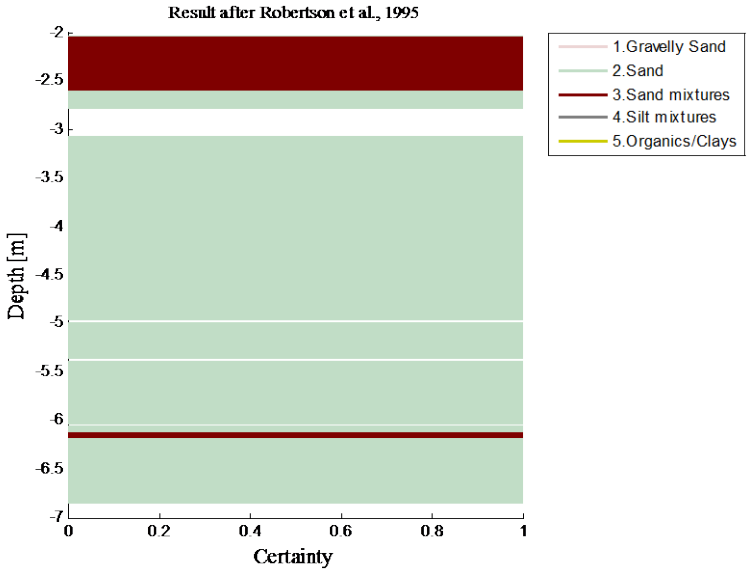

Figure 4-8. Certainty of soil type from the chart after Robertson et al., 1995 – Sounding No. 3 (Sandy site)

- Elasticity theory relates the shear modulus, soil density (ρ) and the shear wave velocity (V_s) as $G_{max} = \rho V^2$. Therefore, by performing seismic cone penetration test in the region, the values of small strain shear moduli needed in the Robertson chart could be obtained.
- The analysis of measurements from all of the soundings reveal that the chart proposed by Robertson et al. (1995) is well-predictive at this site, and in the lack of information due to limited soil samples it seems reliable to use the results of SCPTu to predict the soil type.

Discussion and concluding remarks

SCPT analysis has been performed using two different methods: Cross-correlation and Reverse polarity. Both methods have some merits in calculating the velocity but need some consideration to avoid any misinterpretation. In reverse polarity method two strikes are needed; hence the need for a clear reversal signal may arise. However, it can be argued that this is subject to come uncertainty in the absent of such clear signals. It is advised to use cross-correlation method for data analysis in such cases.

As shown in Figure 6 in the paper, there are some white lines in the certainty diagram. The meaning for these layers is that cone parameters corresponding to these depths fall beyond of the classification chart and no zone could be assigned to them. So the method cannot predict any soil type to these measurements. In the case that these layers are presented many times, reconsideration in the method for soil classification is needed. Also the measurement uncertainty could be a possible reason for these incompatibilities in the diagram.

4.4 Paper 4

Published in *Canadian Geotechnical Journal*, Vol. 51, No. 8, pp. 844-857.

The paper title is "Spatial correlation length of normalized cone data in sand: A case study in the north of Denmark".

The paper focuses on the spatial variability of cone data normalized with respect to vertical stress. The data were collected at two different sites in the north of Denmark. To characterize a random field, the knowledge about how rapidly the field varies in space is needed. This is captured by the covariance structure of the data. By calculating the statistical parameters of the cone data, the spatial correlation length of the field was estimated in the vertical and horizontal directions. At both sites, the cone data show that the vertical and horizontal correlation structures in soil properties are strongly anisotropic, with shorter correlation lengths in the vertical direction.

Main results

The main findings from Paper 4 are:

- The coefficient of variation, COV, is a dimensionless value that quantifies the relative deviation between individual data sets with different means. It is generally more useful than the standard deviation for the comparison of one raw data set with another raw data set. Since COV is an indicator of the degree of variation in soil properties across the site, in soil layers with relatively high COVs, there is expectation for more variability of the soil parameters.
- In the horizontal direction, the maximum COVs occurred in the last layer of sand deposits in the Frederikshavn site. This effect may be due to thinly interbedded silt mixtures within the layer.
- A random field is described concisely in the second moment sense by estimating the spatial correlation length and the coefficient of variation in space. For this purpose, the average coefficient of variation of cone data in vertical and horizontal directions was calculated in two sites, and regression analysis was employed to estimate the spatial correlation length.
- Characterizing the spatial variability of soil properties shows that due to the geological nature of deposits and the material composition of the formations, the vertical and horizontal correlation structures from the cone results are significantly anisotropic, with higher values in the horizontal direction (Figures 4-9 to 4-11).

- Inclination of soil layers has a significant effect on the obtained values of horizontal correlation length. Under the simplifying assumptions that the soil layers are ideally horizontal and homogenous, the measured parameters at the same depth must be highly correlated with the same measured values. Though in reality, due to the inclined layer within the soil deposit, it is more likely for soil parameters to have different values at the same depth and this result in a poor correlation.

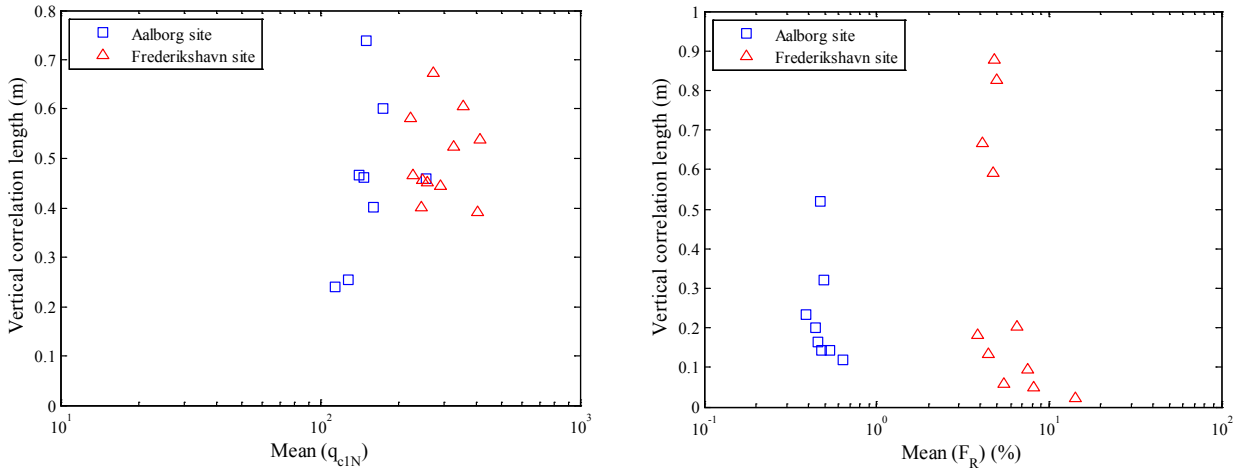

Figure 4-9. Vertical spatial correlation lengths of q_{c1N} and F_R, plotted against the mean, for the Frederikshavn and Aalborg sites

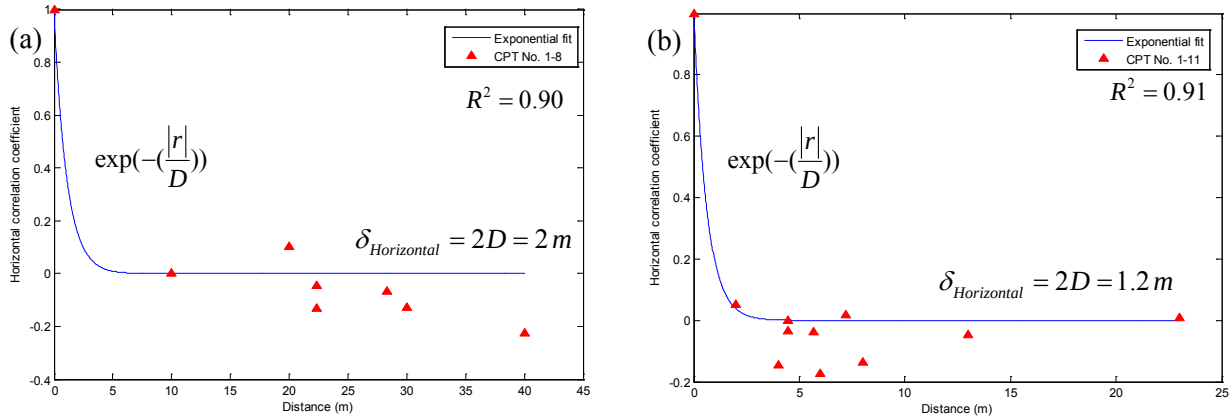

Figure 4-10. Horizontal correlation coefficient of q_{c1N} for all soundings in the sand layer (a) Aalborg, (b) Frederikshavn

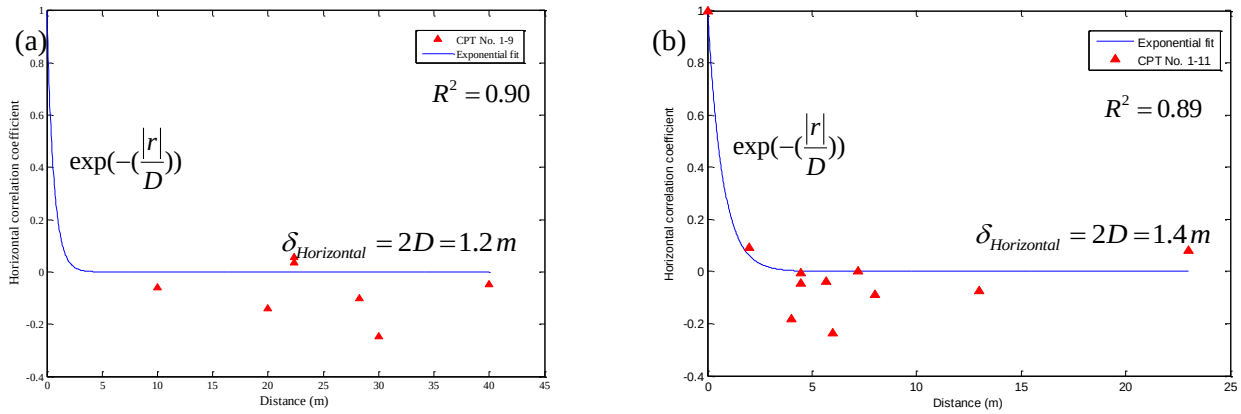

Figure 4-11. Horizontal correlation coefficient of F_R for all soundings in the sand layer (a) Aalborg, (b) Frederikshavn

Discussion and concluding remarks

Since effective overburden stress has a considerable influence on the soil interpretation, CPT measurements have been normalized for vertical stress. To have a certain comparison between two different sites, and avoid the influence of the depth on the results, data normalization proposed by Robertson and Wirde (1998) was used in this study. It should be noted that the Robertson classification method also employs normalized cone data (Q_t and F_R) to estimate the soil type. Therefore, q_{c1N} and Q_t should not be mixed up in the conclusion.

The observed variations of the vertical correlation length in F_R and q_{c1N} imply weaker correlation structure in friction sleeve measurements. A friction sleeve with a length of 133 mm includes 6 consecutive friction readings per each 2 cm penetration. This means that the instrument in itself is correlating the data because each measurement is contributing in the procedure several times. Hence, one could argue that correlation lengths shorter than about 200 mm can hardly be achieved. Such correlation lengths would be expected alone due to the inherent smoothing provided by the sleeve and the process of taking a running average. Therefore, the small correlation length obtained in the vertical direction clearly indicates low correlation over depth.

4.5 Paper 5

Published in Journal of Geotechnical and Geoenvironmental Engineering (ASCE). Vol. 141, No. 12, 04015052. The paper title is “Effect of spatial correlation length on the interpretation of normalized CPT data using a Kriging approach”.

The article presents a Kriging approach applied to the normalized cone resistance of a sandy site in Denmark to interpolate between known borehole data. By generating a 3-D standard Gaussian random field and sampling some values at discrete (“bore-hole”) locations, Kriging was used to interpolate between the discrete values and compared with the original random field. By calculating the difference between Kriging estimation and generated random field, known values of the cone data at the location of the sounding were taken as observation points to estimate the values of cone resistance at any point within the field.

Main results

The main findings from Paper 5 are:

- The correlation length has an inevitable effect on the interpolated values in a way that by increasing the correlation length, more accurate estimates could be obtained at a greater distance.
- Verification of the method using a random field simulation and the small mean value of the error shows that Kriging interpolation approach and assumptions employed in the method are admissible.
- Applying Kriging to real values of cone data help us to analyse the effect of correlation length on the results in both vertical and horizontal directions.
- The results indicate that when the horizontal correlation length increases, the standard deviation of estimated values by the Kriging method decreases, resulting in less uncertainty in prediction of values at intermediate locations.
- Excellent agreement between the predicted values of normalized cone data and the existing test data (at the location of soundings) emphasizes that correlation structure of the field in a statistically homogenous layer is chosen properly.

Discussion and concluding remarks

Even though Kriging is a preferred method for data interpolation, many considerations should take into account to avoid any misinterpretation. Kriging uses a weighting which assigns more influence to the nearest data points in the estimation of values at unknown locations. To calculate the estimate, Kriging depends on spatial and statistical relationships so it is essential to be aware of correlation structure of the data. If a weak correlation is ruling, then estimated points are only an average of the dataset. An example is a field with small spatial correlation length.

The Kriging has a two-step process of semi-variance estimations and performing the interpolation. Some advantages of this method are the incorporation of variable interdependence and the available error estimator output. A disadvantage is that it requires more input from the user and substantially more computing and modelling time.

Kriging belongs to the family of linear least squares estimation algorithms. The estimator error is the difference between estimated and real but unknown values and is the error of prediction. The Kriging predictor is the one that minimizes the variance of the prediction error. In a case study, it is important to be aware of this estimation error to have a better interpretation of the result.

CHAPTER 5: CONCLUSIONS AND FUTURE DIRECTIONS

5.1 Summary overview

The current PhD thesis conveys a comprehensive study on a statistical approach to integrate prior information and project specific test results for probabilistic characterization of soil properties from a limited number of tests. For this, being able to make a consistent classification of soil type and strength parameters at a given site is crucial and this leads to a repeatable and highly standardized method by using cone penetration test due to the large amount of information collected continuously throughout a soil deposit. By focusing on the spatial variability of cone data normalized with respect to vertical stress, the spatial correlation length of the field was estimated in the vertical and horizontal directions to be used in the Kriging interpolation approach to provide a map of normalized cone resistance at the site.

5.2 Geotechnical site assessment using cone penetration test—method verification

- Due to economy, simplicity, continuity, accuracy and efficiency features, cone penetration tests have been turned into an alternative to conventional laboratory testing. One of the most important applications of CPT is in soil stratigraphy and classification profiling. The results can be used further in estimation of shear strength parameters of soils and deformation moduli for the purpose of design and analysis of foundations. Different methods exist for soil profile interpretation from CPT data but their validity still needs to be verified since the original soils used in the chart development are quite different from a local soil. This study attempts to do more investigation on different CPTu-based soil classification method adequacies to have a better assessment of the region soil type. This was done by intact sampling and doing some usual classification laboratory tests and comparison with method predictions. These include methods by Robertson et al. (1986), Robertson (1990), Ramsey (2002), Eslami and Fellenius (2004) and Schneider (2008). The results showed an acceptable reliability in most of the CPT classification methods for estimating the soil type. However some of the methods are much more acceptable with higher certainties in some particular soil types compared to others. This can be the result of differences in the development processes of the chart based on different background data. In this specific site, the method by Robertson (1990) based on pore pressure measurements has the highest compatibility with the soil classification test results on samples in sand and gravelly layers, while the Ramsey (2002) models are more reliable in clayey soils.
- By increasing interest in soil dynamics in the recent years, there is a development of CPT as a seismic piezocone penetration test (SCPTu) with the added ability of taking shear wave velocity measurements simultaneously with measurements of tip resistance (q_c), sleeve friction (f_s) and pore pressure (u). Different empirical correlations have been proposed between cone data and shear wave velocity measurements to estimate soil parameters but their validity still needs to be verified in a local case and uncertainty remains about the choice of any of these empirical correlations. Two analysis methods from

signal traces of seismic data were chosen as "Reverse polarity" and "Cross-correlation". The field test results of SCPTu and CPTu estimations for shear velocities from empirical correlation are in the same range. Results obtained from empirical methods are conservative compare to the measured values. Also calculations based on correlation proposed by Mayne (2006) results in negative values of shear wave velocities due to small sleeve friction measurements which are not reasonable. So this correlation is not preferred to be used for this region.

- A number of seismic cone penetration tests have been done in a sandy site in the north of Denmark and results were used to investigate and verify the soil classification system proposed by Robertson et al. (1995). The chart employs the small strain shear modulus and normalized cone resistance to estimate the soil type in the absence of intact soil samples and laboratory test results. The outcomes have been further compared to the soil classification test results on samples retrieved from boreholes in the site. The value of small strain shear modulus is achieved by multiplying the square of the velocity by the density of the soil to be used in the classification chart. The results are very compatible with the laboratory classification results of samples from boreholes by this fact that it is feasible in the future to apply the Robertson et al. (1995) chart to estimate the soil type from SCPT data in this region. This can significantly reduce the cost of site investigation.

5.3 Probabilistic site description based on cone penetration tests

- Soil variability in CPT test data from two different sites in the north of Denmark has been considered by calculating the COV values of normalized cone data in both directions in homogenous sub-layers identified by the soil classification system proposed by Robertson (1990). In order to characterize the spatial variability of cone resistance and sleeve friction, the autocorrelation function with respect to physical distance has been calculated from measurements of the sand layers. Then by fitting an exponential model to these data, the spatial correlation distance for each variable was estimated. The natural deposition processes of soil causes a significant anisotropy in the vertical and horizontal correlation structures from the cone results, with the vertical length of two to seven times shorter than that in the horizontal direction. Also in the vertical direction, q_{c1N} values are more spatially correlated than F_R, with spatial correlation lengths estimated in the range of 0.5 m and 0.2 m respectively. The same is seen in the horizontal direction. The physical explanation for this is the influences of the soil volume around the cone tip that q_{c1N} measurements are larger than the sampling intervals.
- Kriging is a well-stablished method to predict the values if statistical parameters are available. The purpose was to examine this as a case study. A Kriging interpolation approach has been applied to the normalized cone resistance of the region to provide a best estimate of properties between observation points in the random field. Due to an inevitable effect of correlation length on the map of soil variation by Kriging, a study made to examine the effect of this parameter on estimated values at intermediate locations between known values in the field. This was done for two horizontal correlation lengths in

different depths of 2 m and 4 m through the deposit. Results showed that a greater number of intermediate points could be estimated when the correlation length was increased. In contrast these intermediate points could not be estimated precisely by the method when the correlation length was smaller. This means that the estimated points at intermediate locations are close to the mean value of observation points, which implies a higher uncertainty. By increasing the correlation length, the data show more correlation with each other, and the values are closer at a greater distance.

- A trend in the Kriged q_{c1N} is distinguished and is more obvious by increasing the correlation length. By moving away from the observation point (in a distance larger than correlation length), the method gives an average value of data.
- Kriging is not a random field generator but a best linear unbiased estimator. It means that by defining a correlation length, the method predicts the values within this distance.

5.4 Recommendations for future studies

With the inspiration from the conducted studies through the current PhD thesis, the following recommendations are suggested for the future research in this field:

- Two analysis methods of reverse polarity and cross correlation need to be verified to see which one is more reliable in calculating the shear wave velocity. This can be done by creating a time series with known velocity value and applying both methods to see which one is closer to the desire velocity.
- Considering the soil layers inclination in calculation may result in a lower value of horizontal correlation length due to reflecting a higher correlation between data. The measured data on the border between two different layers may show more correlation than points which are in the same level but from different soil categories. As a future work, it is important to find these inclined layers in a soil deposit.
- Studies such as modelling spatial variability of the site using Kriging can be further developed to reduce the cost of site investigation by providing more reliable interpolated information between limited site CPT data.

REFERENCES

Alonso, E. E. and Krizek, R. J. (1975). "Stochastic formulation of soil properties". *Proc. 2nd Int. Conf. on Applications of Statistics and Probability in Soil and Structural Engineering*, Aachen 2, 9-32

Andrus, R.D and K.H. Stokoe. (2000). "Liquefaction Resistance of Soils Based on Shear Wave Velocity", in *Geo tech. and Geo envir . Engrg*, ASCE, 126 (11), 1015-1026.

ASCE Task Committee on Geostatistical Techniques in Geohydrology (1990). "Review of Geostatisics in Geohydrology, 1. B asic Concepts, 2. Applications, "ASCE Journal of Hydraulic Engineering, 116(5), 612-658.

Baldi, G., R. Bellotti, V.N. Ghionna, M. Jamiolkowski, and D.C.F. LoPresti. (1989). "Modulus of Sands from CPTs and DMTs". *Proc. 12th Int. Conf. on Soil Mechan. and Found. Engrg*., Rio de Janeiro, Balkema, Rotterdam, 1, 165-170.

Baecher G.B. and Christian J.T. (2003). "Reliability and statistics in geotechnical Engineering". John Wiley

Baecher, G. B. (1986). "Geotechnical Error Analysis". *Transportation Research Record*. 1105, 23-31.

Begemann, H. K. S. (1965). "The friction jacket cone as an aid in determining the soil profile". *Proceedings of the 6th International Conference on Soil Mechanics and Foundation Engineering,* ICSMFE, 2, (17–20). Montreal.

Cai, G.J., S.Y. Liu., L.Y. Tong and G.Y. Du. (2009). "Assessment of Direct CPT and CPTU Methods for Predicting the Ultimate Bearing Capacity of Single Piles". *Engrg Geology.,* 104 (1), 211–222.

Cai, G.J., S.Y. Liu and L.Y. Tong. (2010). "Field Evaluation of Deformation Characteristics of a Lacustrine Clay Deposit Using Seismic Piezocone Tests", *Engrg Geology,* 116, 251–260.

Campanella, R.G., P.K. Robertson., D. Gillespie., N. Laing and P.J. Kurfurst. (1987). "Seismic cone penetration testing in the near offshore of the MacKenzie Delta". *Can. Geotech. J*. 24, 154-159.

Campanella, R. G., Wickremesinghe, D. S. and Robertson, P. K. (1987). "Statistical treatment of cone penetrometer test data". *Proc. 5th Int. Conf. on Applications of Statistics and Probability in Soil and Structural Engineering*, Vancouver 2, 1011–1019.

Cetin, K.O., Ozan, C. (2009). "CPT-based probabilistic soil characterization and classification". *Journal of Geotechnical and Geoenvironmental Engineering,* 135 (1), 84–107.

Chen, B.S.Y. and Mayne, P.W. (1996). "Statistical Relationships between Piezocone Measurements and Stress History of Clays". *Canadian Geotechnical Journal,* 33(3), 488–498.

Chiasson, P., and Wang, Y. J. (2006). "Spatial variability of sensitive champlain sea clay and an application of stochastic slope stability analysis of a cut," *in Proceedings of the 2nd International Workshop on Characterisation and Engineering Properties of Natural Soils,* T. S. Tan et al., Eds., Singapore, pp. 2707–2720.

Dasaka, S. M. and Zhang, L. M. (2012). "Scale effect on bias in the estimation of spatial correlation characteristics of soil and rock". *In Proceedings of the 6th Asian Young Geotechnical Engineers Conference (AYGEC),* pp. 192-204.

DeGroot, D. J. (1996). "Analyzing spatial variability of insitu soil properties (invited paper). Uncertainty in the Geologic Environment, From Theory to Practice". *Proceeding of Uncertainty '96, Geotechnical Special Publication.* No. 58.

DeGroot, D. J., and Baecher, G. B. (1993). "Estimating autocovariance of insitu soil properties". *Journal of Geotechnical Engineering*, 119(1), 147-166.

Delhomme, J. P. (1978). "Kriging in the hydrosciences", *Advances in Water Resources*, 1(5), 251-266.

DNV-RP-C207. Recommended practice. (2010). "Statistical presentation of soil data".

Douglas, B. J. and Olsen, R. S. (1981). "Soil classification using electric cone penetrometer". *American Society of Civil Engineers, ASCE, Proceedings of Conference on Cone Penetration Testing and Experience*, (209–227). St. Louis, October 26–30.

Elkateb, T., Chalaturnyk, R. and Robertson, P. K. (2003a). "An overview of soil heterogeneity: quantification and implications on geotechnical field problems". *Canadian Geotechnical Journal,* 40, 1–15.

Elkateb, T., Chalaturnyk, R. and Robertson, P. K. (2003b). "Simplified geostatistical analysis of earthquake-induced ground response at the Wildlife Site, California, USA". *Canadian Geotechnical Journal*. 40, 16–35.

Eslami and B.H. Fellenius. (2004). "CPT and CPTU data for soil profile interpretation: Review of methods and a proposed new approach". *Iranian Journal of Science and Technology*, Transaction B, Vol. 28, No. B1 Printed in Islamic Republic of Iran, 2004.

Fenton, G. A. and Griffiths, D. V. (2008). "Risk assessment in geotechnical engineering". *John wiley and sons*, New York.

Fenton, G. (1999). "Random field modeling of CPT data". *Journal of Geotechnical and Geoenvironmental Engineering*. 125(6), 486–498.

Fenton G.A. and Vanmarcke E.H. (1990). "Simulation of random fields via Local Average Subdivision". *ASCE Journal of Engineering Mechanics*, 116(8),1733-1749.

Fraleigh, J. B., and Beauregard, R. A. (1990). "Linear Algebra". Addison-Wesley, USA.

Goldsworthy, J. S., Jaksa, M. B., Fenton, G. A., Kaggwa, W. S., Griffiths, D. V., and Poulos, H. G. (2007). "Effect of sample location on the reliability based design of pad foundations". *Georisk: Assessment and Management of Risk for Engineered Systems and Geohazards*, 1(3), 155-166.

Griffiths, D. V. and Fenton, G. A. (1993). "Seepage beneath water retaining structures founded on spatially random soil". *Geotechnique*, 43(4),577−587.

Hegazy, Y.A. and P.W. Mayne. (1995). "Statistical Correlations Between Vs and CPT Data for Different Soil Types". *Proc. Symp on Cone Penetration Testing*, Swedish Geotechnical Society, Linköping, Vol., II, pp. 173-178.

IBC. (2000). *International Building Code*, prepared by International Code Council.

Jaksa, M. B., Goldsworthy, J. S., Fenton, G. A., Kaggwa, W. S., Griffiths, D. V., Kuo, Y. L. and Poulos, H.G. (2005). "Towards reliable and effective site investigations". *Géotechnique*, 55(2), 109-121.

Janbu, N., and Senneset, K. (1974). "Effective stress interpretation of in situ static penetration test". *Proc.,European Symp. On Penetration Testing,* ESOPT, 181–193.

JCSS-Cl probabilistic model code (2006). Section 3.7: Soil Properties, Revised Version.

Jefferies, M.G., and Davies, M.P. (1993). "Use of CPTu to estimate equivalent SPT N_{60}". *Geotechnical Testing Journal*, 16(4), 458-467.

Jefferies, M. G. and Davies, M. P. (1991). "Soil classification using the cone penetration test: Discussion". *Canadian Geotechnical Journal, 28*(1), 173–176.

Jendrezejczuk, J.A and M.W. Wambs. (1987). "Surface Measurements of Shear Wave Velocity at the 7-GeV APS Site". *Argonne National Laboratory Report*, LS-129.

Jones, G. A. and Rust, E. (1982). "Piezometer penetration testing, CUPT". *Proceedings of the 2nd European Symposium on Penetration Testing,* ESOPT-2, 2, (607–614). Amsterdam, May 24–27.

Journel, A. G. and C. Huijbregts. (1978). "Mining Geostatistics". *Academic Press*, London, 600 p.

Kulhawy, F. H., Birgisson, B. and Grigoriu, M. D. (1992). "Reliability based foundation design for transmission line structures: Transformation models for in-situ tests". *Report EL-5507(4). Palo Alto*, CA: Electric Power Research Institute.

Krige, D. G. (1951). "A statistical approach to some basic mine valuation problems on Witwatersrand". *J. Chem. Metall. Mining Soc.* South Africa 52, No. 6, 119–139.

Liao, T and P.W. Mayne. (2006). "Automated Post-processing of Shear Wave Signals", *Proc. 8th US. Conf. on Erthq Engrg.*, San Francisco, California, USA.

Liu, S.Y., G.J. Cai., L.Y. Tong and G.Y. Du. (2008). "Approach on the Engineering Properties of Lianyungang Marine Clay from Piezocone Penetration Tests". *Marine Geo resource. and Geo. tech*, 26 (7), 189–210.

Lunne, T., Robertson, P.K. and Powell, J.J.M. (1997). "Cone Penetration Testing in Geotechnical Practice". Blackie Academic/Chapman and Hall, EandFN Spon, 312. pages, 3rd printing.

Mantoglou, A., and Wilson, J.L. (1982). "The Turning Bands Method for Simulation of Random Fields using Line Generation with a Spectral Method". *Water Resources Research*, 18(5), 1379-1394.

Marinoni, O. (2003). "Improving geological models using a combined ordinary–indicator kriging approach". *Engineering Geology*, (69). 37 – 45.

Matheron, G. (1973). "The intrinsic random functions and their applications," Advances in Applied Probability, 5(3), 439–468.

Mayne, P.W and G.J. Rix. (1995). "Correlations between Shear Wave Velocity and Cone Tip Resistance in Natural Clays". *Soils and Founds*, 35(2), 107-110.

Mayne, P.W and G.J. Rix. (1993). "G_{max}–q_c Relationships for Clays". *Geotech Testng J.* 16 (1), pp. 54–60.

Mayne, P.W. (2006). "The 2nd James K. Mitchell Lecture: Undisturbed Sand Strength from Seismic Cone Tests". *Geo. mechnc* and *Geo Engrg*., Taylor and Francis Group, London. Vol., I, No. 4.

Mayne, P.W and G. Campanella. (2005). "Versatile Site Characterization by Seismic Piezocone". *Proc. 16th Int. Conf. on Soil Mechnc. and Geo. tech Engrg*., Osaka, Japan, 2, pp. 721–724.

Moss, R., Seed, R., and Olsen, R. (2006). "Normalizing the CPT for Overburden Stress". *J. Geotech. Geoenviron. Eng,* 132(3),378–387.

Nadim, F. (1986). "Probabilistic site description strategy". *Report 51411–4*: Norwegian Geotechnical Institute. Oslo

Olea, R. A. (1991). "Geostatistical Glossary and Multilingual Dictionary". *Oxford Univ. Press*, New York.

Olsen, R. S. and Mitchell, J. K. (1995). "CPT stress normalization and prediction of soil classification". *Proceedings of International Symposium on Cone Penetration Testing*, *CPT95*, Linköping, 2, (257–262). Sweden, SGI Report 3:95.

O. Magnin and Bertrand Y. (2005). "Guide Seismique Refraction". *Laboratoire Centrale des ponts et chaussées*.

Phoon, K. K., Quek, S. T. and An, P. (2003). "Identification of statistically homogeneous soil layers using modified Bartlett statistics". *J. Geotech. Geoenviron. Engng*, 129(7), 649–659.

Rackwitz, R., Denver, H. and Calle, E. (2002). Rautman, C. A and M. V. Cromer. (1994). "Three- Dimensional Rock Characteristics Models Study Plan: Yucca Mountain Site Characterization Plan SP 8.3.1.4.3.2". *U.S. Department of Energy, Office of Civilian Radioactive Management*, Washington, DC.

Remesy , N. R. (2002). "A calibrated model for the interpretation of cone penetration tests (CPTs) in North Sea quaternary soils". *Proc SUT Conf*, London

Reyna, F. and Chameau, J. L. (1991). "Statistical evaluation of CPT and DMT measurements at the Heber Road Site". *Geotechnical Engineering Congress*, pp. 14–25. New York: American Society of Civil Engineers.

Rix G.J and K.H. Stoke. (1992). "Correlation of Initial Tangent Modulus and Cone Resistance". *Proc. of Int. Symp. On Calibration Chamber Testing*: 351-362.

Robertson, P. K. and Campanella, R. G. (1983). "Interpretation of cone penetrometer tests, Part I sand". *Canadian Geotechnical Journal,* 20(4), 718–733.

Robertson, P. K., Campanella, R. G., Gillespie, D. and Grieg, J. (1986). "Use of piezometer cone data". *Proceedings of American Society of Civil Engineers, ASCE, In-Situ 86 Specialty Conference*, (1263–1280). Edited by S. Clemence, Blacksburg, June 23–25, Geotechnical Special Publication GSP No. 6.

Robertson, P., Campanella, R., Gillespie, D., and Rice, A. (1986). "Seismic Cpt to Measure in Situ Shear Wave Velocity." J. Geotech. Engrg., 112(8), 791–803.

Robertson, P. K. (1990). "Soil classification using the cone penetration test". *Canadian Geotechnical Journal*, 27(1), 151–158.

Robertson, P. K., Fear C.E., Woeller D. J and Weemees I. (1995). "Estimation of sand compressibility from Seismic CPT". *Proc. 48th Canadian Geotechnical Conference*, Vancouver.

Robertson, P.K. and Wride, C.E. (1998). "Evaluating cyclic liquefaction potential using the cone penetration test". *Canadian Geotechnical Journal*. 35:442 – 459.

Rouhani, S. (1996). "Geostatistical estimation: Kriging, Geostatistics for environmental and geotechnical applications". ASTM STP 1283.

Ryti, R. (1993). "Superfund Soil Cleanup: Developing the Piazza Remedial Design". *Journal of Air and Waste Management*, Vol. 43, Febrauary 1993.

Schneider, J.A., Randolph, M.F., Mayne, P.W., Ramsey, N.R.. (2008). "Analysis of factors influencing soil classification using normalized piezocone tip resistance and pore pressure parameters". *Journal of Geotechnical and Geoenvironmental Engineering*, 134 (11), 1569–1586.

Tang, W. H. (1979). "Probabilistic evaluation of penetration resistances". *J. Geotech. Engng Div*., ASCE 105(10),1173–1191.

Uzielli, M., Vannucchi, G. and Phoon, K. K. (2005). "Random field characterisation of stress normalised cone penetration testing parameters". *Géotechnique*, 55(1), 3–20

Vahdatirad, M.J., Griffiths, D. V., Andersen, L.V., Sørensen, J.D. and Fenton, G. A. (2014). "Reliability Analysis of a Gravity Based Foundation for Wind Turbines: A Code-Based Design Assessment". *Géotechnique*, Inpress. DOI: 10.1680/geot./13-P-152.

Vanmarcke, E. H. (1984). Random Fields: Analysis and Synthesis, MIT Press, Cambridge, Massachusetts.

Vanmarcke, E. H. (1977). "Probabilistic Modeling of Soil Profiles". *Journal of Geotechnical Engineering*, ASCE. 103(11), 1227-1246.

Wild, M. and S. Rouhani. (1995). "Taking a Statistical Approach: Geostatistics Brings Logic to Environmental Sampling and Analysis". *Pollution Engineering*, February 1995.

Wroth, C.P. (1984). "The interpretation of in situ soil tests". *Geotechnique*, 34(4), 449-489.

Wu, T. H., Lee, I. M., Potter, J. C. and Kjekstad, O. (1987). "Uncertainties in evaluation of strength of marine sand". *J. Geotech. Engng,* 113(7), 719–738.

Zhang, J., Zhang, L. M., Tang, W. H. (2011)." Kriging numerical models for geotechnical reliability analysis". *Soils and Foundation*, 51(6), 1169-1177.

Zhang, Z., Tumay, M.T. (1996). "Simplification of soil classification charts derived from cone penetration test". *Geotechnical Testing Journal*, 19 (2), 203–216.

APPENDIX A: PAPER 1

CPTu-based geotechnical site assessment for offshore wind turbines—a case study from the Aarhus site in Denmark

IS CITED AS:

Firouzianbandpey, S., Ibsen, L. B., Andersen, L. V. (2012). "CPTu-based geotechnical site assessment for offshore wind turbines—a case study from the Aarhus site in Denmark." ***Proceedings of the Twenty-second International Offshore and Polar Engineering Conference***, Rhodes, Greece, pp. 151–158.

STATUS: Published

Corrigendum: CPTu-based geotechnical site assessment for offshore wind turbines—a case study from the Aarhus site in Denmark

Firouzianbandpey, S., Ibsen, L. B., Andersen, L. V.

Ref.: Proceedings of the Twenty-second International Offshore and Polar Engineering Conference, Rhodes, Greece, pp. 151–158 (2012).

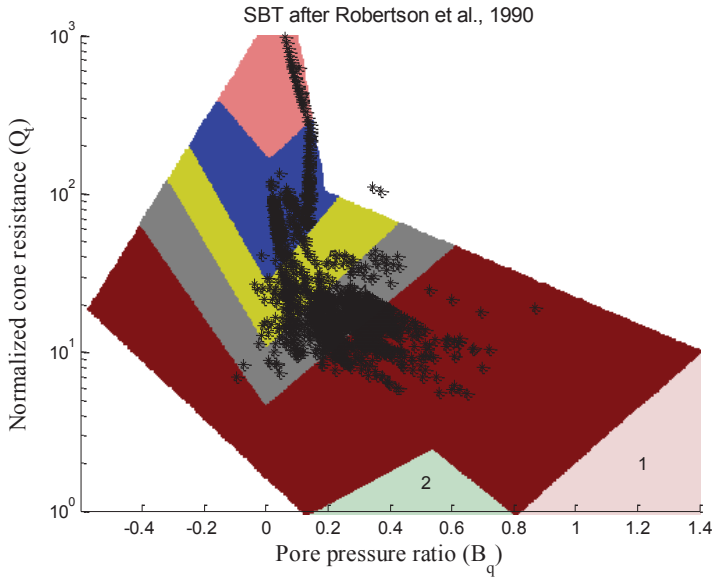

Figure 5. CPTu data plotted on the chart proposed by Robertson et al. (1990). The soil types corresponding to zones 1 to 7 are: 1. Sensitive, fine-grained soils; 2. Organic soils and peat; 3. Clays, clay to silty clay; 4. Silt mixtures, silty clay to clayey silt; 5. Sand mixtures, sandy silt to silty sand; 6. Sands, silty sand to clean sand; 7. Sand to gravelly sand;

Corrigendum: CPTu-based geotechnical site assessment for offshore wind turbines—a case study from the Aarhus site in Denmark

Proceedings of the Twenty-second (2012) International Offshore and Polar Engineering Conference
Rhodes, Greece, June 17–22, 2012

ISBN 978-1-880653-94–4 (Set); ISSN 1098-6189 (Set)

www.isope.org

CPTu-based Geotechnical Site Assessment for Offshore Wind Turbines—a Case Study from the Aarhus Site in Denmark

Sarah Firouzianbandpey, Lars Bo Ibsen, Lars Vabbersgaard Andersen
Department of Civil Engineering, Aalborg University
Aalborg, Denmark

ABSTRACT

Cone penetration testing (CPT) is a fast and reliable means of conducting site investigations. Different methods exist for soil profile interpretation from CPT data but their validity still needs to be verified. A wind farm site at Aarhus, where numerous CPTu tests have been conducted is considered. The raw cone penetration measurements are scrutinized for data connected with physical or mechanical errors, and these are removed. The corrected data then were used for classifying soil by several charts presented in the literature. The results are further compared and verified with laboratory classification of samples retrieved from boreholes.

KEY WORDS: Soil classification; piezocone penetration test; in situ testing; case study.

INTRODUCTION

Cone penetration test has been considered as an alternative to conventional laboratory testing due to its economical, continuously, simplicity, accuracy and efficiency features. CPT, with built-in pressure transducers for the purpose of pore water pressure measurements have been developed in addition to cone tip resistance (q_c) and sleeve friction (f_s) measuring abilities. In CPTu tests, pore pressure generated during penetration depends on the location of the pressure transducer (at the cone face, u_1, behind the base, u_2, or behind the sleeve, u_3). One of the most common applications of CPT is its utilization for soil stratigraphy and classification profiling. The results are used in evaluation of shear strength parameters of soils and deformation modulus in design of foundations and earth retaining structures.

Numerous classification charts have been proposed to estimate soil type using cone data (Begemann, 1965; Douglas and Olsen, 1981; Jones and Rust, 1982; Robertson et al., 1986; Robertson and Campanella, 1988; Robertson, 1990; Jefferies and Davis, 1991; Zhung and Tumay, (1996); Schneider et al., 2008; Cetin and Ozan, 2009). Begemann (1965) pioneered soil profiling from the CPT, showing that, while coarse grained soils generally demonstrate larger values of cone resistance (q_c) and sleeve friction (f_s) than do fine-grained soils, the soil type is not a strict function of either cone resistance or sleeve friction, but of a combination of these values. The Begemann chart was derived from tests in Dutch soil using a mechanical cone. Douglas and Olsen (1981) were the first to propose a soil profiling chart based on tests with an electrical cone penetrometer. Their chart also indicated trends for liquidity index and earth pressure coefficient, as well as sensitive soils and "metastable sands". The soil profiling chart by Jones and Rust (1982) is based on the piezocone using the measured total cone resistance and the measured excess pore water pressure mobilized during cone advancement. The chart is interesting because it also identifies the density (compactness condition) of coarse-grained soils and the consistency of fine-grained soils, but it has the deficiency of classifying soil in a different group due to increasing parameters like cone resistance and friction ratio with depth. Robertson et al. (1986) and Campanella and Robertson (1988) were the first to present a chart based on the piezocone with the cone resistance corrected for pore pressure at the shoulder [$q_t = q_c + u(1–a)$], where q_t is the cone resistance corrected for pore water pressure on shoulder, q_c is the measured cone resistance, u_2 is the pore pressure measured at cone shoulder, a is the ratio between shoulder area (cone base) unaffected by the pore water pressure to total shoulder area.

Robertson (1990) proposed a refinement of the Robertson et al. (1986) profiling chart considering overburden stress. The normalization was proposed to compensate for the cone resistance dependency on the overburden stress. In fact the effective stress at depth is a function of the weight of the soil and, to a greater degree, of the pore pressure distribution with depth (Eslami and Fellinius, 2004). Zhang and Tumay (1996) investigated the uncertainty results in overlaps of different soil types in currently used CPT classification systems. Their methodology is based on the statistical and fuzzy subset approaches and related to the uncertainties in identifying soil type and behaviour using the existing CPT soil engineering classifications. Eslami and Fellenius (2004) developed a soil profiling method based on data from boring, sampling, laboratory testing and routine soil characteristics of cases from 18 sources reporting data from 20 sites in 5 countries.

The Ramsey (2002) Model evolved during the 1990s for classifying soil using data from the corrected tip resistance (q_t) and penetration pore-water pressure at the shoulder (u_2). Ramsey's model has a simple criterion, which distinct it from the other methods. Whenever the charts

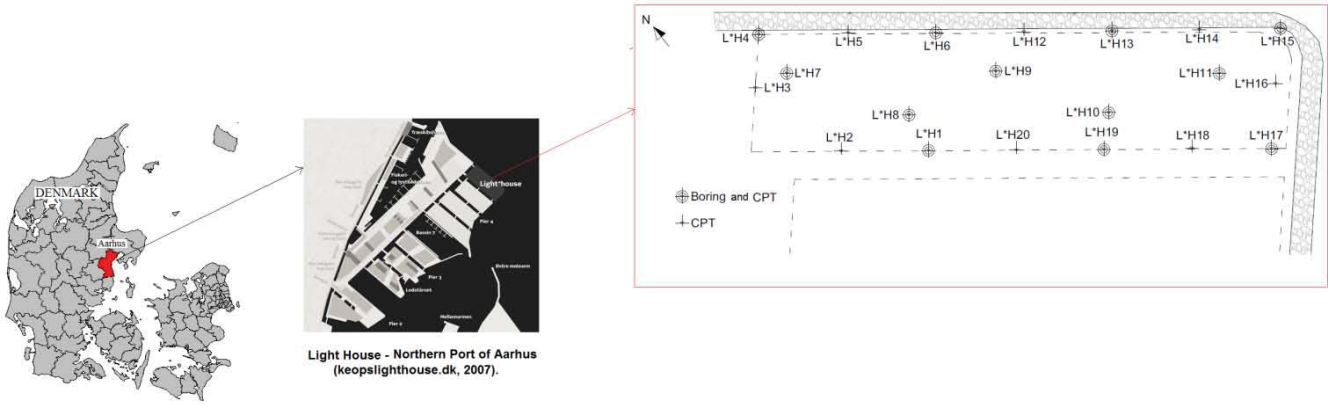

Fig. 1. Map of Aarhus and location of the site selected, borings and CPTs

predict different zones, then the zone with the lower numerical value should be chosen. This is because it is generally more conservative to interpret a soil with higher fines content (Ramsey, 2008). Using parametric studies of analytical solutions, field data, and judgment based on the previous discussions Schneider (2008) recommended soil classification charts based on normalized piezocone parameters. The method proposed three models that are exactly the same but have been plotted in different formats. The models describe soil also as essentially drained sand and transitional soils.

A cone penetration test (CPT) soil classification based on probabilistic methodology, considering the uncertainties intrinsic to the problem proposed by Cetin and Ozan (2009). Despite the probabilistic assessment of soil types using various methods, there are some limitation in their applicability as the index definitions are not clear enough to specify the soil type and parameters unambiguously. Also the boundaries between zones were extensively designated and the databases plenty and Adequacy used in soil charts development are not available. Due to all of these limitations and uncertainties in soil classifying just based on CPTu data, there is an effort in this study to do more investigation and discussion on different CPTu-based soil classification method abilities by verifying and validating with bore-holes and sampling to do a site-specific correlation in order to have a better assessment of the region soil type. These include methods by Robertson et al., (1986), Robertson (1990), Ramsey (2002), Eslami and Fellenius (2004) and Schneider (2008).

FIELD AND LABORATORY TESTS

The investigation was conducted in Arhus in Denmark. Piezocone penetration tests were conducted at 41 locations. Fig. 1 presents a map of Aarhus with approximate locations of the sites selected for this study. The ground water table depth at the test locations varied in the range 1.5–1.75 m. Drilling borings for soil samples were conducted close to the CPTu locations. The distance between CPTu and borehole locations has been shown in Fig. 1**.** A total of 41 CPTu soundings and 12 borings were performed at the site.

Cone penetration testing was conducted using a Memocone MKII Class 1 10 ton Digital Piezocone Penetrometer, and data was acquired using an ENVI data logger (Envi Logger C1 or CS1). The CPTu system consists of a hydraulic pushing and levelling system, 1 m length segmental rods, cone penetrometers and a data acquisition system.

The field tests were performed by Grontmij/Carl Bro and all laboratory tests were carried out at Aalborg University, Denmark. The whole project was done from 3 September 2007 to 21 January 2008.

Fig. 2. A sample of very fat clay from the region.

Cordless CPT system

The Memocone CPT probes and equipments consists of the following main items:

- Continuous Penetrometer, 20 ton maximum capacity;
- 10 cm^2 probe with a tip angle of 60° and 3 channels measuring point resistance, local friction and pore pressure (max. 50 MPa);
- inbuilt temperature compensation and tilt sensor;
- depth synchronization;
- data acquisition system and software;
- CPT-LOG software.

This equipment can be operated with the maximum depth of 40 m with penetration rate of 20 mm/s. The drilling equipment stationed on a jack-up platform was operated to advance the borehole to the required depth.

Laboratory tests

At depths of more than 12 m, high quality tube samples were taken for every 2 metres. ASTM standard tests for determining grain size distribution, moisture content, Atterberg limits and specific gravity are carried out on the samples. The results of laboratory tests conducted on soil samples collected at various locations are presented in Table 1. The

Table 1. Summary of laboratory properties of clays from investigated sites.

Sites	Water content (%)	Liquid limit (%)	Plasticity index (%)	pH
Borehole 07	30-48.6	97.7-109.3	103-213	8.9-9.5
Borehole 08	-	-	97-310	-
Borehole 10	31-52	98.5-107.4	90-280	8.6-9.5
Borehole 11	37.6-49.5	102-107	153.5-235	9-9.7

geological characteristic of the studied sites is generally characterized by very fat clay. In Fig. 2, a sample of the predominant soil type of the region, categorized as very fat clay, is illustrated.

ERROR FILTERING

Even though the cone penetration test is a standard method of assessing soil properties, errors due to measuring can still occur during the test. First of all, measurements with zero cone-tip resistance have been removed as zero cone resistance indicates a cavity in the soil, but this is very unlikely to happen in sand deposits. Two additional criteria for removing uncertain data are described in the following.

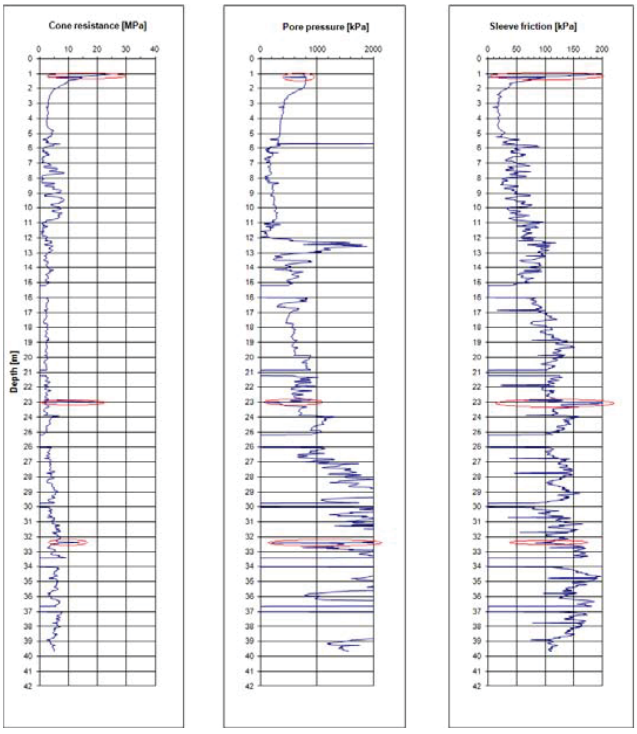

Fig. 3. Example of error filtering in borehole 08.

Errors due to local soil inhomogeneity

Several peaks and drops in the cone resistance as well as the pore pressure appeared during the cone penetration test. Especially, peaks can occur when the cone encounters a thin layer of stiff material such as lenses of stiff silt or sand or a small stone or rock within a deposit. The peaks are removed as they cause a considerable error in predicting the strength parameters of entire layer.

Errors due to halts

Most of the errors occurring in cone penetration tests are due to halts. These errors often appear as large drops in the cone resistance. The halts usually occur due to attachment of new rods, i.e. after penetration of each rod length. When the penetrometer is halted, the pressure on the cone and the sleeve is released. Cone penetration in sands will not occur completely drained, i.e. a small excess pore pressure is always measured. When the cone stops, this small pressure drains away and again builds up during the penetration. In this study, these peaks are removed as they are not representative of inherent soil properties.

Here measurements with considerable peaks are removed. This is basically based on engineering judgment, and is very important as this removal has effects on the classification results. In Fig. 3, an example of this error filtering is illustrated for borehole 08.

EVALUATION OF CPTU DATA FOR SOIL CLASSIFICATION

Different classification methods based on CPT and CPTu data proposed by Robertson et al. (1986), Robertson et al. (1990), Ramsey (2002), Eslami and Fellinus (2004), and Schneider (2008) were evaluated using data achieved from the region. Each of the methods uses different cone parameters like cone resistance, friction ratio, pore water pressure, overburden pressure, or a combination of these three parameters. Further, these methods are compared and verified with laboratory classification results from bore-holes for the purpose of comparison and representation of the most reliable chart for the soil type as a guidance for future investigations of the region soil with less number of bore-holes and a proper CPTu-based assessment.

Fig. 4 illustrates a CPTu profile based on corrected cone resistance, pore pressure ratio and friction ratio as a typical cone penetration test result achieved from the sounding in the region. The water table in different bore-holes is also varying from 1.5 to 1.75 m.

A code for determining the soil types and the related certainties has been made in Matlab. Each chart has been digitalized with a resolution of approximately 2000×2000 pixels. Every pixel in a chart is given a value corresponding to the zone to which is belongs according the classification method. For each data point, a “window” is defined with a number of pixels in each direction away from the central pixel corresponding to the measured data point. The number of pixels with a given zone number are counted and divided by the total number of pixels within the window to provide the certainty with which the soil can be identified as belonging to that zone. In this study, a window with 9×9 pixels is employed. Thus, if 34 pixels lie in zone 3 in a given soil classification chart, the certainty related to soil type 3 is 34/81. It should be noticed that a large window with several pixels in either direction will associate less certainty with the soil type related to the central point of the window. However, it may identify more potential candidates for the soil type. The size of the window is chosen in a heuristic manner.

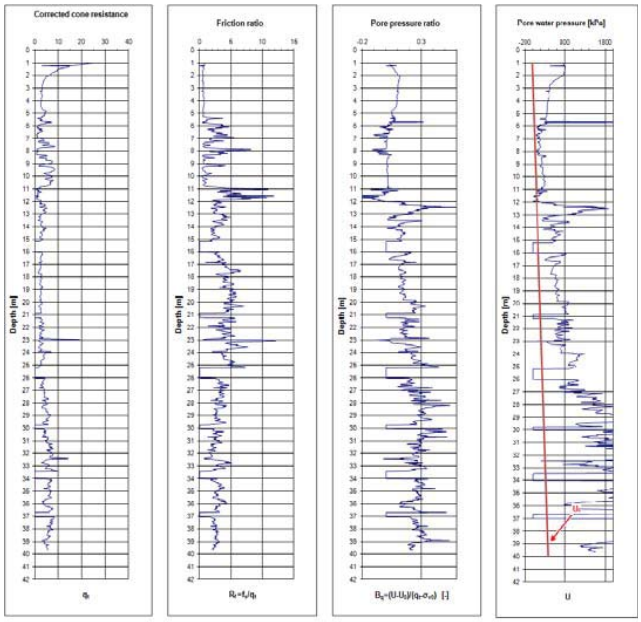

Fig. 4. A typical result of piezocone test at the selected site

Based on the certainties provided by the Matlab code, the soil types are plotted in terms of certainty versus depth. The diagram shows the value of certainty of the related zone within the classification chart for each prediction. When the certainty is 1, it means that the input data has been located somewhere within the chart far away from the boundaries of a given zone. Thus the possibility of being within another zone is zero or, in other words, the chart is completely sure that the input data is related to the zone number that has been predicted. But for certainties less than 1, the input data is close to the boundaries between two zones or more. Hence, the soil may be of another type. For each soil layer, the soil type with higher certainty according to a given classification method will be used to provide the final identification of the soil type for that method. For example, if the certainty of "Sand" in the method proposed by Robertson (1990) is 73%, then the soil is identified as "Sand" in this method. Applying the described methodology, every input data is plotted into the various diagrams and the certainty related to each soil type is determined. By plotting the values of the certainties versus depth, it is possible to compare the soil profiles provided by the CPT-based methods with each other and with the profile achieved from the bore-hole test using standard classification methods as described in the section about laboratory tests.

RESULTS AND DISCUSSIONS

Fig. 5 illustrates the chart proposed by Robertson et al. (1990) and digitalized as described above. To clarify the evaluation process, two kinds of input data with different certainties have been chosen. According to the figure data located in the middle of zone 3 is obviously far away from the boundaries and categorized as zone 3 with a certainty of 1.0, while the data points close to the boundaries between zones 4 and 5 have certainties less than 1.0 depending on their distance from the borders, measured in terms of number of pixels, and may instead be suspected of being categorized as belonging to the neighbouring zone.

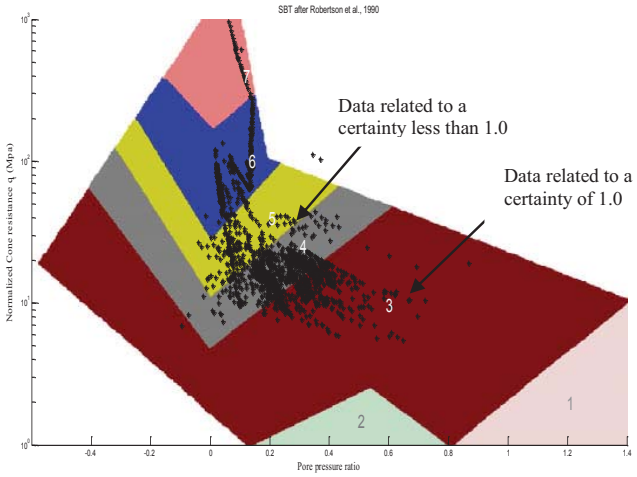

Fig. 5. CPTu data plotted on the chart proposed by Robertson et al. (1990). The soil types corresponding to zones 1 to 7 are: 1. Sensitive, fine-grained soils; 2. Organic soils and peat; 3. Clays, clay to silty clay; 4. Silt mixtures, silty clay to clayey silt; 5. Sand mixtures, sandy silt to silty sand; 6. Sands, silty sand to clean sand; 7. Sand to gravelly sand; 8. Very stiff fine-grained soil; 9. Very stiff, fine-grained, over-consolidated or cemented soil.

Fig. 6 shows an example of varying certainty versus depth for the Robertson-1990 method based on CPT data and penetration depth. Also one of the bore-hole logs has been presented to compare with the diagram for this method.

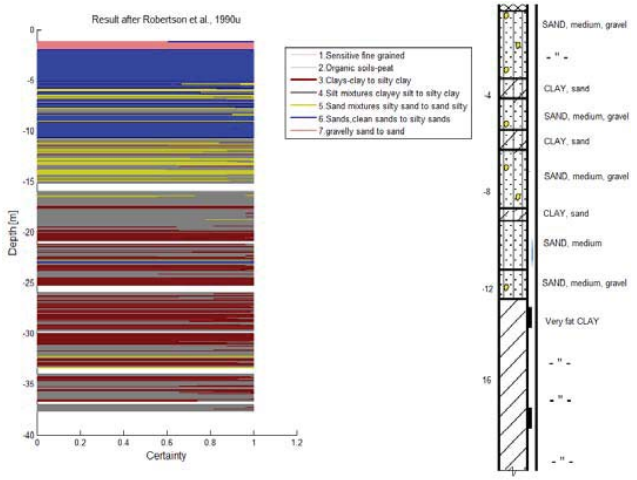

Fig. 6. Different values of certainties versus depth from Robertson et al. (1990) and soil profiling from borehole 07.

According to this method, the first soil layers to a depth of 5 m are classified as "Sands, clean sands to silty sand" and "Gravelly sand to sand" (zones 6 and 7, respectively, in the chart) with a high certainty. This prediction is in close agreement with the classification provided by the bore-hole test. Likewise, clayey soil is identified as the most probable deposit at greater depths, which is in correspondence with the classification made from the borehole.

Table 2: Comparison between different CPT-based classification methods and soil type determined from bore-hole tests at borehole 07.

depth	Soil Type	Method Robertson (1986) f			Method Robertson (1986) u			Method Robertson (1990) f			Method Robertson (1990) u		
		Zone	certainty	Soil Description	Zone	certainty	Soil Description	Zone	certainty	Soil Description	Zone	certainty	Soil Description
0.25-3.0	SAND, medium, gravell	Silty sand to sandy silt	0.32	Sand to silty Sand	Sandy silt to clayey silt	0.53	Sandy silt to clayey silt	Sand; silty sand to clean sand	0.63	Sand; silty sand to clean sand	Sand; silty sand to clean sand	0.60	Sand; silty sand to clean sand-Gravelly sand
		Sand to silty sand	0.38		Silty sand to sandy silt	0.22		Sand to gravelly sand	0.37		Sand to gravelly sand	0.40	
		Sand	0.30		Sand to silty sand	0.16							
					Sand	0.09							
3.0-3.75	CLAY, SAND	Silty sand to sandy silt	1.00	Silty sand to sandy silt	Clayey silt to silty clay	0.30	Sandy silt to clayey silt	Sand; silty sand to clean sand	1.00	Sand; silty sand to clean sand	Sand; silty sand to clean sand	1.00	Sand; silty sand to clean sand
					Sandy silt to clayey silt	0.70							
3.75-6.3	SAND, medium, gravell	Clay	0.02	Silty sand to sandy silt	Clayey silt to silty clay	0.35	Sandy silt to clayey silt	Clays-clay to silty clay	0.06	Sand; silty sand to clean sand	Sand mixtures; sandy silt to silty sand	0.20	Sand; silty sand to clean sand - Sand mixtures
		Silty clay to clay	0.09		Sandy silt to clayey silt	0.44		Silt mixtures; clayey silt to silty clay	0.12		Sand; silty sand to clean sand	0.79	
		Clayey silt to silty clay	0.05		Silty sand to sandy silt	0.20		Sand mixtures; sandy silt to silty	0.18				
		Sandy silt to clayey silt	0.09					Sand; silty sand to clean sand	0.65				
		Silty sand to sandy silt	0.59										
		Sand to silty sand	0.14										
6.3-6.7	SAND,clay	Clay	0.10	Clayey silt to silty clay	Clayey silt to silty clay	0.43	Sandy silt to clayey silt	Clays-clay to silty clay	0.19	Silt and Sand mixtures	Sand mixtures; sandy silt to silty sand	0.65	Sand mixtures; sandy silt to silty sand
		Silty clay to clay	0.14		Sandy silt to clayey silt	0.50		Silt mixtures; clayey silt to silty clay	0.46		Sand; silty sand to clean sand	0.35	
		Clayey silt to silty clay	0.35		Silty sand to sandy silt	0.08		Sand mixtures; sandy silt to silty	0.35				
		Sandy silt to clayey silt	0.41										
6.7-8.2	SAND, medium, gravell	Clay	0.24	Clay, Sand to silty sand	Silty clay to clay	0.08	Clayey silt to silty clay- Sand	Clays-clay to silty clay	0.35	Clays-clay to silty clay- Sand mixtures	Silt mixtures; clayey silt to silty clay	0.24	Sand; silty sand to clean sand-Sand and silt mixtures
		Silty clay to clay	0.12		Clayey silt to silty clay	0.33		Silt mixtures; clayey silt to silty clay	0.19		Sand mixtures; sandy silt to silty sand	0.30	
		Clayey silt to silty clay	0.14		Sandy silt to clayey silt	0.17		Sand mixtures; sandy silt to silty	0.25		Sand; silty sand to clean sand	0.47	
		Sandy silt to clayey silt	0.15		Silty sand to sandy silt	0.20		Sand; silty sand to clean sand	0.22				
		Silty sand to sandy silt	0.15		Sand to silty sand	0.21							
		Sand to silty sand	0.20										
8.2-10.3	SAND, CLAY	Clay	0.04	Silty clay to Clay	Silty clay to clay	0.06	Sand to silty sand	Clays-clay to silty clay	0.09	Sand; silty sand to clean sand	Silt mixtures; clayey silt to silty clay	0.06	Sand; silty sand to clean sand
		Silty clay to clay	0.04		Sandy silt to clayey silt	0.13		Silt mixtures; clayey silt to silty clay	0.07		Sand mixtures; sandy silt to silty sand	0.11	
					Silty sand to sandy silt	0.27		Sand mixtures; sandy silt to silty sand	0.25		Sand; silty sand to clean sand	0.83	
					Sand to silty sand	0.55		Sand; silty sand to clean sand	0.60				
10.3-10.8	SAND	Silty sand to sandy silt	0.10	Sand to silty Sand	Silty sand to sandy silt	0.13	Sand to silty sand	Sand mixtures; sandy silt to silty sand	0.26	Sand; silty sand to clean sand	Sand mixtures; sandy silt to silty sand	0.03	Sand; silty sand to clean sand
		Sand to silty sand	0.90		Sand to silty sand	0.87		Sand; silty sand to clean sand	0.74		Sand; silty sand to clean sand	0.97	
10.8-11.125	SAND, medium, gravell	Clay	0.31	Clay, Silty clay to clay	Clayey silt to silty clay	0.23	Sandy silt to clayey silt	Clays-clay to silty clay	0.62	Clays-clay to silty clay- Silt mixtures	Silt mixtures; clayey silt to silty clay	0.31	Sand mixtures; sandy silt to silty sand
		Silty clay to clay	0.22		Sandy silt to clayey silt	0.69		Silt mixtures; clayey silt to silty clay	0.31		Sand mixtures; sandy silt to silty sand	0.67	
		Clayey silt to silty clay	0.31		Silty sand to sandy silt	0.08		Sand mixtures; sandy silt to silty sand	0.08				
		Sandy silt to clayey silt	0.08										
		Silty sand to sandy silt	0.08										
11.25-40	very fat CLAY	Clay	0.19	Clayey silt, Clay	Silty clay to clay	0.16	Clayey silt to silty clay	Clays-clay to silty clay	0.65	Clays-clay to silty clay- Silt mixtures	Clays-clay to silty clay	0.35	Silt mixtures; Clay to silty clay
		Silty clay to clay	0.14		Clayey silt to silty clay	0.72		Silt mixtures; clayey silt to silty clay	0.32		Silt mixtures; clayey silt to silty clay	0.56	
		Clayey silt to silty clay	0.27		Sandy silt to clayey silt	0.09					Sand mixtures; sandy silt to silty sand	0.08	
		Sandy silt to clayey silt	0.31										
		Silty sand to sandy silt	0.09										

Table 2–continued: Comparison between different CPT-based classification methods and soil type determined from bore-hole tests at borehole 07.

depth	Soil Type	Method Ramsey (2002) f			Method Ramsey (2002) u			Method Eslami (2004)			Method Schneider (2008)		
		Zone	certainty	Soil Description	Zone	certainty	Soil Description	Zone	certainty	Soil Description	Zone	certainty	Soil Description
0.25-3.0	SAND, medium, gravell	clean to slightly silty SAND/GRAVEL	1.00	clean to slightly silty SAND/GRAVEL	CLAY(su/po>1) clayey SAND	0.90 0.10	CLAY(su/po>1)	Sandy SILT SAND	0.53 0.47	DAND and Sandy SILT	-	0.00	-
3.0-3.75	CLAY, SAND	silty SAND clean to slightly silty SAND/GRAVEL	0.80 0.20	silty SAND	CLAY(su/po>1)	1.00	CLAY(su/po>1)	Sandy SILT	1.00	Sandy SILT	-	0.00	-
3.75-6.3	SAND, medium, gravell	CLAY(su/po>1) clayey SAND silty SAND clean to slightly silty SAND/GRAVEL	0.21 0.07 0.68 0.04	silty SAND	CLAY(su/po>1) clayey SAND	0.96 0.02	CLAY(su/po>1)	CLAY SILT Silty CLAY Silty SAND Sandy SILT	0.12 0.08 0.03 0.75	Sandy SILT	Silts and Low Ir Clays Transitional soils	0.96 0.04	Silts and Low Ir Clays
6.3-6.7	SAND,clay	CLAY(su/po<=1) CLAY(su/po>1)	0.04 0.96	CLAY(su/po>1)	CLAY(su/po>1)	1.00	CLAY(su/po>1)	CLAY SILT Silty CLAY Silty SAND	0.33 0.49 0.18	Silty CLAY	Silts and Low Ir Clays Transitional soils	0.89 0.11	Silts and Low Ir Clays
6.7-8.2	SAND, medium, gravell	CLAY(su/po<=1) CLAY(su/po>1) clayey SAND silty SAND clean to slightly silty SAND/GRAVEL	0.20 0.41 0.14 0.19 0.05	CLAY - silty SAND	CLAY(su/po<=1) CLAY(su/po>1) clayey SAND silty SAND clean to slightly silty SAND/GRAVEL	0.03 0.54 0.17 0.11 0.13	CLAY(su/po>1) - clayey SAND	CLAY SILT Silty CLAY Silty SAND Sandy SILT SAND	0.40 0.17 0.18 0.15 0.11	CLAY SILT - Silty SAND	Silts and Low Ir Clays Transitional soils	0.32 0.68	Transitional soils
8.2-10.3	SAND, CLAY	CLAY(su/po<=1) CLAY(su/po>1) clayey SAND sandy SILT silty SAND	0.05 0.12 0.08 0.02 0.73	silty SAND- Clay	CLAY(su/po<=1) CLAY(su/po>1) clayey SAND silty SAND clean to slightly silty SAND/GRAVEL	0.05 0.21 0.40 0.21 0.14	clayey SAND- silty SAND	CLAY SILT Silty CLAY Silty SAND Sandy SILT SAND	0.06 0.09 0.29 0.23 0.33	SAND -Silty SAND	Silts and Low Ir Clays Transitional soils	0.15 0.85	Transitional soils
10.3-10.8	SAND	clayey SAND silty SAND	0.04 0.95	silty SAND	CLAY(su/po>1) clayey SAND silty SAND clean to slightly silty SAND/GRAVEL	0.07 0.61 0.28 0.03	clayey SAND	Silty SAND Sandy SILT SAND	0.43 0.23 0.34	Silty SAND	Transitional soils	0.99	Transitional soils
10.8-11.125	SAND, medium, gravell	CLAY(su/po<=1) CLAY(su/po>1) clayey SAND	0.23 0.70 0.08	CLAY(su/po>1)	CLAY(su/po>1) sandy very clayey SILT	0.88 0.10	CLAY(su/po>1)	CLAY SILT Silty CLAY Silty SAND Sandy SILT	0.31 0.54 0.11 0.04	Silty CLAY	Silts and Low Ir Clays Transitional soils	0.55 0.30	Silts and Low Ir Clays
11.25-40	very fat CLAY	CLAY(su/po<=1) CLAY(su/po>1)	0.34 0.63	CLAY	CLAY(su/po<=1) CLAY(su/po>1)	0.26 0.72	CLAY(su/po>1)	CLAY SILT Silty CLAY Silty SAND	0.19 0.66 0.14	Silty CLAY	Silts and Low Ir Clays CLAYS Transitional soils	0.40 0.55 0.04	Silts and Low Ir Clays

This way of interpretation can be applied to the other CPT-based classification methods as well. In Table 2, the soil types and the corresponding certainties for each method are presented for borehole 07. The soil description for each method is provided in the table, and based on the certainties, the soil type is identified.

In Table 2, "Method Robertson 1986 (f)" is the proposed chart based on the friction ratio and the cone resistance, while "Method Robertson 1986 (u)" is based on the pore pressure ratio and the cone resistance. This means that the first chart does not take the pore pressure ratio into account. This is similar in the other proposed methods which present two types of charts, thus considering the pore pressure ratio as well as the friction ratio. In this context, the methods proposed by Eslami (2004) and Schneider (2008) are different, since they only consider the sleeve friction and the pore pressure ratio, respectively.

The soil descriptions in the different methods are not exactly the same. In some methods, the soil type is fully described, e.g. as "Silty sand to sandy silt" in Robertson (1986), while in other methods the soil type is determined in brevity, e.g. as "Transitional soils" in Schneider (2008). Further, soil type descriptions as either "CLAY ($S_u/P_0>1$)" or "CLAY ($S_u/P_0\leq1$)" in the method suggested by Ramsey (2002) describe the degree of consolidation in clayey soils in terms of undrained shear strength and initial overburden pressure ratio.

SUMMARY AND CONCLUSION

There have been lots of efforts on the development of in-situ techniques to classify soils and predicting the important engineering parameters such as strength and stiffness properties. Even if there are different methods to classify soil just based on CPTu data, but their validity still needs to be verified for a better prediction since the original soils used in the charts development are quite different from a local soil. So a site-specific correlation using boring and sampling should be performed in order to a more reliable site assessment. In this paper, a site in the harbour of Aarhus in Denmark, where wind turbines are installed, has been considered. Here 41 CPTu tests and five bore-hole tests have been carried out, and different CPT-based classification methods by Robertson et al. (1986), Robertson et al. (1990), Ramsey (2002), Eslami (2004) and Schneider (2008) have been considered for the purpose of interpretation and comparison of soil types of the region.

The results showed that most of CPT classification methods, in general, are reliable for classifying the soil with an acceptable accuracy. Nevertheless some of methods are more confident with high certainties in some particular soil types and others are less confident. It means that different methods have different capabilities in identifying correctly various soil types. This is possibly due to the differences in the development processes behind the charts, i.e. the various CPT-based classification charts rely on different background data.

Using these comparisons between different methods and verifications of CPTu-based soil classifications by bore-holes, there will be a guidance for classification of the region soil with less bore-holes and samples that would be more efficient in time and cost.

Also the results show, some of the methods are unexpectedly unreliable regarding the prediction of soil types. For instance Ramsey (2002) considering pore water pressure is quite incompatible with the other methods, and Schneider (2008) is not agreeing well with borehole classification in gravels and sands. This is especially surprising, since the methods are relatively new and consider the pore pressure ratio as an effective parameter instead of the friction ratio.

As a final conclusion it can be summarized that the Robertson 1990 (u) method has the most compliance with the classification based on borehole tests in sand and gravelly layers, while the Ramsey (2002) models are more reliable in clayey layers in this specific region.

With the limited amount of data available in the present analysis, a general conclusion cannot be made regarding the model uncertainties related to each of the CPT-based soil classification methods. Future research will be carried out on the basis of further cone-penetration tests performed along the Danish coast line.

ACKNOWLEDGEMENTS

The authors kindly acknowledge the financial support from the Danish Council for Strategic Research within the programme "Reliability-based analysis applied for reduction of cost of energy for offshore wind turbines".

REFERENCES

Begemann, H. K. S., (1965). The friction jacket cone as an aid in determining the soil profile. *Proceedings of the 6th International Conference on Soil Mechanics and Foundation Engineering,* ICSMFE, 2, (17–20). Montreal.

Cetin, K.O., Ozan, C., 2009. CPT-based probabilistic soil characterization and classification. *Journal of Geotechnical and Geoenvironmental Engineering* 135 (1), 84–107.

Chen, B.S.Y. and Mayne, P.W. (1996). Statistical Relationships between Piezocone Measurements and Stress History of Clays. *Canadian Geotechnical Journal,* Vol. 33, No. 3, pp. 488–498.

Douglas, B. J. & Olsen, R. S., (1981). Soil classification using electric cone penetrometer. *American Society of Civil Engineers, ASCE, Proceedings of Conference on Cone Penetration Testing and Experience*, (209–227). St. Louis, October 26–30.

Eslami and B.H. Fellenius., (2004). CPT and CPTU data for soil profile interpretation: Review of methods and a proposed new approach. *Iranian Journal of Science & Technology*, Transaction B, Vol. 28, No. B1 Printed in Islamic Republic of Iran, 2004.

Janbu, N., and Senneset, K. (1974). Effective stress interpretation of in situ static penetration test. *Proc.,European Symp. On Penetration Testing,* ESOPT, 181–193.

Jefferies, M. G. & Davies, M. P., (1991). Soil classification using the cone penetration test: Discussion. *Canadian Geotechnical Journal, 28*(1), 173–176.

Jefferies, M.G., and Davies, M.P. (1993). Use of CPTu to estimate equivalent SPT N_{60}. *Geotechnical Testing Journal*, 16(4): 458-467.

Jones, G. A. & Rust, E., (1982). Piezometer penetration testing, CUPT. *Proceedings of the 2nd European Symposium on Penetration Testing,* ESOPT-2, 2, (607–614). Amsterdam, May 24–27.

Lunne, T., Robertson, P.K. and Powell, J.J.M., (1997). *Cone Penetration Testing in Geotechnical Practice.* Blackie Academic/Chapman & Hall, E&FN Spon, 312. pages, 3rd printing.

Olsen, R. S. & Mitchell, J. K., (1995). CPT stress normalization and prediction of soil classification. *Proceedings of International Symposium on Cone Penetration Testing*, *CPT95*, Linköping, 2, (257–262). Sweden, SGI Report 3:95.

Remesy , N. R., (2002). A calibrated model for the interpretation of cone penetration tests (CPTs) in North Sea quaternary soils. *Proc SUT Conf*, London

Robertson, P. K. & Campanella, R. G., (1983). Interpretation of cone penetrometer tests, Part I sand. *Canadian Geotechnical Journal*,

20(4), 718–733.
Robertson, P. K., Campanella, R. G., Gillespie, D. & Grieg, J., (1986). Use of piezometer cone data. *Proceedings of American Society of Civil Engineers, ASCE, In-Situ 86 Specialty Conference*, (1263–1280). Edited by S. Clemence, Blacksburg, June 23–25, Geotechnical Special Publication GSP No. 6.
Robertson, P. K., (1990). Soil classification using the cone penetration test. *Canadian Geotechnical Journal*, 27(1), 151–158.
Schneider, J.A., Randolph, M.F., Mayne, P.W., Ramsey, N.R.,(2008). Analysis of factors influencing soil classification using normalized piezocone tip resistance and pore pressure parameters. *Journal of Geotechnical and Geoenvironmental Engineering*, 134 (11), 1569–1586.
Zhang, Z., Tumay, M.T., (1996). Simplification of soil classification charts derived from cone penetration test. *Geotechnical Testing Journal*, 19 (2), 203–216.

APPENDIX B: PAPER 2

Geotechnical site assessment by seismic piezocone test in north of Denmark

IS CITED AS:

Firouzianbandpey, S., Nielsen, B. N., Andersen, L. V., Ibsen, L. B. (2013). "Geotechnical site assessment by seismic piezocone test in north of Denmark." ***Proceedings of 7th International Conference on Case Stories in Geotechnical Engineering: and Symposium in Honor of Clyde Baker***, ed. / Prakash, S., Missouri University of Science and Technology, Paper No. 2.34.

STATUS: Published

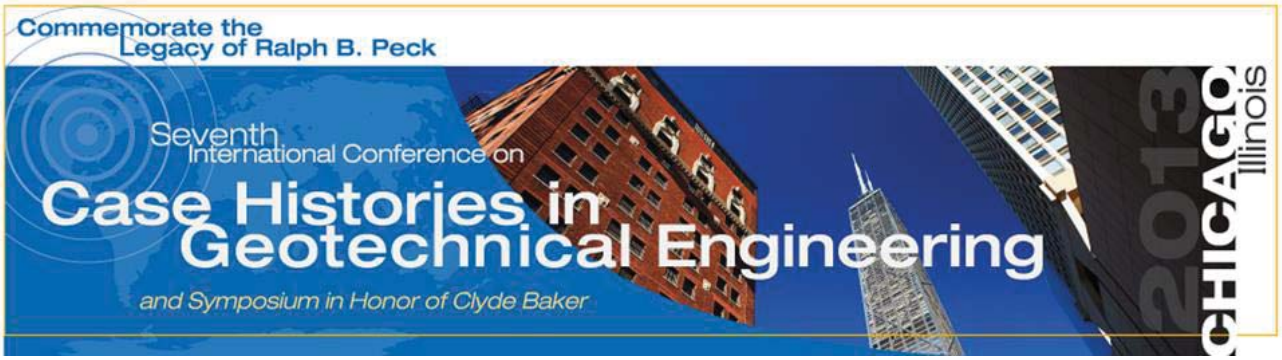

Corrigendum: Geotechnical site assessment by seismic piezocone test in north of Denmark

Firouzianbandpey, S., Nielsen, B. N., Andersen, L. V., Ibsen, L. B.

Ref.: Proceedings of 7th International Conference on Case Stories in Geotechnical Engineering: and Symposium in Honor of Clyde Baker, ed. / Prakash, S., Missouri University of Science and Technology, Paper No. 2.34. (2013).

Figure 2 is modified to:

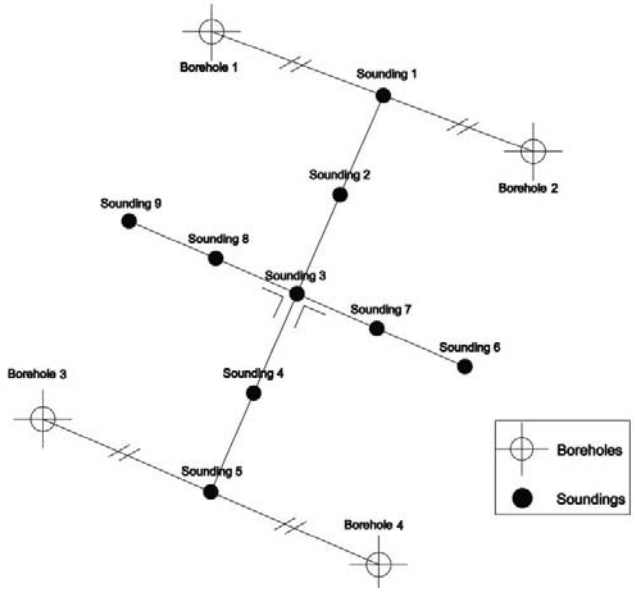

Figure 2 Position of boreholes and SCPTu (Sandy site)

Figure 3 is modified to:

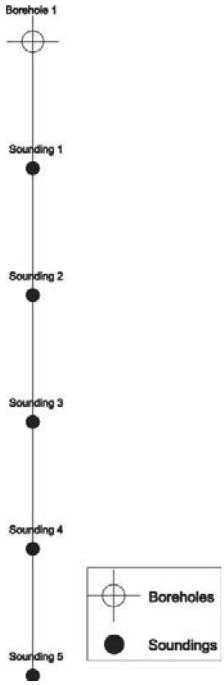

Figure 3 View of the field test area (Clayey site)

The Caption of Figure 4 is changed to:

Figure 4 (a): Sand (Borehole 1) – CPT 3

Figure 4 (b): Clay (Borehole 1) – CPT 5

Table 1. Water content results for sand

Borehole 100 is changed to Borehole 1

Borehole 200 is changed to Borehole 2

Table 2. Specific gravity of soil (Sand)

Sample No.	Borehole No.	Sample depth (m)	Specific gravity of soil solid, Gs, [-]	*Density*, ρ (kg / m^3) from laboratory tests on samples
9	1	3.8	2.66	1853
14	1	6.3	2.65	1675
25	3	3.2	2.65	2042
34	3	7.8	2.66	2047

Table 3. Water content results for clay

Sample No.	Borehole No.	Sample depth (m)	Water content (%)
22	1	7.4	34-36
13	1	4.4	36-37

Commemorate the Legacy of Ralph B. Peck
April 29 - May 4, 2013 CHICAGO
Seventh International Conference on
Case Histories in Geotechnical Engineering
and Symposium in Honor of Clyde Baker

GEOTECHNICAL SITE ASSESSMENT BY SEISMIC PIEZOCONE TEST IN NORTH OF DENMARK

Sarah Firouzianbandpey
Dept. of Civil Engineering, Aalborg University
9000 Aalborg, Denmark

B.N. Nielsen, L.V. Andersen, L.B. Ibsen
Dept. of Civil Engineering, Aalborg University
9000 Aalborg, Denmark

ABSTRACT

These days cone penetration tests (CPT) have gained more popularity as an alternative to the conventional laboratory tests for subsurface investigation and estimation of soil parameters. Due to increasing interest in soil dynamics in the last decades, there is a development of CPT as a seismic piezocone penetration test (SCPTU) which provides shear wave velocity measurements simultaneously with measurements of tip resistance (q_c), sleeve friction (f_s) and pore pressure (u). The results can be used for determination of deformation parameters of soil. In this regard there have been proposed different empirical correlations between cone data and shear wave velocity measurements to estimate geotechnical parameters but their validity still needs to be verified in a case study and uncertainty remains about the choice of empirical correlations. In this study a site at the East Harbor of Aalborg (sandy site) and another at the Harbor of Frederikshavn (clayey site) in Denmark, where several SCPTU tests have been conducted, are considered. The data were used and analyzed based on different correlations presented in the literature. The results are further compared and verified with the measurements of shear wave velocity achieved from SCPTU tests.

Key Words: Seismic cone penetration test, Shear wave velocity, Small strain shear modulus, Denmark.

INTRODUCTION

To obtain a proper design in the ultimate limit state as well as the serviceability limit state, various properties of the soil underneath a wind turbine must be known including the strength of the soil and the deformation properties of large and small strain magnitudes. Recently, focus has been on assessment of dynamic properties as well. The seismic piezocone penetration test (SCPTu), which provides multipoint simultaneous measurement of tip resistance (q_t), sleeve friction (f_s), pore pressure (u_2), and shear wave velocity (V_s), appears to be a reliable tool in estimation of geotechnical parameters (Lunne et al., 1997; Mayne and Campanella, 2005; Liu et al., 2008; Cai et al., 2009). During the test, a geophone integrated in a cone measures the waves generated by a shock between a hammer and a steel plate on the ground surface as a down-hole test. When the polarized shear wave is generated, the time is measured for the shear wave to travel a known distance to the geophone in the borehole.

Determination of shear wave velocity (V_s) can be crucial in obtaining information regarding the soil properties. V_s is used in geotechnical seismic design methods (e.g., IBC 2000 code), in soil liquefaction evaluations (e.g. Andrus and Stokoe, 2000), as well as in deriving the small-strain shear modulus ($G_{max} = \rho V^2$). In the absence of direct measure of shear wave velocity, correlations have been developed between shear wave velocity and several commonly measured geotechnical properties (cone resistance and sleeve friction); however, uncertainty remains about the choice of empirical correlations to determine the constrained modulus, small strain shear modulus and other deformation parameters (Cai, 2010).

The current study will present a description of performed SCPTu and shear wave types in north of Denmark as a case study along with two different methods of finding S-wave velocities in order to analyze and compare with the values obtained from empirical correlations.

FIELD TEST

Two sites located in Alborg in the north of Denmark are assessed: one with sandy soil and one with clayey soil (Fig. 1). The tests performed in sand are located in the east of Aalborg, an industrial part of the city. A wind turbine blade deposit will be constructed in this area. The clayey site is in the center of Aalborg, next to the main train station and bus terminal.

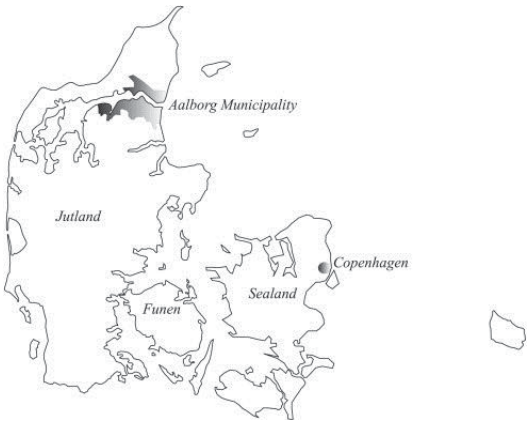

Fig. 1. View of the field test area.

The sandy site is situated a few meters from the Limfjord which means it is a basin deposit area. The upper four meters top layer is a marine deposit of clay/gyttia, while the lower layers are mostly silty sand. The SCPTu tests were performed to approx. 8 meters depth.

Nine soundings are executed in a cross-shaped position on a line separated by a distance of ten meters and four bore-holes have been located in the corners (Fig. 2).

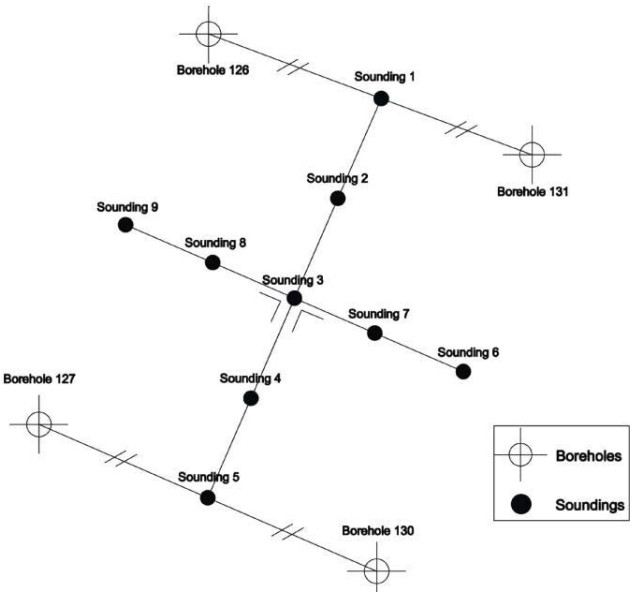

Fig. 2. Position of Boreholes and SCPTu (Sandy site).

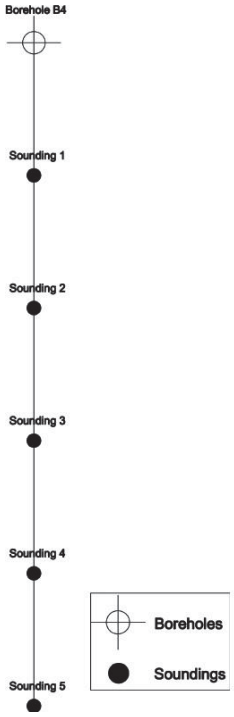

Fig. 3. View of the field test area (Clayey site).

In the clayey site, five SCPTu where executed with a top layer of 2-3 meters sand and the rest as clay. Soundings are aligned by a distance of five meters and one bore-hole as the same distance from the first sounding. The profile is illustrated in Fig. 3.

Description of the cone

The used Geotech SCPT equipment consists of the following main items:

- A conical tip;
- A 10 cm^2 probe with a tip angle of 60°;
- 7 channels measuring point resistance (q_c), local sleeve friction f_s, pore pressure u, tilt, temperature, electric conductivity, seismic, uniaxial for shear wave measurements.
- Depth synchronization;
- Data acquisition system and software;
- Data interpretation, CPT-LOG software.

The friction sleeve is placed above the conical tip and has a standard dimension of 150 cm^2. A pore pressure transducer is installed to measure the pore pressure during the penetration. The cone is pushed into the soil at a standard speed of 20 mm/s. the acoustic transmitter is located just above the CPT probe in 480 mm length and 36 mm diameter. The power supply is 4 LR14 1.5 V Alkalin batteries. The measured values of piezocone data and the results of the bore hole tests are given in Fig. 4 which u_0 is initial pore water pressure.

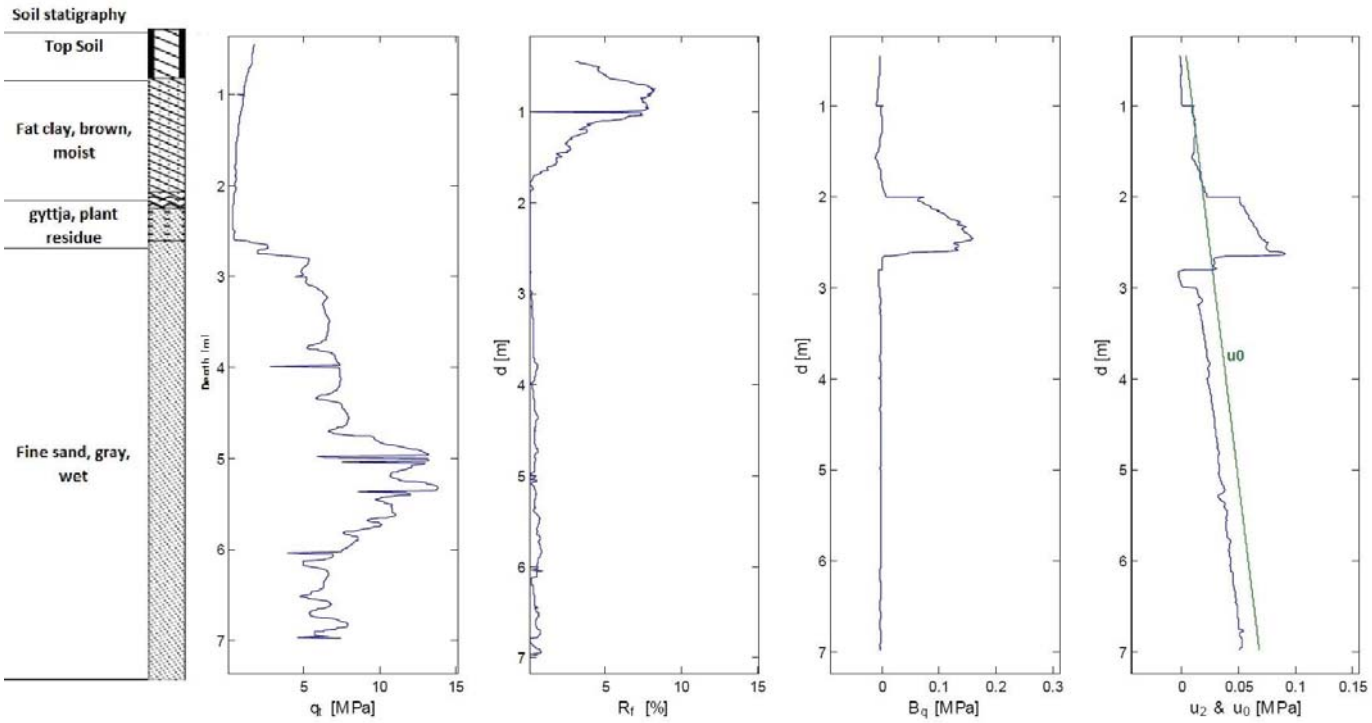

(a) Sand (Bore-hole 09)

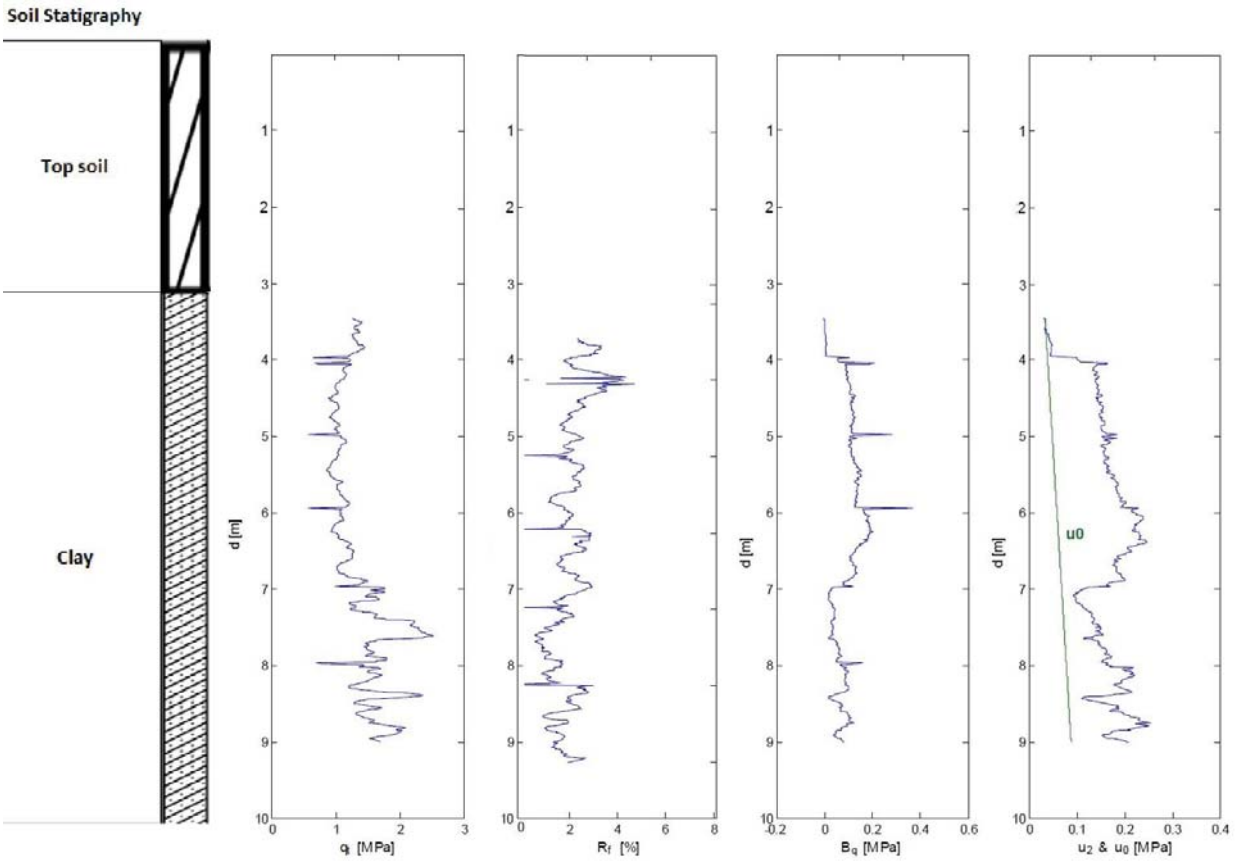

(b) Clay

Fig. 4. Borehole profile and CPTu results from field test (Bore-hole 01) .

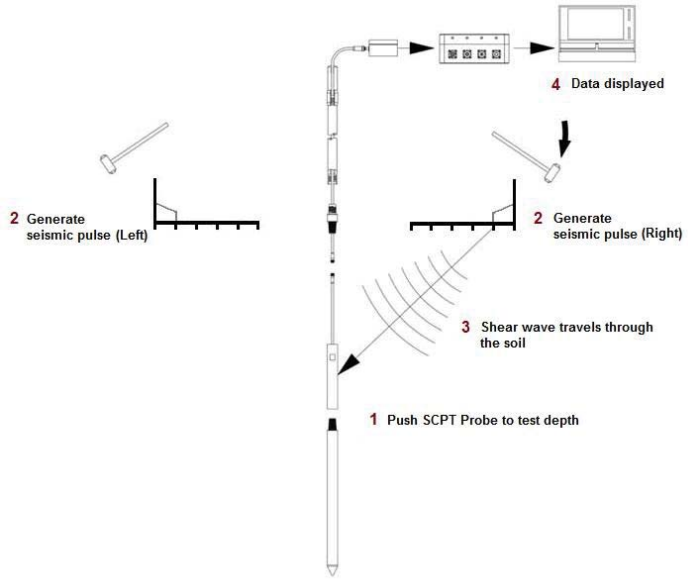

Fig. 5. Layout of source-trigger receiver.

Test setup

For the S-waves generation, two plates on both sides of the sounding hole are placed considering that the left and the right part of the S wave testing are aligned and a sledge hammer was blown on them, respectively (Fig 5). The sledge hammer and one of the plates can be seen in Fig. 6. These plates are "L" shaped and the bottom of the plates should be equipped with transversal teeth to improve the contact with the ground. The distance between the place where the hammer hits and the sounding hole is 1.4 meters (Fig. 7).

Fig. 6. L plate and sledge hammer for S waves generation.

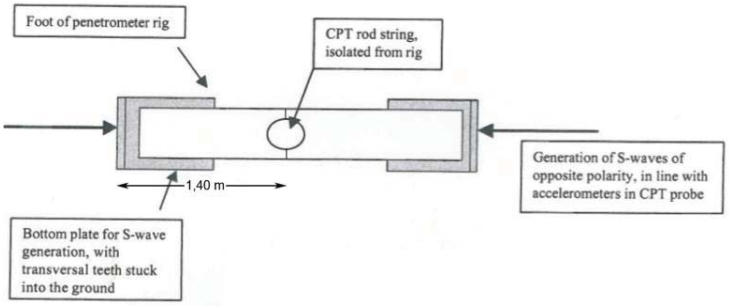

Fig. 7. SCPT field set up, (Geotech 2004).

The seismic part of the test is performed every each meter. When the rod string reaches to the desire depth, the engine of the penetrometer or drill rig is stopped. This is done to give the possibility to realize the SCPT test which is noise sensitive. The shear velocity can be easily checked on site, for quality assessment. As soon as the seismic part is finished the CPT can continue.

LABORATORY TESTS

Sand. From boreholes seen in Fig. 4a, soil samples were taken in order to perform soil classification tests. The laboratory testing program included basic soil characterization tests such as grain size distribution, hydrometer tests, relative density and water content. Results from laboratory tests as water content and particle density can be observed in Table 1 and 2, respectively.

Table 1. Water content results for sand

	Layer	Water content (%)
Borehole 100	Topsoil - clay	23-38
	Gyttia	46-62
	Fine sand	17-27
Borehole 200	Topsoil - clay	26-55
	Gyttia	54-56
	Fine sand	20-24

Using water content (w), Specific gravity of soil solid (G_s) and water level surface at depth 0.3, the soil considers saturated and density of soil can be calculated. Final values from laboratory tests are given in Table 2.

Table 2. Specific gravity of soils results (Sand)

Sample No.	Specific gravity of soil solid, Gs, [-]	*Density*, ρ (kg / m^3)
9	2.66	1853
14	2.65	1675
25	2.65	2042
34	2.66	2047

Clay. As for the sandy site, two samples from the borehole have been taken in the clay site in order to perform common laboratory tests. The results are given in table 3 and 4.

Table 3. Water content results for clay

Sample No.	Water content (%)
22	34-36
13	36-37

Table 4. Specific gravity of soils results (Clay)

Sample No.	Specific gravity of soil solid, Gs, [-]	*Density*, ρ (kg/m^3)
22	2.69	1853
13	2.72	1890

SHEAR WAVE VELOCITY

There are many empirical correlations proposed by different authors that relate the shear wave velocity to SCPT/CPT results. Based on sleeve friction and cone resistance, for all type of soils Equation (1), (Mayne, 2006) and Equation (2), (Hegazy and Mayne, 1995) can be used:

$$v_s(m/s) = 118.8(m/s)\log_{10}\left(\frac{f_s}{1Mpa}\right) + 18.5(m/s) \quad (1)$$

$$v_s(m/s) = [(10.1\log_{10}(q_t/1kPa) - 11.4]^{1.67}\left[100\frac{f_s}{q_t}\right]^{0.3} \quad (2)$$

Shear wave velocity (v_s) is measured in meters per second and tip resistance (q_t) are measured in kPa.

In the correlation proposed by Mayne (2006), if the values of sleeve friction and cone resistance are too low, taking logarithm results in negative values in shear wave velocity which is not rational. So in a case study, consideration should be taken when using this correlation as no limitation has been considered in developing the correlation for such condition.

Based on studies on Po River Sands and Gioia Taura Sands, Baldi et al., (1986) proposed Equation (3) for shear wave velocity from CPT data for clean quartz sands ,

$$v_s(m/s) = 277(q_t/1MPa)^{0.13}(\sigma'_{v0}/1MPa)^{0.27} \quad (3)$$

Shear wave velocity (v_s) is measured in meters per second and tip resistance (q_t) and effective overburden stress (σ'_{v0}) are measured in MPa.

Based on tests on intact and fissured samples from 31 different clay sites, Mayne and Rix (1995) proposed Equation (4) for soft to stiff, intact and fissured clays,

$$v_s(m/s) = 1.75(q_t/1kPa)^{0.627} \quad (4)$$

where q_t is in (kPa).

SHEAR MODULUS

In projects dealing with analyzing and designing wind turbine foundations, information about G_{max} as a key parameter in performing dynamic analysis of foundation response is essential. This is very important since traditional CPT leads to properties that are relevant for the ULS (Ultimate Limit State), but usually wind turbines fail in the FLS (Fatigue Limit State) and this means that small strain parameters for the soil are more important than large-deformation properties including the shear strength.

Shear modulus obtained from SCPT

The low strain shear modulus, G_{max}, can be found using the geotechnical method of Seismic Cone Penetration Test. Elastic theory relates the shear modulus, soil density (ρ) and the shear wave velocity as

$$G_{max} = \rho V_s^2 \quad (5)$$

The shear strain amplitude in seismic test is usually low which allow finding the very low strain level of dynamic shear modulus, G_{max}.

To obtain the shear modulus a seismometer is placed in the horizontal direction and orientated transverse to the signal source to detect the different components of the shear wave (horizontal and transversal). The ideal seismic signal source should generate a large amplitude shear wave with little or no compressional wave component. The signal can be generated by a hammer hitting a plate.

To obtain the measurements a rugged velocity seismometer has been incorporated into the cone penetrometer. It is placed in the horizontal direction and oriented transverse to the signal source to detect the horizontal component of the shear wave arrivals.

Shear modulus obtained from CPT

The value of small-strain shear modulus, G_{max} applies strictly to the nondestructive range of strains where shear strain $\gamma<10^{-4}$ (Cai, 2010). Different correlations for determining G_{max} have been proposed based on cone resistance for a large variety of soils, either granular (Baldi et al., 1989) or cohesive (Mayne and Rix, 1993) or both soils (Hegazy and Mayne, 1995). Based on calibration chamber results and field

measurements, Rix and Stokoe (1992) proposed a correlation for cohesionless soils as Equation (6) (T. Lunne, 1997).

$$\frac{G_0}{q_c} = 1634\left(\frac{q_c}{\sqrt{\sigma'_{v0}}}\right)^{-0.75} \quad (6)$$

where
G_0: Small strain shear modulud in kPa
q_c : Cone resistance in kPa
σ'_{v0} : Effective overburden stress in kpa

The major disadvantage of all these correlations is that G_{max} is a parameter determined at very small shear strain levels whereas q_t is a quantity measured at large deformations involving yielding and failure of the soil surrounding the cone. However, Mayne and Rix (1993) showed that the small strain shear modulus varied with in situ void ratio (e_0) and cone penetration resistance (q_t) for a wide range of clays and can be expressed as (Cai, 2010):

$$G_0 = 99.5(P_a)^{0.305}\frac{(q_t)^{0.695}}{(e_0)^{1.130}} \quad (7)$$

P_a : Atmospheric reference pressure in the same units as G_0 and q_t.
e_0 : In-situ void ratio

CORECTION OF MEASURED DATA FOR THE CPT

Considering to this fact that the cone penetration test is always accompanied by several errors due to halts, soil irregularities (thin layers of stiff materials and etc.), then there is a need for these measurements to be corrected. Also the cone resistance and the sleeve friction need to be corrected in order to account for the specific cone design, which influences how the pore water pressure alters the measurements. This is in particular important in the soft normally consolidated or low consolidated soil where the pore pressure behind the cone may be large. The cone resistance and the sleeve friction are corrected using Equation 8 and 9 respectively (T. Lunne, 1997):

$$q_t = q_c + u_2(1-a) \quad (8)$$

$$f_t = f_s - \frac{(u_2 A_{sb} - u_3 A_{st})}{A_s} \quad (9)$$

where
q_t: Corrected cone resistance in MPa
a: Cone area ratio [$a = \frac{A_n}{A_c}$] which A_n and A_c are cross section area of the shaft and the cone respectively.
u_2: Pore pressure behind the cone
f_t: Corrected sleeve friction
A_{sb}: Cross section area of sleeve bottom
A_{st}: Cross section area of sleeve top
A_{sb}: Friction sleeve surface area

SCPT ANALYSIS

Two different interpretation methods were used to determine the shear velocity, Vs, from SCPTu data as follows:

Cross-Correlation

Cross-correlation refers to the correlation of two independent series, and can be used to measure the degree to which the two series are related (Liao and Mayne, 2006). The cross-correlation function of x(t) and y(t) for a time shift 's' is defined as Equation (10) which x(t) and y(t) are two continuous signals with respect to time 't'.

$$z(s) = \int_{-\infty}^{\infty} x(t)y(t+s)dt \quad (10)$$

These series are measured at acoustic transmitter located just behind the sleeve friction in 48 cm length. For two signals of the same shape, the cross-correlation function may be used to calculate their difference in their arrival times, which is equal to the time shift that results in the peak of the cross-correlation function (Liao and Mayne, 2006).

Reverse Polarity

Interpolation of the shear wave velocity from SCPTu data consists of dividing an increment shear wave travel time into an increment of travel path. The test procedure involves generating shear waves with reverse polarity, by impacting opposite sources, for example two ends of a steel beam, (left and right). Subsequent processing and analysis are then applied on recorded acceleration time traces for each impact. Actually, in analyzing the data, the true shear waves should reverse polarity, as the most important identifying characteristic (Jendrezejczuk, 1987). In some surveys, the shear waves are readily obvious and identifying is not so difficult while in others, there may be numerous other arrivals and noise signals that make identification difficult; hence the need for a clear reversal signature may arise.

It has been found that the reverse polarity of the source greatly facilitates the identification of the S-wave and the time for the first cross-over point (shear wave changes sign) is easily identified from the polarized waves (forward and reverse) and provides the most repeatable reference arrival time, (Campanella, 1987). An example, using the traces is given in Fig. 9.

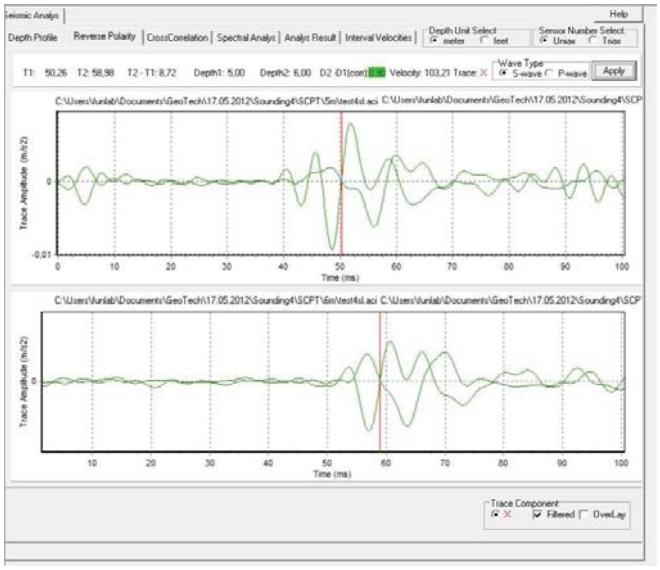

Fig. 9. Seismic analysis using reverse polarity, (Geotech, 2004).

INTERPRETATION OF RESULTS

Shear wave velocity

For a better understanding and comparison of the value ranges, all the results calculated from the empirical methods to estimate shear velocity have been plotted together with the shear velocities obtained from seismic CPT. Figure 10 illustrates these values for both clayey and sandy sites. estimate shear velocity have been plotted together with the shear velocities obtained from seismic CPT. Figure 10 illustrates these values for both clayey and sandy sites.

For sand, SCPTu results from reverse polarity and cross-correlation are in the same range of values. Both methods have negative shear velocities, which are in the first meters of sounding and doesn't seem reasonable and fit well with values obtained from empirical methods. These irrational values are results of not considering the deposition layout of different soil layers in calculation of shear wave velocities. When the shear wave passes through one layer, the values of velocity is equal to the distance divided by the travel time of the wave. But if during the passage, the wave encounters to a change in the layer, due to the change in the density of the media the direction of the wave will be diverted. It means that traveled distance varies and the mentioned formula is not true. This is the main reason of errors in shear wave velocity calculations in the soil. One way is decreasing in the interval between pals but there is a limitation for this as most general errors identified in cone penetration tests are registered due to halts. So a good knowledge about soil type and condition of layers in the deposit could help in better understanding and interpretation of results.

By increasing the depth in all profiles, the results from analysis using both of reverse polarity and cross-correlation methods give reasonable values which are in the range but the cross-correlation method gives conservative values compare to the reveres polarity.

The values obtained from correlation proposed by Mayne (2006) second layer is negative which is not reasonable. This is due to the small values of sleeve friction in this layer which results in the negative values according to Equation (1) after taking the logarithm. It means that this correlation cannot be used for this region because there is no limited range for shear wave velocity in this formula for soils with low sleeve friction.

Also for clay site, cross-correlation results are compatible to the results obtained from the reverse polarization and the field test. The range between the two methods is similar going from 0 to 200 m/s which are in the range.

Shear Modulus

Using equation (6) and (7), shear modulus for coarse and fine grained soils are obtained and compared to values from SCPTu field data as seen in (Fig. 11).

In sands, by increasing the depth, the difference between values obtained from two different analysis increased. For both sand and clays, the values from empirical correlations are over estimated.

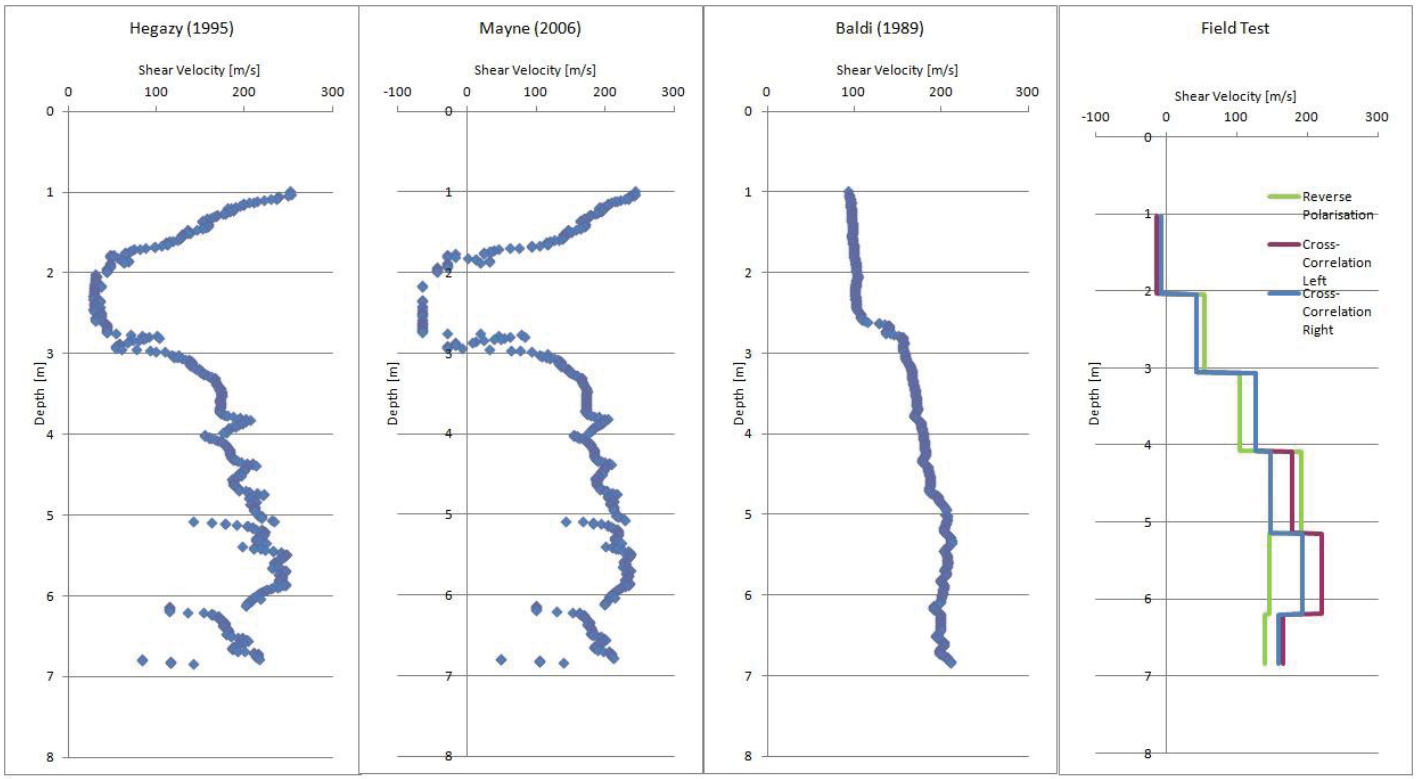

(a) Sand

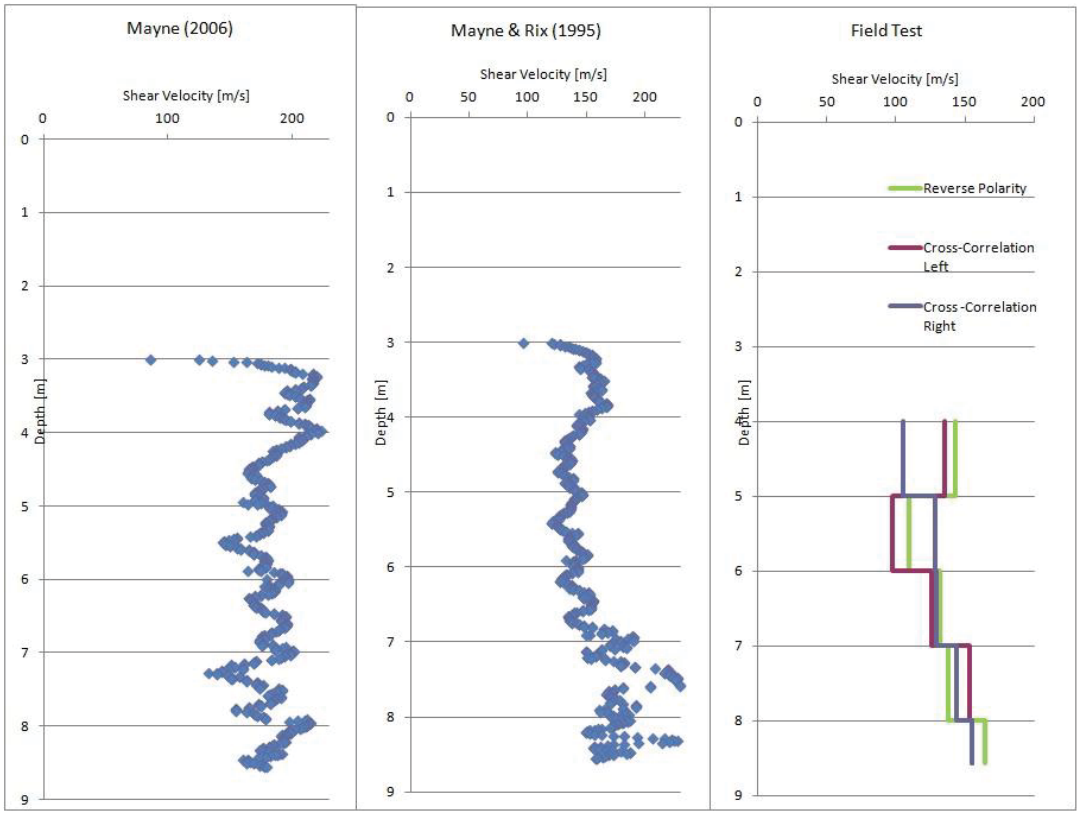

(b) Clay

Fig. 10. Shear velocities obtained from empirical methods and field test results.

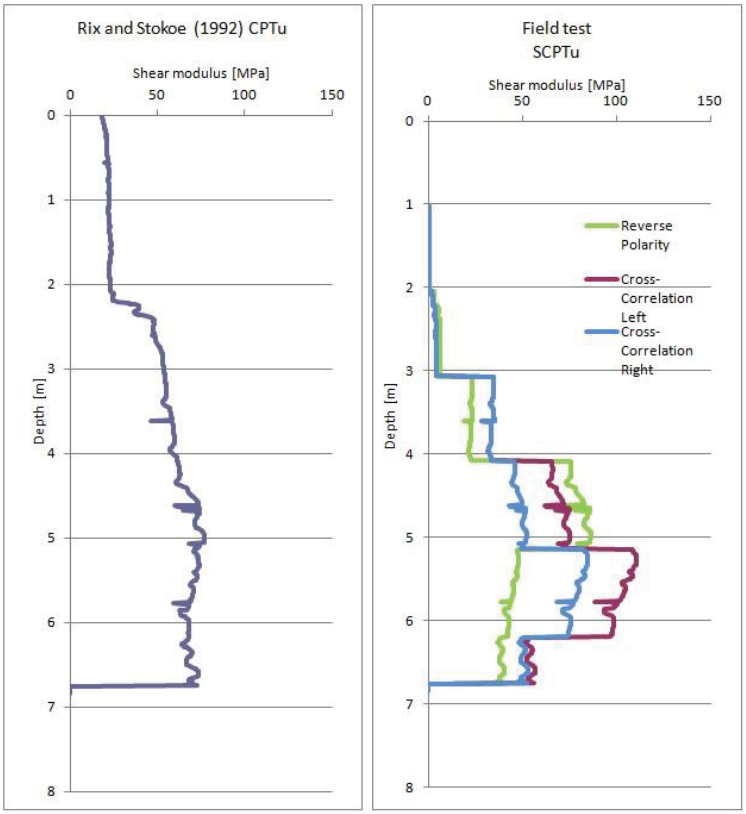

(a) Sand

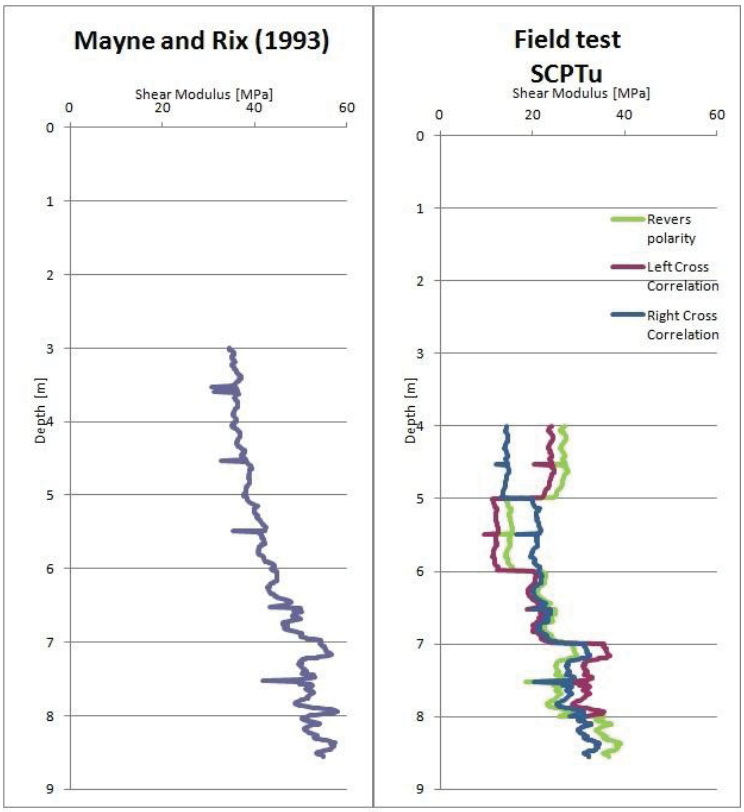

(b) Clay

Fig. 11. Shear modulus results obtained from empirical methods and field data.

CONCLUSION

There are different correlation methods reported to predict shear modulus from CPTu data, but their validity still needs to be verified for a local case as the original soils used in the empirical formula development are different from other region soils. This justifies the need for a case study in large projects and site-specific correlations should be developed based on field tests.

The SCPTu is concluded to be time and cost efficient and to provide reliable results, regarding the fact that is the first time performed in Denmark.

Based on different correlations between shear wave velocity and shear modulus from cone data two sites, one with mostly clayey soil and the other with mostly sand in the north of Denmark have been considered as a case study. Several seismic cone penetration tests were performed and values of shear velocity and cone data were recorded. Also common laboratory tests have been carried out on intact samples taken from boreholes to achieve soil density and void ratio of the region soil. Two methods of analyzing the signal traces of seismic data was chosen as "Reverse polarity" and "Cross-correlation".

In this study, correction of the measured CPTu data has been applied according to Equation (8) and (9), thus no error filtering due to halts on data was performed.

Actually the field test results of SCPTu and CPTu estimations for shear velocities from empirical correlation are in the same range, as it can be seen in Figure 10. Also the values are in the range for shear velocities in clays and sands.

Comparing the shear velocities calculated based on empirical correlations from CPTu data to the SCPTu field test results, it can be stated the empirical methods are over estimated. Also calculations based on correlation proposed by Mayne (2006) results in negative values for shear wave velocities which is not reasonable due to small values of sleeve friction. So this correlation doesn't seem to predict well the values of shear wave velocity from cone data for this region.

Due to a very agglomerate area as the center of the city, different errors could appear in the results of shear velocity in clay site. These errors can be generated by the construction site situated next to the testing site or the presence of the main bus terminal and train station. The works from the site along with the passing of the trains, buses and cars produce mild vibrations that could reach the cone, which is very sensitive on interference. In addition, another cause for possible errors in the results could be the appearance of the site. The SCPTu were performed on pavement stones and asphalt. The asphalt in comparison with normal soil, or even the pavement stones, absorbs the energy, which causes a poor signal for the waves, therefore errors in the results.

REFRENCES

Andrus, R.D and K.H. Stokoe [2000]. "Liquefaction Resistance of Soils Based on Shear Wave Velocity", in *Geo tech. and Geo envir . Engrg*, ASCE, 126 (11), pp. 1015-1026.

Baldi, G., R. Bellotti, V.N. Ghionna, M. Jamiolkowski, and D.C.F. LoPresti. [1989]. "Modulus of Sands from CPTs and DMTs". *Proc. 12th Int. Conf. on Soil Mechan. & Found. Engrg*., Rio de Janeiro, Balkema, Rotterdam, Vol. I, pp. 165-170.

Cai, G.J., S.Y. Liu., L.Y. Tong and G.Y. Du. [2009]. "Assessment of Direct CPT and CPTU Methods for Predicting the Ultimate Bearing Capacity of Single Piles". *Engrg Geology.,* 104 (1), pp. 211–222.

Cai, G.J., S.Y. Liu and L.Y. Tong. [2010]. "Field Evaluation of Deformation Characteristics of a Lacustrine Clay Deposit Using Seismic Piezocone Tests", *Engrg Geology.*, No. 116, pp. 251–260.

Campanella, R.G., P.K. Robertson., D. Gillespie., N. Laing and P.J. Kurfurst. [1987]. "Seismic cone penetration testing in the near offshore of the MacKenzie Delta". *Can. Geotech. J*. 24. pp. 154-159.

Hegazy, Y.A. and P.W. Mayne. [1995]. "Statistical Correlations Between Vs and CPT Data for Different Soil Types". *Proc. Symp on Cone Penetration Testing*, Swedish Geotechnical Society, Linköping, Vol., II, pp. 173-178.

IBC. [2000]. *International Building Code*, prepared by International Code Council.

Jendrezejczuk, J.A and M.W. Wambs. [1987]. "Surface Measurements of Shear Wave Velocity at the 7-GeV APS Site". *Argonne National Laboratory Report*, LS-129.

Liao, T and P.W. Mayne. [2006]. "Automated Post-processing of Shear Wave Signals", *Proc. 8th US. Conf. on Erthq Engrg.*, San Francisco, California, USA.

Liu, S.Y., G.J. Cai., L.Y. Tong and G.Y. Du [2008]. "Approach on the Engineering Properties of Lianyungang Marine Clay from Piezocone Penetration Tests". *Marine Geo resource. and Geo. tech*, 26 (7), pp. 189–210.

Lunne, T., P.K. Robertson and J.J.M. Powell. [1997]. "Cone Penetration Testing in Geotechnical Practice". *Blackie Academic/Chapman & Hall*, E&FN Spon, 312. pages, 3rd printing.

Mayne, P.W and G.J. Rix. [1993]. "G_{max}–q_c Relationships for Clays". *Geotech Testng J.* 16 (1), pp. 54–60.

Mayne, P.W and G.J. Rix. [1995]. "Correlations between

Shear Wave Velocity and Cone Tip Resistance in Natural Clays". *Soils and Founds*, 35 (2), pp. 107-110.

Mayne, P.W and G. Campanella. [2005]. "Versatile Site Characterization by Seismic Piezocone". *Proc. 16th Int. Conf. on Soil Mechnc. & Geo. tech Engrg*., Osaka, Japan, 2, pp. 721–724.

Mayne, P.W. [2006]. "The 2nd James K. Mitchell Lecture: Undisturbed Sand Strength from Seismic Cone Tests". *Geo. mechnc & Geo Engrg*., Taylor & Francis Group, London. Vol., I, No. 4.

O. Magnin and Bertrand Y. [2005]. "Guide Seismique Refraction". *Laboratoire Centrale des ponts et chaussées*.

Rix G.J and K.H. Stoke. [1992]. "Correlation of Initial Tangent Modulus and Cone Resistance". *Proc. of Int. Symp. On Calibration Chamber Testing*: 351-362.

APPENDIX C: PAPER 3

Estimation of soil type behavior based on shear wave velocity and normalized cone data in the north of Denmark

IS CITED AS:

Firouzianbandpey, S., Ibsen, L. B., Andersen, L. V. (2014). "Estimation of soil type behavior based on shear wave velocity and normalized cone data in the north of Denmark." ***Proceedings of 3rd International Symposium on Cone Penetration Testing***, Las Vegas, Nevada, USA, pp. 621–628.

STATUS: Published

3rd International Symposium on Cone Penetration Testing :: May 12-14, 2014 - Las Vegas, Nevada

Corrigendum: Estimation of soil type behavior based on shear wave velocity and normalized cone data in the north of Denmark

Firouzianbandpey, S., Ibsen, L. B., Andersen, L. V.

Ref.: Proceedings of 3rd International Symposium on Cone Penetration Testing, Las Vegas, Nevada, USA, pp. 621–628 (2014).

Figure 1 is modified to:

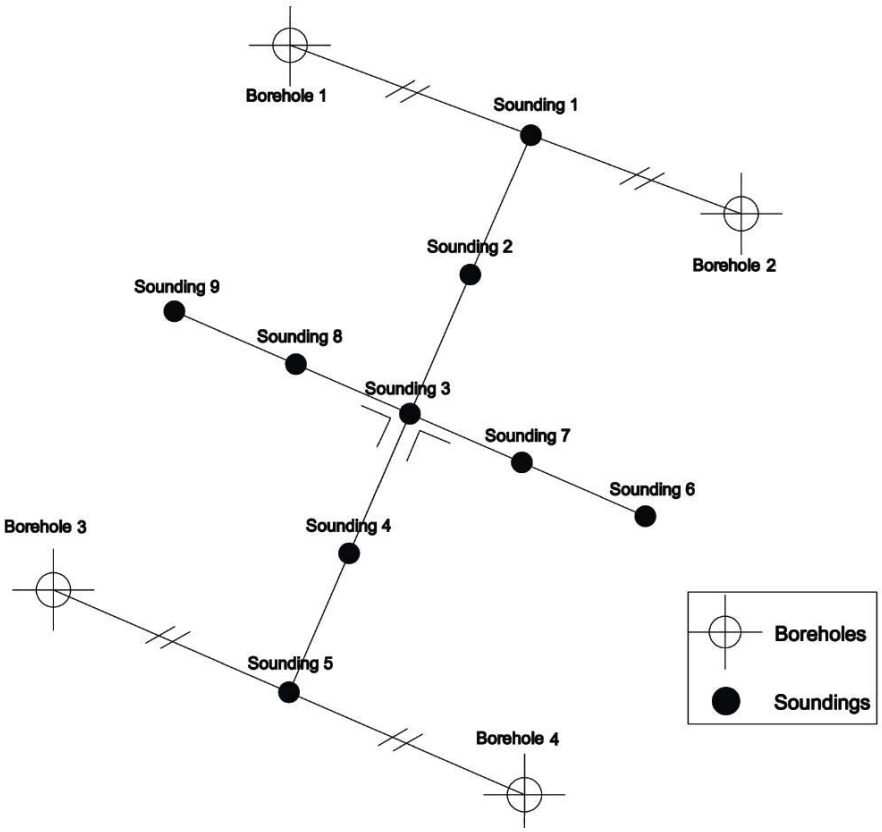

Figure. 1. Position of boreholes and soundings

The caption of Figure 2 is changed to:

Figure 2: Boreholes profile and CPTu results from field test: Borehole 1– CPT 3

Table 1:

Borehole 100 is changed to Borehole 1

Borehole 200 is changed to Borehole 2

Table 2: Specific gravity of soil results (Sand)

Sample No.	Borehole No.	Sample depth (m)	Specific gravity of soil solid, Gs, [-]	*Density*, ρ (kg / m^3)
9	1	3.8	2.66	1853
14	1	6.3	2.65	1675
25	3	3.2	2.65	2042
34	3	7.8	2.66	2047

Figure 6 (left):

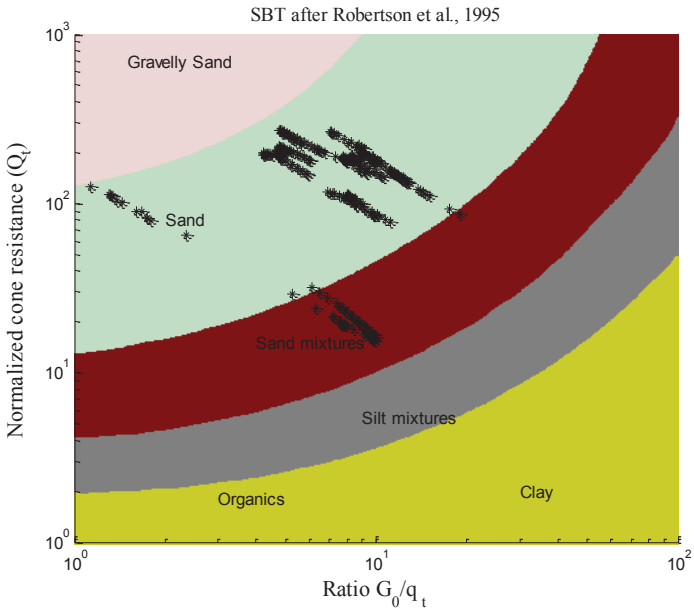

Figure 6 Results from the data in the soil classification chart after Robertson et al., 1995 – Sounding No. 3 (Sandy site)

Estimation of soil type behavior based on shear wave velocity and normalized cone data in the north of Denmark

Sarah Firouzianbandpey, Lars Bo Ibsen and Lars Vabbersgaard Andersen
Department of Civil Engineering, Aalborg University, Aalborg, Denmark

ABSTRACT: As a recent development, the CPTu with added shear wave velocity measurement, known as Seismic Cone Penetration Test (SCPTu), turned into an inimitable in-situ testing method. There are different classification charts proposed in the literature to predict the soil behavior type from cone data. Shear wave velocity measurements from SCPTu tests carried out at a sandy site in the north of Denmark were used in the classification chart based on small strain shear modulus and normalized cone resistance to verify the soil classification system in the region. The results are further compared and verified with the classification test results of samples retrieved from boreholes on the site. The results seem to be very compatible with the soil classification results of samples from boreholes.

1 INTRODUCTION

Cone penetration tests (CPT) have been considered as an alternative to conventional laboratory testing due to economical reasons and their ability to provide continuous data over depth that can be converted into geotechnical in-situ properties of soil. Numerous classification charts have been proposed to estimate soil type using cone data (Begemann, 1965; Douglas and Olsen, 1981; Jones and Rust, 1982; Robertson et al., 1986; Robertson and Campanella, 1983; Robertson, 1990; Jefferies and Davis, 1991; Zhung and Tumay, (1996); Schneider et al., 2008; Cetin and Ozan, 2009). The seismic piezocone penetration test (SCPTu) which provides multipoint simultaneous measurement of tip resistance (q_t), sleeve friction (f_s), pore pressure (u_2), and shear wave velocity (V_s), appears to be a reliable tool in estimation of geotechnical parameters (Lunne et al., 1997; Mayne and Campanella, 2005; Liu et al., 2008; Cai et al., 2009). During the test, a geophone integrated in the cone measures the arrival time of a seismic wave generated by a hammer impact on a steel plate on the ground surface. This can be regarded as a down-hole test. When a polarized shear wave is generated, the time is measured for the shear wave to travel a known distance to the geophone in the cone.

Determination of shear wave velocity (V_s) can be crucial in obtaining information regarding the soil properties. V_s is used in geotechnical seismic design methods (e.g., IBC 2000 code), in soil liquefaction evaluations (e.g. Andrus and Stokoe, 2000), as well as in deriving the small-strain shear modulus ($G_{max} = \rho V^2$). In the absence of a direct measure of the shear wave velocity, correlations have been developed between shear wave velocity and several commonly measured geotechnical properties (cone resistance and sleeve friction). However, uncertainty remains about the choice of

empirical correlations to determine the constrained modulus, small strain shear modulus and other deformation parameters (Cai, 2010) (Firouzianbandpey et al., 2012).

Using the data from SCPTu carried out in a sandy site, the chart by Robertson et al. 1995 based on small strain shear modulus and normalized cone resistance was employed to classify the soil. The data from the seismic part were used in two different analysis methods to obtain shear wave velocity and subsequently small strain shear modulus to be used in the chart. To verify the method, the results were further compared with the soil classification test results on the samples retrieved from boreholes.

2 FIELD AND LABORATORY TESTS

The tests performed in the sandy site are located in the east of Aalborg, an industrial part of the city. A wind turbine blade storage will be constructed at this location. Nine soundings are executed in a cross-shaped pattern with 10 m between the positions of the individual soundings. Four boreholes have been located in the corners (Fig. 1). From the boreholes shown in Fig. 2, soil samples were taken in order to perform soil classification tests. The laboratory testing program included basic soil characterization tests such as grain size distribution, hydrometer tests, relative density and water content. Results from laboratory tests in terms of water content and particle density can be observed in Tables 1 and 2, respectively.

Based on the water content (w), specific gravity of the soil solid (G_s) and a water surface level at a depth of 0.3 m, the soil is considered saturated and the density of the soil can be calculated. Final values from laboratory tests are given in Table 2.

2.1 *Test set up*

For the S-wave generation, one plate is placed on either side of the sounding hole (Fig 3a). A sledge hammer was used to hit the two plates in turn, thereby providing an impact on the ground leading to wave propagation into the soil. The sledge hammer and one of the plates can be seen in Fig. 6. These plates are "L" shaped and the bottom of the plates is equipped with transversal teeth to improve the contact with the ground. The distance between the sounding hole and the place where the hammer hits the plates is 1.4 meters (Fig. 3b).

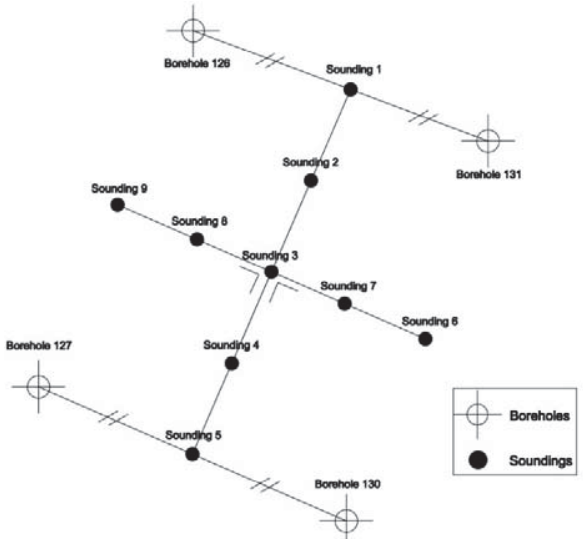

Fig. 1. Position of Boreholes and SCPTu soundings (Sandy site

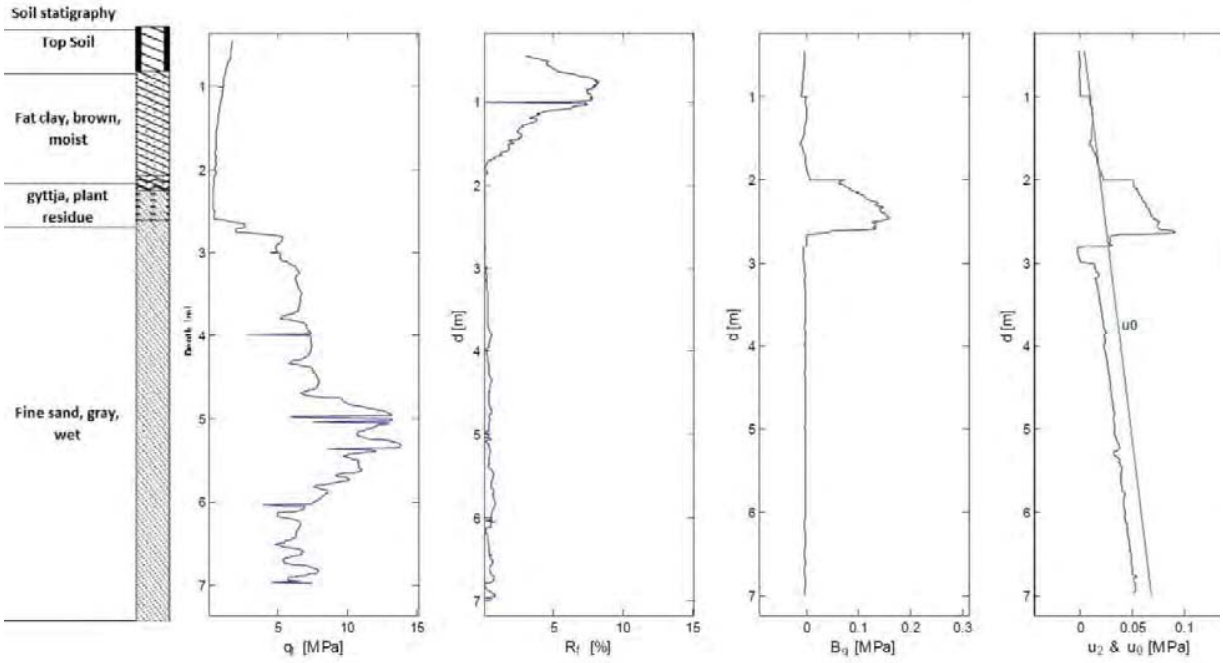

Fig. 2. Borehole profile and CPTu results from field test (Borehole 09).

Table 1. Water content results for sand

Borehole No.	Layer	Water content (%)
100	Topsoil - clay	23-38
	Gyttia	46-62
	Fine sand	17-27
200	Topsoil - clay	26-55
	Gyttia	54-56
	Fine sand	20-24

Table 2. Specific gravity of soils results (Sand)

Sample No.	Specific gravity of soil solid, *Gs*, [-]	*Density*, ρ (kg / m^3)
9	2.66	1853
14	2.65	1675
25	2.65	2042
34	2.66	2047

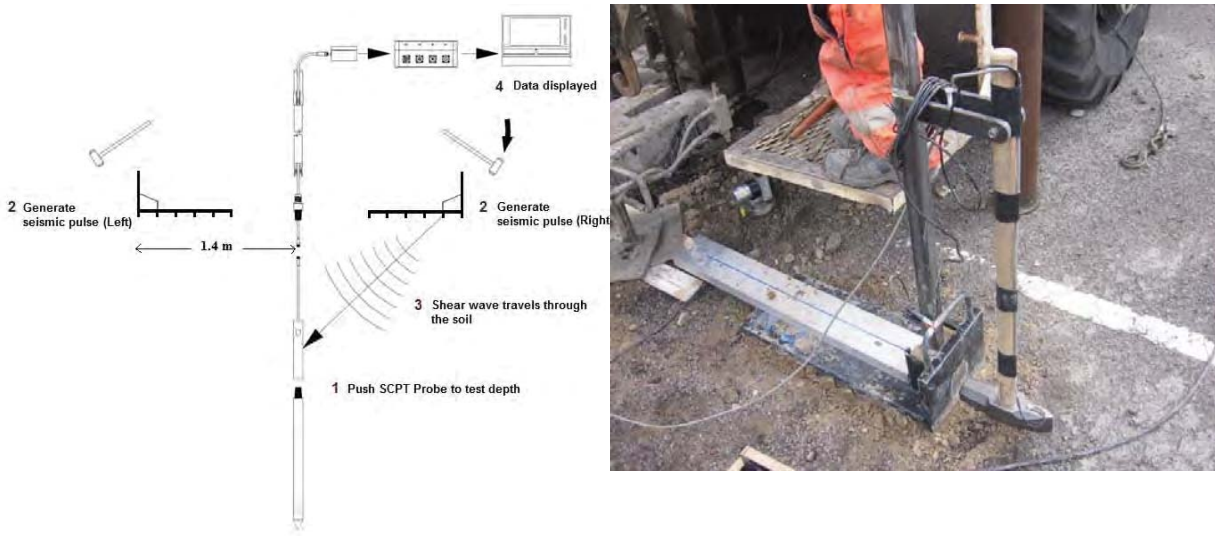

Fig. 3. (a) Layout of source-trigger receiver, (b) L plate and sledge hammer for S-wave generation

The seismic part of the test is performed for each 1 m of penetration. When the cone reaches the desired depth, the engine of the penetrometer or drill rig is stopped. This is done to give the possibility to realize the SCPT test with maximum signal-to-noise ratio. Performing the seismic test during penetration will lead to an inaccurate acceleration measurement, and it will disallow impacts on the two plates to be performed at the same penetration depth. The shear velocity can be easily checked on site, for quality assessment. As soon as the seismic part is finished, the CPT can continue.

3 CORRECTION OF MEASURED DATA FOR THE CPT

Considering that the CPT is accompanied by several possible errors due to halts, soil irregularities (thin layers of stiff materials and etc.), there is a need for these measurements to be corrected. Also the cone resistance and the sleeve friction need to be corrected in order to account for the specific cone design which influences how the pore water pressure alters the measurements. This is in particular important in soft normally consolidated or lightly overconsolidated soil where the pore pressure behind the cone may be large. The cone resistance and the sleeve friction are corrected using Equations (1) and (2) respectively (Lunne et al, 1997):

$$q_t = q_c + u_2(1 - a) \quad (1)$$

$$f_t = f_s - \frac{(u_2 A_{sb} - u_3 A_{st})}{A_s} \quad (2)$$

Where q_t is the corrected cone resistance (in MPa), a is the cone area ratio ($a = \frac{A_n}{A_c}$) with A_n and A_c denoting the cross section area of the shaft and the cone, respectively. Further u_2 is the pore pressure behind the cone and f_t is the corrected sleeve friction. A_{sb} and A_{st} are cross section area of the sleeve bottom and top, respectively. Also A_s is the friction sleeve surface area.

4 SCPT ANALYSIS

Two different interpretation methods were used to determine the shear wave velocity, V_s, from SCPTu data. A short description of the methods is given blow.

4.1 Cross-Correlation

Cross-correlation refers to the correlation of two independent series and can be used to measure the degree to which the two series are related (Liao and Mayne, 2006). The cross-correlation function of x(t) and y(t) for a time shift "s" is defined as Equation (3) in which x(t) and y(t) are two continuous signals with respect to time, t.

$$z(s) = \int_{-\infty}^{\infty} x(t)\, y(t+s)\, dt \quad (3)$$

These series are measured with a geophone located 48 cm behind the friction sleeve. The time shift "s" providing the maximum value of the cross correlation function z(s) can be interpreted as the difference in arrival time of the waves at two positions for two signals of the same shape (Liao and Mayne, 2006).

4.2 Reverse Polarity

Interpolation of the shear wave velocity from SCPTu data consists of dividing an increment in shear wave travel time into an increment of the travel path. The test procedure involves generating shear waves with reverse polarity, by impacting opposite sources, for example two ends of a steel beam, (left and right). Subsequent processing and analysis are then applied on recorded acceleration time traces for each impact. Actually, in analyzing the data, the true shear waves should have reverse

polarity, as the most important identifying characteristic (Jendrezejczuk and Wambs, 1987). In some surveys, the shear waves are readily obvious and identification is not so difficult, while in other cases there may be numerous other arrivals and noise signals that make identification difficult; hence the need for a clear reversal signature may arise. It has been found that the reverse polarity of the source greatly facilitates the identification of the S-wave and the time for the first cross-over point (shear wave changes sign) is easily identified from the polarized waves (forward and reverse) and provides the most repeatable reference arrival time, (Campanella et al, 1987). An example, using the traces, is, given in Fig. 4.

5 SOIL CLASSIFICATION USING SHEAR WAVE VELOCITY MEASUTMENTS

With the addition of shear wave velocity measurements using the seismic CPT (SCPT), Robertson et al. (1995) suggested a chart based on normalized cone resistance (Q_t) and the ratio of small strain shear modulus (G_0) to cone resistance (G_0/q_c).

Normalized cone resistance can be achieved by considering the effect of overburden pressure estimated by the density of the soil and cone depth at the measured data:

$$Q_t = \frac{q_t - \sigma_{v0}}{\sigma'_{v0}} \qquad (4)$$

Where q_t is the measured resistance, σ_{v0} and σ'_{v0} are the effective and total overburden pressure, respectively.

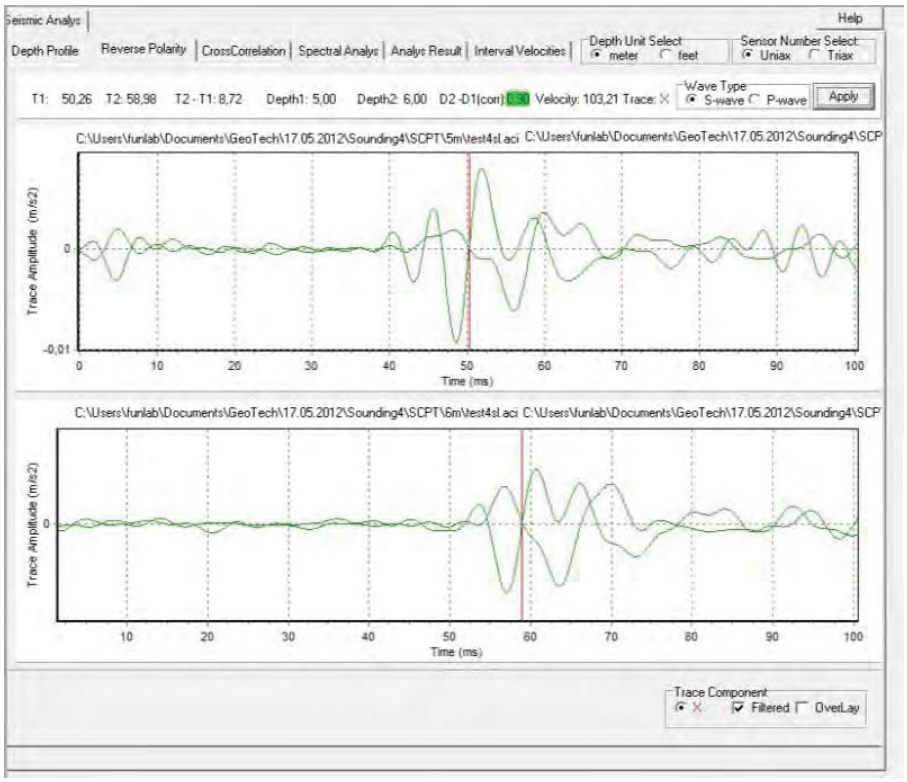

Fig. 4. Seismic analysis using reverse polarity, (Geotech, 2004).

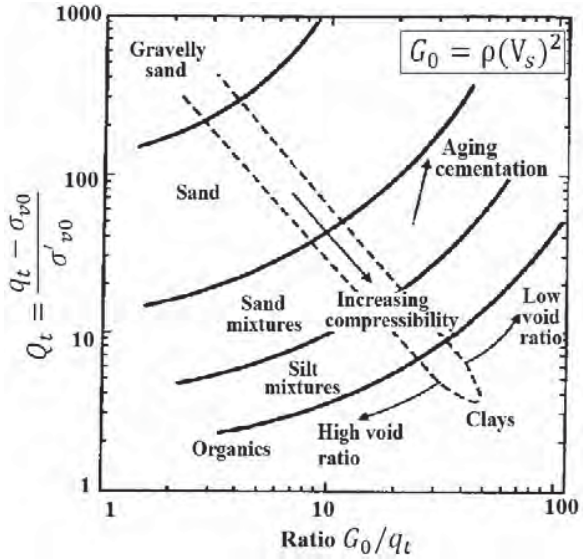

Figure 5. Soil classification chart based on normalized cone resistance and small strain shear modulus (Lunne et al., 1997)

Elasticity theory relates the shear modulus, soil density (ρ) and the shear wave velocity (V_s) as

$$G_{max} = \rho V^2 \qquad (5)$$

The chart shown in Figure 5 can be used to identify different soils. The shear strain amplitude in seismic test is usually low, which allows finding the low-strain shear modulus, G_{max}. To obtain the shear modulus, a seismometer is placed in the horizontal direction and orientated transverse to the signal source to detect the different components of the soil displacement (horizontal and transversal). The ideal seismic signal source should generate a large amplitude shear wave with little or no compressional wave component. The signal can be generated by a hammer hitting a plate. To obtain the measurements, a rugged velocity seismometer has been incorporated into the cone penetrometer. It is placed in the horizontal direction and oriented transverse to the signal source to detect the horizontal component of the shear wave arrivals.

6 RESULTS FROM THE TESTS

After correction of measured data from the CPT and normalizing the cone resistance for the effect of overburden pressure, the data were used in the chart proposed by Robertson et al. (1995) based on shear wave velocity measurements. Results are illustrated in Figures 6 and 7 for a representative SCPT sounding profile. As shown in Figure 6, data points very close to the zone borders may be misclassified. This is an inherent uncertainty of the soil classification chart that should be considered in the estimation of soil type by using the method. For this purpose, the chart domain is discretized into approximately 2000×2000 pixels. For each measured data point, a square "window" is defined centered on the pixel containing the measurement. The probability that a measurement is classified in a zone is calculated as the number of pixels belonging to the zone divided by the total number of pixels in the window. The present study employs a 9×9 window (a heuristic choice that gives good results). Consequently, a larger window implies that the soil types assigned to measurements near zone boundaries are less certain. However, it may also identify more candidates for the underlying soil type (Firouzianbandpey et al., 2012).

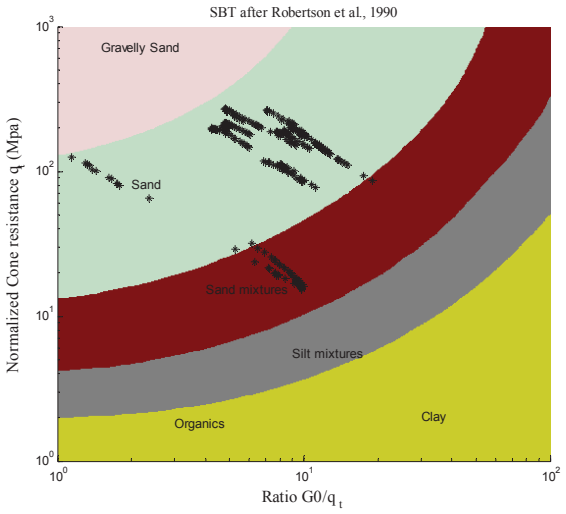

Figure 6. Results from the data in the soil classification chart after Robertson et al., 1995- Sounding No. 3 (Sandy site)

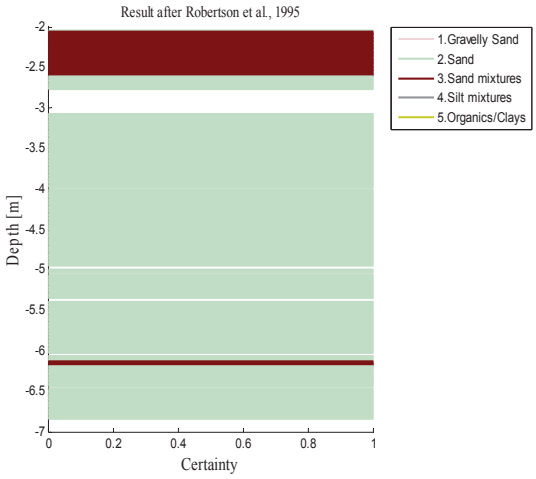

Figure 7. Certainty of soil type from the chart after Robertson et al., 1995 – Sounding No. 3 (Sandy site)

From Figures 6 and 7, the chart predicts the soil type of the region using shear wave velocity measurements as sand and sand mixtures. This is very compatible with the soil classification results of samples from the laboratory tests. The analysis of measurements from all of soundings reveal that the chart proposed by Robertson et al. (1995) is well-predictive at this site, and in the lack of information due to limited soil samples it seems reliable to use the results of SCPTu to predict the soil type.

7 CONCLUSION

The results of seismic cone penetration tests have been used for a sandy site in the north of Denmark to study and verify the soil classification system proposed by Robertson et al. (1995). The chart uses the small strain shear modulus and normalized cone resistance to predict the soil type in the absence of intact soil samples. As a case study, the outcomes have been compared to the results of soil classification tests on samples retrieved from boreholes on the site. Two different interpretation methods were used to determine the shear wave velocity, V_s, from SCPTu data: the reverse polarity method and the cross-correlation method. The values of velocity multiplied by the density of the soil provide small strain shear modulus to be used in the classification chart. The results seem to be very compatible with the soil classification results of samples from boreholes. This leads to the observation that in the future it is possible to use the Robertson et al. (1995) chart to estimate the soil type from SCPT data. This can reduce the cost of site investigation considerably.

REFRENCES

Andrus, R.D and K.H. Stokoe. 2000. Liquefaction Resistance of Soils Based on Shear Wave Velocity, *in Geotechnical and Geo environmental engineering, ASCE*, 126 (11), pp. 1015-1026.

Begemann, H. K. S. 1965. The friction jacket cone as an aid in determining the soil profile. *Proceedings of the 6th International Conference on Soil Mechanics and Foundation Engineering,* ICSMFE, 2, (17–20). Montreal.

Cai, G.J., S.Y. Liu and L.Y. Tong. 2010. Field Evaluation of Deformation Characteristics of a Lacustrine Clay Deposit Using Seismic Piezocone Tests, *Engineering Geology*., No. 116, pp. 251–260.

Cai, G.J., S.Y. Liu., L.Y. Tong and G.Y. Du. 2009. Assessment of Direct CPT and CPTU Methods for Predicting the Ultimate Bearing Capacity of Single Piles. *Engineering Geology*., 104 (1), pp. 211–222.

Campanella, R.G., P.K. Robertson., D. Gillespie., N. Laing and P.J. Kurfurst. 1987. Seismic cone penetration testing in the near offshore of the MacKenzie Delta. *Canadian Geotechnical Journal*. 24. pp. 154-159.

Cetin, K.O., Ozan, C. 2009. CPT-based probabilistic soil characterization and classification. *Journal of Geotechnical and Geoenvironmental Engineering*. 135 (1), 84–107.

Douglas, B. J. & Olsen, R. S. 1981. Soil classification using electric cone penetrometer. *American Society of Civil Engineers, ASCE, Proceedings of Conference on Cone Penetration Testing and Experience*, (209–227). St. Louis, October 26–30.

Firouzianbandpey, S. Ibsen, L.B & Vabbersgaard Andersen, L. 2012. CPTu-based Geotechnical Site Assessment for Offshore Wind Turbines—a Case Study from the Aarhus Site in Denmark, *Proc. Twenty-second International Offshore and Polar Engineering Conference.* June 17–22, 2012. Rhodes, Greece.

Jefferies, M.G., and Davies, M.P. 1993. Use of CPTu to estimate equivalent SPT N6o. *Geotechnical Testing Journal*. 16(4): 458-467.

Jendrezejczuk, J.A and M.W. Wambs. 1987. Surface Measurements of Shear Wave Velocity at the 7-GeV APS Site. *Argonne National Laboratory Report*, LS-129.

Jones, G. A. & Rust, E. 1982. Piezometer penetration testing, CUPT. *Proc. 2nd European Symposium on Penetration Testing*, ESOPT-2, 2, (607–614). Amsterdam, May 24–27.

IBC. 2000. *International Building Code*, prepared by International Code Council.

Liu, S.Y., G.J. Cai., L.Y. Tong and G.Y. Du. 2008. Approach on the Engineering Properties of Lianyungang Marine Clay from Piezocone Penetration Tests. *Marine Geo resource. and Geotechnical*, 26 (7), pp. 189–210.

Liao, T & Mayne, P.W. 2006. Automated Post-processing of Shear Wave Signals", *Proc. 8th US. Conf. on Erthq Engrg.* San Francisco, California, USA.

Lunne, T., Robertson, P.K. and Powell, J.J.M. 1997. *Cone Penetration Testing in Geotechnical Practice*. Blackie Academic/Chapman & Hall, E&FN Spon, 312. pages, 3rd printing.

Mayne, P.W and G. Campanella. 2005. Versatile Site Characterization by Seismic Piezocone. *Proc. 16th Int. Conf. on Soil Mechnc. & Geo. tech Engrg*. Osaka, Japan, 2, pp. 721–724.

Robertson, P. K. 1990. Soil classification using the cone penetration test. *Canadian Geotechnical Journal*, 27(1), 151–158.

Robertson, P. K., Campanella, R. G., Gillespie, D. & Grieg, J. 1986. Use of piezometer cone data. *Proc. American Society of Civil Engineers, ASCE*, In-Situ 86 Specialty Conference, (1263–1280). Edited by S. Clemence, Blacksburg, June 23–25, Geotechnical Special Publication GSP No. 6.

Robertson, P. K. & Campanella, R. G. 1983. Interpretation of cone penetrometer tests, Part I sand. *Canadian Geotechnical Journal*. 20(4), 718–733.

Robertson, P. K., Fear C.E., Woeller D. J and Weemees I. 1995. Estimation of sand compressibility from Seismic CPT, *Proc. 48th Canadian Geotechnical Conference*, Vancouver.

Schneider, J.A., Randolph, M.F., Mayne, P.W., Ramsey, N.R. 2008. Analysis of factors influencing soil classification using normalized piezocone tip resistance and pore pressure parameters. *Journal of Geotechnical and Geoenvironmental Engineering*. 134 (11), 1569–1586.

Zhang, Z., Tumay, M.T. 1996. Simplification of soil classification charts derived from cone penetration test. *Geotechnical Testing Journal*. 19 (2), 203–216.

APPENDIX D: PAPER 4

Spatial correlation length of normalized cone data in sand: case study in the north of Denmark

IS CITED AS:

Firouzianbandpey, S., Griffiths, D. V., Ibsen, L. B., Andersen, L. V. (2014). "Spatial correlation length of normalized cone data in sand: case study in the north of Denmark." ***Canadian Geotechnical Journal***, 51, 844–857.

STATUS: Published

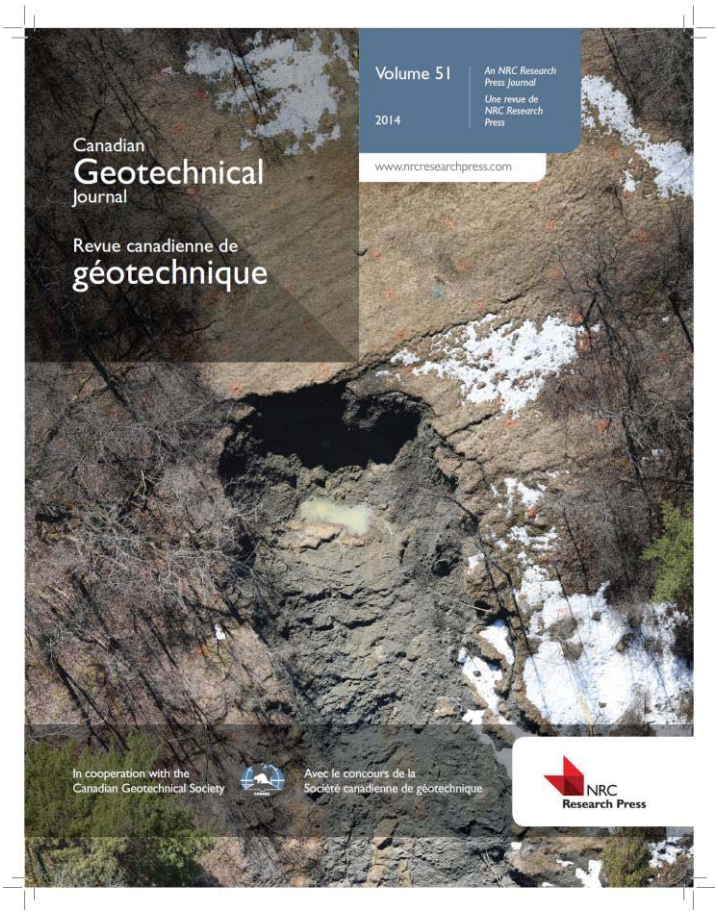

NRC Research Press

CORRIGENDUM

Corrigendum: Spatial correlation length of normalized cone data in sand: case study in the north of Denmark

S. Firouzianbandpey, D.V. Griffiths, L.B. Ibsen, and L.V. Andersen

Ref.: Can. Geotech. J. **51**(8): 844–857 (2014). dx.doi.org/10.1139/cgj-2013-0294.

Figures 3 and 4 on pages 846 and 847, respectively, should be replaced with the figures shown herein. In Figs. 5*a* and 6*a*, on pages 848 and 849, respectively, "q_t (MPa)" should be replaced with "Q_t".

Tables 1 and 2 on page 850 should be replaced with the tables shown herein. In Tables 3 and 4 on p. 853, "Number of samples" should be replaced with "Number of samples*", with the following footnote added below each table: "*In each sounding."

Table 1. Results of spatial variability of cone data for different soil layers at the Aalborg site.

		Soil type (Robertson 1990)			
Cone parameter	Statistical parameters	Gravelly sand	Sands, clean sands	Silty sand, sand mixtures	Clayey silt to silty clay, silt mixtures
Normalized cone resistance	Number of samples	1109	2399	272	229
	COV (%)	38	33	26	21
	Mean	260.93	112.75	27.39	16.22
Normalized friction ratio	Number of samples	1109	2399	272	229
	COV (%)	65	51	61	46
	Mean	1.01	0.97	1.25	1.83

Table 2. Results of spatial variability of cone data for different soil layers at the Frederikshavn site.

		Soil type (Robertson 1990)			
Cone parameter	Statistical parameters	Gravelly sand	Sands, clean sands	Silty sand, sand mixtures	Clayey silt to silty clay, silt mixtures
Normalized cone resistance	Number of samples	382	1999	1110	43
	COV (%)	56	47	13	21
	Mean	376.28	87.58	44.07	31.29
Normalized friction ratio	Number of samples	382	1999	1110	43
	COV (%)	48	25	23	35
	Mean	3.28	5.05	5.3	4.17

Received 23 May 2015. Accepted 19 June 2015.

S. Firouzianbandpey, L.B. Ibsen, and L.V. Andersen. Department of Civil Engineering, Aalborg University, 9000 Aalborg, Denmark.
D.V. Griffiths. Department of Civil and Environmental Engineering, Colorado School of Mines, Golden, CO 80401, USA; Australian Research Council Centre of Excellence for Geotechnical Science and Engineering, University of Newcastle, Callaghan NSW 2308, Australia.
Corresponding author: S. Firouzianbandpey (e-mail: sf@civil.aau.dk).

Published at www.nrcresearchpress.com/cgj on 10 July 2015.

Fig. 3. Position of boreholes and CPTu: (*a*) Aalborg site; (*b*) Frederikshavn site.

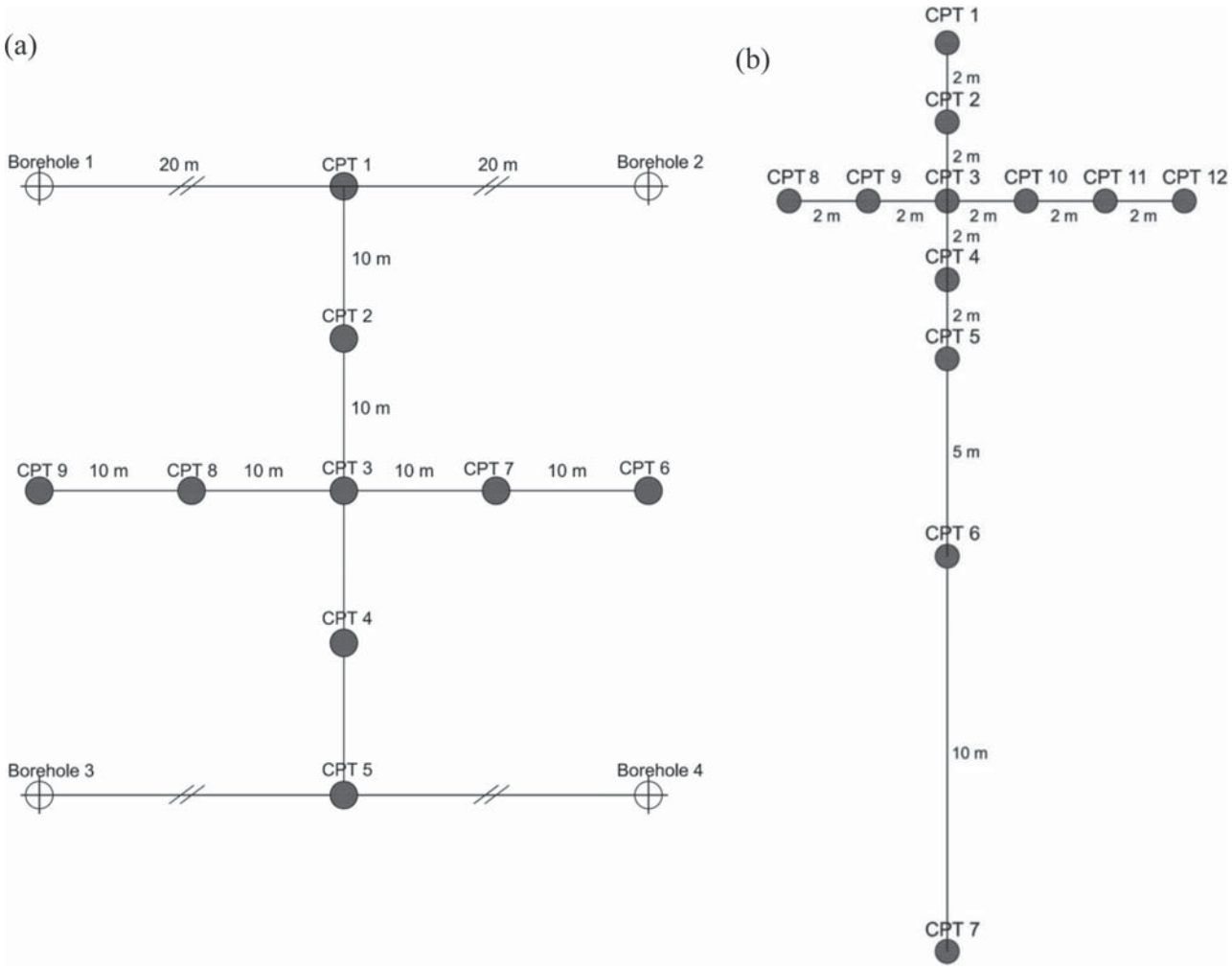

Fig. 4. Representative CPT profiles obtained at (*a*) Aalborg and (*b*) Frederikshavn – CPT 4. u_0, hydrostatic pore pressure induced by water level surface of the region.

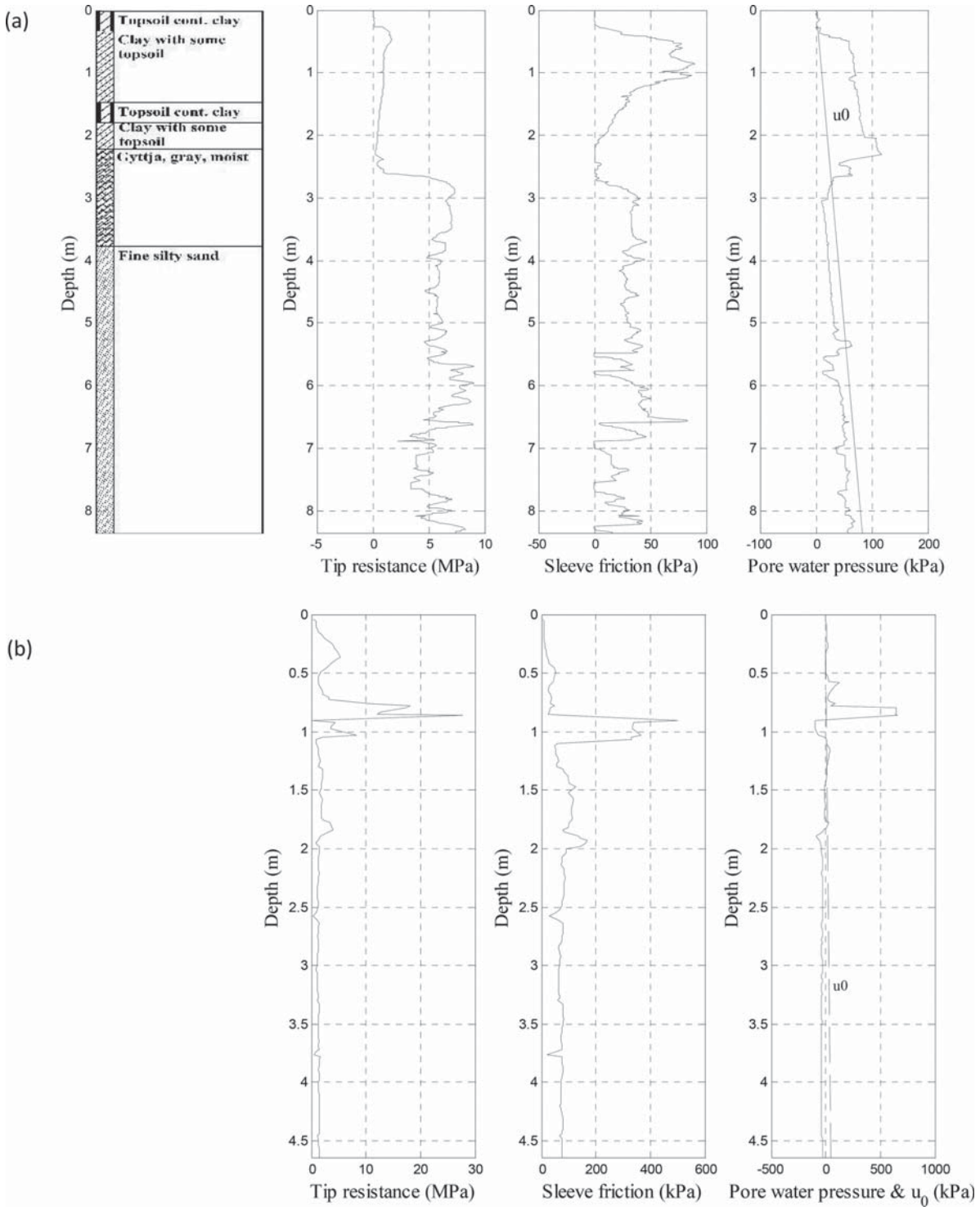

NRC Research Press

ARTICLE

Spatial correlation length of normalized cone data in sand: case study in the north of Denmark

S. Firouzianbandpey, D.V. Griffiths, L.B. Ibsen, and L.V. Andersen

Abstract: The main topic of this study is to assess the anisotropic spatial correlation lengths of a sand layer deposit based on cone penetration testing with pore pressure measurement (CPTu) data. Spatial correlation length can be an important factor in reliability analysis of geotechnical systems, yet it is rarely estimated during routine site investigations. Results from two different sites in the north of Denmark are reported in this paper, indicating quite strong anisotropy due to the depositional process, with significantly shorter spatial correlation lengths in the vertical direction. It is observed that the normalized cone resistance is a better estimator of spatial trends than the normalized friction ratio.

Key words: spatial correlation length, cone penetration testing with pore pressure measurement (CPTu), soil inhomogeneity, normalized cone resistance, normalized friction ratio.

Résumé : Le sujet principal de cette étude est l'évaluation des longueurs de corrélation spatiale anisotrope d'un dépôt sous forme de couches de sable, à partir de résultats d'essais de pénétration du cône avec la mesure des pressions interstitielle (CPTu. La longueur de corrélation spatiale est considérée comme un facteur important lors de la réalisation d'analyses de fiabilité de systèmes géotechniques, cependant elle est rarement estimée durant les investigations de routine sur le terrain. Les résultats provenant de deux sites différents dans le nord du Danemark sont présentés dans cet article. Ces résultats indiquent une anisotropie relativement forte associée au processus de déposition, en raison de longueurs de corrélation spatiale significativement plus faibles dans la direction verticale. Il est observé que la résistance normalisée du cône est un meilleur paramètre pour l'estimation des tendances spatiales plutôt que le ratio de friction normalisé. [Traduit par la Rédaction]

Mots-clés : longueur de corrélation spatiale, essai de pénétration du cône avec la mesure des pressions interstitielle (CPTu), inhomogénéité du sol, résistance normalisée du cône, ratio de friction normalisé.

Introduction

An understanding of the variability of soil properties for the purpose of foundation design and analysis, and as a basis for the calibration of new design codes, is of considerable importance in geotechnical engineering. Soil data used in foundation design is usually accompanied with significant uncertainty because of limited site data and natural variability.

In addition to the mean and standard deviation of soil parameters, the spatial correlation has been increasingly recognized as an influential property in determining probabilistic outcomes. This paper seeks to estimate anisotropic spatial correlation length at two sand deposits in northern Denmark, by analysis of the measured spatial variability of sampled soil properties using statistical trends and correlations, and to interpolate soil properties at unsampled locations. When the available information is very limited, geotechnical design is inevitably more conservative (e.g., Baecher 1986). In this study, we study the results of stress normalized cone penetration testing with pore pressure (CPTu) data to estimate spatial correlation length. Numerous studies, such as Alonso and Krizek (1975), Tang (1979), Nadim (1986), Campanella et al. (1987), Wu et al. (1987), Reyna and Chameau (1991), Kulhawy et al. (1992), Fenton (1999), Elkateb et al. (2003*a*, 2003*b*), and Phoon et al. (2003), have reported assessments of inherent soil variability using cone penetration tests (CPT). However, results using stress-normalized CPT data are more limited (Uzielli et al. 2005).

There are several different methods for modeling the inherent variability of a soil property represented as a random field. For example, the local average subdivision method, as proposed by Fenton and Vanmarcke (1990) was subsequently combined with finite element methods to analyze geotechnical problems of practical interest (see Griffiths and Fenton 1993; Fenton and Griffiths 2008). The local average subdivision method requires probability density functions (pdf) of key input parameters described by the mean, μ, and standard deviation, σ, of the property at each point in space, and a spatial correlation length δ. These parameters can be estimated from field data obtained at discrete locations across a site.

The present study focuses on the spatial variability of cone data normalized with respect to vertical stress. The data were collected at two different sites in the north of Denmark, where the ambient soil type is classified as either sand or silty sand. By calculating the statistical parameters of the cone data, the spatial correlation length of the field was estimated in the vertical and horizontal directions.

Vanmarcke (1977) estimated spatial correlation functions and spatial correlation lengths using common functions such as exponential, exponential oscillatory, quadratic exponential oscillatory, and bilinear. In the present research, the function describing spatial correlation with respect to relative distance is an exponential model. Furthermore, the parameter of the model, D, is calculated separately in the horizontal and vertical directions. At both

Received 31 July 2013. Accepted 5 March 2014.

S. Firouzianbandpey, L.B. Ibsen, and L.V. Andersen. Department of Civil Engineering, Aalborg University, 9000 Aalborg, Denmark.
D.V. Griffiths. Department of Civil and Environmental Engineering, Colorado School of Mines, 80401 Golden, CO, USA, and Australian Research Council Centre of Excellence for Geotechnical Science and Engineering, University of Newcastle, Callaghan NSW 2308, Australia.
Corresponding author: S. Firouzianbandpey (e-mail: sf@civil.aau.dk).

Published at www.nrcresearchpress.com/cgj on 25 March 2014.

Fig. 1. Terminology for cone penetrometers.

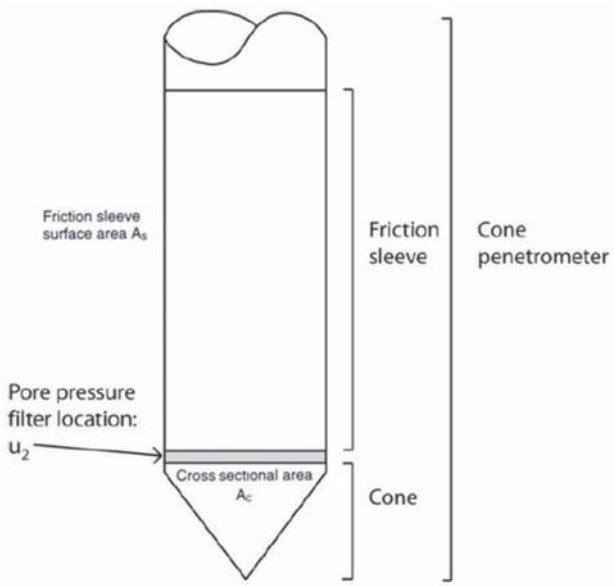

Fig. 2. Map of field test area.

sites, the cone data show that the vertical and horizontal correlation structures in soil properties are strongly anisotropic, with shorter correlation lengths in the vertical direction. Also in the vertical direction, it was observed that cone resistance normalized by vertical stress is more spatially correlated than normalized values of the friction ratio, with spatial correlation lengths estimated in the range of 0.5 and 0.2 m, respectively.

Cone penetration test

The cone penetration test (CPT) and its enhanced versions (i.e., piezocone-CPTu and seismic-CPT) have various applications in a wide range of soils. During testing, a cone mounted on a series of rods is pushed into the ground at a constant rate, while continuous measurements are made of the resistance to the penetration of the cone and of a surface sleeve surrounding the rods. The CPTu is preferred among other in situ testing methods because of the advantages of fast and continuous profiling, repeatable and reliable data (not operator-dependent), being economical and productive to conduct, and having a strong theoretical basis for interpretation.

Figure 1 illustrates the main parts of a cone penetrometer. The total force acting on the cone, Q_c, divided by the projected area of the cone, A_c, produces the cone resistance, q_c. The total force acting on the friction sleeve, F_s, divided by the surface area of the friction sleeve, A_s, is the sleeve friction, f_s. A piezocone also measures pore water pressure, typically just behind the cone in the location u_2, as shown in Fig. 1.

Description of the sites

As illustrated in Fig. 2, the analysis concerns two different sites located in Jutland, in the north of Denmark, a few metres from the sea. Statistical characteristics of cone tip resistance in the Aalborg site were estimated using piezocone penetration test (CPTu) data of nine soundings obtained from the industrial part of the city. A wind turbine blade storage will be constructed at this location. The site is close to the Limfjord river, meaning it is a basin deposit area. The soil sediment is 1–4 m of clay/gyttia marine deposits, while the lower layers are mostly silty sand. The CPTu tests reached a depth of approximately 8 m. The nine soundings are arranged in a cross-shaped pattern, with 10 m separation between the holes. The cross is framed by four bore holes (Fig. 3*a*). In both sites and all CPT soundings, the interval distance between the samples in the vertical direction is 2 cm. Figure 4*a* shows a representative CPT profile performed in the field. Statistical analysis of the CPT data was performed using MATLAB, after programming the soil behavior classification system suggested by Robertson (1990) as shown in Fig. 5.

The second site is located in the northeast of Denmark, at the harbor of Frederikshavn. The soil layers are mostly sand, with some thinly interbedded stiff clays. Twelve soundings were performed at this site to depths of 7–8 m, in a cross-shaped pattern as illustrated in Fig. 3*b*. Figure 4*b* shows a representative CPT profile from this site. The soil types inferred from the representative cone profile, based on the Robertson classification chart, are plotted in Fig. 6. The ambient layers are various types of sands, gravelly sands, and sand mixtures.

Normalized cone data

Effective overburden stress can have a significant influence on CPT measurements and lead to an incorrect assessment of soil strength parameters. Low overburden stresses result in a reduced sleeve and tip resistance, whereas at greater soil depths, a logarithmically pronounced increase occurs in measured tip and sleeve resistance (Moss et al. 2006).

Different methods are used in the literature for normalizing CPT measurements for vertical stress. This study applies the technique proposed by Robertson and Wride (1998) to cone tip resistance measurements:

$$(1) \qquad q_{c1N} = \left(\frac{q_c}{P_a}\right)C_Q, \quad C_Q = \left(\frac{P_a}{\sigma'_{v0}}\right)^n$$

where q_{c1N} is the dimensionless cone resistance normalized by the weight of soil above the cone, q_c is the measured cone tip resistance, and C_Q is a correction for overburden stress. The exponent n takes the values 0.5, 1.0, and 0.7 for cohesionless, cohesive, and intermediate soils respectively, while σ'_{v0} is the effective vertical stress, and P_a is the reference pressure (atmospheric pressure) in the same units as σ'_{v0} and q_c, respectively. q_{c1N} is a dimensionless cone resistance normalized by the weight of the soil on top of the cone. In most studies, this value is used instead of the raw cone resistance in the correlations.

Fig. 3. Position of boreholes and CPTu: (*a*) Aalborg site; (*b*) Frederikshavn site.

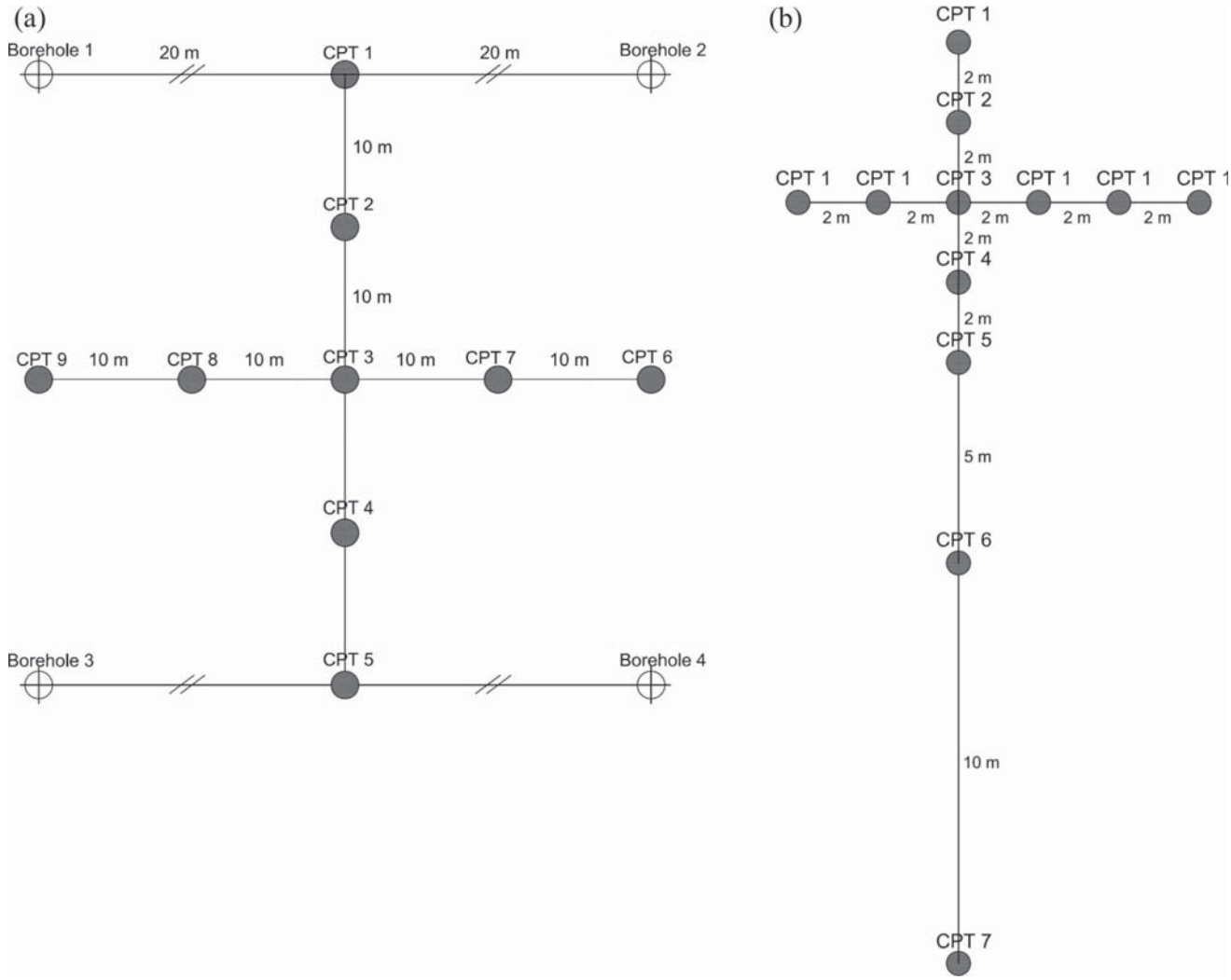

Also, the normalized friction ratio is calculated using the equation proposed by Wroth (1984)

$$F_R = 100\frac{f_s}{q_c - \sigma_{v0}} \quad (2)$$

where f_s is the measured sleeve friction and σ_{v0} is the total vertical stress. In this case, q_c, σ_{v0}, and f_s are all in the same units.

These procedures were applied to all soil types, to decrease the effect of overburden pressure on the results.

Estimation of soil behavior type from cone data

The two charts shown in Figs. 5*a* and 6*a* represent the classification system proposed by Robertson (1990) that incorporates two pieces of normalized cone data (tip resistance and pore water pressure). Using the chart, the soil type can be estimated using cone data after a normalization in which the overburden pressure and the initial water level surface is accounted for. Seven different zones can be identified in the chart by plotting the data for the normalized cone resistance and pore pressure ratio.

The normalized tip resistance is calculated as

$$Q_t = \frac{q_t - \sigma_{v0}}{\sigma'_{v0}} \quad (3)$$

where q_t is the measured resistance, and σ_{v0} and σ'_{v0} are the total and effective overburden pressures estimated by the density of the soil and cone depth at the measured data, respectively. The normalized pore pressure (also known as the pore pressure ratio in the soil classification chart by Robertson 1990) is defined as follows:

$$B_q = \frac{u_2 - u_0}{q_t - \sigma_{v0}} \quad (4)$$

where u_0 is the initial pore pressure and u_2 is the pore pressure measurement at the back of the cone penetrometer.

Regarding the certainty with which a classification method (in this case the method proposed by Robertson 1990) identifies a given soil type, a distinction must be made between two aspects. Firstly, a classification method may be more or less accurate in identifying a soil type. This may be regarded as a model uncertainty, and as proposed by Firouzianbandpey et al. (2012) this uncertainty can be identified by comparing the classification made from the CPT from a classification made from soil samples taken within a bore hole. The present work does not consider this kind of uncertainty, but previous studies indicate that the method provides a reliable overall identification of soil types for regions with the considered type of soil deposits.

Fig. 4. Representative CPT profiles obtained at (*a*) Aalborg site and (*b*) Frederikshavn. u_0, hydrostatic pore pressure induced by water level surface of the region.

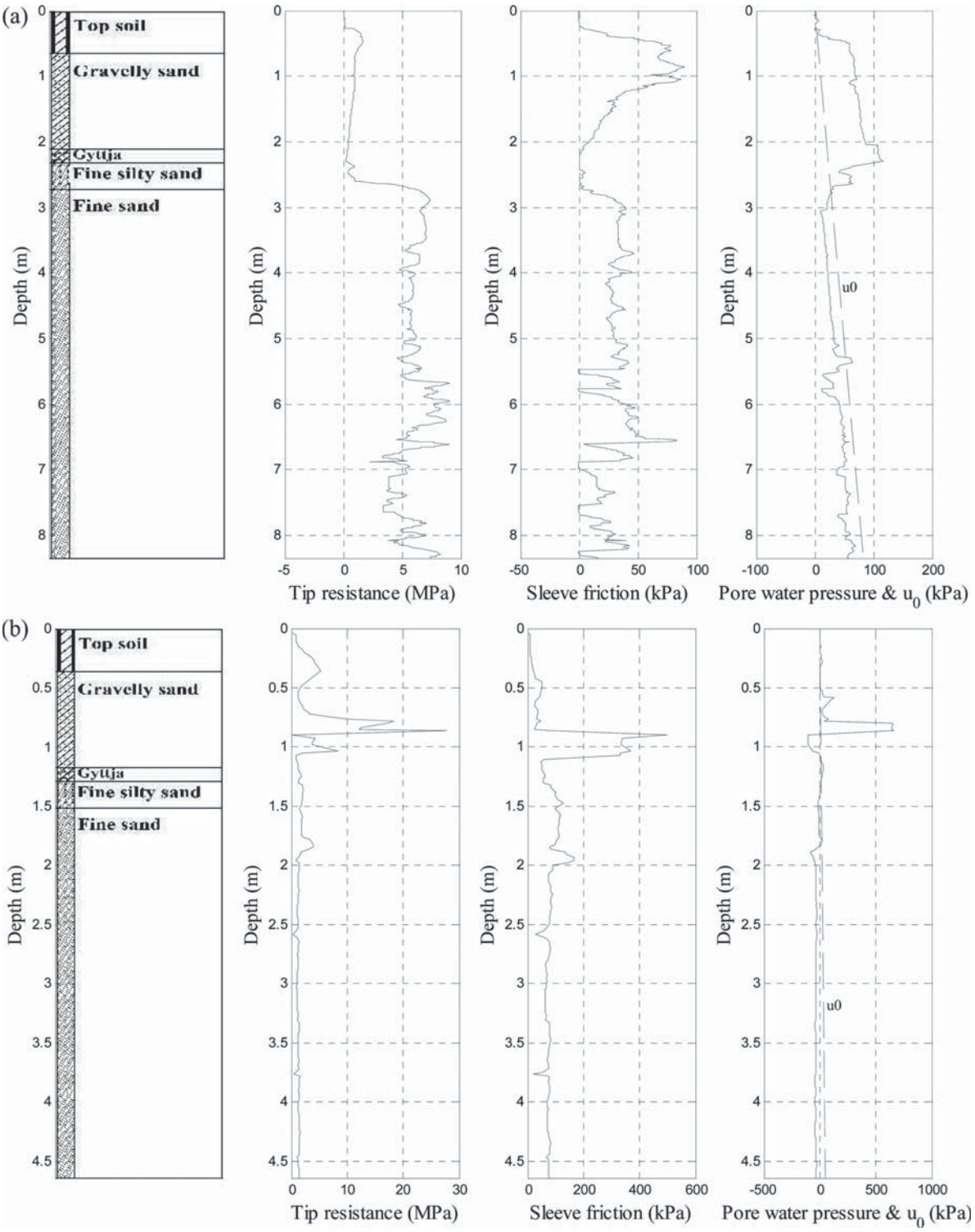

Secondly, each CPT classification method is based on the idea that combinations of raw CPT data (in this case pore pressure and cone resistance) falling within a "zone" in the classification diagram are related to a particular type of soil. However, the borders between these "zones" are subject to uncertainty in the sense that the engineer has to decide whether a given data point is in one zone or another. One idea would be to define a borderline of no extent such that it is uniquely defined to which zone a given data point belongs. However, in this paper another approach is considered. Thus, the classification diagram is digitalized (in this case a resolution of about 2000 × 2000 pixels is used) and a window is defined around a given data point as illustrated in Fig. 7. The size

Fig. 5. Soil classification results of a representative CPT sounding (CPT No. 5) performed at the Aalborg site (after Robertson 1990): (*a*) Soil behavior type (SBT) classification from CPTu data, using the method of Robertson (1990). Zones 1 to 7 are: 1, sensitive, fine-grained soils; 2, organic soils and peat; 3, clays, clay to silty clay; 4, silt mixtures, silty clay to clayey silt; 5, sand mixtures, sandy silt to silty sand; 6, sands, silty sand to clean sand; 7, sand to gravelly sand. (*b*) Possible soil type for each measurement versus depth. The shades of grey are the same as the zones in Fig. 5*a*.

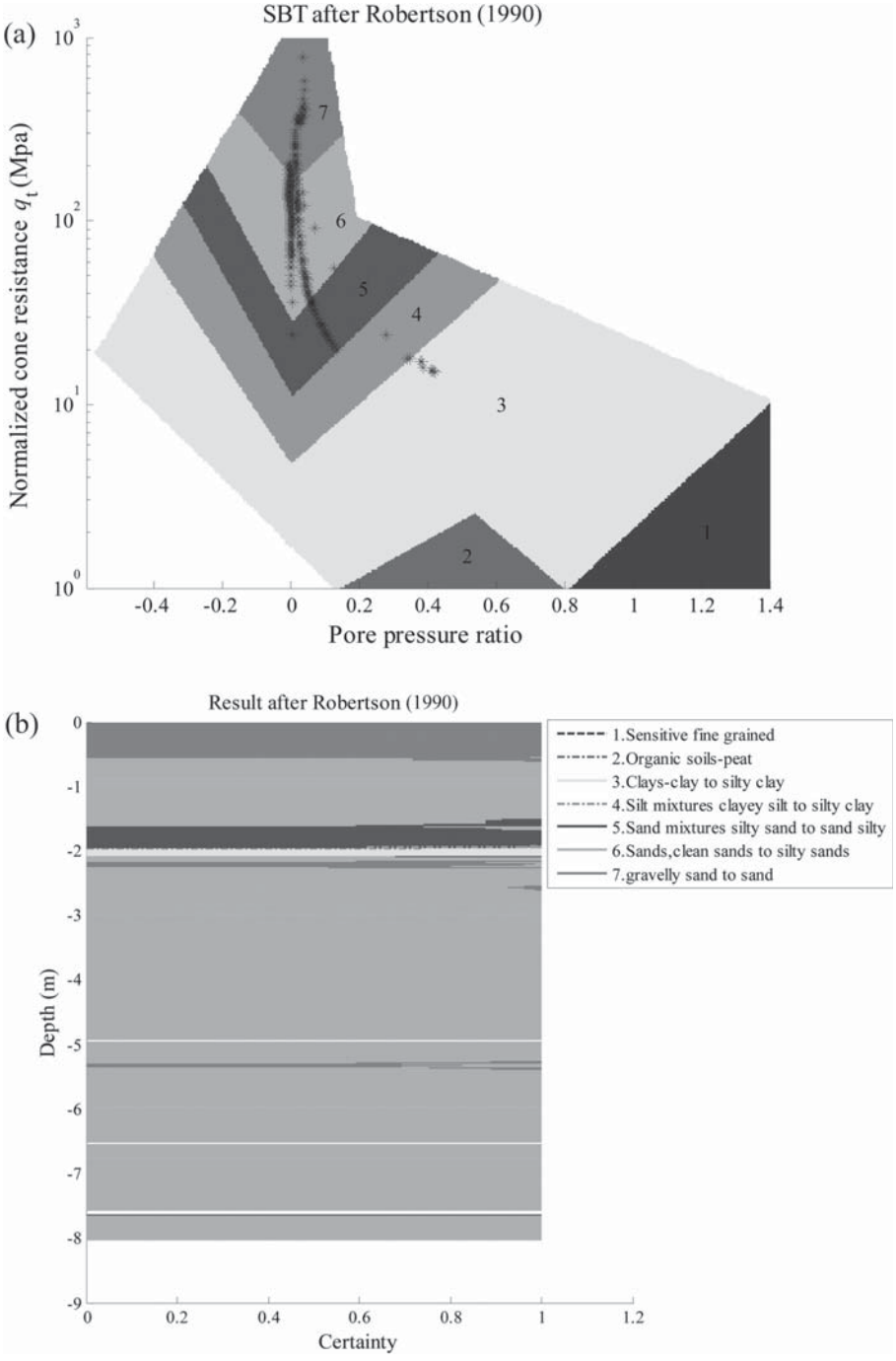

of the window is a heuristic choice, however, the basic idea is that it should be chosen such that it reflects the uncertainty related to an engineer performing a visual interpretation of the printed diagram. A larger window implies that the soil types assigned to measurements near zone boundaries are identified with less confidence, and more candidates for the underlying soil type may be proposed by the classification method.

The size of the window is chosen to be 9 × 9 pixels in the present study, but for comparison, Fig. 7 illustrates the principle for a smaller window of the size 5 × 5 pixels as well. The number of pixels in the window occurring in each zone is now counted and compared to the total number of pixels in the window. In this context, the ratio between the number of pixels in the window residing in a given zone and the number of total pixels in the

Fig. 6. Soil classification results of a representative CPT sounding (CPT No. 8) performed in Frederikshavn site (after Robertson 1990): (*a*) Soil behavior type classification from CPTu data, according to Robertson (1990). The soil types corresponding to zones 1 to 7 are the same as defined in the caption of Fig. 5*a*. (*b*) Possible soil type for each measurement versus depth. The shades of grey are the same as the zones in Fig. 6*a*.

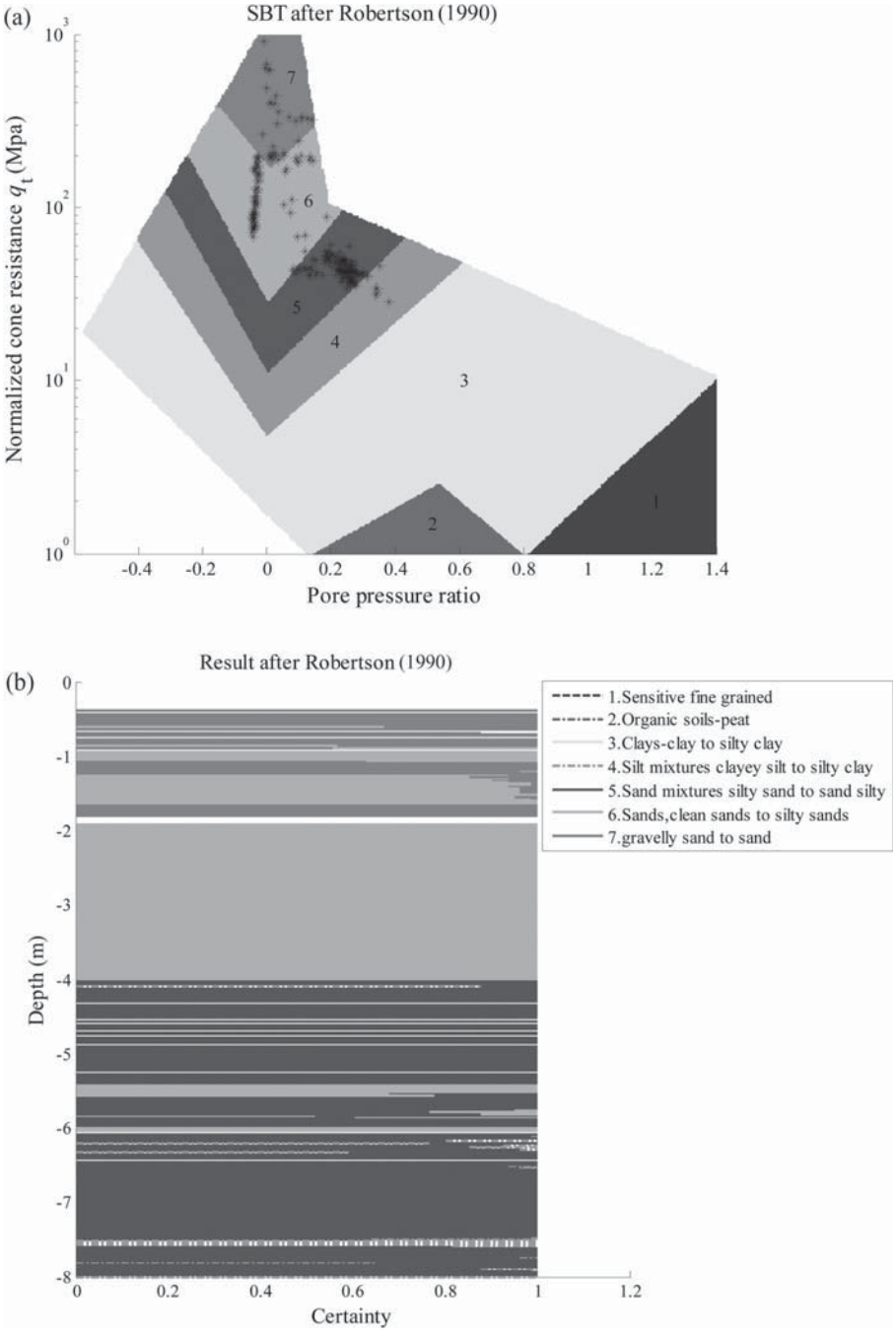

window provides a number that may be regarded as a classification certainty related to a given classification method. The terminology "classification certainty" will be used in what follows in accordance with this definition. As an example, for the data point indicated in Fig. 7, the classification certainty related to the green zone 6 becomes 24/25 = 0.96 for the small window and 66/81 = 0.81 (i.e., the classification certainty related to the zone in wherein the data point resides decreases with increasing size of the window).

Next, Figs. 5*b* and 6*b* show the soil profile resulting from this method. For each depth, a horizontal line is drawn and divided into segments proportional to the certainty of each soil type in the window. The most certain soil type is plotted first, so the left vertical axis represents the most likely form of the soil profile. When the certainty is 1, the input data measurement is located well within a zone, far away from the boundaries.

It is evident from Figs. 5 and 6 that the soil types predicted by the 1990 Robertson chart method are mostly sand, sand mixtures,

Fig. 7. 5 × 5 and 9 × 9 pixel windows for determination of classification certainty related to a CPT data point.

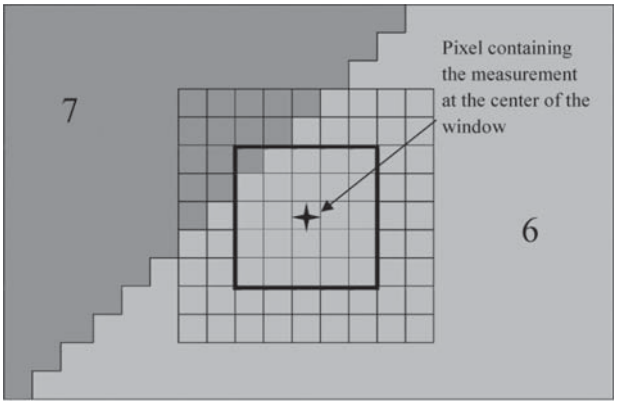

and gravelly sand. These results agree with the classification of soil samples retrieved from the boreholes.

Coefficient of variation (COV) of cone data in vertical direction

Using data from sub layers identified as spatially homogeneous by the soil-behavior-type classification system suggested by Robertson (1990), the coefficients of variation of the CPT data in the Aalborg site and Frederikshavn site have been estimated. Tables 1 and 2 provide the mean and coefficient of variation of the "normalized cone resistance" and "normalized friction ratio" at the two different sites. All CPT data have been classified based on the Robertson (1990) chart. Then the data points that were classified in the same zone were counted. The total number of samples is the number of CPT data obtained from the soundings.

Table 1 shows that the gravelly sand layers of the Frederikshavn site have much higher coefficient of variation (COV) values between the different soundings than other soil types, for both cone resistance and sleeve friction. At the Aalborg site, the sleeve friction is always highly variable, but the COV values for cone resistance are higher in gravelly sands than in other layers.

Silt mixtures exhibit the most consistent cone resistance measurements at both sites (low COV). The soil type with the lowest sleeve friction variability is silty sands and sand mixtures in Frederikshavn, but clayey silt layers in Aalborg.

Since COV is an indicator of the degree of variation in soil properties across the site, in soil layers with relatively high COVs, there is more expectation for variability of the soil parameters.

Correlation structure of the field

To characterize a random field, knowledge about how rapidly the field varies in space is needed. This is captured by the second moment of the field's joint distribution, which is expressed by the covariance function,

$$(5)\qquad C(t',t^*) = \mathrm{Cov}[X(t'),X(t^*)] = E[X(t')X(t^*)] - \mu_X(t')\mu_X(t^*)$$

where $\mu_X(t)$ is the mean of X at the position t. A more meaningful measure about the degree of linear dependence between $X(t')$ and $X(t^*)$ is the correlation function

$$(6)\qquad \rho(t',t^*) = \frac{C(t',t^*)}{\sigma_X(t')\sigma_X(t^*)}$$

where $\sigma_X(t)$ is the standard deviation of X at the position t.

Table 1. Results of spatial variability of cone data for different soil layers at the Aalborg site.

		Soil type (Robertson 1990)			
Cone parameter	Statistical parameter	Gravelly sand	Sands, clean sands	Silty sand, sand mixtures	Clayey silt to silty clay, silt mixtures
Normalized cone resistance	Number of samples	1109	2399	272	229
	COV (%)	61	56	23	11
	Mean	3.2	2.7	0.1	0.04
Normalized friction ratio	Number of samples	1109	2399	272	229
	COV (%)	60	60	81	53
	Mean	0.03	0.01	0.004	0.001

Table 2. Results of spatial variability of cone data for different soil layers at the Frederikshavn site.

		Soil type (Robertson 1990)			
Cone parameter	Statistical parameter	Gravelly sand	Sands, clean sands	Silty sand, sand mixtures	Clayey silt to silty clay, silt mixtures
Normalized cone resistance	Number of samples	382	1999	1110	43
	COV (%)	82	28	15	12
	Mean	2.69	0.6	0.31	0.16
Normalized friction ratio	Number of samples	382	1999	1110	43
	COV (%)	51	22	2	32
	Mean	0.08	0.09	1	0.03

Fig. 8. Schematic view of an ideally horizontal homogeneous sublayer of soil and data points in the vertical and horizontal directions.

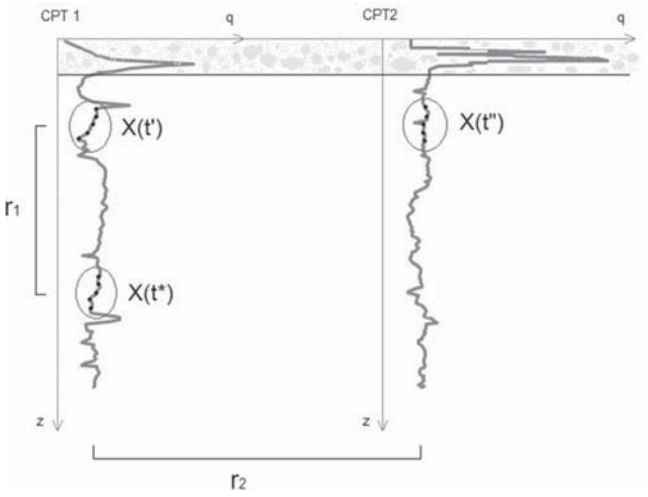

A commonly applied model of the correlation function for soil parameters is a single exponential curve (e.g., Vanmarcke 1977; DeGroot 1996; DNV 2010).

In this study an attempt is made to estimate the spatial correlation length of normalized cone data in the horizontal and vertical directions by fitting an exponential model to the results (correlation coefficients of normalized cone data versus distance). This method was preferred to the maximum likelihood method because of the lack of information about the model function of the error.

Fig. 9. Vertical correlation coefficient of q_{c1N} for (*a*) a representative sounding (CPT No. 8) and (*b*) for all soundings in sand layer (Frederikshavn site).

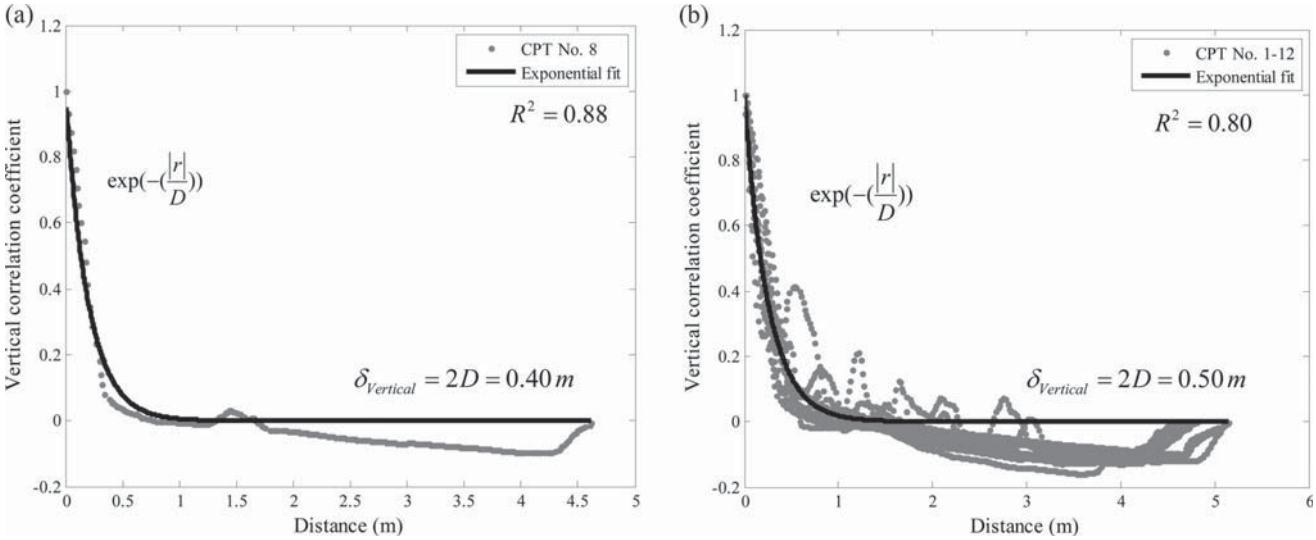

Fig. 10. Vertical correlation coefficient of q_{c1N} for (*a*) a representative sounding (CPT No. 1) and (*b*) for all soundings in sand layer (Aalborg east site).

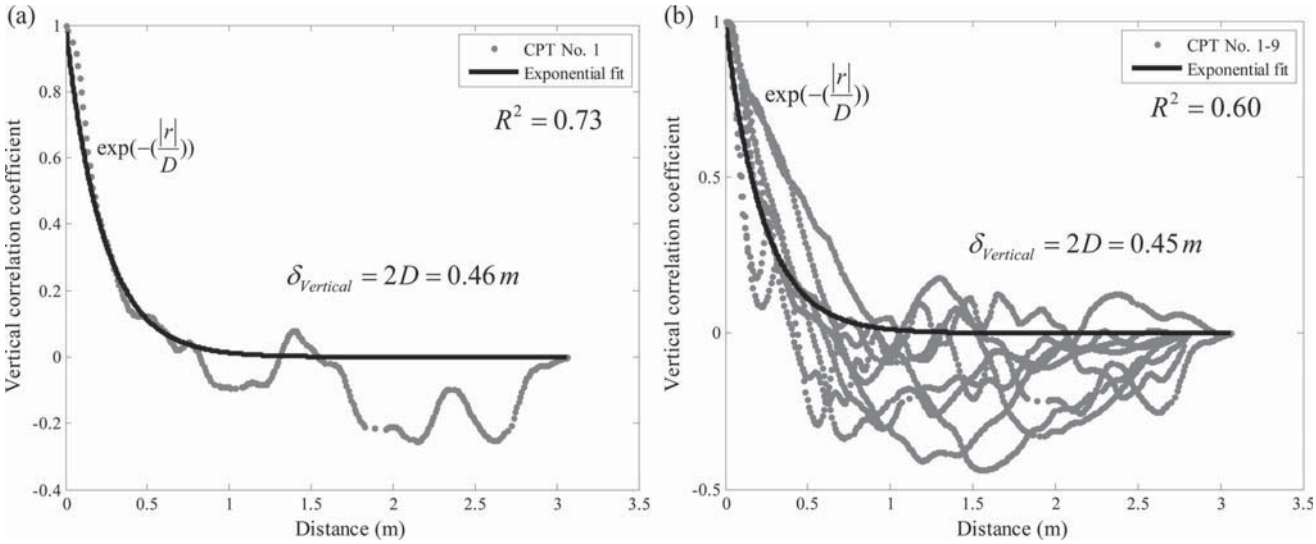

In the vertical direction, each sounding is considered as a set of data with a number of CPT points. Then five measurements in each homogeneous sublayer were taken and the correlation coefficient of them was calculated by eq. (6). The distance r was the difference between two sequences of depth in the position of mean value of each data set (Fig. 8). By fitting an exponential model to these points, the D parameter was estimated to give the value of spatial correlation length. In the horizontal direction, the same approach was employed, but where r was the distance between two sounding locations.

By assuming two sampling zone with the same length (i.e., x_i, $i = 1, 2, \ldots, n$ and y_i, $i = 1, 2, \ldots, n$), the sample means and sample variances have been estimated and sample correlation coefficients are found with eq. (6).

To convert the data set to a random field with a stationary mean and variance, eq. (7) is used:

$$(7) \qquad x_i' = \frac{x_i - \overline{X}}{S_X} \quad y_i' = \frac{y_i - \overline{Y}}{S_Y}$$

The correlation coefficients are calculated between one fixed cone penetration test and the remaining tests. To incorporate as many different intervals between the cone penetration tests, all data sets are fixed in turn (with no repetition).

This was also done for the horizontal direction except that each 5 data points were taken from each sounding, and as shown in Fig. 8, the distance between data points was the distance between CPT soundings (r_2).

Spatial correlation length (vertical direction)

The spatial correlation length, also known as the scale of fluctuation, is a concise indicator of the variability of a strongly correlated domain. There are various techniques available in the geotechnical literature for the estimation of the spatial correlation length. Vanmarcke (1977) approximated correlation functions and corresponding correlation lengths of residuals by use of these common models. For example, using the exponential model, DeGroot and Baecher (1993) estimated the horizontal correlation length of undrained shear strength in a soft marine clay

Fig. 11. Vertical correlation coefficient of F_R for (*a*) a representative sounding (CPT No. 2) and (*b*) for all soundings in the sand layer (Frederikshavn site).

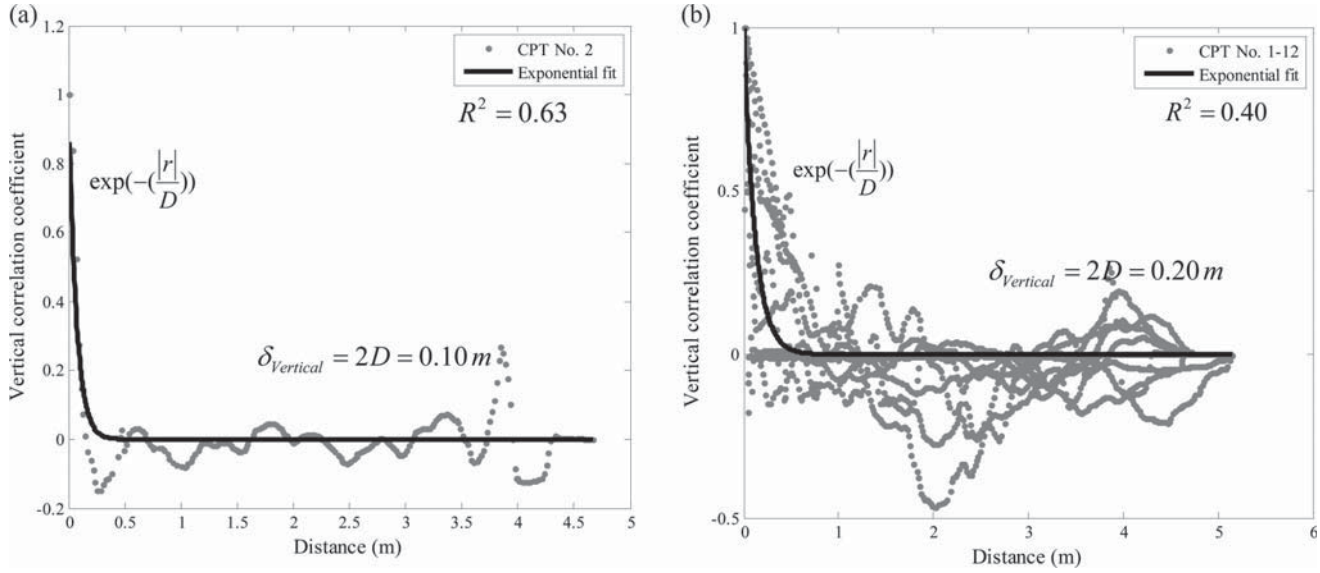

Fig. 12. Vertical correlation coefficient of F_R for (*a*) a representative sounding (CPT No. 1) and (*b*) for all soundings in the sand layer (Aalborg site).

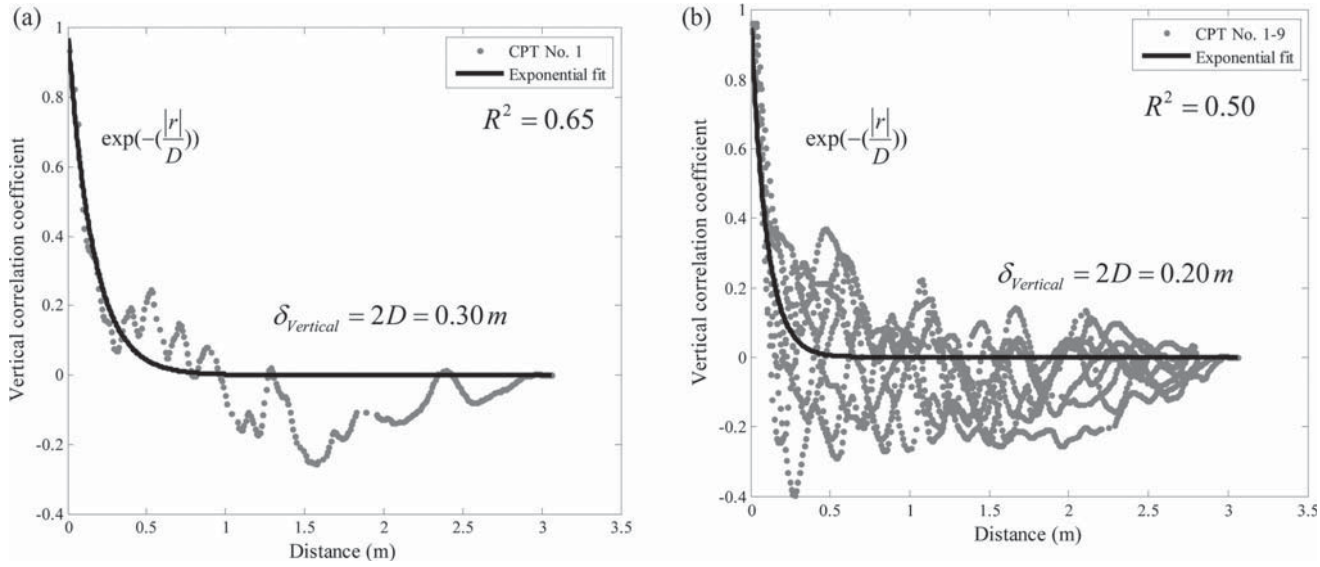

layer, and Tang (1979) employed the quadratic exponential model to estimate the horizontal correlation length of cone resistance of CPT data in a marine clay layer.

Figures 9 and 10 display the correlation coefficient functions and spatial correlation lengths of vertical CPT tip resistance data in all sand layers at a given site. The resistance data are normalized by the vertical effective stresses, as described in eq. (1). The best-fit exponential models for each function are determined using regression analysis. The result of a single representative CPT is shown in Figs. 9*a* and 10*a*, while the exponential model that best fits all correlation coefficient functions from a site is shown in Figs. 9*b* and 10*b*.

The vertical spatial correlation lengths of the cone tip resistance are similar at the two sites. At the Frederikshavn site, the parameter D of the best-fit exponential model is 0.25 m, so the spatial correlation length is 0.5 m. At the Aalborg site, the spatial correlation length is 0.45 m.

The R^2 parameter is also estimated in each case, showing that the model is a reasonable fit to the data, although for the Aalborg site, the scatter in the data are greater.

The spatial correlation length of the normalized friction ratio in the vertical direction in each site is also estimated by fitting the exponential model proposed by Vanmarcke (1977) in Table 3. The vertical spatial correlation length of the friction ratio is 0.2 m at both sites, as illustrated in Figs. 11 and 12. The low values of the R^2 parameter show a greater scatter of data in the sand layer.

Figure 13 plots the spatial correlation lengths obtained by fitting exponential models to each individual CPT sand layer profile against the corresponding mean values of q_{c1N} and F_R. Figure 13*a* shows that the spatial correlation lengths and mean values of cone tip resistance (q_{c1N}) fall into similar ranges at the two sites. However, Fig. 13*b* shows that the mean values of F_R in the Frederikshavn site are greater than in the Aalborg site. The latter is mostly of a clean sand type while the former also contains silty

Fig. 13. Vertical spatial correlation lengths of (*a*) q_{c1N} and (*b*) F_R, plotted against the mean, for the Frederikshavn and Aalborg sites.

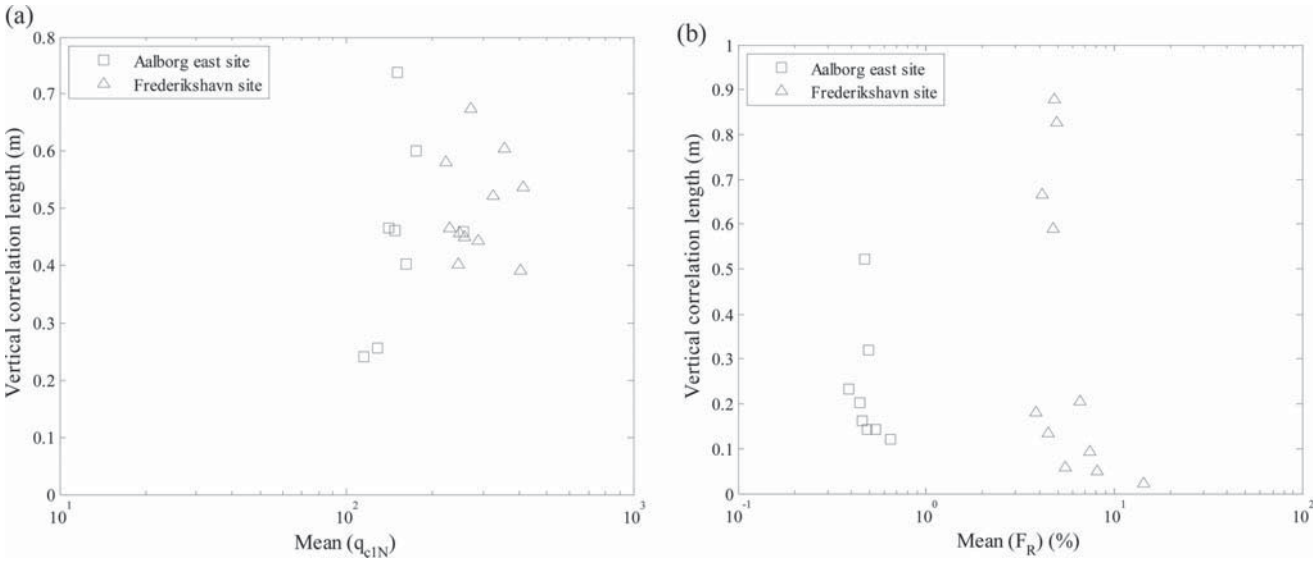

Table 3. Results of spatial variability of cone data for sand layer in the horizontal direction (Aalborg site).

		Layer thickness (m)				
Cone parameter	Statistical parameter	0–1	1–2	2–3	3–4	4–5
Normalized cone resistance	Number of samples	50	50	50	50	50
	COV (%)	28	32	26	31	36
	Mean	52.75	56.94	42.93	48.04	46.93
Normalized friction ratio	Number of samples	50	50	50	50	50
	COV (%)	24	16	24	35	30
	Mean	0.5	0.5	0.46	0.51	0.46

Table 4. Results of spatial variability of cone data for sand layer in the horizontal direction (Frederikshavn site).

		Layer thickness (m)				
Cone parameter	Statistical parameter	0–1	1–2	2–3	3–4	4–5
Normalized cone resistance	Number of samples	50	50	50	50	50
	COV (%)	29	30	26	45	95
	Mean	14.91	15.64	13.56	25.82	62.25
Normalized friction ratio	Number of samples	50	50	50	50	50
	COV (%)	53	37	70	27	100
	Mean	3.96	4.32	5.54	4.48	20.07

sands, and this may not come as a surprise given that the friction ratio increases by increasing the fine content.

In both sites, the lower and upper bounds of the spatial correlation length in F_R are greater than the bounds in q_{c1N}. The absence of a strong correlation structure in F_R is justified by the fact that sleeve friction measurements are inherently much more erratic than tip resistance measurements. The sleeve friction is affected only by adjacent soil, while q_{c1N} is influenced by a volume of soil around the cone tip that is larger than the sampling interval. Therefore, a few consecutive values of q_{c1N} are affected by the same volume of soil as the cone penetrates.

Spatial correlation length (horizontal direction)

This section estimates horizontal correlation coefficient structures using the CPT datasets collected at Aalborg and Frederikshavn. Tables 3 and 4 summarize the horizontal variability of normalized CPT measurements in one-metre interval layers obtained from the last five metres of soundings, which consist mostly of sand and silty sand at both sites. The COV values of normalized cone resistance and friction ratio measurements taken at the Aalborg site are all in a fairly narrow range. In Frederikshavn, however, the COV values are much higher and more variable. In particular, the last metre has a COV larger than 95% for both CPT measurements, testifying to the high variability of this region.

Note that each sublayer with one metre thickness is considered a separate statistical domain with limited data. The correlation coefficient of data in each layer was estimated with a distance as described earlier and regression analysis was employed to determine the *D* parameter and spatial correlation length as proposed by Vanmarcke (1977) in the exponential model. Figures 14–17 show the correlation coefficient of normalized cone data versus relative distance in two sites and the best fit exponential curves. By estimating the *D* parameters of the model, the average spatial correlation length of the normalized cone resistance is 2 m in horizontal direction for the Aalborg site, and 1.2 m for the Frederikshavn site. The average horizontal spatial correlation lengths of the normalized friction ratio are 1.2 and 1.4 m for the Aalborg

Fig. 14. (*a*) Horizontal correlation coefficient of q_{c1N} for all soundings in the sand layer. (*b*) Fitting an exponential curve to the mean values (Aalborg site).

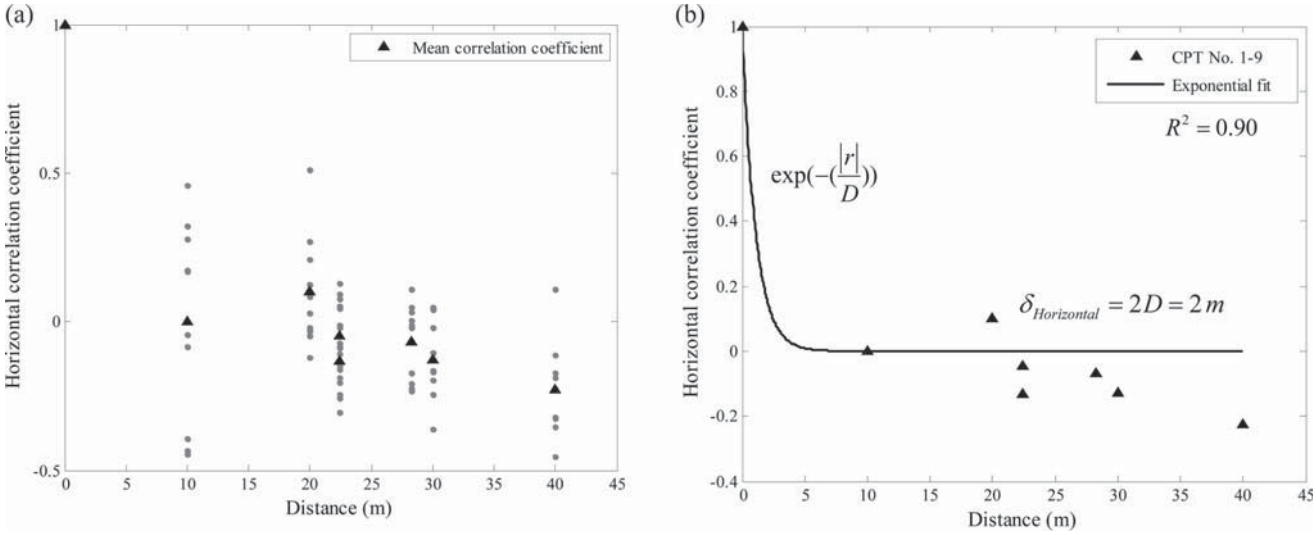

Fig. 15. (*a*) Horizontal correlation coefficient of q_{c1N} for all soundings in the sand layer. (*b*) Fitting an exponential curve to the mean values (Frederikshavn site).

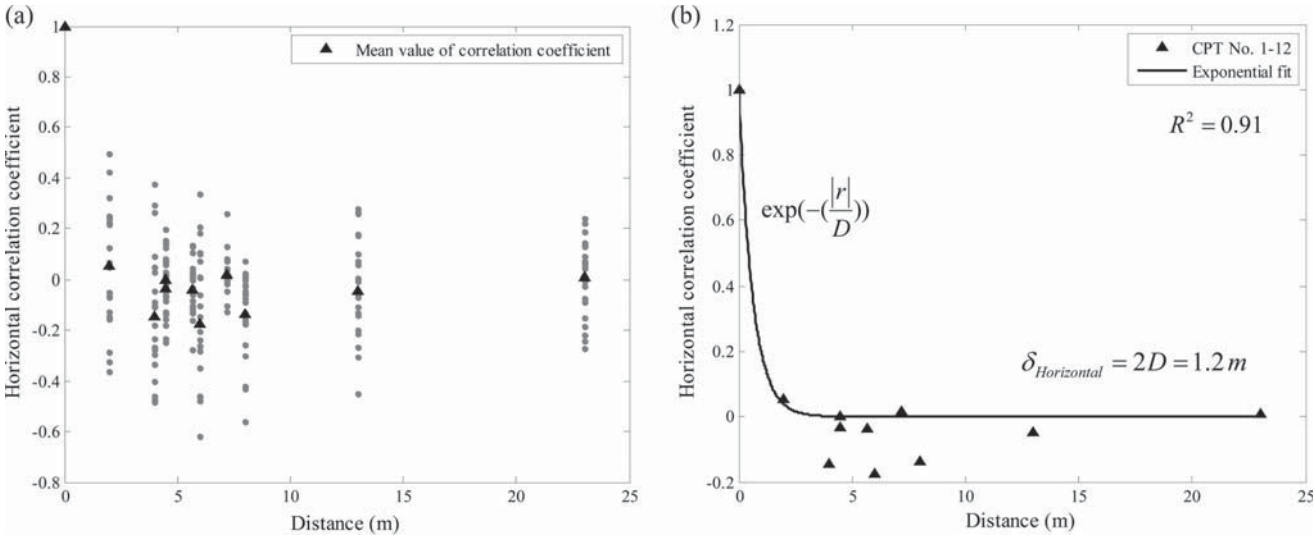

and Frederikshavn sites respectively. The values of R^2 near 0.90 indicates that the regression curve fits the data quite well in all charts.

Summary of results and discussions

For both sites, the values of correlation length for normalized cone resistance and friction ratio are summarized in Table 5. What we have in Table 5 is the correlation length estimated after fitting the model to all soundings (in the vertical direction) and all layers in the horizontal direction. These values are the mean of the correlation length in each direction. Table 5 indicates anisotropic spatial correlation lengths, with the vertical spatial correlation length being anywhere from two to seven times shorter than that in the horizontal direction.

Comparing the values of correlation length and distance between sample points in both directions reveals a high variability in the random field. This can be expressed in terms of inhomogeneities of the soil deposit because of the inclination of soil layers. Under the simplifying assumptions that the soil layers are ideally horizontal and homogenous, we did not consider the big influence of inclined soil layers on the results. If there is an inclination in the soil layers, then the data points taken from different layers show a poor correlation. This can happen in the horizontal as well as the vertical directions. As shown in Fig. 18, the measured data at the border between two layers of sand and clay may show more correlation than points that are in the same level as they are. The consideration of inclined layers will be let for future work.

Conclusion

This paper considered soil variability in CPT test data from two different sites in the north of Denmark. The cone resistance and sleeve friction measurements were first normalized for vertical stress, and then used to identify homogonous sublayers following the soil classification system proposed by Robertson (1990). First, the COV values of normalized cone data in both directions were determined. For both sites, the vertical COV values of normalized cone resistance are higher in coarse-grained sands than in fine soil. This is also the case for the normalized sleeve friction in the

Fig. 16. (*a*) Horizontal correlation coefficient of F_R for all soundings in the sand layer. (*b*) Fitting an exponential curve to the mean values (Aalborg site).

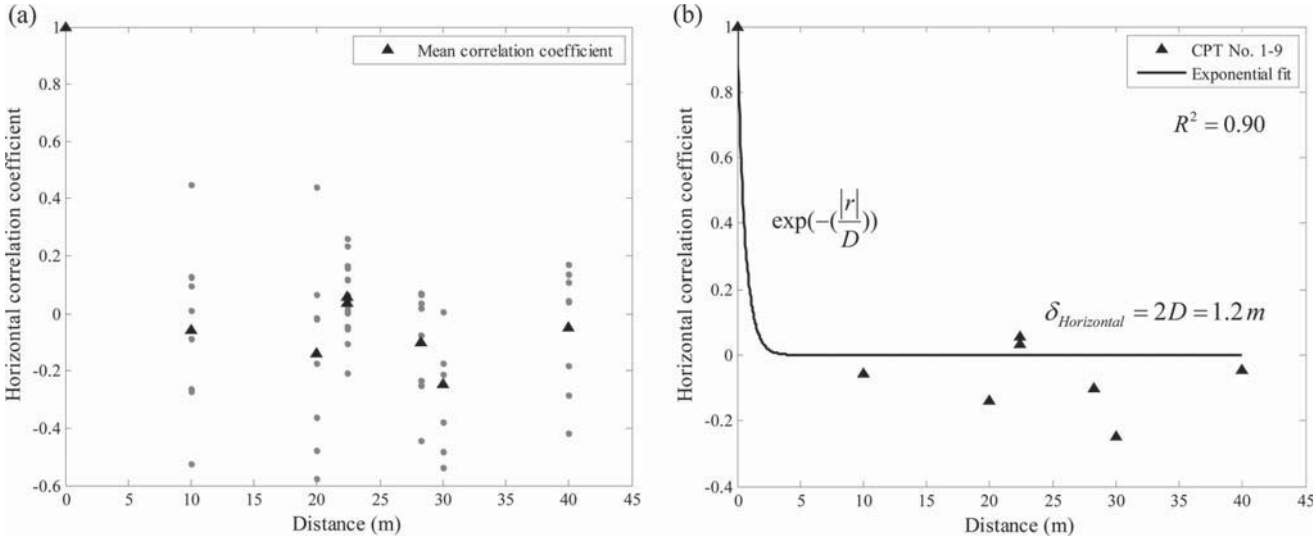

Fig. 17. (*a*) Horizontal correlation coefficient of F_R for all soundings in the sand layer. (*b*) Fitting an exponential curve to the mean values (Frederikshavn site).

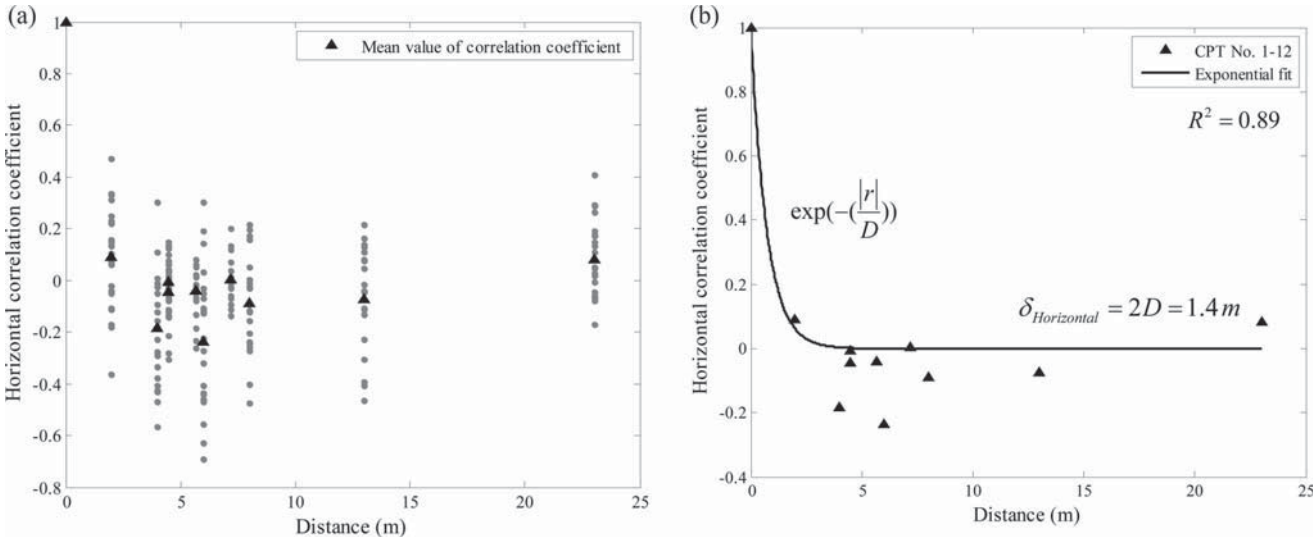

Table 5. Mean values of spatial correlation length in vertical and horizontal direction at both sites.

Site	Cone parameter	Vertical correlation length (mean value)	Horizontal correlation length (mean value)
Frederikshavn	Normalized cone resistance (q_{c1N})	0.5	1.2
	Normalized friction ratio (F_R)	0.2	1.4
Aalborg	Normalized cone resistance (q_{c1N})	0.45	2.0
	Normalized friction ratio (F_R)	0.2	1.2

Aalborg site. However, no such trend exists in the vertical COV values of normalized sleeve friction in Frederikshavn. The expectation that very fine-grained soil layers tend to have less variation of soil parameters than granular soil layers is consistent with this finding.

In the horizontal direction, the maximum COVs occur in the last layer of sand deposits in the Frederikshavn site. This effect may be because of thinly interbedded silt mixtures within the layer (Fig. 7*b*).

To more precisely characterize the spatial variability of the cone resistance and sleeve friction, the autocorrelation function with respect to physical distance was calculated on measurements from sand layers. The spatial correlation distance for each variable was estimated by fitting a simple exponential model to these data.

To describe a random field concisely in the second moment sense, the spatial correlation length and the coefficient of variation in both directions were estimated. For this purpose, the average coefficient of variation of cone data in the vertical and

Fig. 18. Example of CPT soundings in an inclined soil layer.

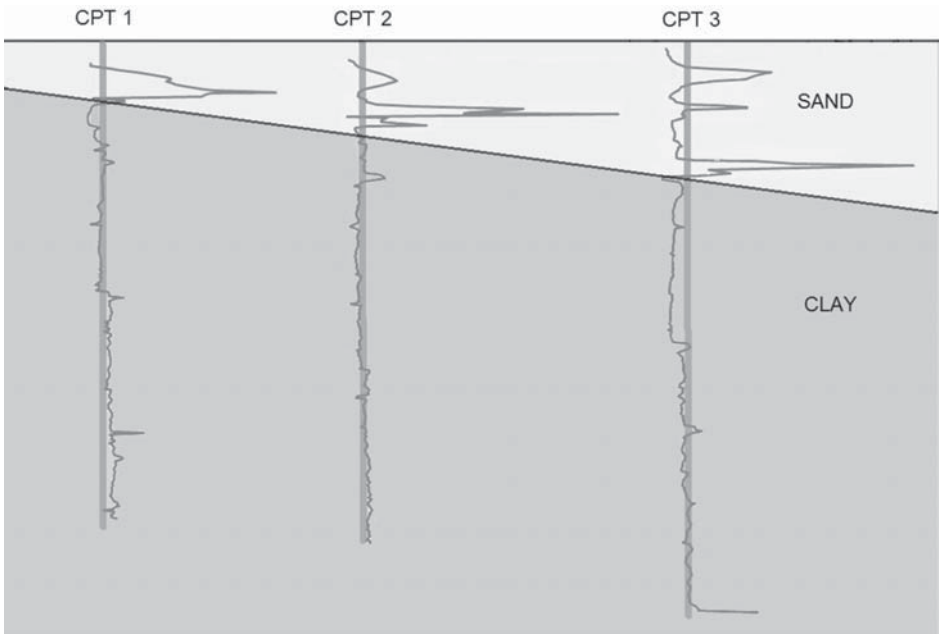

horizontal directions was calculated in both sites, and regression analysis was employed to estimate the spatial correlation length.

Because of natural deposition and soil formation processes, the vertical and horizontal correlation structures from the cone results indicated significant anisotropy, with the vertical length being anywhere from two to seven times shorter than that in the horizontal direction. Also in the vertical direction, it was observed that q_{c1N} is more spatially correlated than F_R, with spatial correlation lengths estimated in the range of 0.5 m and 0.2 m respectively. The same is true in the horizontal direction. The physical meaning of this observation is that the volume of soil around the cone tip that influences q_{c1N} is larger than the sampling interval. As the cone penetrates, several consecutive values of q_{c1N} are affected by almost the same volume of soil, while F_R is affected only by the local soil adjacent to the cone.

References

Alonso, E.E., and Krizek, R.J. 1975. Stochastic formulation of soil properties. *In* Proceedings, 2nd International Conference on Applications of Statistics & Probability in Soil and Structural Engineering, Aachen. Vol. 2, pp. 9–32.

Baecher, G.B. 1986. Geotechnical error analysis. Transportation Research Record, **1105**: 23–31.

Campanella, R.G., Wickremesinghe, D.S., and Robertson, P.K. 1987. Statistical treatment of cone penetrometer test data. *In* Proceedings of the 5th International Conference on Applications of Statistics and Probability in Soil and Structural Engineering, Vancouver. Vol. 2, pp. 1011–1019.

DeGroot, D.J. 1996. Analyzing spatial variability of in situ soil properties. [Invited paper.] *In* Uncertainty in the Geologic Environment, From Theory to Practice, Proceedings of Uncertainty '96. Geotechnical Special Publication No. 58.

DeGroot, D.J., and Baecher, G.B. 1993. Estimating autocovariance of in-situ soil properties. Journal of Geotechnical Engineering, **119**(1): 147–166. doi:10.1061/(ASCE)0733-9410(1993)119:1(147).

DNV. 2010. Recommended practice. Statistical presentation of soil data. DNV standard DNV-RPC207. Det Norske Veritas AS (DNV).

Elkateb, T., Chalaturnyk, R., and Robertson, P.K. 2003*a*. An overview of soil heterogeneity: quantification and implications on geotechnical field problems. Canadian Geotechnical Journal, **40**(1): 1–15. doi:10.1139/t02-090.

Elkateb, T., Chalaturnyk, R., and Robertson, P.K. 2003*b*. Simplified geostatistical analysis of earthquake-induced ground response at the Wildlife Site, California, U.S.A. Canadian Geotechnical Journal, **40**(1): 16–35. doi:10.1139/t02-089.

Fenton, G.A. 1999. Random field modeling of CPT data. Journal of Geotechnical and Geoenvironmental Engineering, **125**(6): 486–498. doi:10.1061/(ASCE)1090-0241(1999)125:6(486).

Fenton, G.A., and Vanmarcke, E.H. 1990. Simulation of random fields via local average subdivision. Journal of Engineering Mechanics, **116**(8): 1733–1749. doi:10.1061/(ASCE)0733-9399(1990)116:8(1733).

Fenton, G.A., and Griffiths, D.V. 2008. Risk assessment in geotechnical engineering. John Wiley and Sons, New York.

Firouzianbandpey, S., Ibsen, L.B., and Vabbersgaard Andersen, L. 2012. CPTu-based geotechnical site assessment for offshore wind turbines—a case study from the Aarhus Site in Denmark. *In* Proceedings of the 22nd International Offshore and Polar Engineering Conference, 17–22 June 2012, Rhodes, Greece.

Griffiths, D.V., and Fenton, G.A. 1993. Seepage beneath water retaining structures founded on spatially random soil. Géotechnique, **43**(4): 577–587. doi:10.1680/geot.1993.43.4.577.

Kulhawy, F.H., Birgisson, B., and Grigoriu, M.D. 1992. Reliability based foundation design for transmission line structures: transformation models for in-situ tests. Report EL-5507(4). Electric Power Research Institute, Palo Alto, Calif.

Moss, R.E., Seed, R.B., and Olsen, R.S. 2006. Normalizing the CPT for overburden stress. Journal of Geotechnical and Geoenvironmental Engineering, **132**(3): 378–387. doi:10.1061/(ASCE)1090-0241(2006)132:3(378).

Nadim, F. 1986. Probabilistic site description strategy. Report 51411–4. Norwegian Geotechnical Institute, Oslo.

Phoon, K.K., Quek, S.T., and An, P. 2003. Identification of statistically homogeneous soil layers using modified Bartlett statistics. Journal of Geotechnical and Geoenvironmental Engineering, **129**(7): 649–659. doi:10.1061/(ASCE)1090-0241(2003)129:7(649).

Reyna, F., and Chameau, J.L. 1991. Statistical evaluation of CPT & DMT measurements at the Heber Road Site. *In* Proceedings of the Geotechnical Engineering Congress. American Society of Civil Engineers, New York, pp. 14–25.

Robertson, P.K. 1990. Soil classification using the cone penetration test. Canadian Geotechnical Journal, **27**(1): 151–158. doi:10.1139/t90-014.

Robertson, P.K., and Wride, C.E. (Fear). 1998. Evaluating cyclic liquefaction potential using the cone penetration test. Canadian Geotechnical Journal, **35**(3): 442–459. doi:10.1139/t98-017.

Tang, W.H. 1979. Probabilistic evaluation of penetration resistances. Journal of Geotechnical Engineering Division, ASCE, **105**(10): 1173–1191.

Uzielli, M., Vannucchi, G., and Phoon, K.K. 2005. Random field characterisation of stress-normalised cone penetration testing parameters. Géotechnique, **55**(1): 3–20. doi:10.1680/geot.2005.55.1.3.

Vanmarcke, E.H. 1977. Probabilistic modeling of soil profiles. Journal of Geotechnical Engineering, **103**(11): 1227–1246.

Wroth, C.P. 1984. The interpretation of in situ soil tests. Géotechnique, **34**(4): 449–489. doi:10.1680/geot.1984.34.4.449.

Wu, T.H., Lee, I.-M., Potter, J.C., and Kjekstad, O. 1987. Uncertainties in evaluation of strength of marine sand. Journal of Geotechnical Engineering, **113**(7): 719–738. doi:10.1061/(ASCE)0733-9410(1987)113:7(719).

List of symbols

A_c projected area of the cone
A_s surface area of the friction sleeve

B_q pore water pressure ratio
COV coefficient of variation
C_Q correction for overburden stress
$C(t)$ covariance function of variable t
D model parameter
F_R normalized friction ratio
F_s sleeve friction
f_s measured sleeve friction
i data point
n correction value for overburden pressure (0.5, 0.7, 1.0 for cohesionless, intermediate, and cohesive soils, respectively)
P_a reference pressure in compatible unit in the equation
Q_c total force acting on the cone
Q_t normalized tip resistance
q_c measured cone tip resistance
q_{c1N} normalized cone resistance
q_t measured resistance
R^2 regression parameter (fit-goodness)
r_1 vertical separation distance between set of data in each sounding
r_2 horizontal separation distance between soundings
S_X, S_Y variance of the sample zones
u_0 initial pore water pressure
u_2 pore water pressure measurement at the back of the cone penetometer
$\overline{X}$, $\overline{Y}$ mean of the sample zones
$X(t)$ observation point at the position X
x_i, y_i sample zones
x_i', y_i' conversion of sample zones to a stationary random field
$\delta_{Vertical}$, $\delta_{Horizontal}$ vertical and horizontal correlation length
$\mu_X(t)$ mean of X at the position t
$\rho(t)$ correlation function
$\sigma_X(t)$ standard deviation of X at the position t
σ_{v0} total vertical stress
σ_{v0}' effective vertical stress

APPENDIX E: PAPER 5

Effect of spatial correlation length on the interpretation of normalized CPT data using a Kriging approach

IS CITED AS:

Firouzianbandpey, S., Ibsen, L. B., Griffiths, D. V., Vahdatirad, M. J., Andersen, L. V., Sørensen, J. D. (2015). "Effect of spatial correlation length on the interpretation of normalized CPT data using a Kriging approach." ***Journal of Geotechnical and Geoenvironmental Engineering***, ASCE. DOI:10.1061/(ASCE)GT.1943-5606.0001358

STATUS: Published

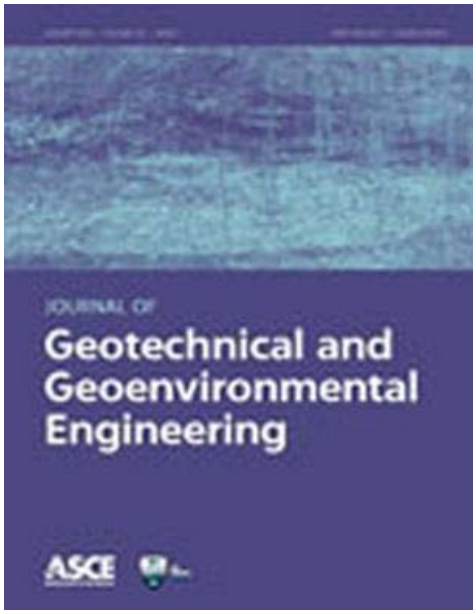

Effect of Spatial Correlation Length on the Interpretation of Normalized CPT Data Using a Kriging Approach

S. Firouzianbandpey, Ph.D.[1]; L. B. Ibsen[2]; D. V. Griffiths[3]; M. J. Vahdatirad, Ph.D.[4]; L. V. Andersen[5]; and J. D. Sørensen[6]

Abstract: In geotechnical engineering analysis and design, the frequency and spacing of borehole information is of great interest, especially when field data are limited. This paper uses random field models to deal with uncertainty in soil properties owing to spatial variability, by analyzing in-situ cone penetration test (CPT) data from a sandy site in northern Denmark. To provide a best estimate of properties between observation points in the random field, a Kriging interpolation approach has been applied. As expected, for small correlation lengths, the estimated field quantities at intermediate locations between data points are close to the mean value of the measured results, and a high uncertainty is associated with the estimate. A longer correlation length reduces the error and implies more variation in the estimated values between the data points. **DOI: 10.1061/(ASCE)GT.1943-5606.0001358.**

Author Keywords: Geostatistics; Kriging; Spatial correlation length; Cone penetration test (CPT); Random field; Normalized cone data.

Introduction

In geotechnical investigations, the scope is often governed by how much the client and project manager are willing to spend, rather than by what is needed to characterize the subsurface conditions (e.g., Jaksa et al. 2005). To design and analyze a foundation, practitioners ideally would like to know the soil properties at many locations; but achieving this goal can be unrealistic and expensive. Researchers are searching for new ways to determine these parameters using statistical approaches. Probabilistic methods have been applied in geotechnical engineering for assessing the effects of uncertainties in geotechnical predictions (e.g., Zhang et al. 2011), and the application of geostatistics to large geotechnical projects has also proved to be a powerful tool, allowing coordination of field data in analysis and design (e.g., Ryti 1993; Rautman and Cromer 1994; Wild and Rouhani 1995; Rouhani 1996).

When uncertainties occur, they may often be attributable to limited sampling, rather than inaccuracies/measurement uncertainties in the soil tests themselves (e.g., Goldsworthy et al. 2007). In-situ tests in particular can provide a good characterization of soil properties at the locations where tests were performed, but inevitable uncertainty remains at locations which have not been examined.

A more formal mathematical characterization of spatial variability using random fields (e.g., Fenton and Griffiths 2008), can quantify probabilistically how the variability at one location can be used to represent the variability at another location some distance away. The well-established Kriging method, based on D. G. Krige's empirical work for evaluating mineral resources (Krige 1951), and later formalized by Matheron (1963) into a statistical approach in geostatistics can also be used to perform spatial interpolation between known borehole data. In addition to generating a best, linear unbiased estimate of a random field between known data, Kriging has the added ability of estimating certain aspects of the mean trend by using a weighted linear combination of the values of a random field at each observation point (e.g., Fenton and Griffiths 2008). In environmental and geotechnical engineering, Kriging is commonly applied to the mapping of soil parameters and piezometric surfaces (e.g., Journel and Huijbegts 1978; Delhomme 1978; ASCE 1990).

Kriging has numerous advantages compared with other common interpolation techniques. For example, Kriging can produce site- and variable-specific interpolation schemes by directly incorporating a model of the spatial variability of the data (Rouhani 1996). As a collection of linear regression techniques, Kriging accounts for the stochastic dependence among the data (Olea 1991). The geological processes result in a *stochastic* dependency, which may have acted over a large area across geological time scales (e.g., sedimentation in large basins) or in fairly small domains for only a short time (e.g., turbiditic sedimentation, glacio-fluviatile sedimentation). Geological characteristics that form in a slow and steady geological environment are better correlated to each other than those that result from an often abruptly changing geological process.

The purpose of this study is to interpolate normalized cone data in a sandy site by using the Kriging method and investigate the effect of spatial correlation length on the results. This statistical analysis procedure consists of two main parts:

1. Verification of the method using a random field simulation. In this part the Kriging method has been applied to a simulated 3D Gaussian random field and then at given intermediate points, these simulated values compared with the best estimate

[1]Engineer, Dept. of Civil Engineering, Aalborg Univ., 9000 Aalborg, Denmark (corresponding author). E-mail: sf@civil.aau.dk

[2]Professor, Dept. of Civil Engineering, Aalborg Univ., 9000 Aalborg, Denmark.

[3]Professor, Dept. of Civil and Environmental Engineering, Colorado School of Mines, Golden, CO 80401; and Australian Research Council Centre of Excellence for Geotechnical Science and Engineering, Univ. of Newcastle, Callaghan, NSW 2308, Australia.

[4]Engineer, Dept. of Civil Engineering, Aalborg Univ., 9000 Aalborg, Denmark.

[5]Associate Professor, Dept. of Civil Engineering, Aalborg Univ., 9000 Aalborg, Denmark.

[6]Professor, Dept. of Civil Engineering, Aalborg Univ., 9000 Aalborg, Denmark.

Note. This manuscript was submitted on July 8, 2014; approved on April 29, 2015; published online on June 30, 2015. Discussion period open until November 30, 2015; separate discussions must be submitted for individual papers. This paper is part of the ***Journal of Geotechnical and Geoenvironmental Engineering***, © ASCE, ISSN 1090-0241/04015052(9)/$25.00.

Kriging values and estimates of the standard deviation or the coefficient of variation of the error.
2. Applying Kriging to real values of cone data. Kriged values are also estimated at different depths below the surface based on two different horizontal correlation lengths to analyze the effect of correlation length on the results.

The results indicate that by increasing the horizontal correlation length, the standard deviation of estimated values by the Kriging method decreases, resulting in less uncertainty in prediction of values at intermediate locations. It is worth noting that in this procedure, it is assumed that the data represent samples from a statistical homogeneous domain.

Normalization of Cone Data

Because of the significant influence of the effective overburden stress on CPT measurements (e.g., Moss et al. 2006), various methods have been proposed for normalizing CPT data to account for this effect. In this study, the technique proposed by Robertson and Wride (1998) has been applied to the measurements of cone tip resistance, i.e.

$$q_{c1N} = \left(\frac{q_c}{P_a}\right) C_Q, \qquad C_Q = \left(\frac{P_a}{\sigma'_{v0}}\right)^n \tag{1}$$

where q_{c1N} is the dimensionless cone resistance normalized by the weight of soil on top of the cone, q_c is the measured cone tip resistance, and C_Q is the correction for overburden stress. The power n takes the values 0.5, 1.0 and 0.7 for cohesionless, cohesive and intermediate soils, respectively, whereas σ'_{v0} is the effective vertical stress and P_a is the reference pressure (atmospheric pressure) in the same units as σ'_{v0} and q_c.

Description of the Site

This study concerns a site close to Aalborg in northern Denmark where a wind turbine blade storage facility is to be constructed. The site is a basin deposit area as it is close to the Limfjord. The soil layers consist of 4 m clay on top and silty sand in the lower layers. Using piezocone penetration test (CPTu) data, the statistical characteristics of the cone tip resistance at the site have been estimated. A total of nine cone penetration tests was conducted using a Geotech NOVA Acoustic system and a 20 t digital piezocone penetrometer, and data was acquired digitally. The CPTu system also consists of a hydraulic pushing and leveling system and 1-m long segmental rods. Fig. 1 shows a schematic cross section of the CPT probe. All CPTu soundings reached a depth of approximately 8 m. The nine soundings were arranged in a cross-shaped pattern with a 10-m separation distance between holes, and the cross was framed by four boreholes (Fig. 2). CPT data were sampled at 20-mm intervals. Fig. 3 illustrates a representative CPT profile obtained in the field. Standard classification test results were carried out on samples retrieved from the boreholes showing that the soil deposit is primarily sand and a sand–silt mixture.

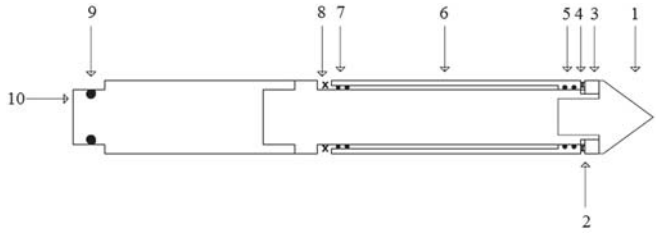

Item	Description	Item	Description
1.	Point/ Tip, 10 cm^2	6.	Friction sleeve
2.	Support ring under the X-ring	7.	Friction sleeve, 2 pcs O-ring
3.	Filter ring brass, 10 cm^2 – Pore pressure	8.	X-ring
4.	X-ring	9.	O-ring, battery pack, 10 cm^2
5.	Friction sleeve, 2 pcs O-ring	10.	Serial number of the probe

Fig. 1. CPT probe, 10 cm^2

Modeling Spatial Variability of the Site Using Kriging

Kriging is essentially a best, linear unbiased estimation with the added benefit of being able to estimate the mean. The main objective is to provide a best estimate of the random field at unobserved points. The Kriging estimate is modeled as a linear combination of the observations

$$\hat{X} = \sum_{k=1}^{n} \beta_k X_k \tag{2}$$

where x is the spatial position of the unobserved value being estimated. The unknown coefficients β_i are determined by considering the covariance between the observations and the prediction point.

To assess the effect of known data at an intermediate position, maps were created by using kriging on the cone resistance data from CPT soundings in the region. This approach provided a best estimate of a random field between known data to estimate the random field at any location using a weighted linear combination of the values of the random field at observation points. The following steps are applied for this procedure:

Assume a correlation length of the site (θ) (in this study two arbitrary correlation lengths have been chosen).

Estimate the correlation coefficient of the data (ρ) assuming a homogeneous random field

$$\rho(\mathbf{x_i}, \mathbf{x_j}) = \exp\left(\frac{-2|\tau_{ij}|}{\theta}\right) \qquad \tau_{ij} = |\mathbf{x_i} - \mathbf{x_j}| \tag{3}$$

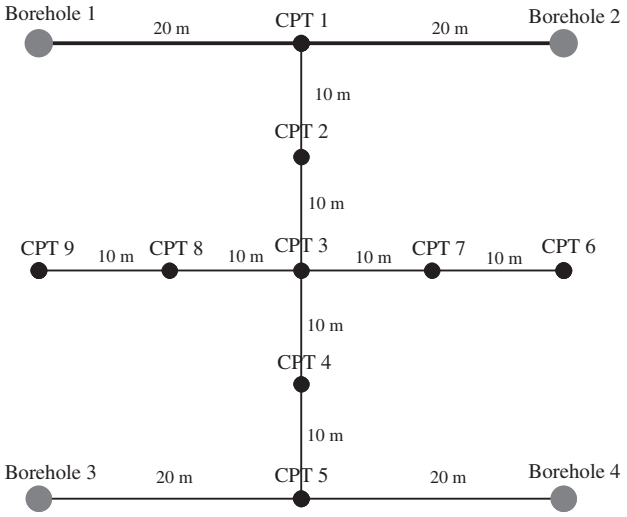

Fig. 2. Plan of boreholes and CPTu positions

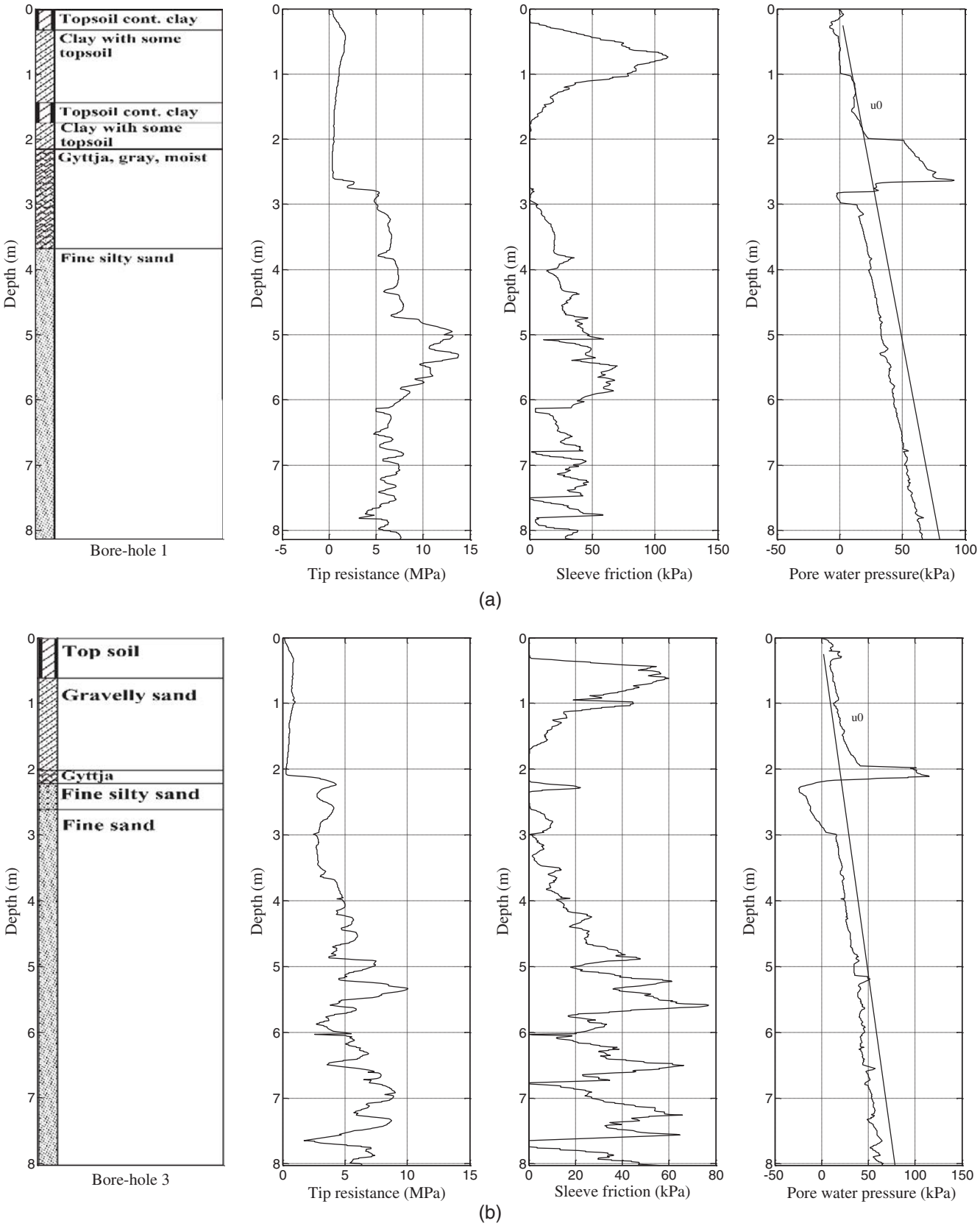

Fig. 3. Two representative CPT profiles obtained from the site. u_0 is the hydrostatic pore pressure induced by the phreatic level of the region (CPT 3 and 5)

Calculate the covariance between data (between $\mathbf{x}_i$ and $\mathbf{x}_j$)

$$C_{ij} = \sigma_x^2 \exp\left(\frac{-2|\tau_{ij}|}{\theta}\right), \qquad \left(\text{Note:}\rho(\tau) = \frac{C(\tau)}{\sigma_x^2}\right) \tag{4}$$

In Kriging it is assumed that the mean can be expressed as in a regression analysis

$$\mu(X) = \sum_{i=1}^{m} a_i g_i(x) \tag{5}$$

where a_i is an unknown coefficient and $g_1(x) = 1$, $g_2(x) = x$, $g_3(x) = x^2$, and so on (in a one-dimensional case). A similar approach is used in higher dimensions (Fenton and Griffiths 2008).

Estimate of the Kriging matrix $\mathbf{K}$

$$\mathbf{K} = \begin{bmatrix} C_{11} & C_{12} & \cdots & C_{1n} & g_1(x_1) & g_2(x_1) & \cdots & g_m(x_1) \\ C_{21} & C_{22} & \cdots & C_{2n} & g_1(x_2) & g_2(x_2) & \cdots & g_m(x_2) \\ \cdot & \cdot & \cdot & \cdot & \cdot & \cdot & \cdot & \cdot \\ \cdot & \cdot & \cdot & \cdot & \cdot & \cdot & \cdot & \cdot \\ \cdot & \cdot & \cdot & \cdot & \cdot & \cdot & \cdot & \cdot \\ C_{n1} & C_{n2} & \cdots & C_{nn} & g_1(x_n) & g_2(x_n) & \cdots & g_m(x_n) \\ g_1(x_1) & g_1(x_2) & \cdots & g_1(x_n) & 0 & 0 & \cdots & 0 \\ g_2(x_1) & g_2(x_2) & \cdots & g_2(x_n) & 0 & 0 & \cdots & 0 \\ \cdot & \cdot & \cdot & \cdot & \cdot & \cdot & \cdot & \cdot \\ \cdot & \cdot & \cdot & \cdot & \cdot & \cdot & \cdot & \cdot \\ \cdot & \cdot & \cdot & \cdot & \cdot & \cdot & \cdot & \cdot \\ g_m(x_1) & g_m(x_2) & \cdots & g_m(x_n) & 0 & 0 & \cdots & 0 \end{bmatrix}. \tag{6}$$

Because $\mathbf{K}$ is a function of the observation point locations and covariance between them, it could be inverted and used repeatedly at different spatial points to build up the best estimate of the random field.

Calculate the covariance between the ith observation point and a given, intermediate spatial point $\mathbf{x}$

$$\mathbf{M} = \begin{Bmatrix} C_{1\mathbf{x}} \\ C_{2\mathbf{x}} \\ \cdot \\ \cdot \\ \cdot \\ C_{n\mathbf{x}} \\ g_1(\mathbf{x}) \\ g_2(\mathbf{x}) \\ \cdot \\ \cdot \\ \cdot \\ g_m(\mathbf{x}) \end{Bmatrix} \tag{7}$$

By definition, the so-called best linear unbiased predictor $\hat{X}$ of X implies that it is linear. So the n unknown weights β_k in Eq. (2) have to be determined to find the best estimate at the point $\mathbf{x}$

$$\mathbf{K}\boldsymbol{\beta} = \mathbf{M}, \qquad \boldsymbol{\beta} = \begin{Bmatrix} \beta_1 \\ \beta_2 \\ \cdot \\ \cdot \\ \cdot \\ \beta_n \\ -\eta_1 \\ -\eta_2 \\ \cdot \\ \cdot \\ \cdot \\ -\eta_m \end{Bmatrix} \tag{8}$$

For each specific point, $\mathbf{M}$ changes, as does the vector of weights, β. The quantities η_i are a set of Lagrangian parameters used to solve the variance minimization problem subject to the unbiased conditions.

Estimate unknown values at the desired location

$$\hat{X}(x) = \sum_{k=1}^{n} \beta_k x_k \tag{9}$$

where the hat indicates that this is an estimate, and $x_1, x_2, \ldots, x_k$ are observation points.

Concerning step 1 in the procedure listed above, there are different techniques available in the literature for the estimation of the correlation length using geotechnical data of the field (Vanmarcke 1977; DeGroot and Baecher 1993; Tang 1979; DNV 2010). If sufficient data are available, then it is possible to use one of those techniques. The correlation coefficient between each pair of data can be calculated and plotted versus the spatial distance between the corresponding positions. Then an admissible type of autocorrelation function is fitted to them and using the regression analysis, the *best* values for the model parameters (incl. correlation length parameter) can be estimated (JCSS-C1 2006). For example, in the quadratic exponential model, the correlation length is the double of the D factor (Firouzianbandpey et al. 2014).

With regard to step 4 of the procedure, an assumption that the mean is either constant (i.e., $m = 1$, $g_1(x) = 1$, $a_1 = \mu(X)$ or linearly varying ($m = 2$, $\mu(X) = a_1 + a_2 x$) is usually sufficient. The correct form of the mean trend can be determined by plotting the results and visually checking the mean trend. The trend can also be found by performing a regression analysis or performing a more complex structural analysis (Journel and Huijbergts 1978).

Method Verification Using Random Field Simulation

In this study, the Kriging method has been applied to a generated 3D Gaussian random field using the correlation matrix decomposition method. The procedure was as follows:

1. Simulate a realization of the random field

Using the simulated values in the soundings positions, establish a Kriging model.

The best estimate Kriging values of cone data are then compared with the simulated values at given intermediate points. This was also undertaken for the purpose of verification of the procedure in assuming a constant mean trend and ignoring Lagrangian parameters.

The mean and standard deviation of the normalized cone data from the field q_{c1N} (e.g.) were used to generate the random field. A Markovian correlation function

$$\rho_{\text{field}} = \exp\left(-\frac{2|\Delta x|}{\delta_x} - \frac{2|\Delta y|}{\delta_y} - \frac{2|\Delta z|}{\delta_z}\right) \tag{10}$$

has been used for modeling the random field (for example, Vahdatirad et al. 2014) and the correlation between points in the field was modeled as an exponentially decaying function of the absolute distance between the points. In Eq. (10), Δx, Δy and Δz are the spatial distances in the horizontal and vertical directions, respectively, and δ_x, δ_y and δ_z are correlation lengths in the appropriate directions. The real correlation lengths of cone data in the region (δ_x, $\delta_y = 2$ m and $\delta_z = 0.45$ m) have been estimated and used in the model (Firouzianbandpey et al. 2014).

For each realization, a vector of standard Gaussian random seeds, U_x, is generated for each random field with the same size as the number of integration points. The correlation matrix $\tilde{R}$ is constructed with the correlation function specified in Eq. (10) and decomposed as

$$\tilde{L} \times \tilde{L}^T = \tilde{R} \tag{11a}$$

$$G(x) = \tilde{L} \times U(x) \tag{11b}$$

where $\tilde{L}$ is the lower triangular matrix used for transferring U_x to the correlated field with zero mean $G(x)$.

For each random variable, transformation to the random fields with real distribution is:

$$Y = \exp(\mu_{\ln} + \sigma_{\ln} G)$$

where $\mu_{\ln}$ and $\sigma_{\ln}$ are lognormal mean value and lognormal standard deviation for q_{c1N}, respectively.

After 1,000 Monte Carlo simulations, the mean values of the random field at the same position as the soundings were used to estimate the Kriging values at intermediate positions in the field. Then the difference between the Kriging estimations and those generated by the random fields has been calculated and by fitting a normal distribution, the mean value of the error has been found. As shown in Fig. 4(a), the mean value of the error is very small, and it indicates that the method is quite acceptable in estimating values. Fig. 4 illustrates the results in the simulated random field. The black circles identify the location of the CPT soundings.

Applying Kriging to the Real Values of Cone Data

Kriged values were also estimated at a depth of 2 m below the surface based on two different horizontal correlation lengths: 5 and 10.5 m (half of the mean distance between soundings which was

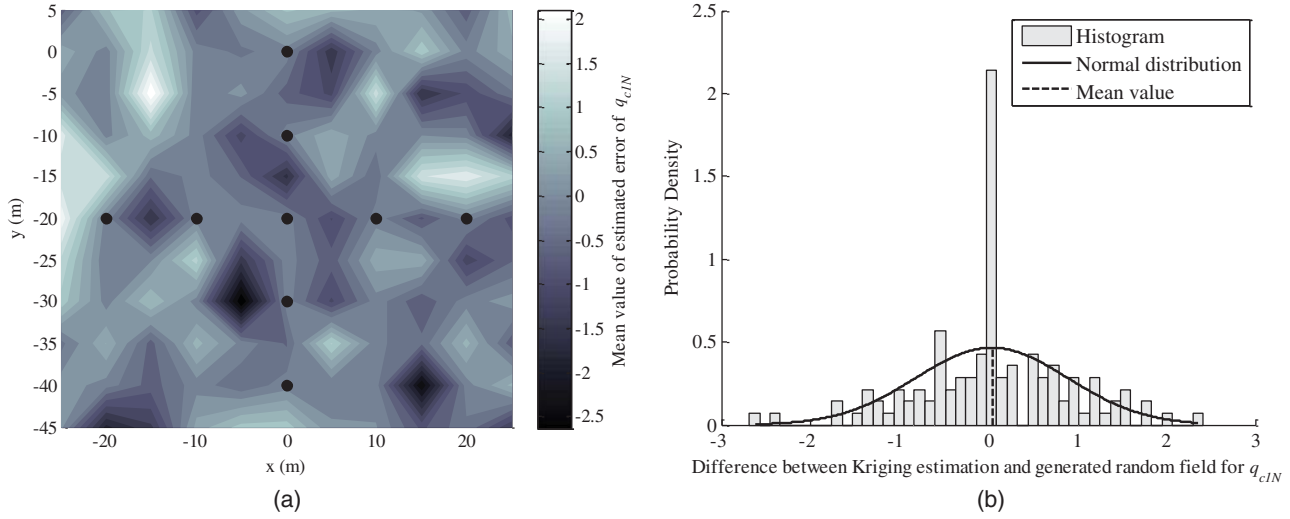

Fig. 4. Kriging estimation: (a) estimated random field at 2 m depth; (b) difference between Kriging estimation and generated random field ($\mu_{qc1N} = 129.7$, $\sigma_{qc1N} = 25$)

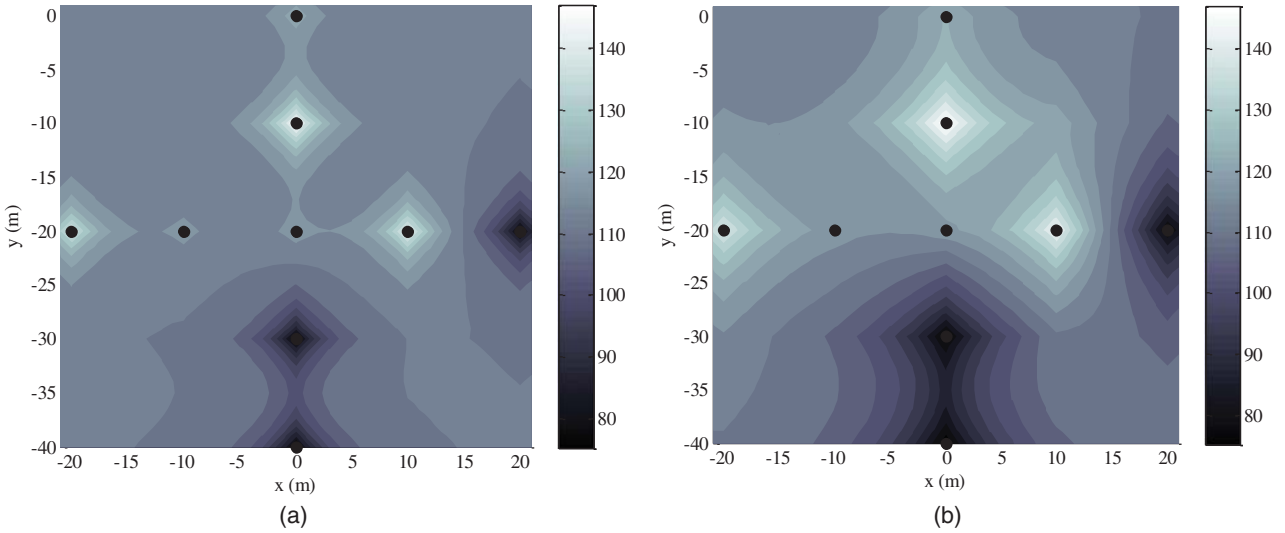

Fig. 5. Normalized cone resistances estimated by Kriging at a depth of 2 m with $\theta_v = 0.45\,m$: (a)$\theta_h = 5\,m$; (b)$\theta_h = 10.5\,m$

21 m), are used to examine the effect of the correlation length on the kriged values. For the vertical direction, the real value of vertical correlation length of the region ($\theta_v = 0.45$ m) was applied. Because the real estimated horizontal correlation length of data was too small, it was preferred in the study to employ two representative values of this parameter for the purpose of comparison and inference.

Fig. 5 shows a map of the estimated normalized cone resistances with two different correlation lengths at the chosen depths. To reflect the variability of this parameter in two directions, the normalized cone resistance values are shown as contours throughout the site plan. The black circles again identify the locations of the CPT soundings. As the distances between these points are increased, the correlation between the values of normalized cone resistances decreases. In other words, the values are increasingly different as the distances between the points increase. When the correlation length is large, the data are highly correlated, and the values are much closer to each other for a greater distance. This fact can be seen by comparing two plots with different horizontal correlation lengths. When the correlation length increases, points with the same color are distributed in a wider separation distance from fixed known locations, which implies a higher dependency in space. In the figures, θ_h and θ_v denote horizontal and vertical correlation lengths, respectively.

Estimator Error

Owing to a finite number of observations, there is always an error associated with any estimate of a random process. This error should be calculated to achieve the accuracy of the estimate. The difference between the estimated $\hat{X}(x)$ and its true (but unknown and random) value $X(x)$ can be given by

$$\mu_E = E[X(x) - \hat{X}(x)] = 0 \tag{12}$$

$$\sigma_E^2 = E[X(x) - \hat{X}(x)^2] = \sigma_X^2 + \beta_n^T(K_{n\times n}\beta_n - 2M_n) \tag{13}$$

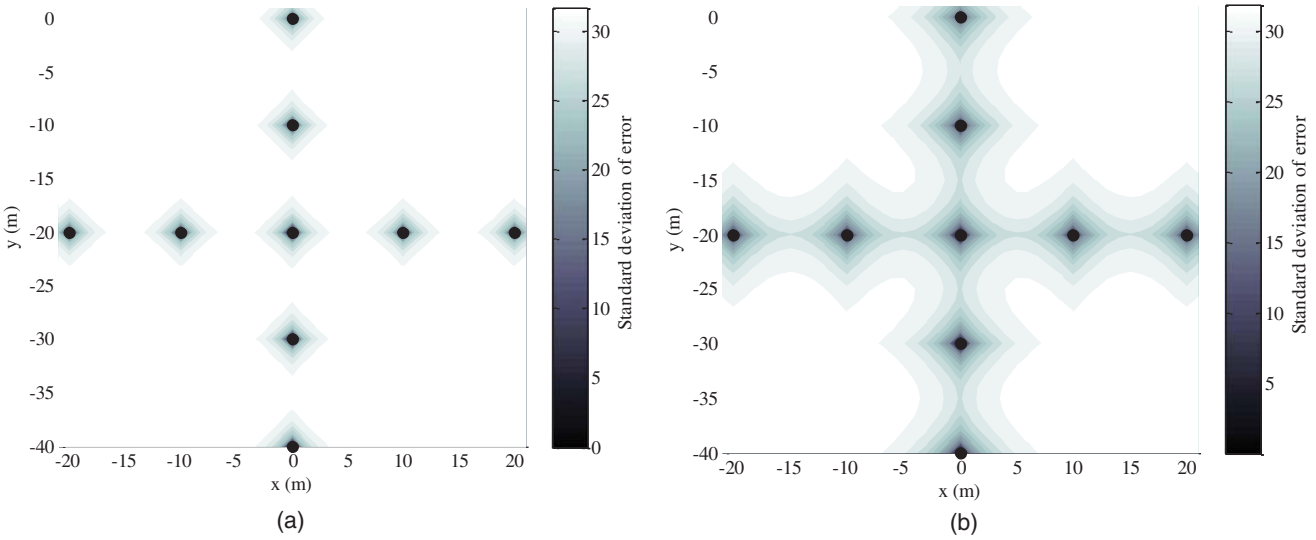

Fig. 6. Estimated standard deviation of the error at a depth of 2 m with $\theta_v = 0.45\,m$: (a)$\theta_h = 5\,m$; (b) $\theta_h = 10.5\,m$

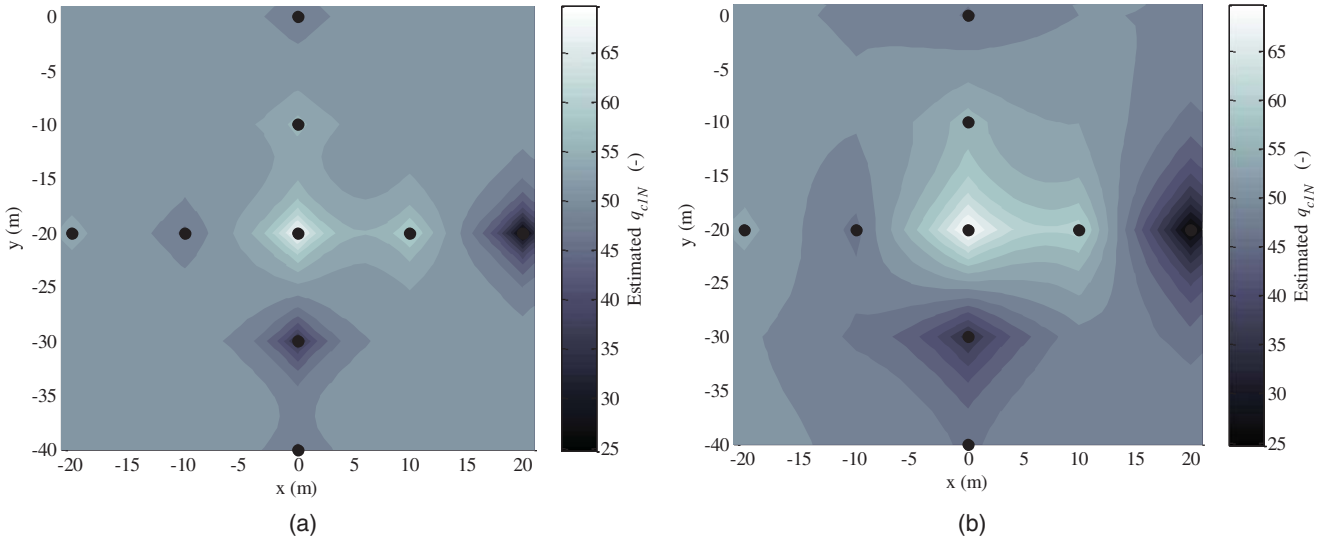

Fig. 7. Estimated normalized cone resistance by Kriging. Depth = 4 m, $\theta_v = 0.45\,m$: (a) $\theta_h = 5\,m$; (b) $\theta_h = 10.5\,m$

where β_n and M_n are the first n elements of $\boldsymbol{\beta}$ and $\mathbf{M}$, and $K_{n\times n}$ is the $n \times n$ upper left submatrix of K containing the covariances. Also β_n^T is the transpose of β_n. The individual standard deviation of the error has been estimated for two different correlation lengths (Fig. 6). As shown in Fig. 6 (left), the standard deviation of the error is small when it is close to the observation points and increases by increasing the distance. In Fig. 6 (right), with a higher horizontal correlation length, the standard deviation of error is obviously smaller in a larger domain around each observation point.

This procedure was applied to a different depth (4 m) to illustrate how the normalized cone resistance varied in the horizontal and vertical directions with correlation length. By understanding the correlation structure of the field, the values of a desired parameter of the soil can be estimated at intermediate locations. Fig. 7 provides information about the variation of normalized cone

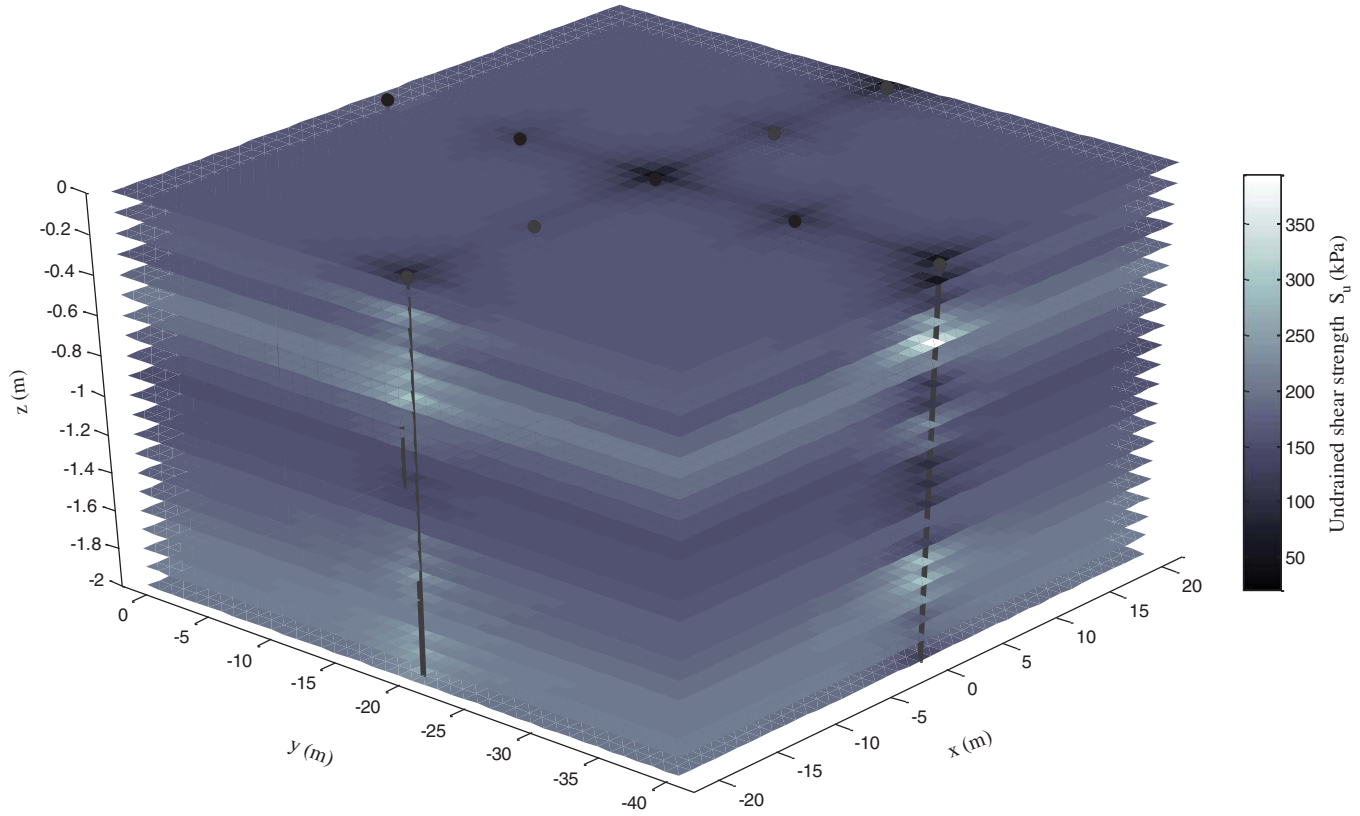

Fig. 8. Estimated undrained shear strength by Kriging. Depth = 0–2 m

resistance in the region. If one could estimate the correlation length of the site by probabilistic analysis, the value of the cone resistance could easily be determined at any point of the site.

Application of Kriging—Illustrative Example

From a consideration of soil type, drainage conditions, and initial stress state, CPTu data can be used to estimate numerous geotechnical parameters, e.g., friction angle, relative density, small strain shear modulus, undrained shear strength, and OCR. An example is now presented to explain how Kriging can be used to estimate the undrained shear strength of a clayey layer in the region under consideration in this paper.

Studies for predicting the undrained shear strength using CPT have progressed empirically and theoretically. The results of these studies show that the correlation between cone resistance and undrained shear strength of clays can make use of the following equation (Baligh et al. 1980)

$$s_u = \frac{(q_c - \sigma_{v0})}{N_{kt}} \tag{14}$$

where N_{kt} is an empirical cone factor and σ_{v0} is the total in-situ vertical stress. A considerable amount of data has been reported on this equation (e.g., Lunne et al. 1997), indicating N_{kt} of approximately 15–20. Previous studies on Danish clay showed N_{kt} varying from 8.5 to 12, with 10 as an average [Luke (1992)]. For larger projects, site-specific correlations should be developed. By having Kriged q_c values, σ_{v0} and $N_{kt} = 10$, the values of s_u can be determined at any point through the layer by Eq. 14. Fig. 8 shows estimated Kriged values of s_u of the clayey layer at 10-cm intervals in the vertical direction. The approach allows limited CPT data to be fully exploited over a much wider volume of the site. The estimated strength parameters might then be available for use in a comprehensive numerical model of foundation performance on the heterogeneous soil layer.

Conclusion

A Kriging approach has been applied to the normalized cone resistance of a sandy site in Denmark to interpolate between known borehole data. First, a verification process has been performed by generating a 3D random field using statistical parameters of cone data. Some values at discrete borehole locations were sampled as known observation points and then Kriging was used to interpolate between the discrete values and compared with the original random field. These estimated Kriging values are compared with the simulated values at given intermediate points. This procedure was performed to verify some assumptions as a constant mean trend and ignoring Lagrangian parameters. After calculating the difference between the Kriging estimation and the generated random field, known values of the cone data at the location of the sounding were taken as observation points to estimate the values of cone resistance at any point within the field by the Kriging method. Because changes in the correlation length have an inevitable effect on the map of soil variation by Kriging, two values of horizontal correlation length were applied at two depth levels by the Kriging method, to examine the effect of correlation length on estimated values at intermediate locations between known field values. This was undertaken for two depths of 2 and 4 m through the deposit. The results showed that when the correlation length was increased, a good (accurate) estimate could be obtained at a greater number of intermediate points. In contrast, when the correlation length was smaller, these values could not be estimated precisely by Kriging. In the latter case, the estimated values at intermediate locations are approximately equal to the mean values of the data at the observation points, which implies a higher uncertainty. When the correlation length was increased, the data were more correlated with each other, and the values were closer at a greater distance. This observation was clear from the contours of cone values, in which the colors varied more gradually.

This study has used a Kriging technique based on measured field values, to provide a map of normalized cone resistances at a site with known or estimated spatial correlation properties. By having the values of normalized cone data at any desired location, the values of strength parameters for the soil needed for the design and analysis of any type of earth structure can be estimated and, consequently, can highly reduce the expenses of future site investigations. Studies such as this can be further developed to reduce the cost of site investigation by providing more reliable interpolated information for sites possessing limited CPT data.

Notation

The following symbols are used in this paper:

a_i = unknown coefficient;
C_{ij} = covariance between data;
C_Q = correlation for overburden stress;
$g_i(x)$ = regression function;
$G(x)$ = correlated random field with zero mean;
K = Kriging matrix (a function of observation point locations and their covariance);
$\tilde{L}$ = lower triangular matrix;
M = covariance between the observation point and the intermediate point;
N_{kt} = empirical cone factor;
n = results from the correction for overburden pressure (0.5, 0.7, 1.0 for cohesionless, intermediate and cohesive soils, respectively);
P_a = atmospheric pressure;
q_c = measured cone tip resistance;
q_{c1N} = normalized cone resistance;
$\tilde{R}$ = correlation matrix;
s_u = Undrained shear strength;
$U(x)$ = standard Gaussian random seeds;
x = spatial position of unobserved value;
$\tilde{X}$ = estimation of x;
β_i = Kriging coefficient or unknown Kriging weight;
$\delta_{x,y,z}$ = correlation length in x, y and z direction;
η_i = Lagrangian parameter;
θ_h = horizontal correlation length;
θ_v = vertical correlation length;
μ_E = mean value of the estimator error;
$\mu_{\ln}$ = Lognormal mean value of q_{c1N};
μ_X = mean function;
ρ = correlation length;
σ_E = standard deviation of the estimator error;
$\sigma_{\ln}$ = Lognormal standard deviation of q_{c1N};
σ'_{v0} = effective vertical stress;
σ_{v0} = total vertical stress; and
τ = lag distance between observation points.

References

ASCE Task Committee on Geostatistical Techniques in Geohydrology of the Ground Water Hydrology Committee of the ASCE Hydraulics Division. (1990). "Review of geostatistics in geohydrology. I: Basic

concepts." *J. Hydraul. Eng.*, 10.1061/(ASCE)0733-9429(1990)116:5(612), 612–658.
Baecher, G. B., and Christian, J. T. (2003). *Reliability and statistics in geotechnical engineering*, Wiley, West Sussex, England.
Baligh, M. M., Azzouz, A. S., and Martin, R. T. (1980). "Cone penetration tests offshore the Venezuelan Coast." *M.I.T. Rep. No. R80–21*, Massachusetts Institute of Technology, Cambridge, MA.
DeGroot, D. J., and Baecher, G. B. (1993). "Estimating autocovariance of in-situ soil properties." *ASCE J. Geotech. Eng.*, 119(1), 147–166.
Delhomme, J. P. (1978). "Kriging in the hydrosciences." *Adv. Water Resour.*, 1(5), 251–266.
DNV (Det Norske Veritas). (2010). "Statistical representation of soil data." *DNV-RP-C207*, Oslo, Norway.
Fenton, G. A., and Griffiths, D. V. (2008). *Risk assessment in geotechnical engineering*, John Wiley and Sons, Hoboken, NJ.
Firouzianbandpey, S., Griffiths, D. V., Ibsen, L. B., and Andersen, L. V. (2014). "Spatial correlation length of normalized cone data in sand: A case study in the North of Denmark." *Can. Geotech. J.*, 51(8), 844–857.
Goldsworthy, J. S., Jaksa, M. B., Fenton, G. A., Kaggwa, W. S., Griffiths, D. V., and Poulos, H. G. (2007). "Effect of sample location on the reliability based design of pad foundations." *Georisk Assess. Manage. Risk Eng. Syst. Geohazards*, 1(3), 155–166.
Jaksa, M. B.,, et al. (2005). "Towards reliable and effective site investigations."*Géotech.*, 55(2), 109–121.
JCSS (Joint Committee on Structural Safety). (2006). "JCSS-Cl: Probabilistic model code. Section 3.7: Soil properties." Technical Univ. of Denmark, Denmark.
Journel, A. G., and Huijbregts, C. (1978). *Mining geostatistics*, Academic, London, 600.
Krige, D. G. (1951). "A statistical approach to some basic mine valuation problems on Witwatersrand." *J. Chem. Metall. Mining Soc. South Africa*, 52(6), 119–139.
Luke, K. (1992). "Measuring undrained shear strength using CPT and field vane." *NGM-92: Proc., from 11. Norwesian Geotechnical meeting, Aalborg*, Vol. 1, 95–100.
Lunne, T., Robertson, P. K., and Powell, J. J. M. (1997). "Cone penetration testing in geotechnical practice." Blackie Academic/Chapman & Hall, E&FN Spon, London, 312.
Matheron, G. (1963). "Principles of geostatistics." *Econ. Geol.*, 58(8), 1246–1266.
Moss, R. E., Seed, R. B., and Olsen, R. (2006). "Normalizing the CPT for overburden stress." *J. Geotech. Geoenviron. Eng.*, 10.1061/(ASCE)1090-0241(2006)132:3(378), 378–387.
Olea, R. A. (1991). *Geostatistical glossary and multilingual dictionary*, Oxford Univ. Press, New York.
Rautman, C. A., and Cromer, M. V. (1994). *Three-dimensional rock characteristics models study plan: Yucca mountain site characterization plan SP 8.3.1.4.3.2*, U.S. Dept. of Energy, Office of Civilian Radioactive Management, Washington, DC.
Robertson, P. K., and Wride, C. E. (1998). "Evaluating cyclic liquefaction potential using the cone penetration test." *Can. Geotech. J.*, 35(3), 442–459.
Rouhani, S. (1996). "Geostatistical estimation: Kriging." *Geostat. Environ. Geotech. Appl.*, 1283, 20–31.
Ryti, R. (1993). "Superfund soil cleanup: Developing the piazza remedial design." *J. Air Waste Manage. Assoc.*, 43(2), 197–202.
Tang, W. H. (1979). "Probabilistic evaluation of penetration resistance." *ASCE J. Geotech. Eng. Div.*, 105(GT10), 1173–1191.
Vahdatirad, M. J., Griffiths, D. V., Andersen, L. V., Sørensen, J. D., and Fenton, G. A. (2014). "Reliability analysis of a gravity based foundation for wind turbines: A code-based design assessment." *Géotechn.*, 64 (8), 635–645.
Vanmarcke, E. (1977). "Probabilistic modeling of soil profiles." *ASCE J. Geotech. Eng. Div.*, 103(11), 1227–1246.
Wild, M., and Rouhani, S. (1996). "Effective use of field screening techniques in environmental investigations: A multivariate geostatistical approach." *ASTM Special Technical Publication 1283*, 88–101.
Zhang, J., Zhang, L. M., and Tang, W. H. (2011). "Kriging numerical models for geotechnical reliability analysis." *Soils Found.*, 51(6), 1169–1177.

APPENDIX F: CPT PROFILES

AARHUS SITE - LIGHT HOUSE

CPT 1

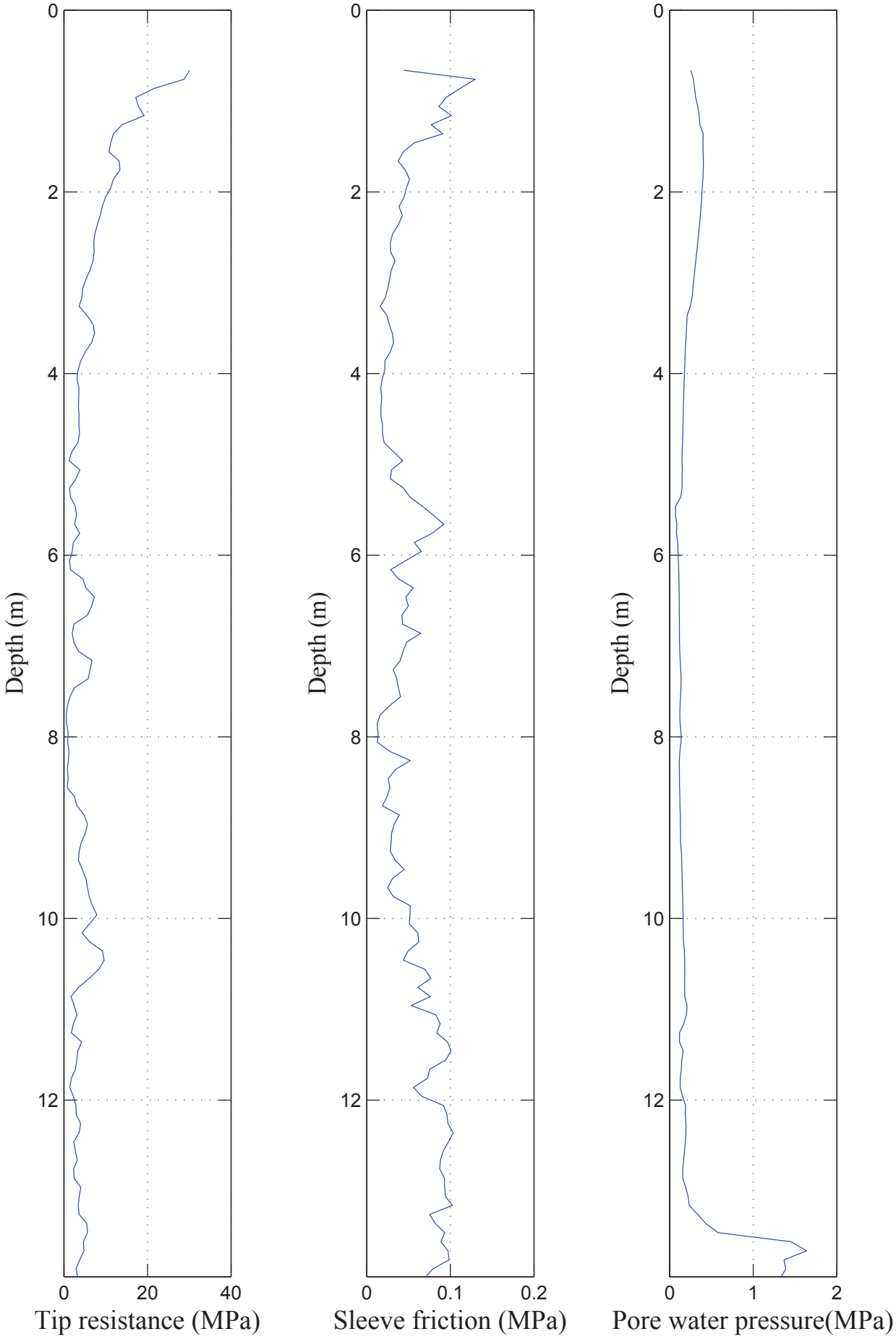
Depth (m)
0
2
4
6
8
10
12
0
20
40
Tip resistance (MPa)
Depth (m)
0
2
4
6
8
10
12
0
0.1
0.2
Sleeve friction (MPa)
Depth (m)
0
2
4
6
8
10
12
0
1
2
Pore water pressure(MPa)

CPT 2

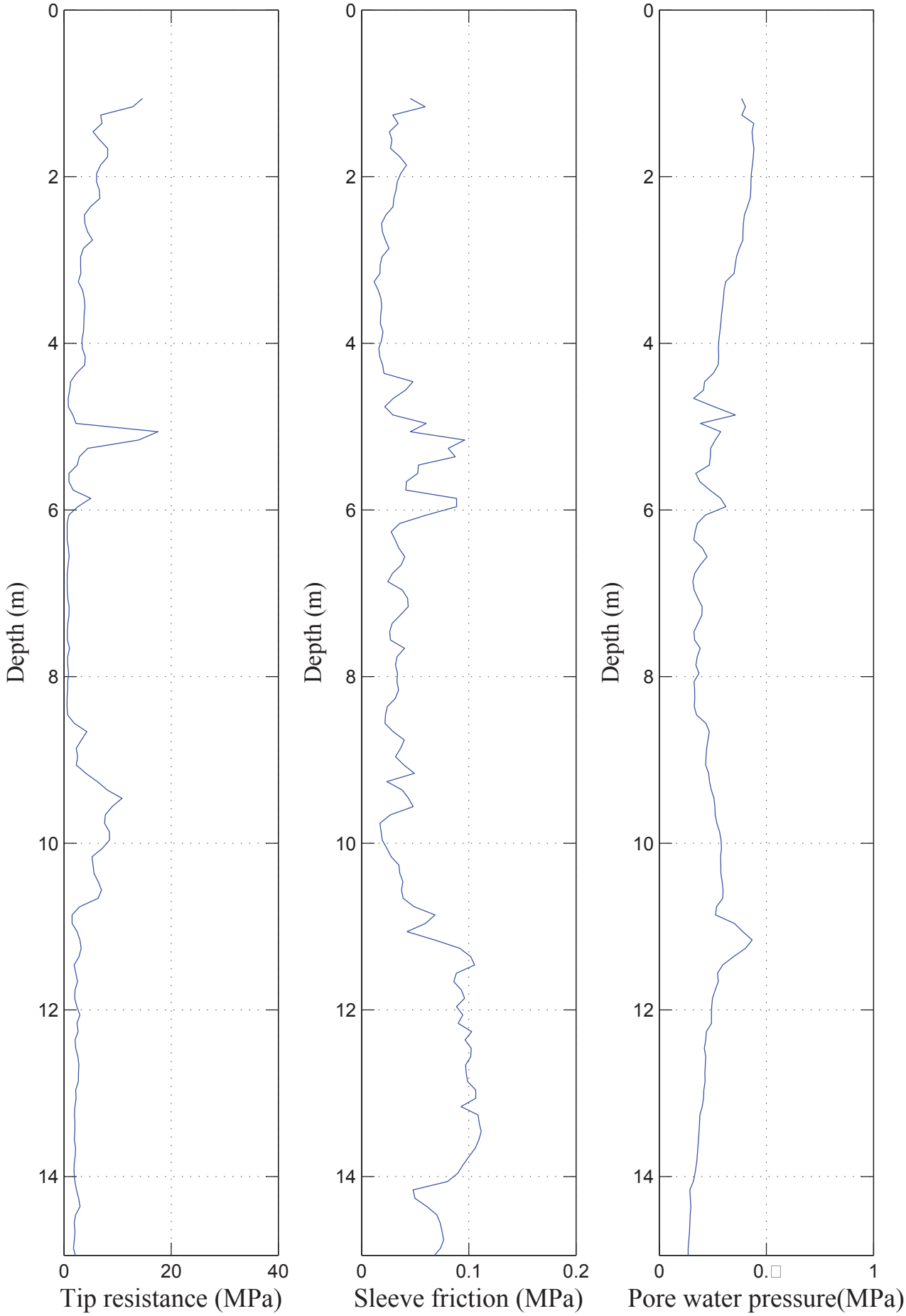
Depth (m)
0
2
4
6
8
10
12
14
0
20
40
Tip resistance (MPa)
0
0.1
0.2
Sleeve friction (MPa)
0
1
Pore water pressure(MPa)

CPT 3

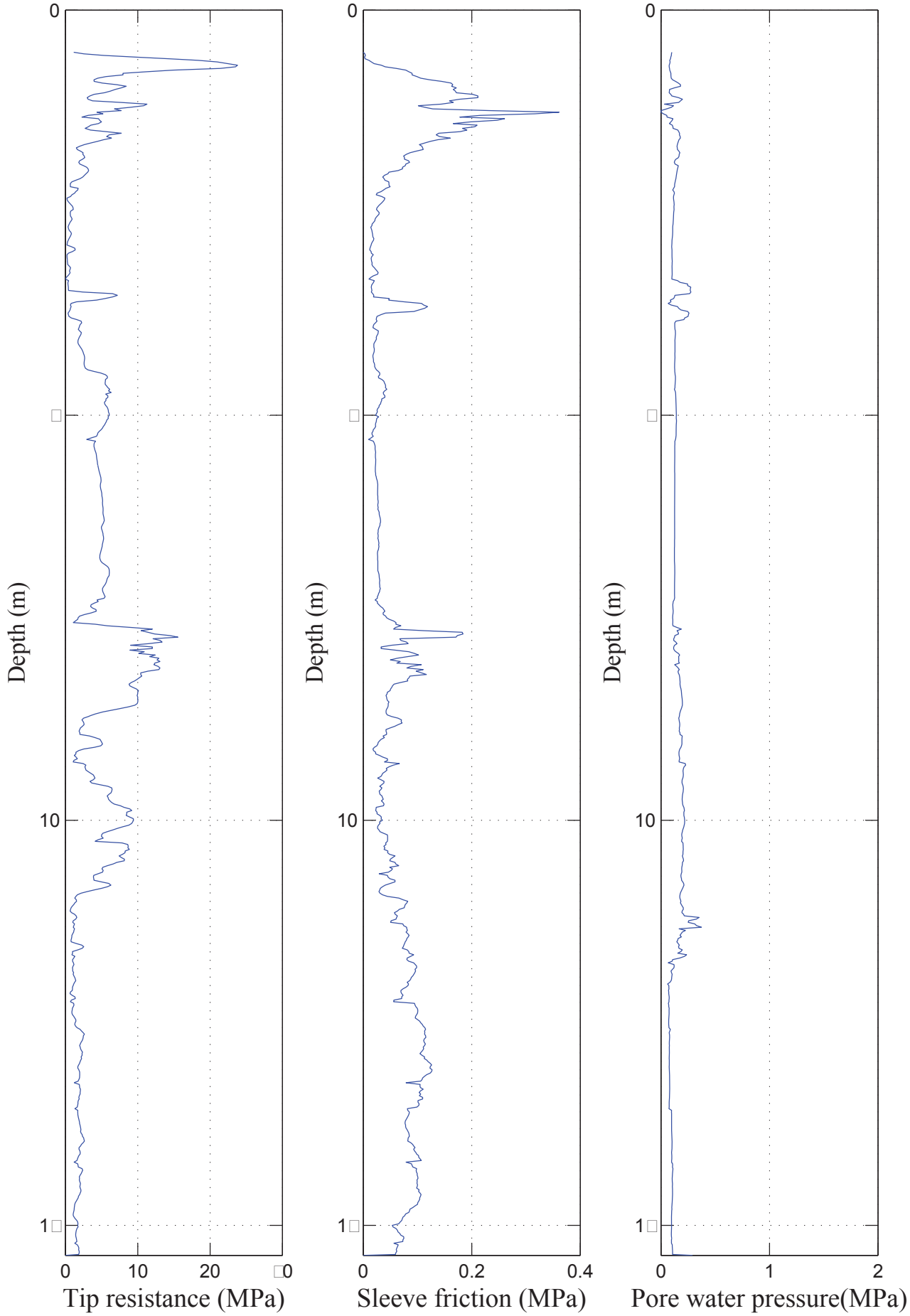
Depth (m)
0
10
Tip resistance (MPa)
0
10
20
Sleeve friction (MPa)
0.2
0.4
Pore water pressure(MPa)
1
2

CPT 4

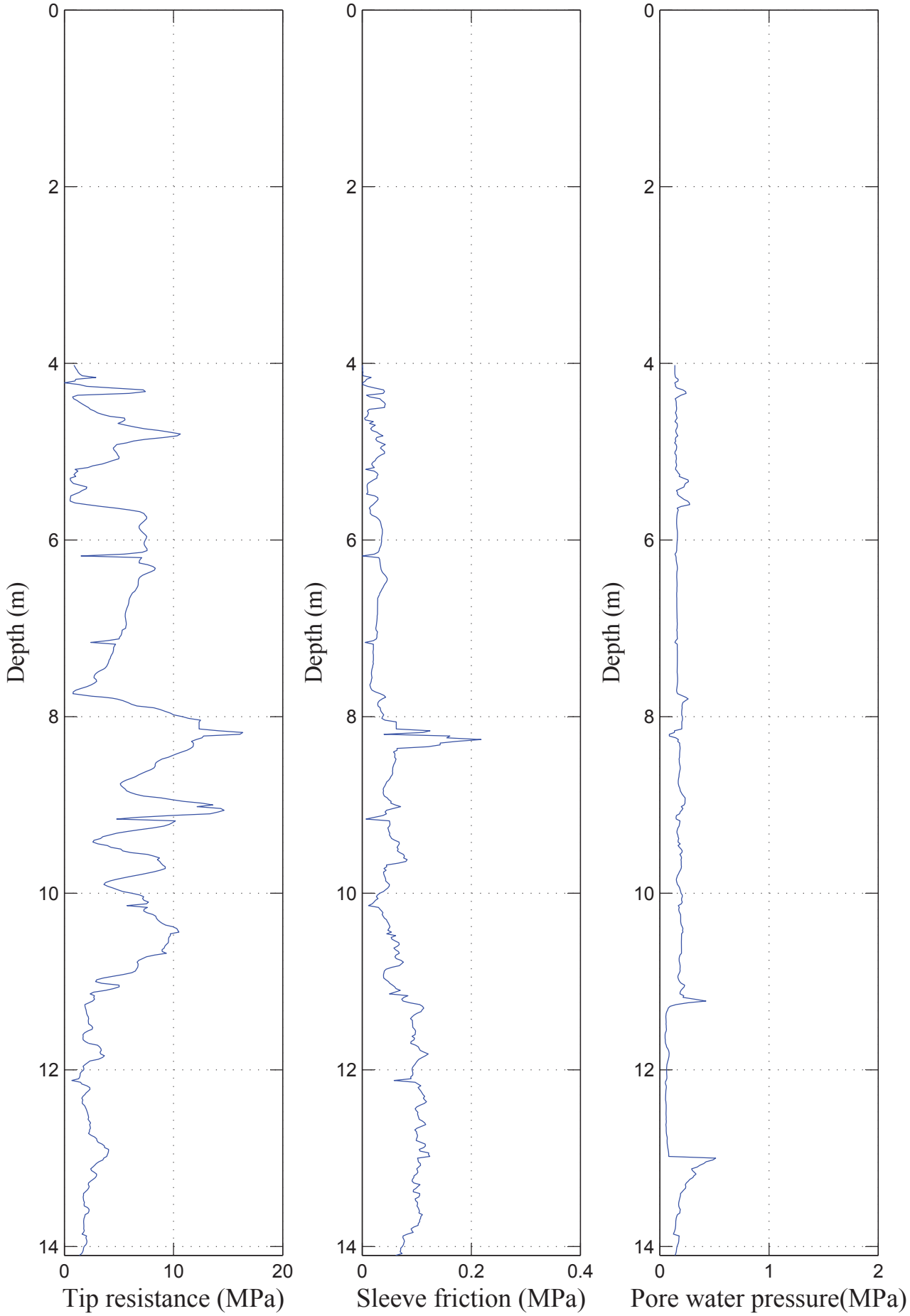
Depth (m)
0
2
4
6
8
10
12
14
0
10
20
Tip resistance (MPa)
Depth (m)
0
2
4
6
8
10
12
14
0
0.2
0.4
Sleeve friction (MPa)
Depth (m)
0
2
4
6
8
10
12
14
0
1
2
Pore water pressure(MPa)

CPT 5

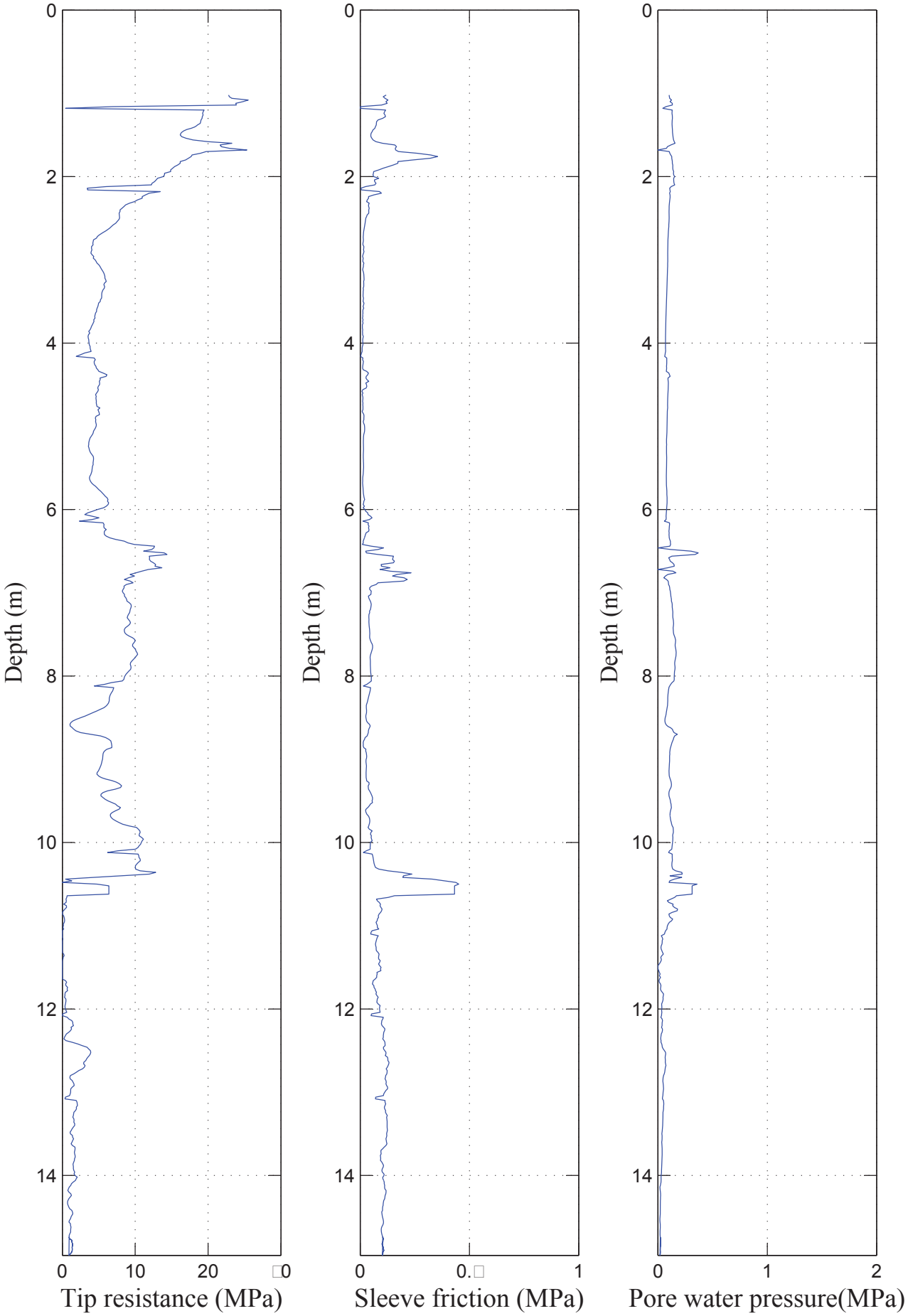
Depth (m)
0
2
4
6
8
10
12
14
0
10
20
Tip resistance (MPa)
Depth (m)
0
2
4
6
8
10
12
14
0
0.
1
Sleeve friction (MPa)
Depth (m)
0
2
4
6
8
10
12
14
0
1
2
Pore water pressure(MPa)

CPT 6

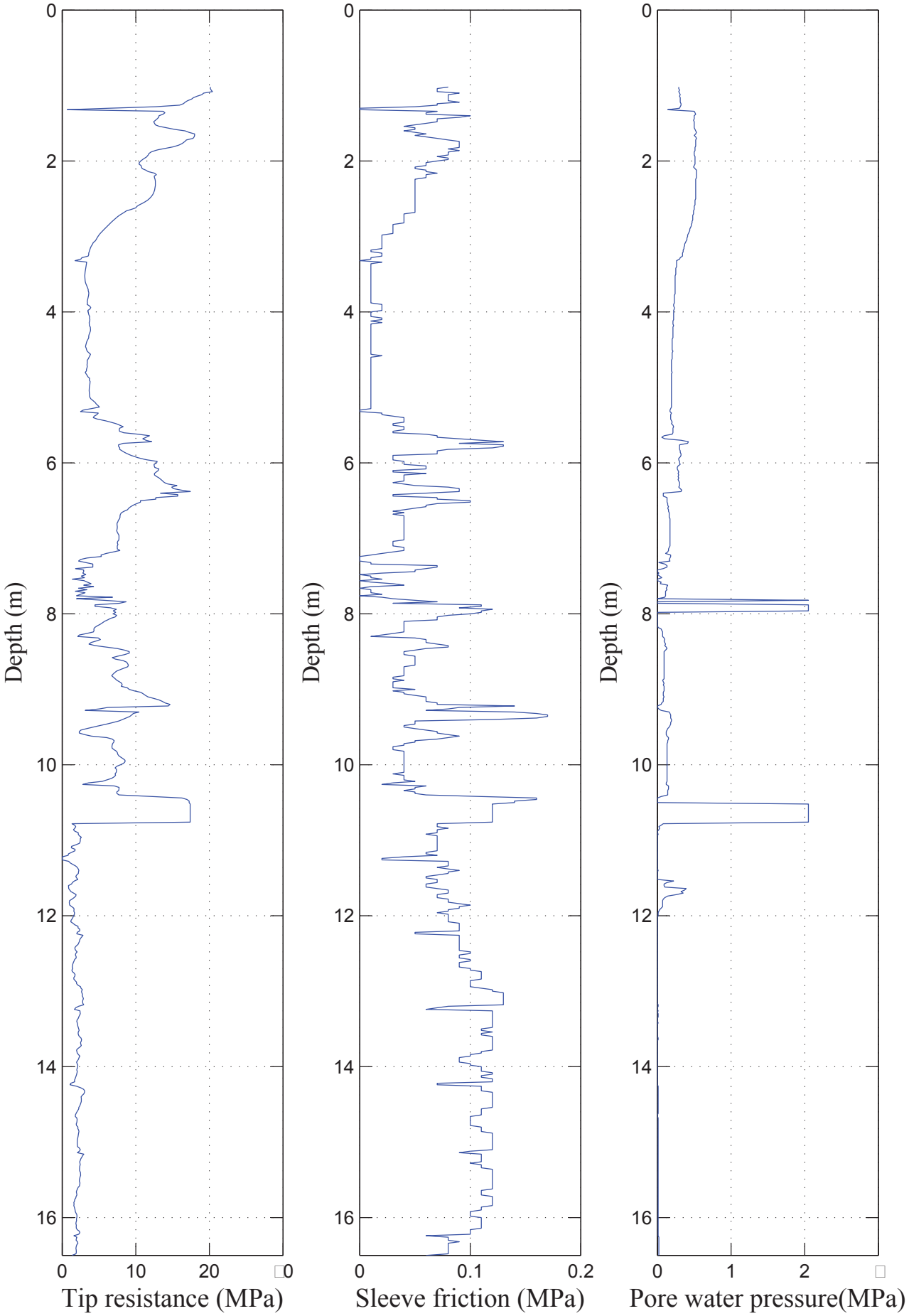
Depth (m)
0
2
4
6
8
10
12
14
16
0
10
20
Tip resistance (MPa)
Depth (m)
0
0.1
0.2
Sleeve friction (MPa)
Depth (m)
0
1
2
Pore water pressure(MPa)

CPT 7

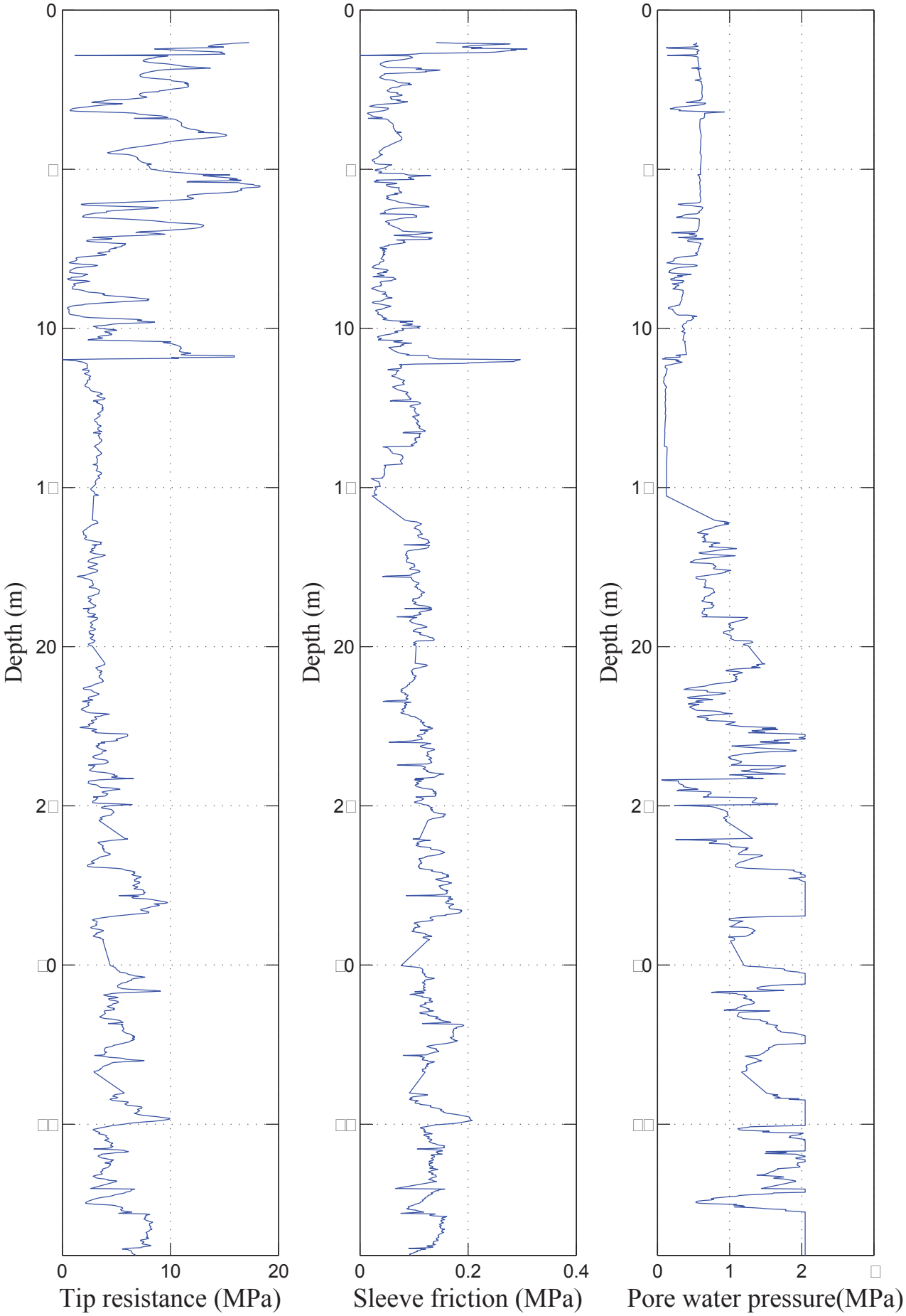
Depth (m)
0
10
20
0
10
20
Tip resistance (MPa)
Depth (m)
0
0.2
0.4
Sleeve friction (MPa)
Depth (m)
0
1
2
Pore water pressure(MPa)

CPT 8

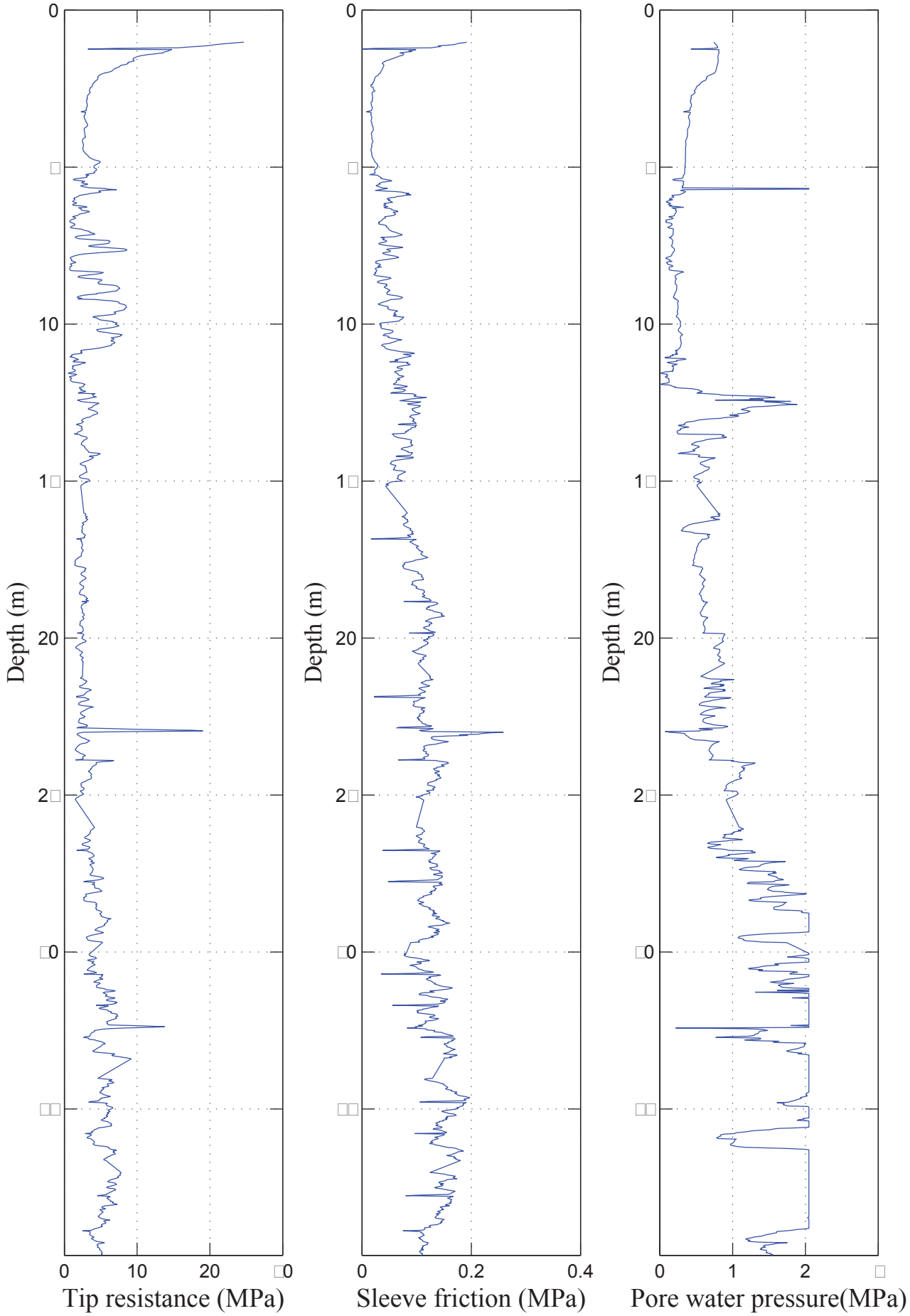
Depth (m)
Tip resistance (MPa)
Sleeve friction (MPa)
Pore water pressure(MPa)

CPT 9

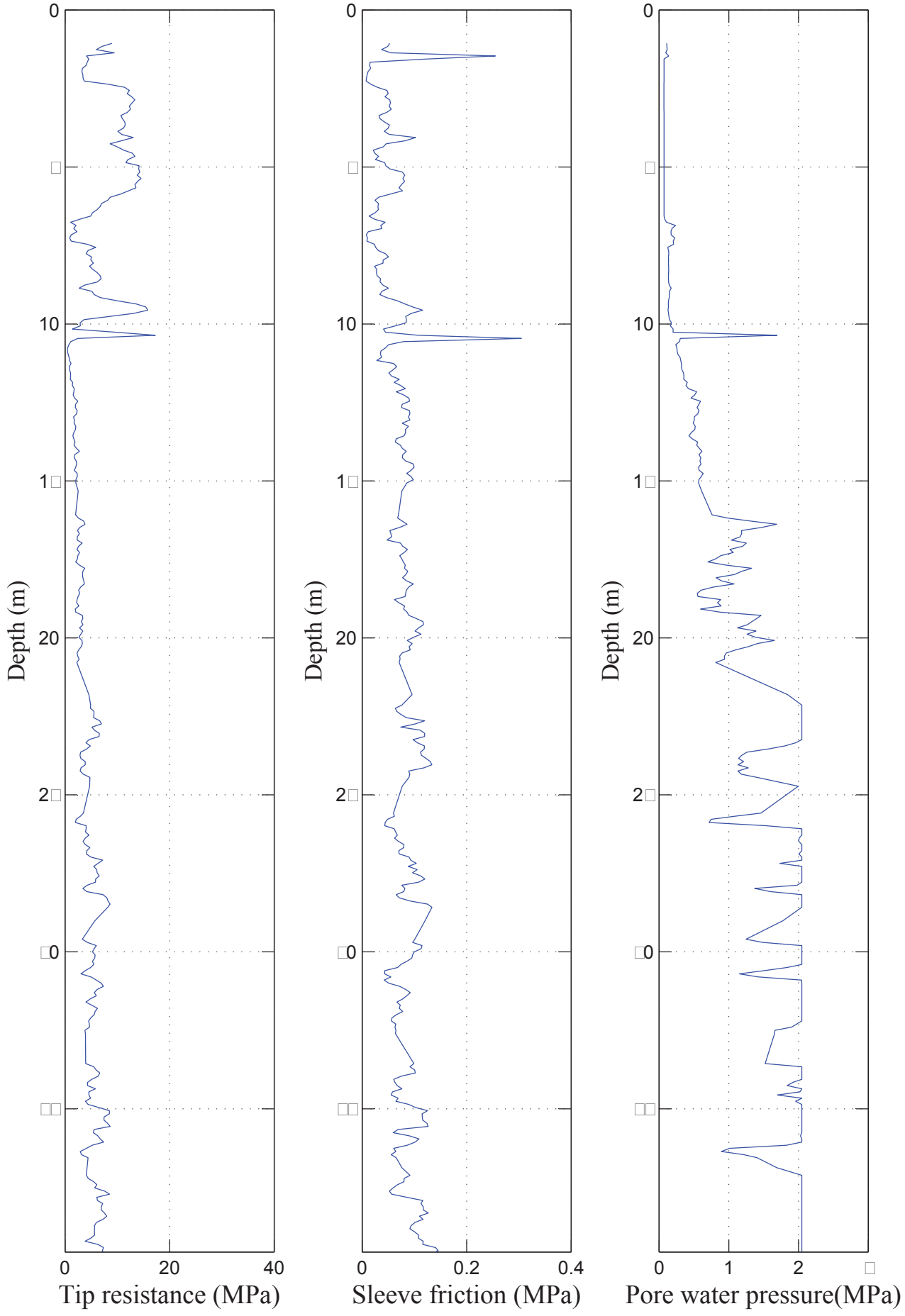
Depth (m)
0
10
20
0
20
40
Tip resistance (MPa)
Depth (m)
0
10
20
0
0.2
0.4
Sleeve friction (MPa)
Depth (m)
0
10
20
0
1
2
Pore water pressure(MPa)

CPT 10

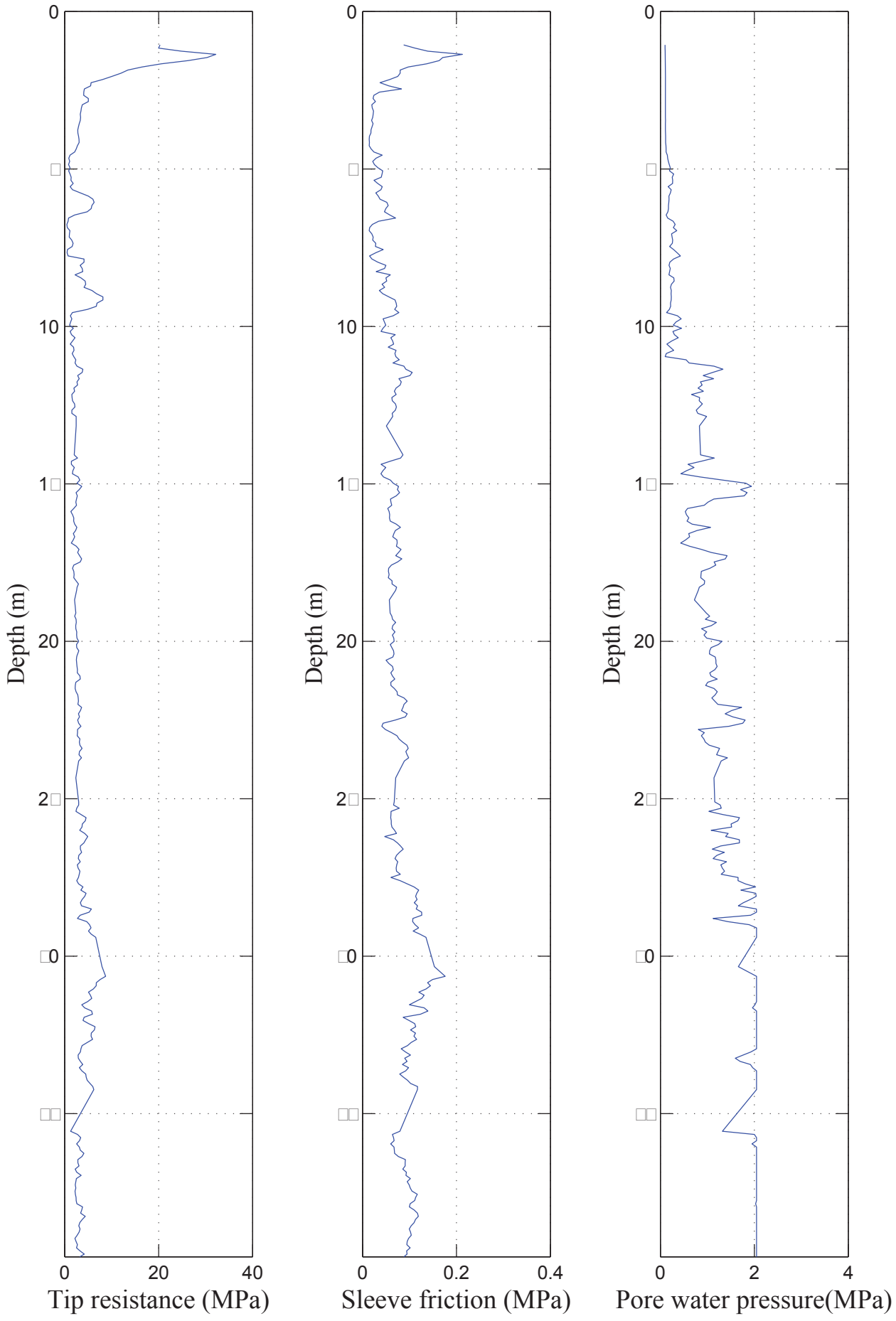
Depth (m)
0
10
20
0
20
40
Tip resistance (MPa)
Depth (m)
0
10
20
0
0.2
0.4
Sleeve friction (MPa)
Depth (m)
0
10
20
0
2
4
Pore water pressure(MPa)

CPT 11

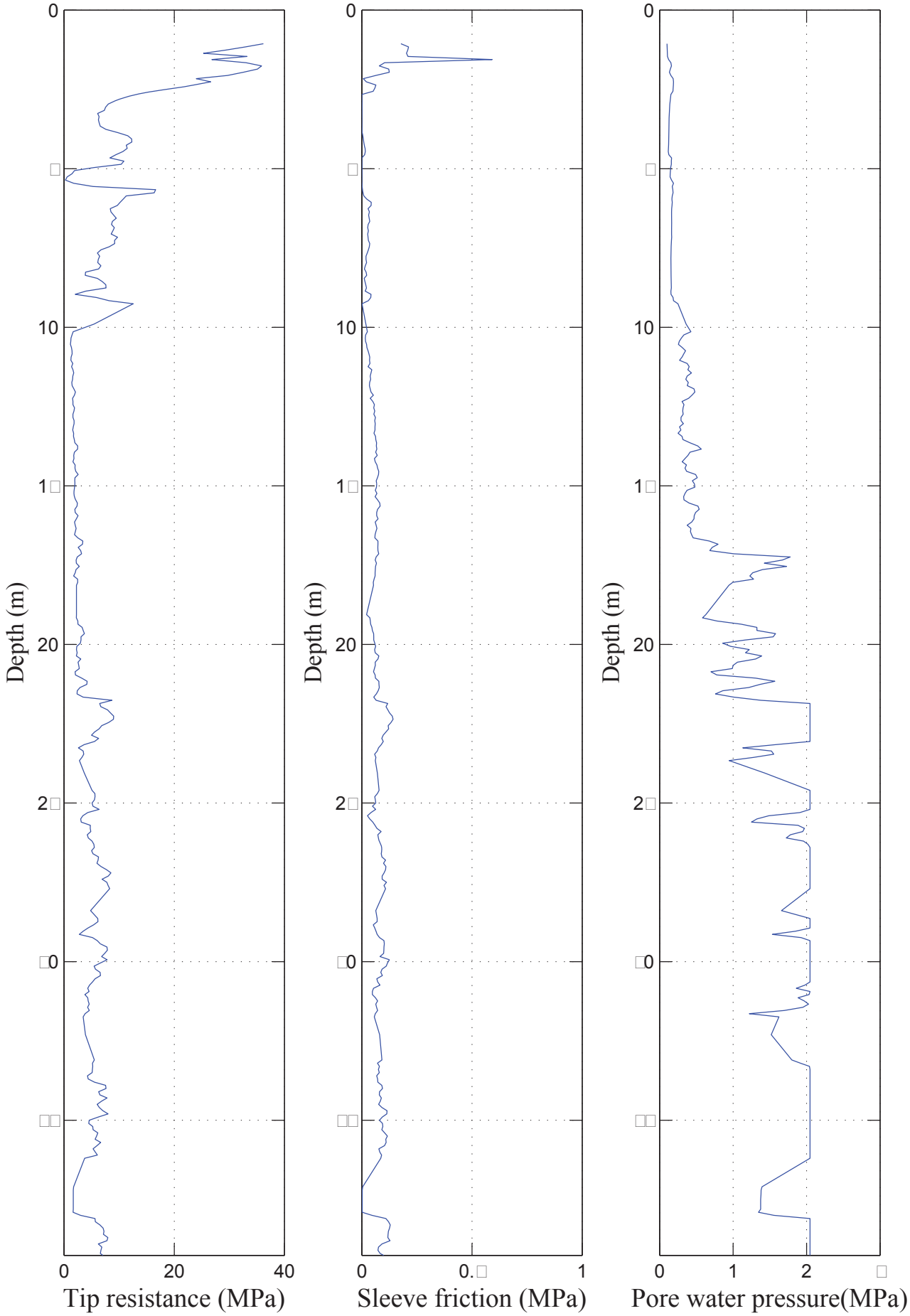
Depth (m)
0
10
20
0
20
40
Tip resistance (MPa)
Depth (m)
0
10
20
0
1
Sleeve friction (MPa)
Depth (m)
0
10
20
0
1
2
Pore water pressure(MPa)

CPT 12

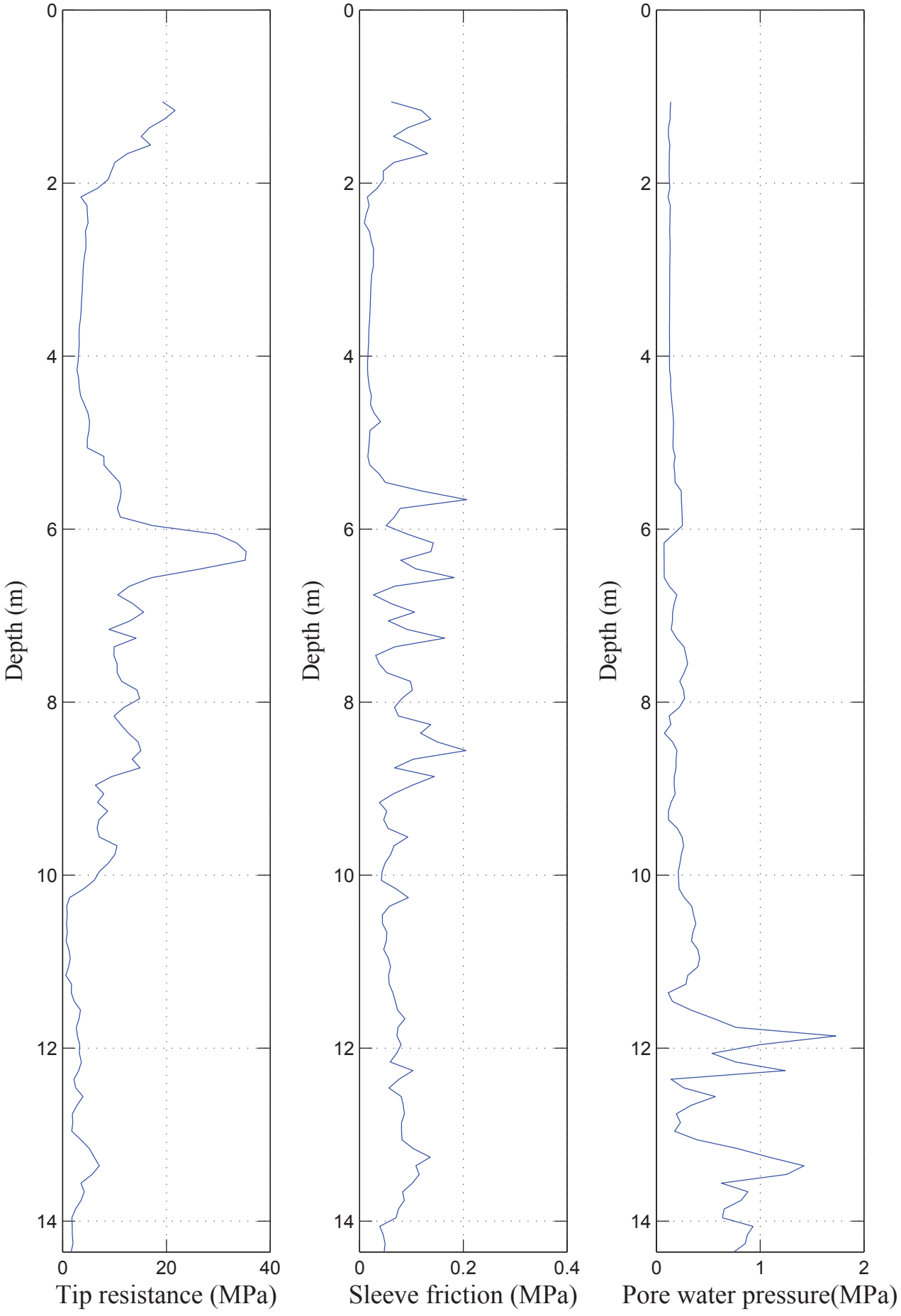
Depth (m)
0
2
4
6
8
10
12
14
0
20
40
Tip resistance (MPa)
Depth (m)
0
2
4
6
8
10
12
14
0
0.2
0.4
Sleeve friction (MPa)
Depth (m)
0
2
4
6
8
10
12
14
0
1
2
Pore water pressure(MPa)

CPT 13

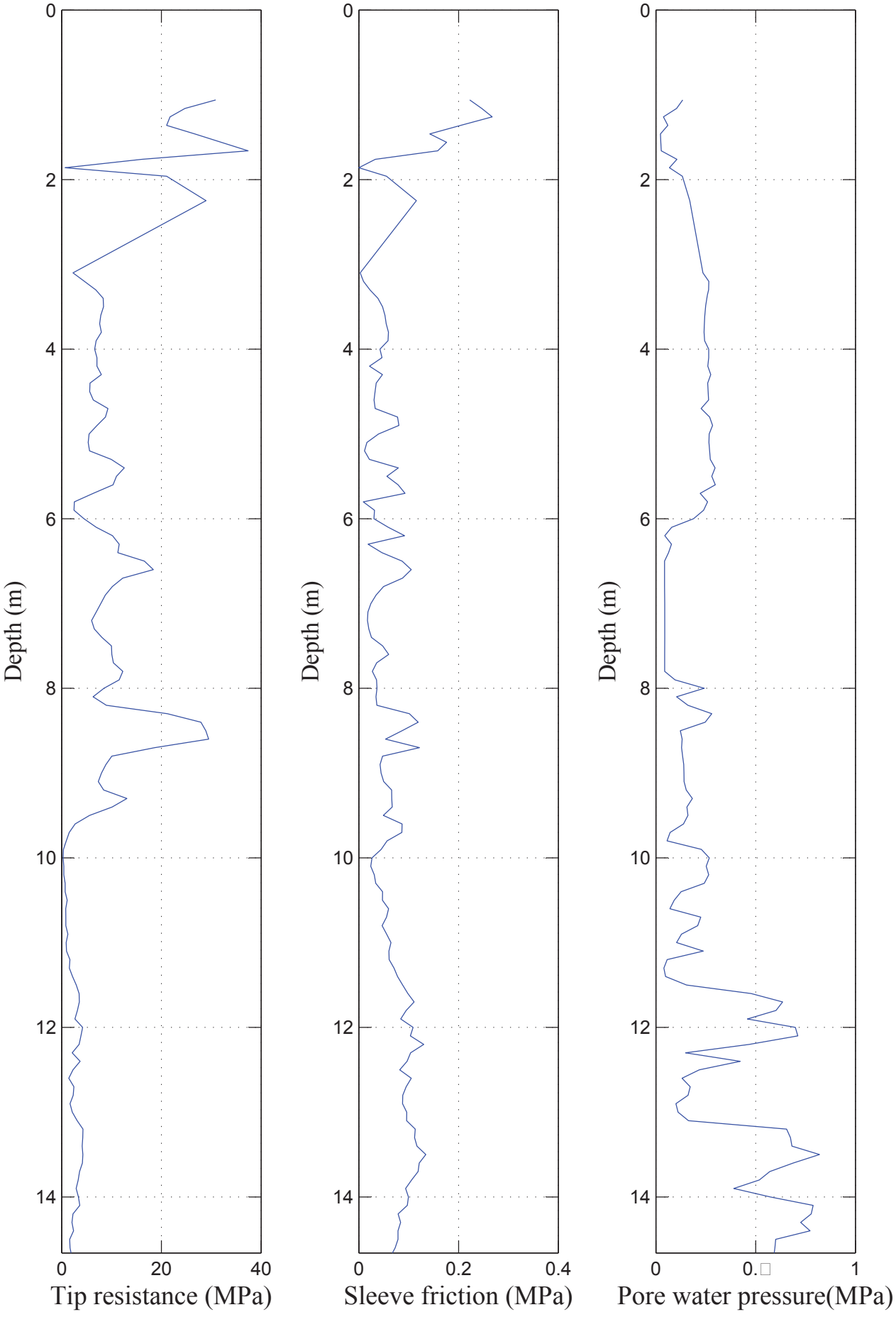
Depth (m)
0
2
4
6
8
10
12
14
0
20
40
Tip resistance (MPa)
Depth (m)
0
2
4
6
8
10
12
14
0
0.2
0.4
Sleeve friction (MPa)
Depth (m)
0
2
4
6
8
10
12
14
0
1
Pore water pressure(MPa)

CPT 14

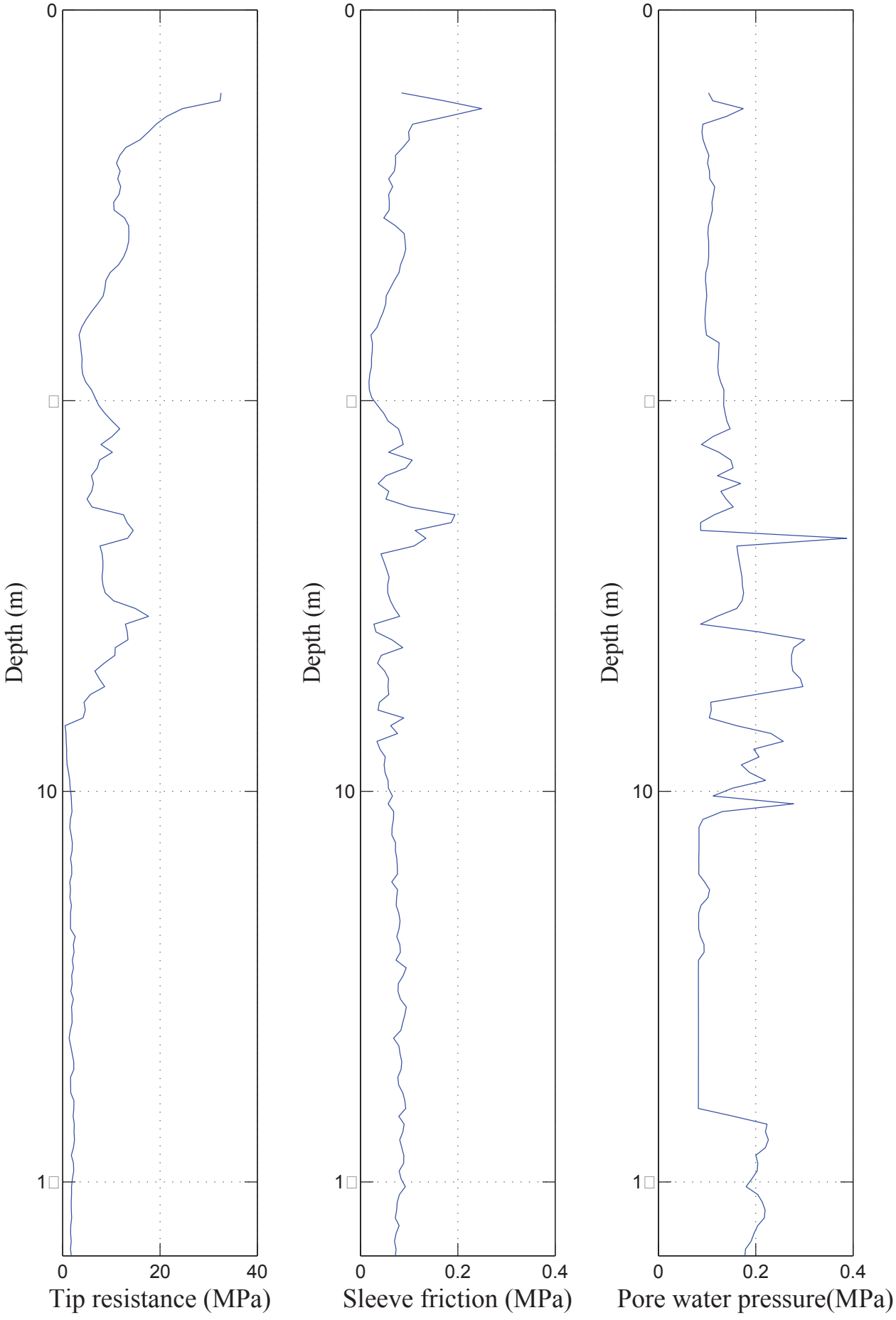
0
10
Depth (m)
0
20
40
Tip resistance (MPa)
0
10
Depth (m)
0
0.2
0.4
Sleeve friction (MPa)
0
10
Depth (m)
0
0.2
0.4
Pore water pressure(MPa)

CPT 15

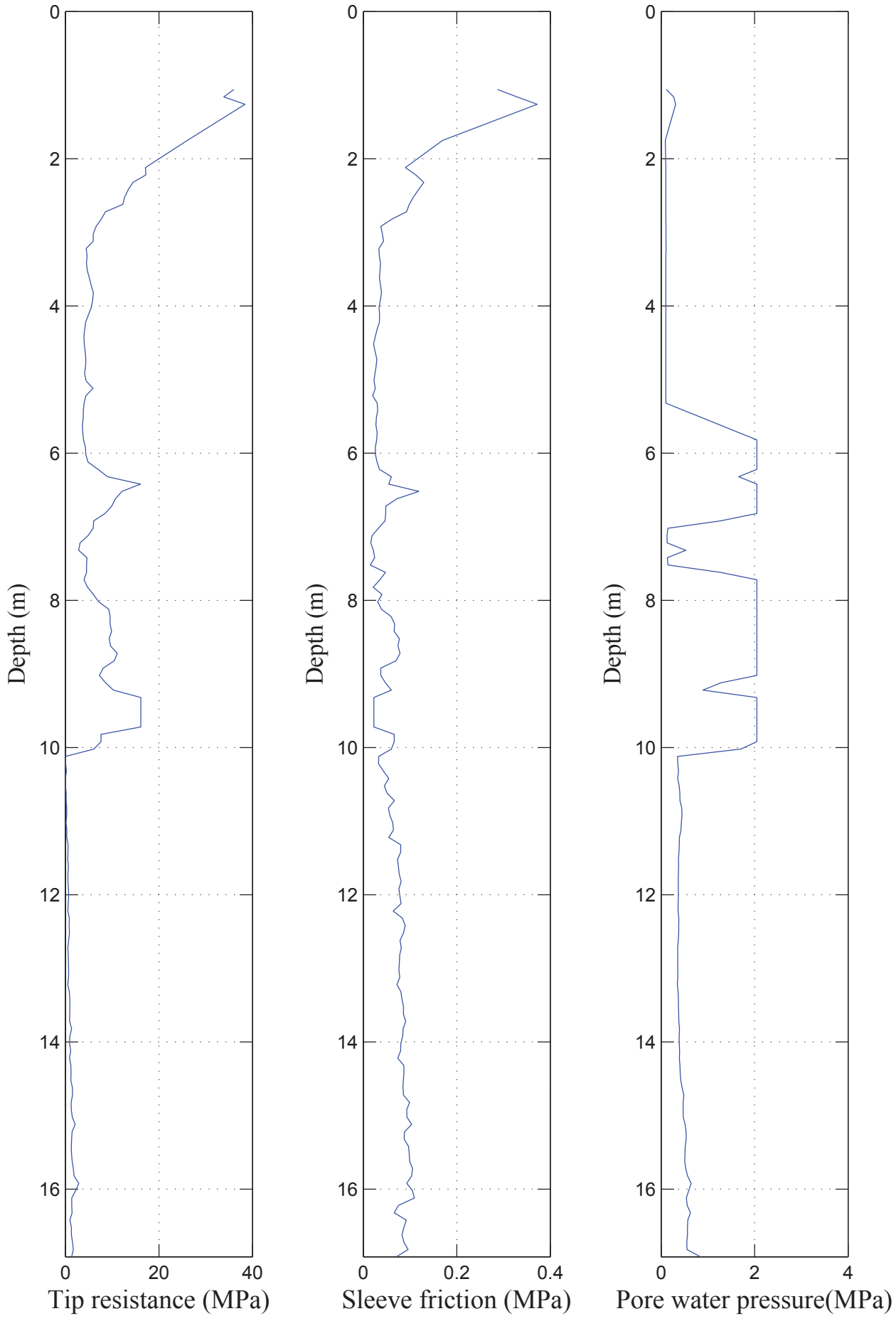
Depth (m)
0
2
4
6
8
10
12
14
16
0
20
40
Tip resistance (MPa)
Depth (m)
0
2
4
6
8
10
12
14
16
0
0.2
0.4
Sleeve friction (MPa)
Depth (m)
0
2
4
6
8
10
12
14
16
0
2
4
Pore water pressure(MPa)

CPT 16

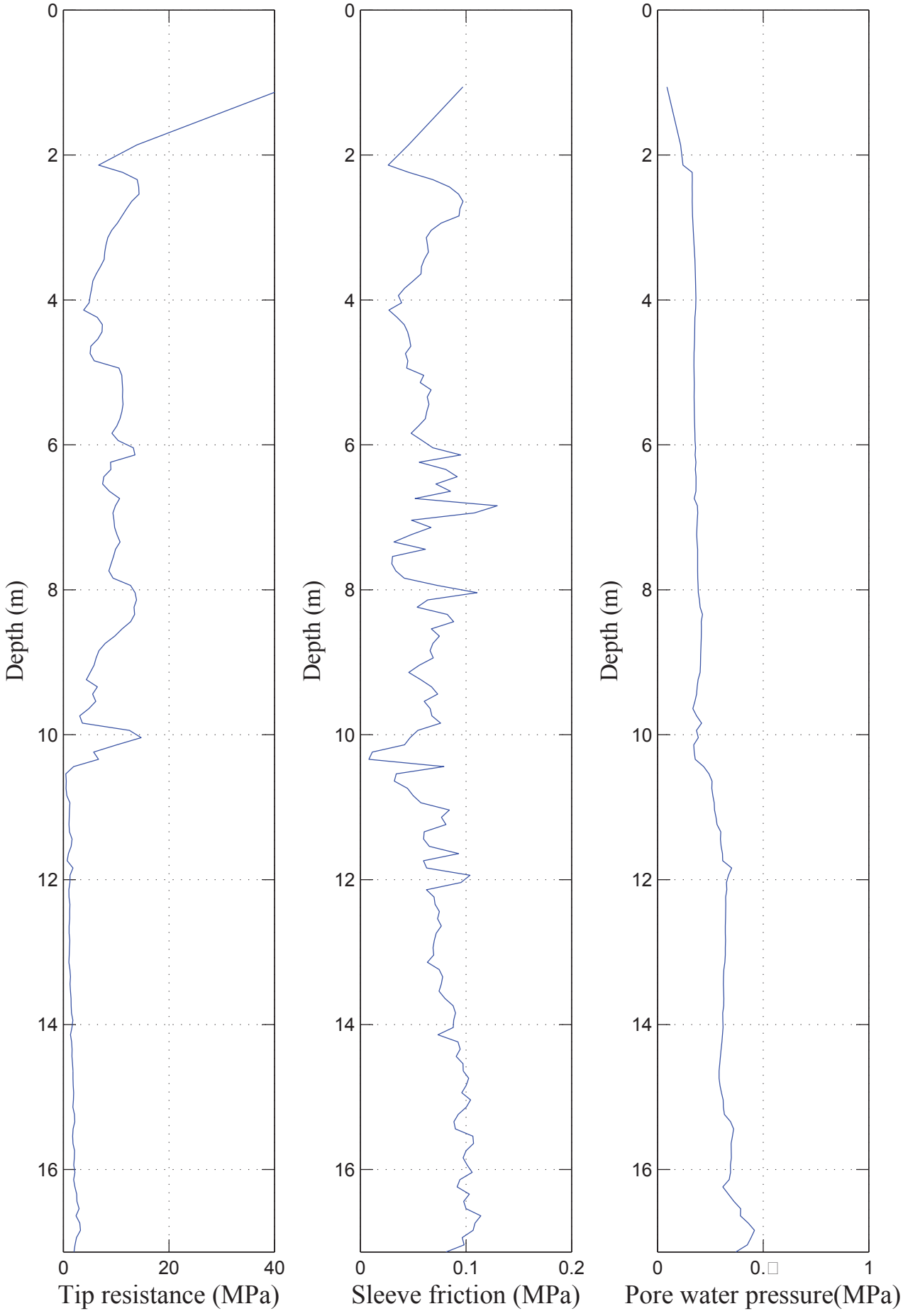
Depth (m)
0
2
4
6
8
10
12
14
16
0
20
40
Tip resistance (MPa)
Depth (m)
0
0.1
0.2
Sleeve friction (MPa)
Depth (m)
0
1
Pore water pressure(MPa)

CPT 17

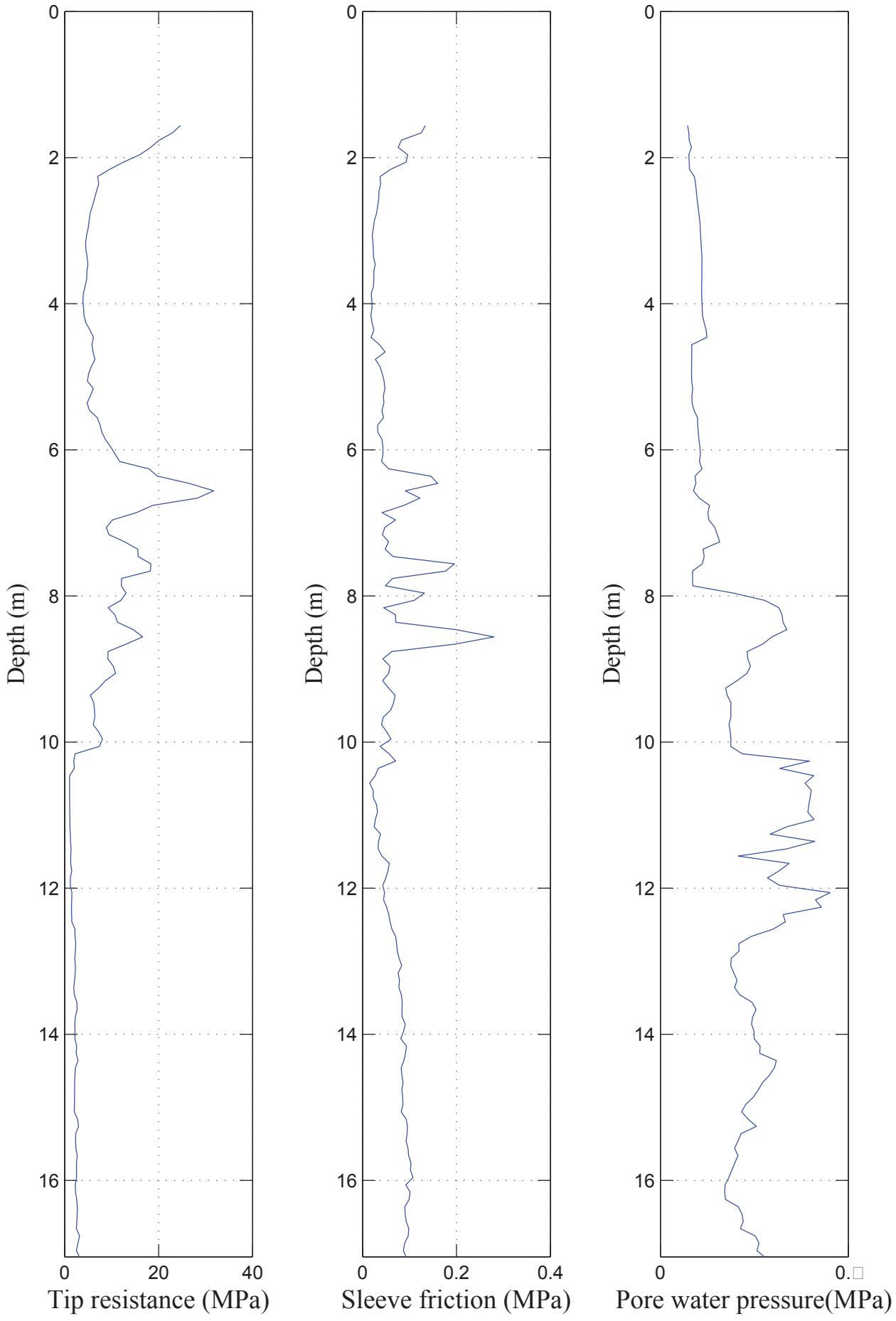
Depth (m)
0
2
4
6
8
10
12
14
16
0
20
40
Tip resistance (MPa)
Depth (m)
0
2
4
6
8
10
12
14
16
0
0.2
0.4
Sleeve friction (MPa)
Depth (m)
0
2
4
6
8
10
12
14
16
0
0.
Pore water pressure(MPa)

CPT 18

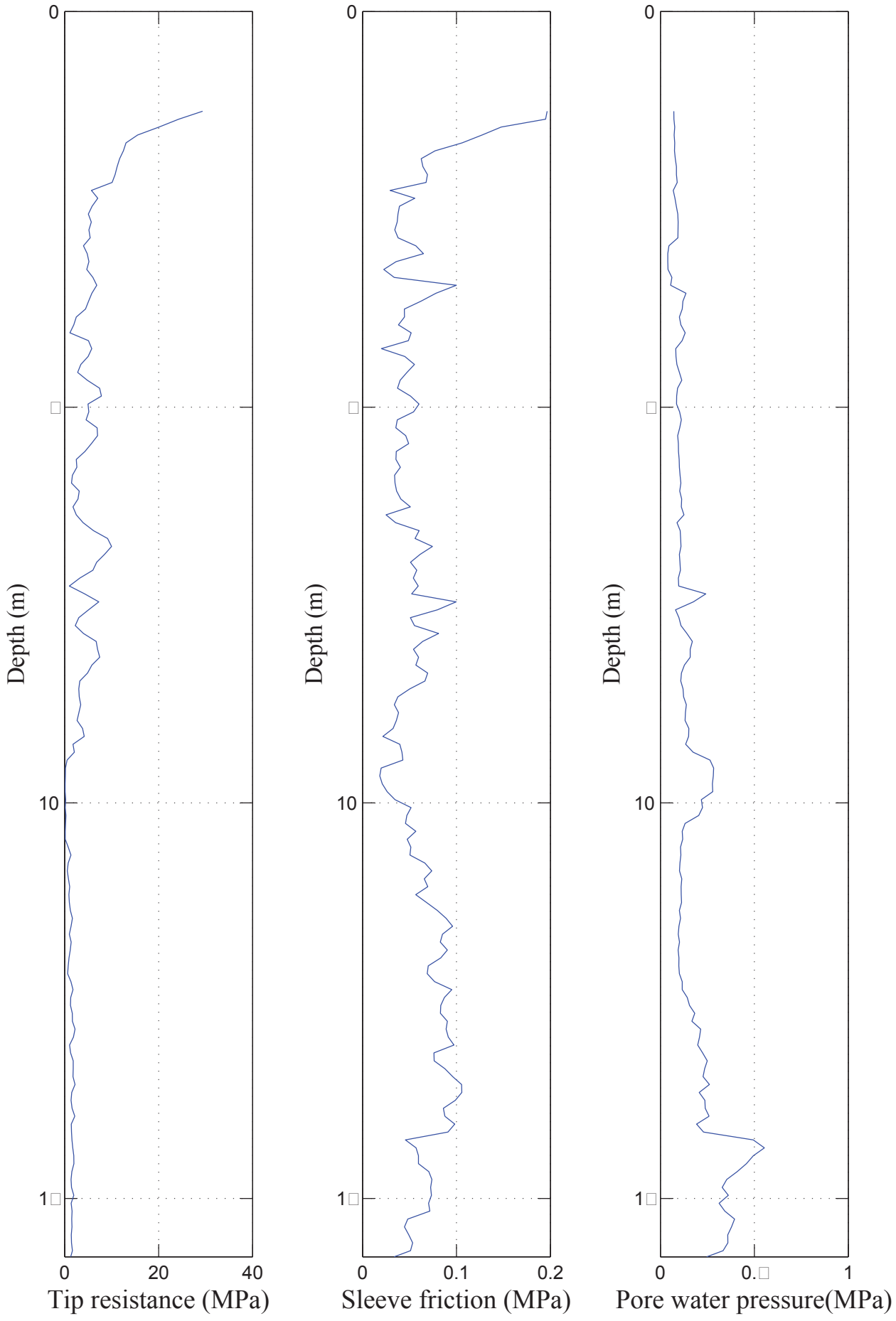
0
10
1
Depth (m)
0
20
40
Tip resistance (MPa)
0
0.1
0.2
Sleeve friction (MPa)
0
0.
1
Pore water pressure(MPa)

CPT 19

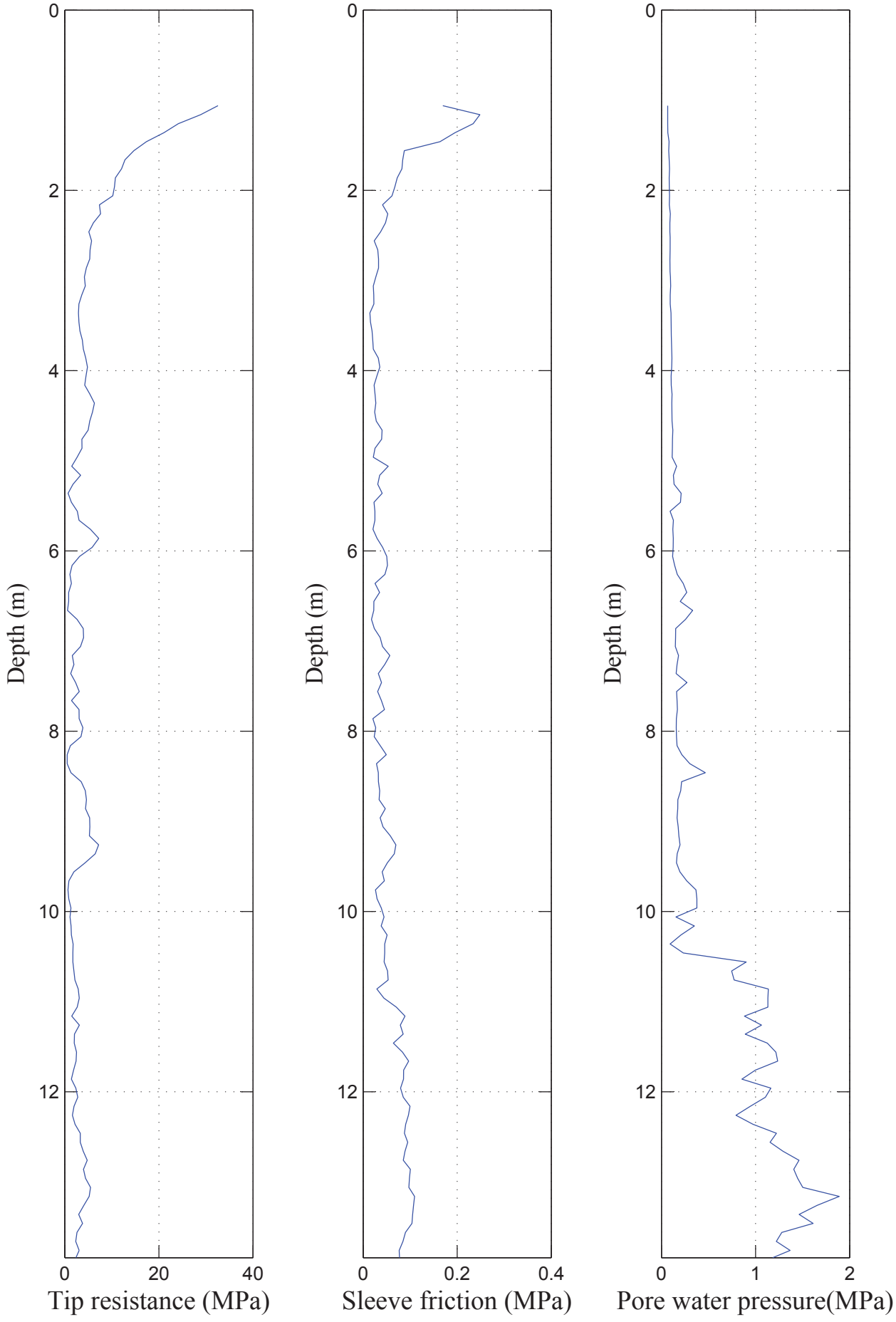
Depth (m)
0
2
4
6
8
10
12
0
20
40
Tip resistance (MPa)
Depth (m)
0
2
4
6
8
10
12
0
0.2
0.4
Sleeve friction (MPa)
Depth (m)
0
2
4
6
8
10
12
0
1
2
Pore water pressure(MPa)

CPT 20

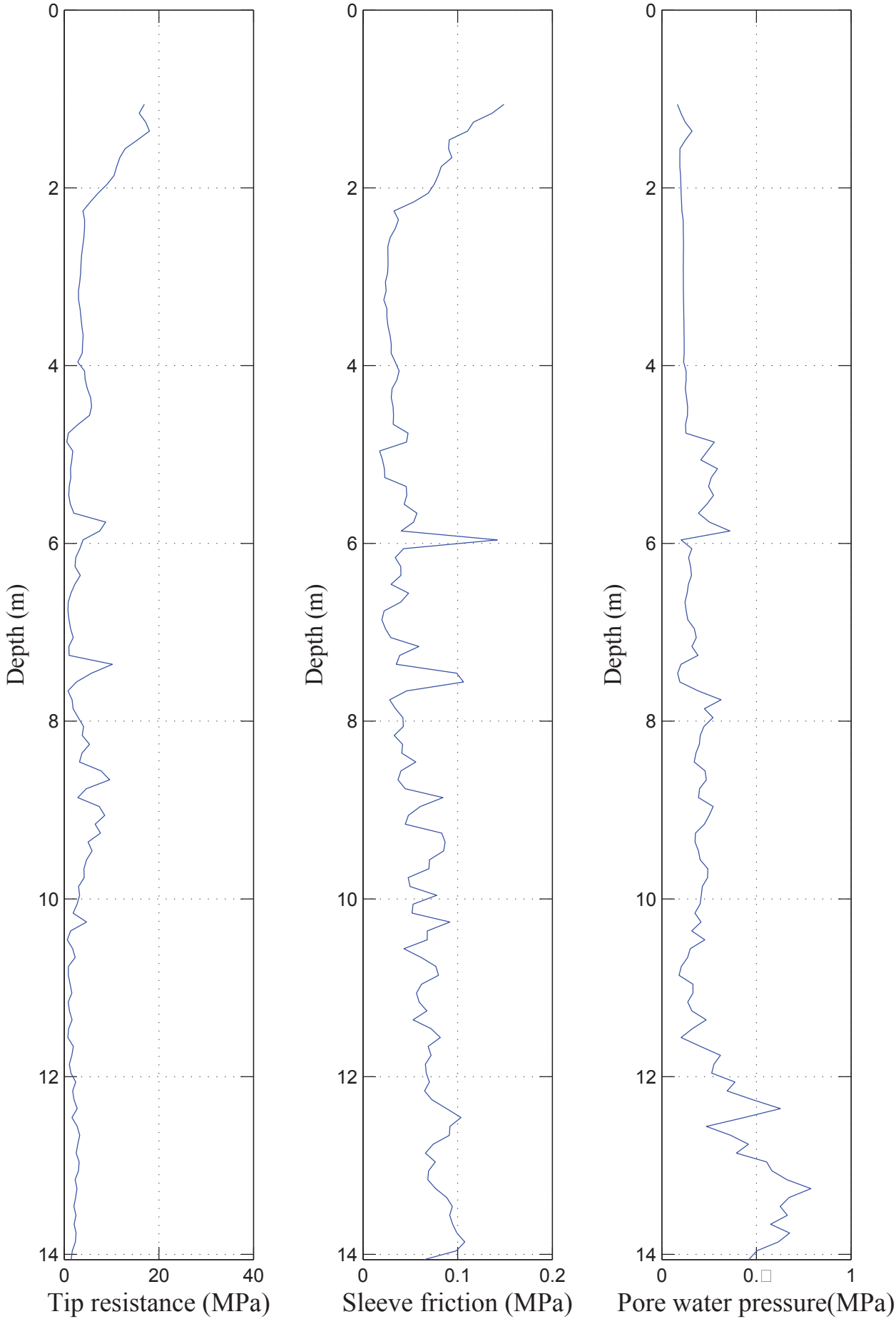
Depth (m)
0
2
4
6
8
10
12
14
0
20
40
Tip resistance (MPa)
Depth (m)
0
2
4
6
8
10
12
14
0
0.1
0.2
Sleeve friction (MPa)
Depth (m)
0
2
4
6
8
10
12
14
0
1
Pore water pressure(MPa)

APPENDIX F: CPT PROFILES

AALBORG SITE - SAND

CPT 1

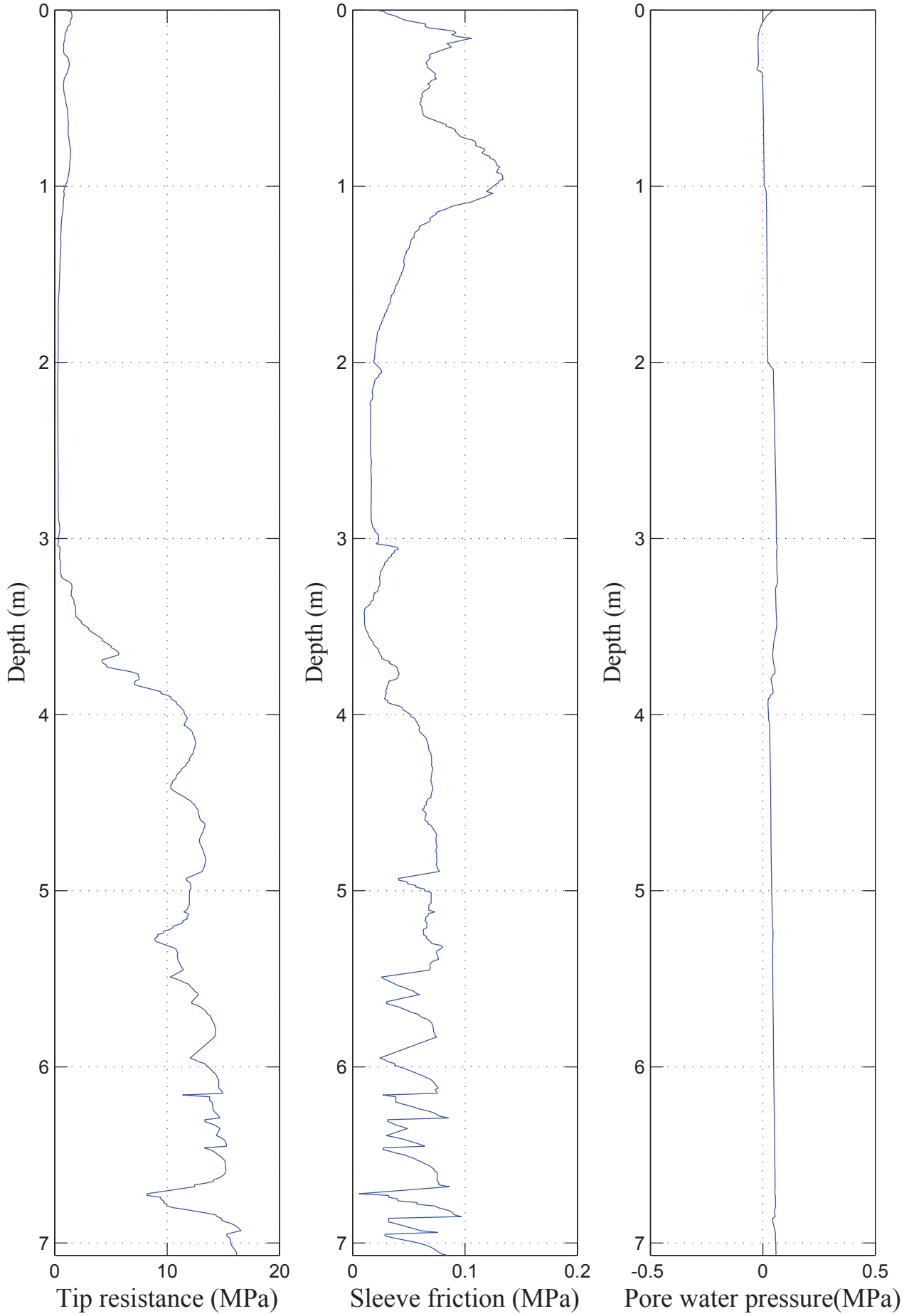
Depth (m)
0
1
2
3
4
5
6
7
0
10
20
Tip resistance (MPa)
Depth (m)
0
0.1
0.2
Sleeve friction (MPa)
Depth (m)
-0.5
0
0.5
Pore water pressure(MPa)

CPT 2

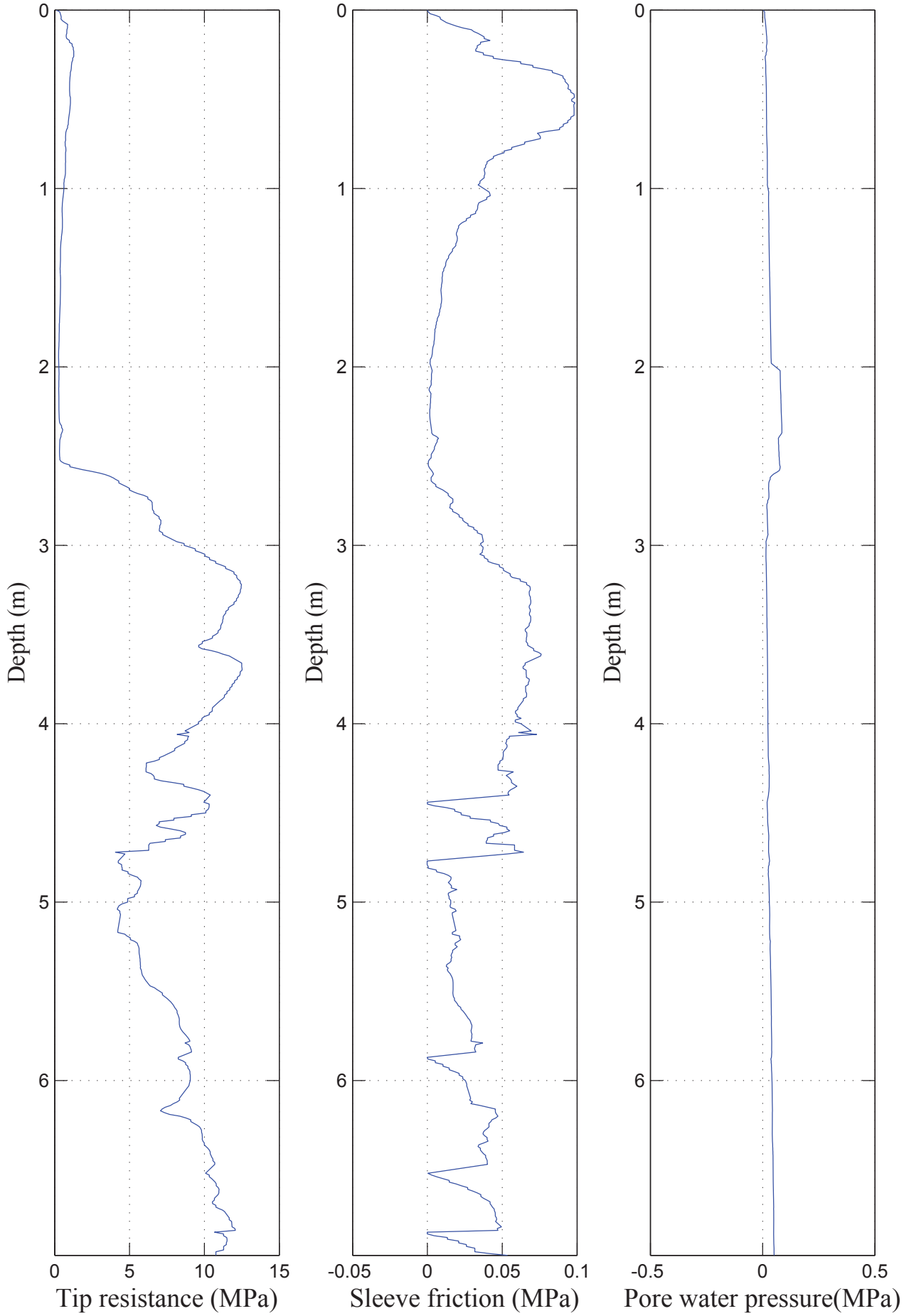
Depth (m)
0
1
2
3
4
5
6
0
5
10
15
Tip resistance (MPa)
-0.05
0
0.05
0.1
Sleeve friction (MPa)
-0.5
0
0.5
Pore water pressure(MPa)

CPT 3

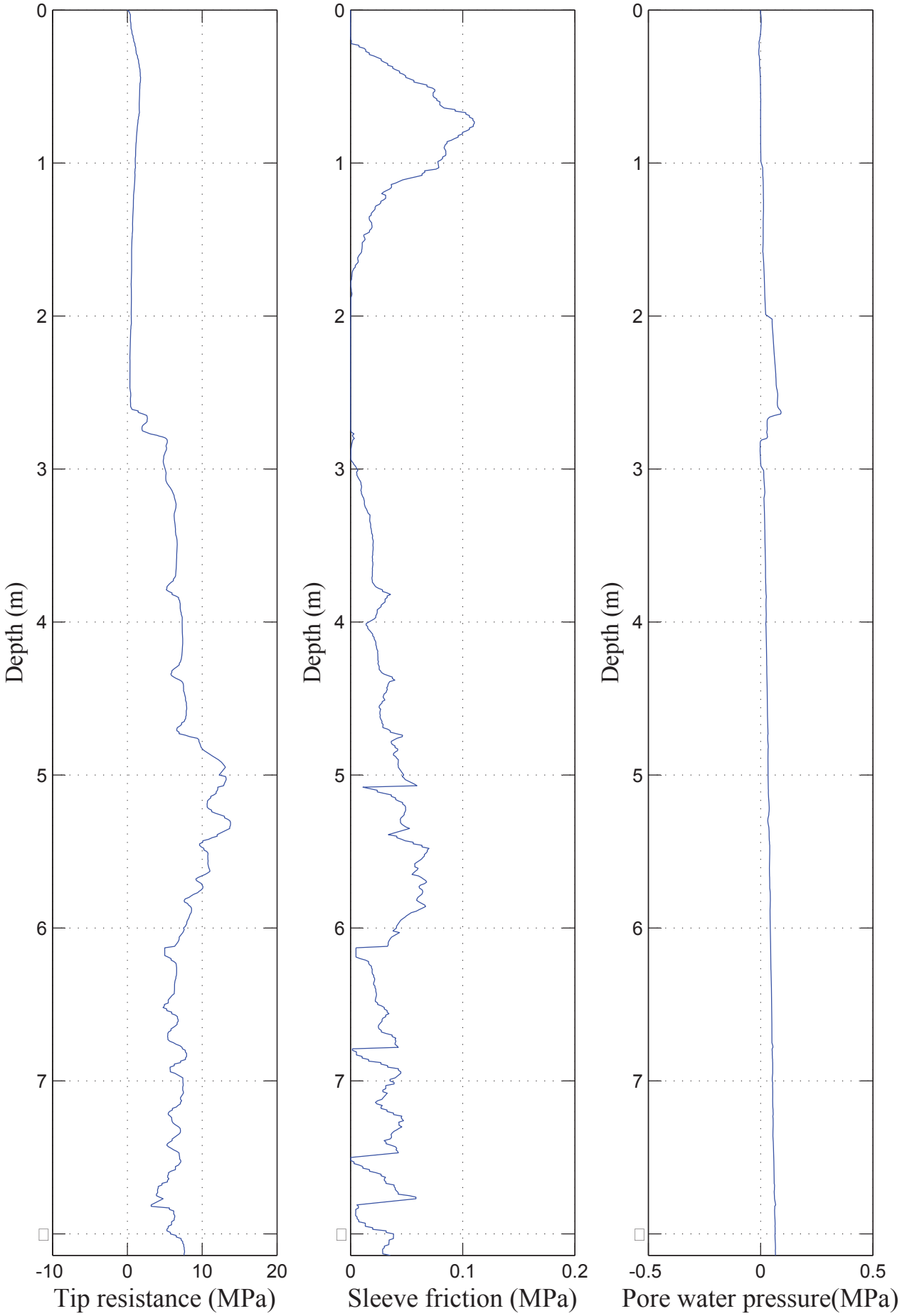
Depth (m)
0
1
2
3
4
5
6
7
-10
0
10
20
Tip resistance (MPa)
Depth (m)
0
0.1
0.2
Sleeve friction (MPa)
Depth (m)
-0.5
0
0.5
Pore water pressure(MPa)

CPT 4

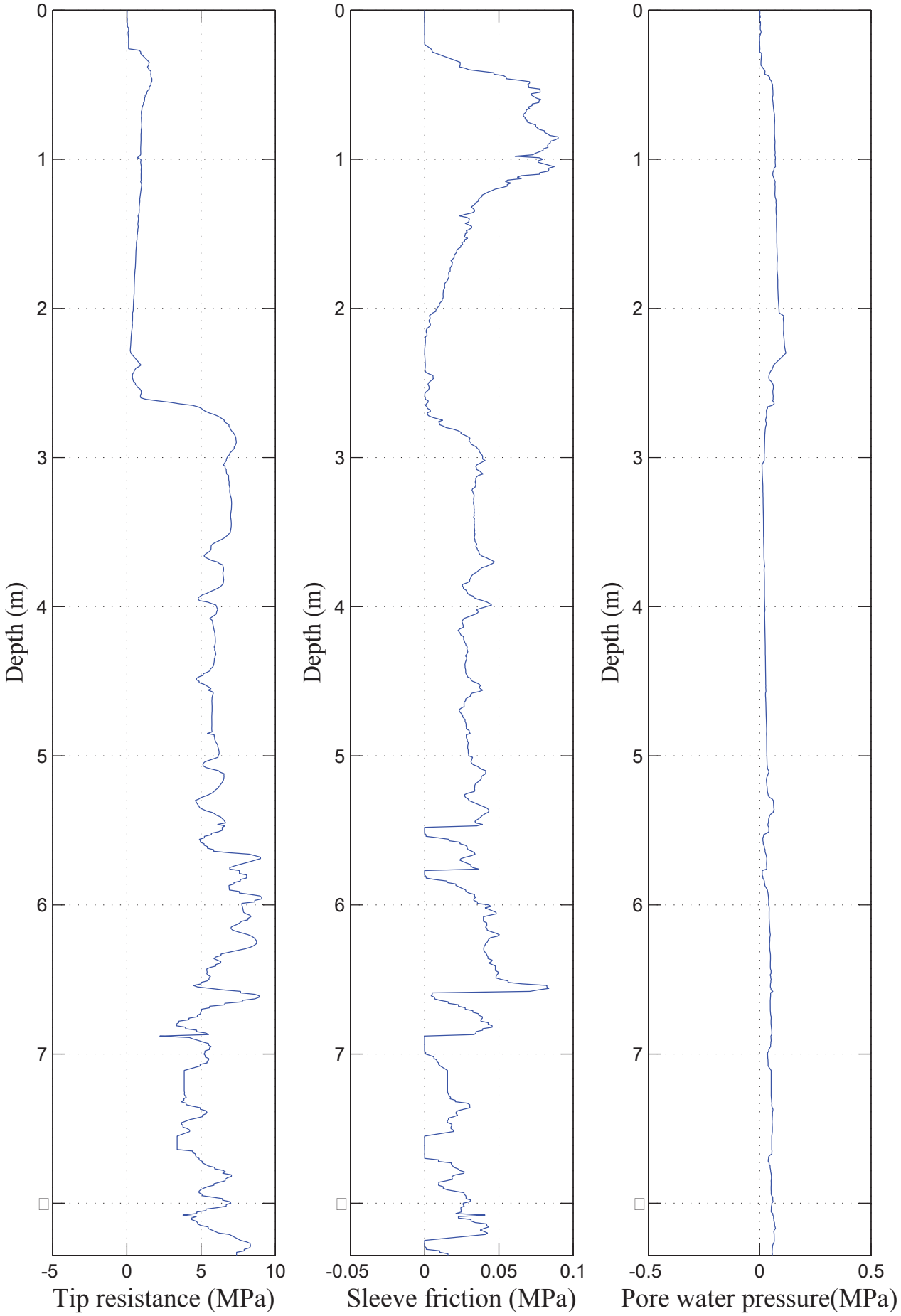
Depth (m)
0
1
2
3
4
5
6
7
-5
0
5
10
Tip resistance (MPa)
Depth (m)
-0.05
0
0.05
0.1
Sleeve friction (MPa)
Depth (m)
-0.5
0
0.5
Pore water pressure(MPa)

CPT 5

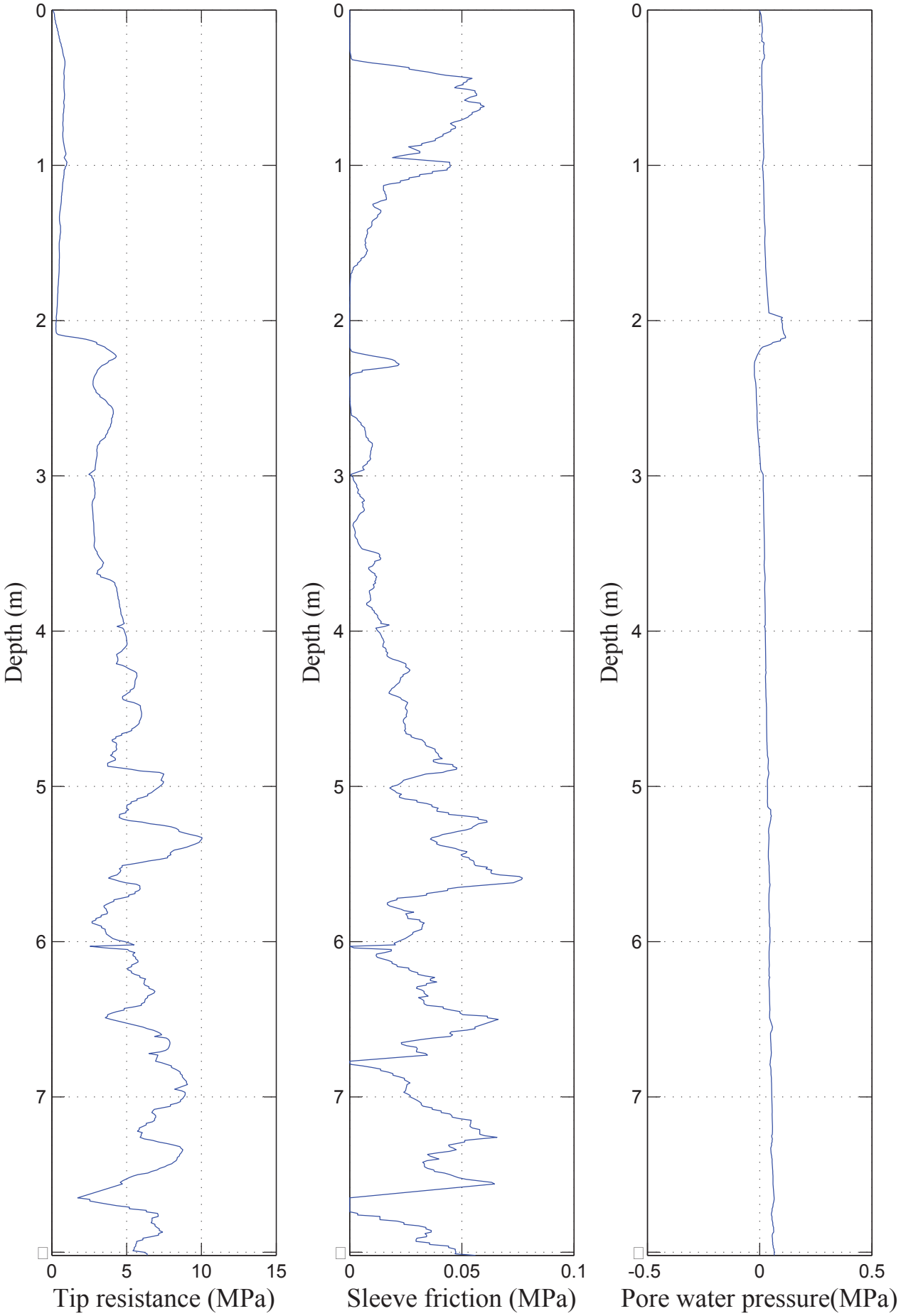
Depth (m)
0
1
2
3
4
5
6
7
0
5
10
15
Tip resistance (MPa)
Depth (m)
0
0.05
0.1
Sleeve friction (MPa)
Depth (m)
-0.5
0
0.5
Pore water pressure(MPa)

CPT 6

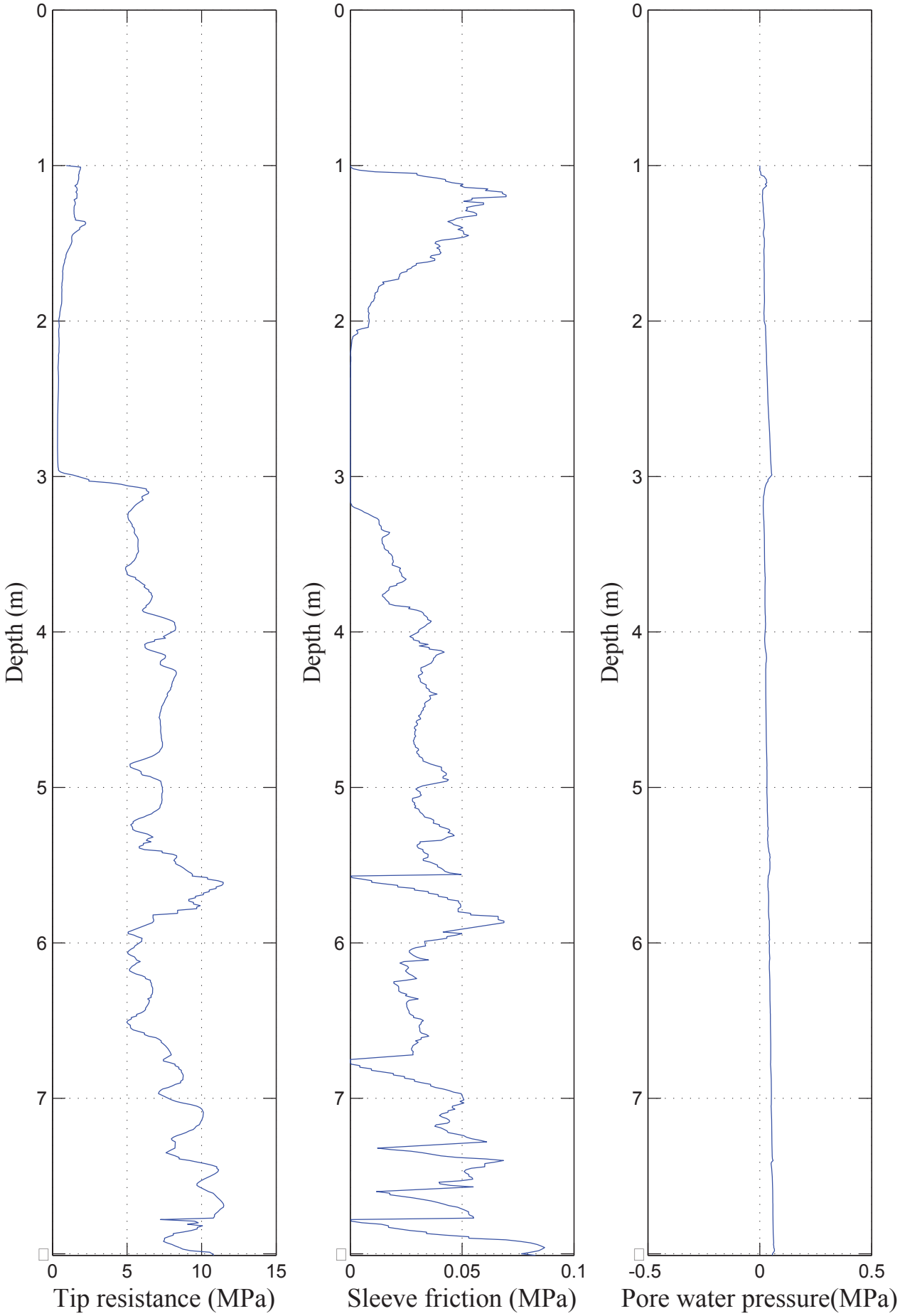
Depth (m)
0
1
2
3
4
5
6
7
0
5
10
15
Tip resistance (MPa)
Depth (m)
0
0.05
0.1
Sleeve friction (MPa)
Depth (m)
-0.5
0
0.5
Pore water pressure(MPa)

CPT 7

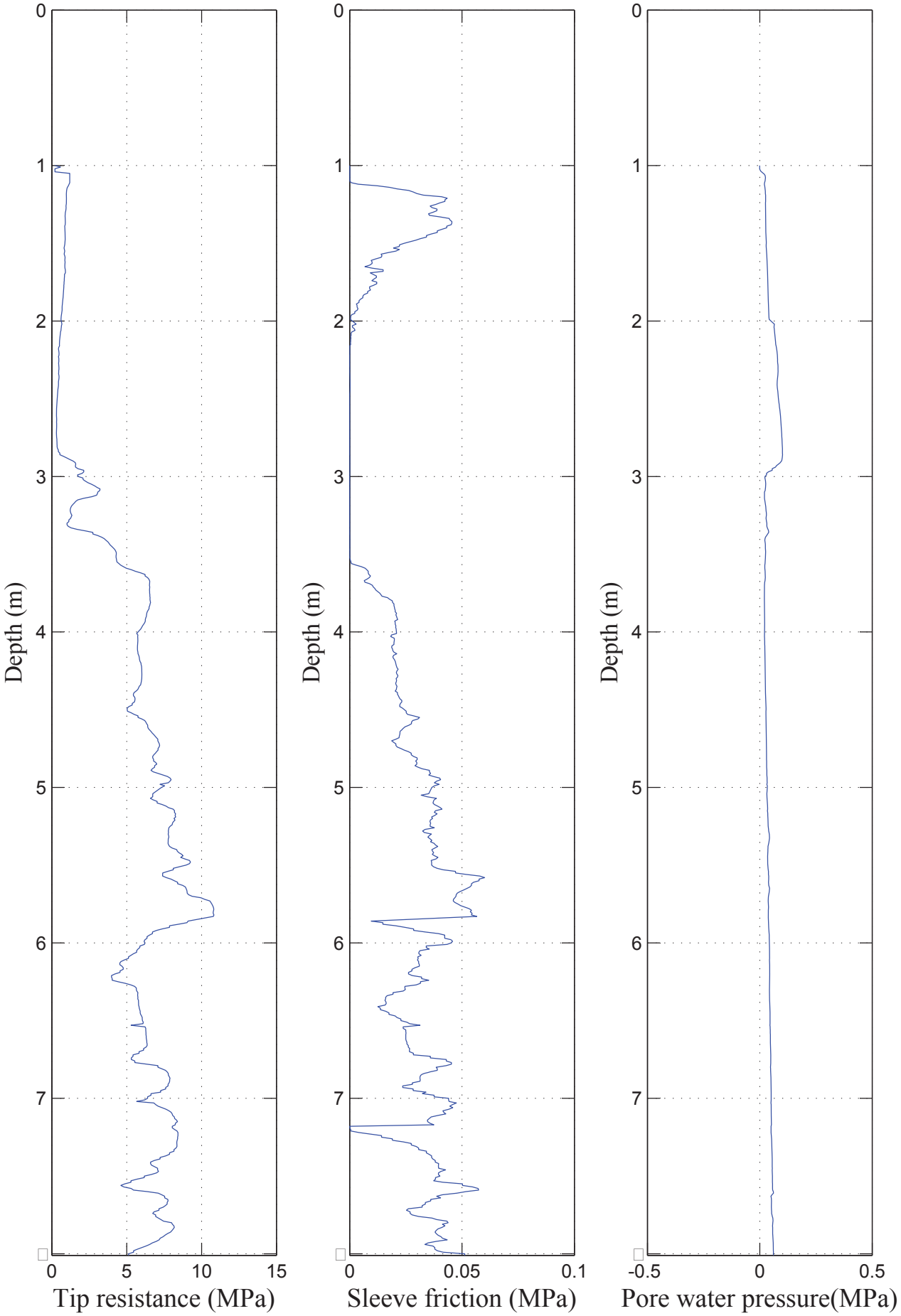
Depth (m)
0
1
2
3
4
5
6
7
0
5
10
15
Tip resistance (MPa)
Depth (m)
0
0.05
0.1
Sleeve friction (MPa)
Depth (m)
-0.5
0
0.5
Pore water pressure(MPa)

CPT 8

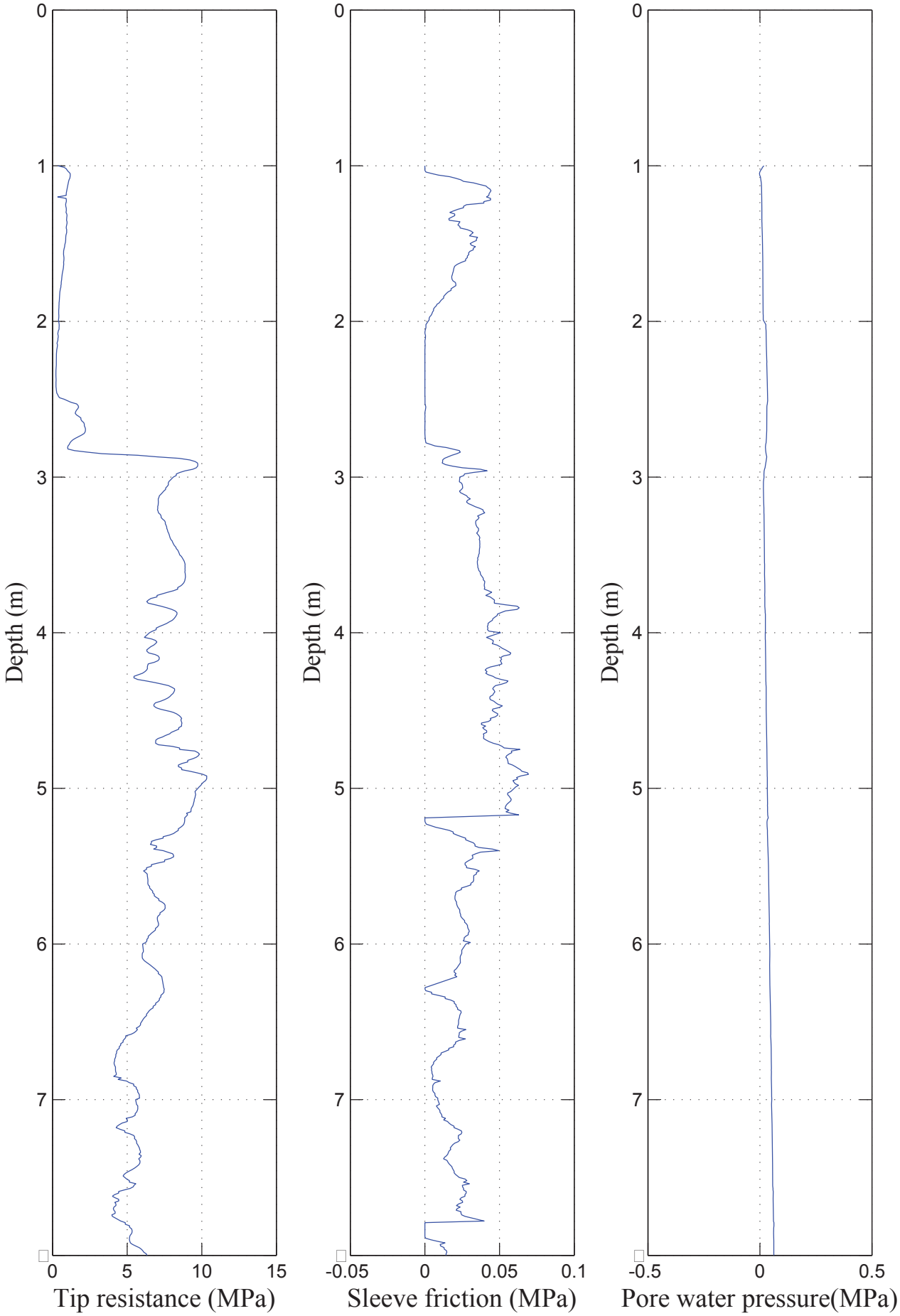
Depth (m)
0
1
2
3
4
5
6
7
0
5
10
15
Tip resistance (MPa)
Depth (m)
-0.05
0
0.05
0.1
Sleeve friction (MPa)
Depth (m)
-0.5
0
0.5
Pore water pressure(MPa)

CPT 9

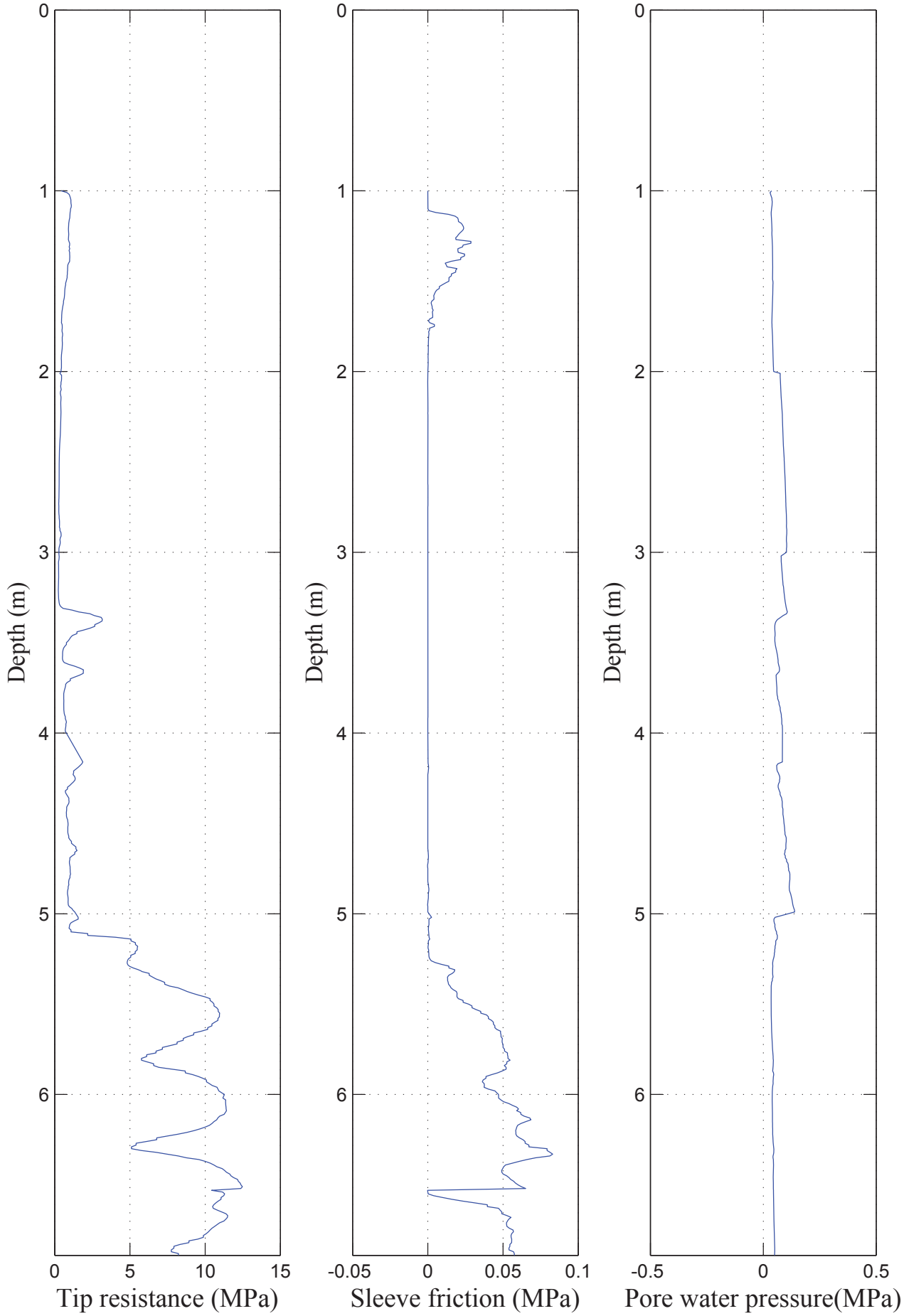
Depth (m)
0
1
2
3
4
5
6
0
5
10
15
Tip resistance (MPa)
-0.05
0
0.05
0.1
Sleeve friction (MPa)
-0.5
0
0.5
Pore water pressure(MPa)

APPENDIX F: CPT PROFILES

AALBORG SITE - CLAY

CPT 1

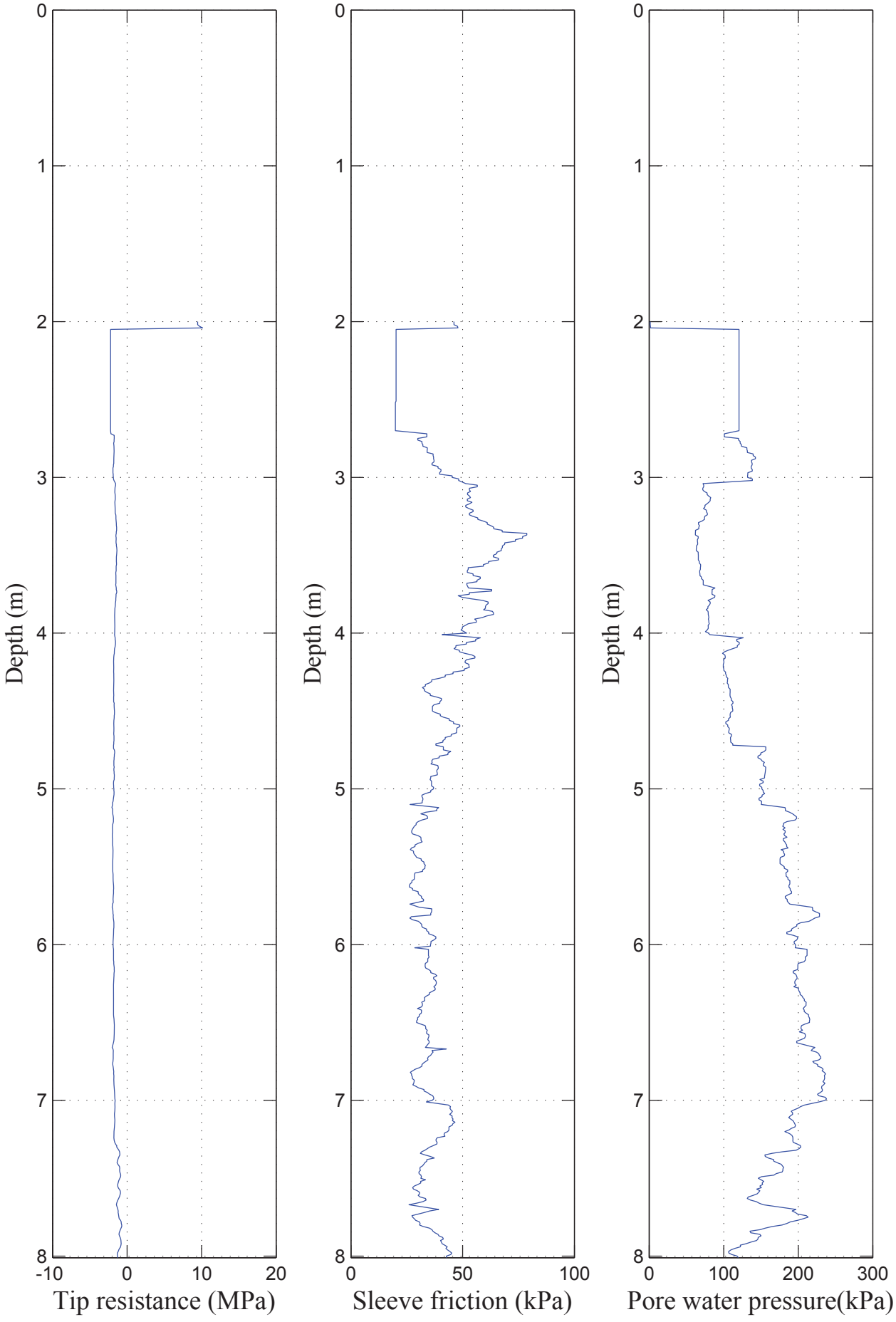
Depth (m)
0
1
2
3
4
5
6
7
8
-10
0
10
20
Tip resistance (MPa)
Depth (m)
0
50
100
Sleeve friction (kPa)
Depth (m)
0
100
200
300
Pore water pressure(kPa)

CPT 2

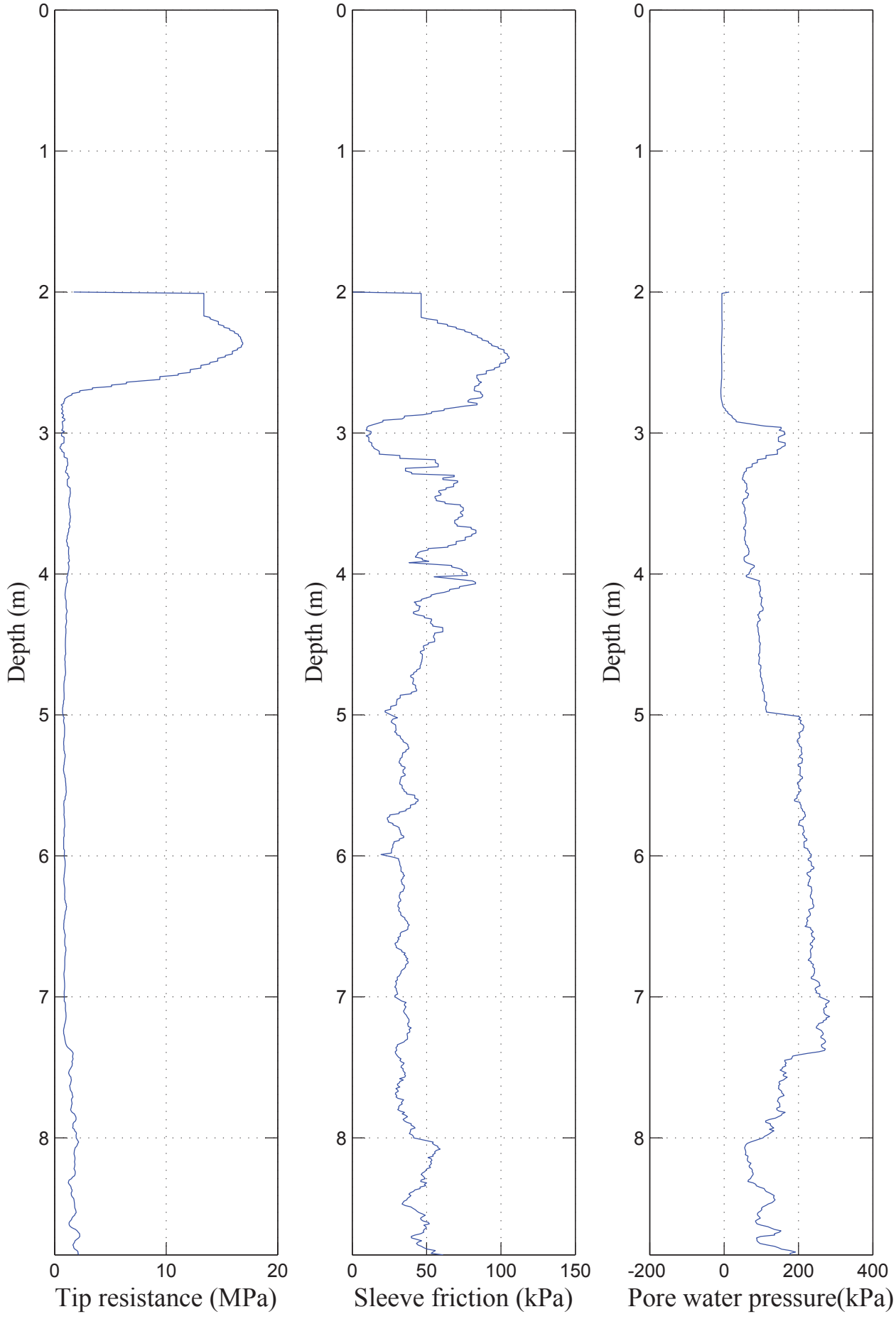
Depth (m)
0
1
2
3
4
5
6
7
8
0
10
20
Tip resistance (MPa)
0
50
100
150
Sleeve friction (kPa)
-200
0
200
400
Pore water pressure(kPa)

CPT 3

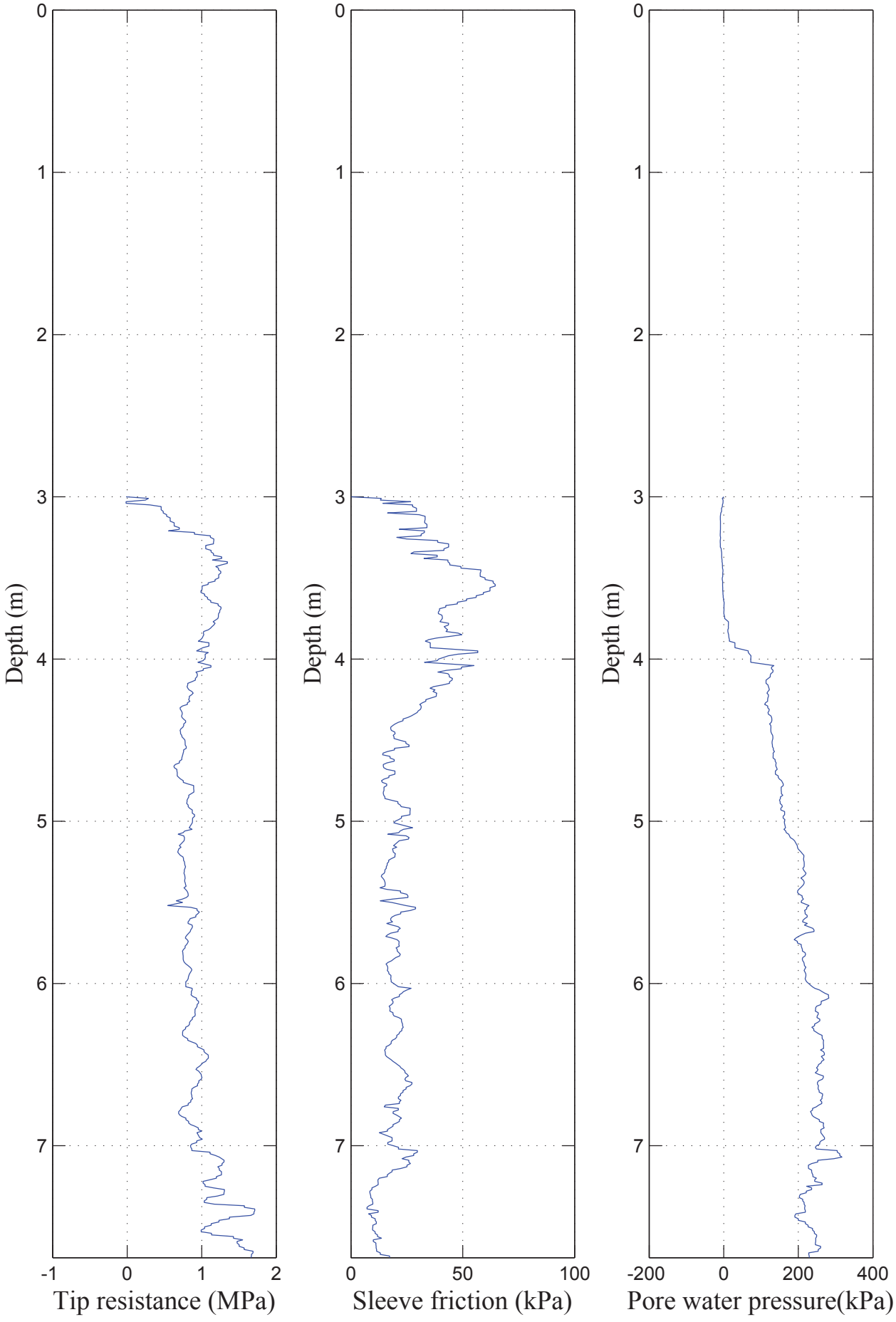
Depth (m)
0
1
2
3
4
5
6
7
-1
0
1
2
Tip resistance (MPa)
Depth (m)
0
50
100
Sleeve friction (kPa)
Depth (m)
-200
0
200
400
Pore water pressure(kPa)

CPT 4

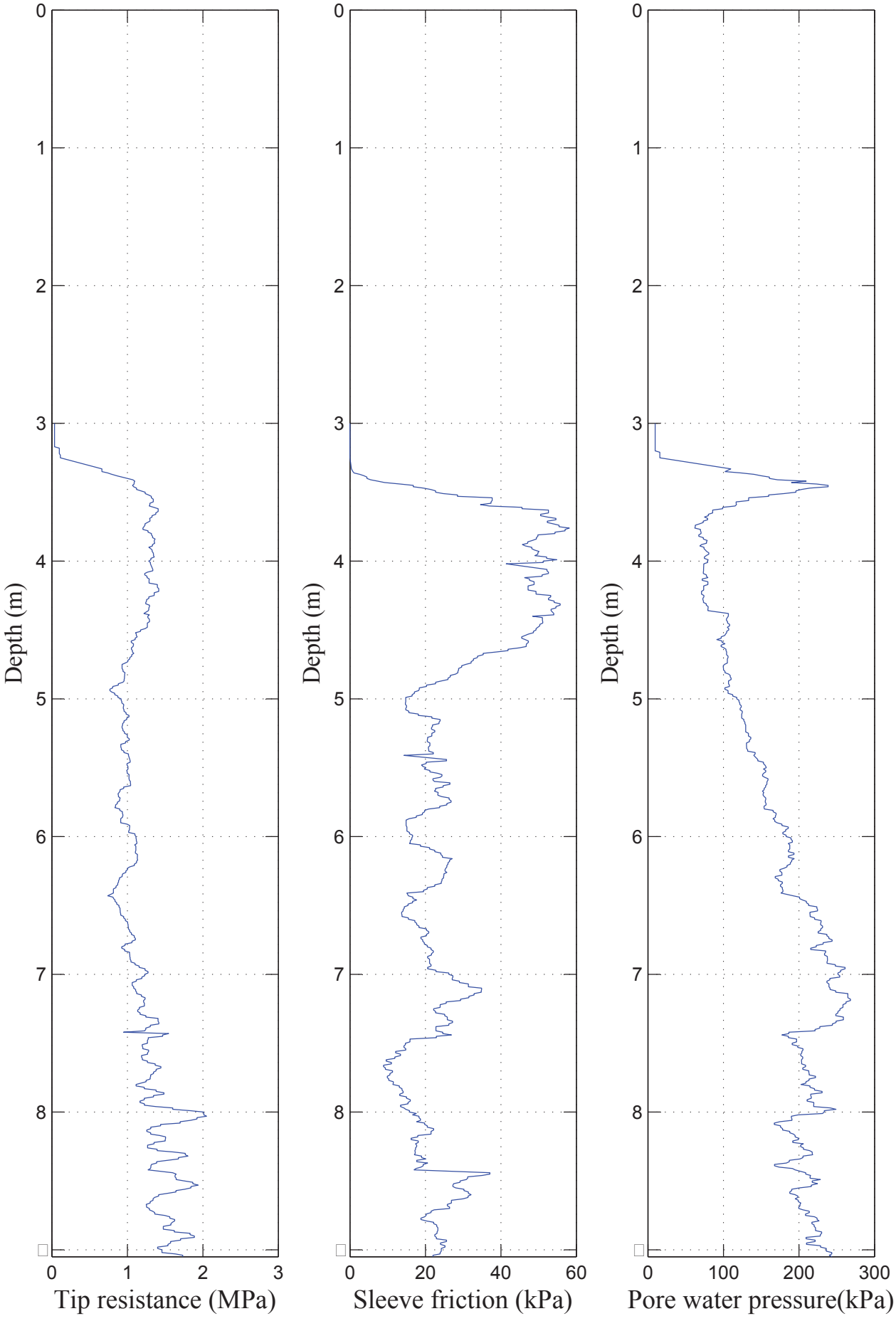
Depth (m)
0
1
2
3
4
5
6
7
8
Tip resistance (MPa)
0
1
2
3
Sleeve friction (kPa)
0
20
40
60
Pore water pressure(kPa)
0
100
200
300

CPT 5

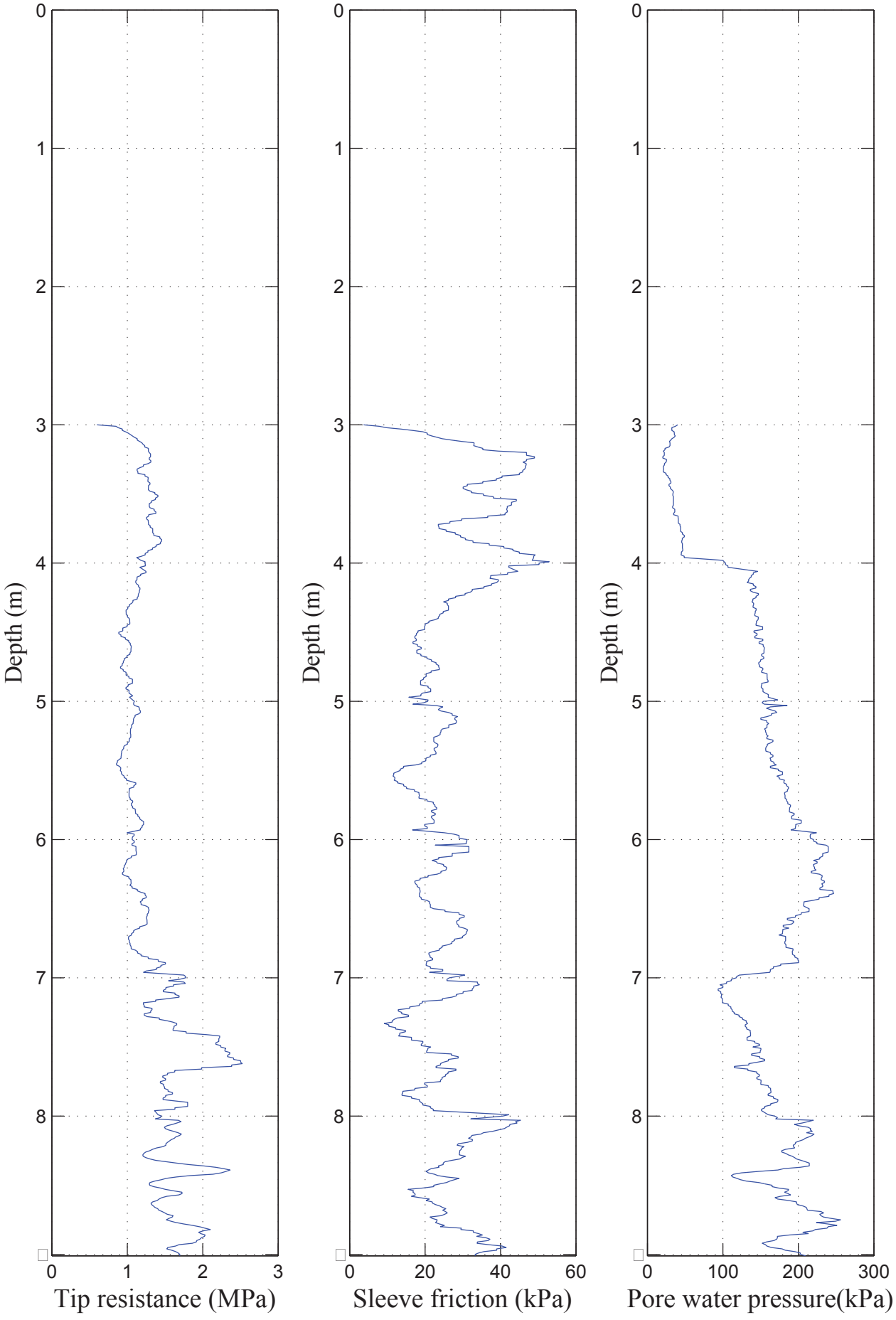
Depth (m)
0
1
2
3
4
5
6
7
8
0
1
2
3
Tip resistance (MPa)
Depth (m)
0
20
40
60
Sleeve friction (kPa)
Depth (m)
0
100
200
300
Pore water pressure(kPa)

APPENDIX F: CPT PROFILES

FREDERIKSHAVN SITE

CPT 1

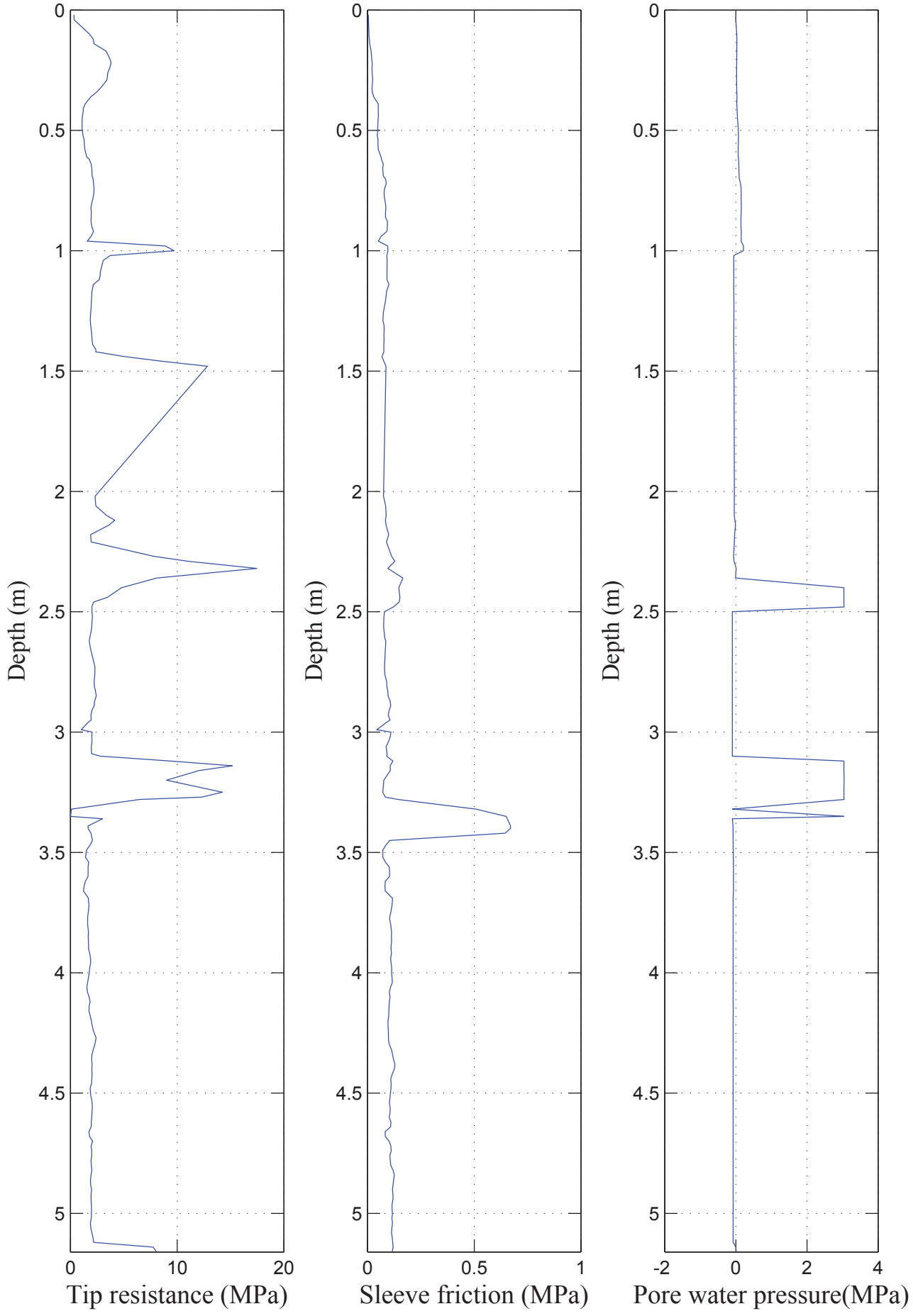
Depth (m)
0
0.5
1
1.5
2
2.5
3
3.5
4
4.5
5
0
10
20
Tip resistance (MPa)
0
0.5
1
Sleeve friction (MPa)
-2
0
2
4
Pore water pressure(MPa)

CPT 2

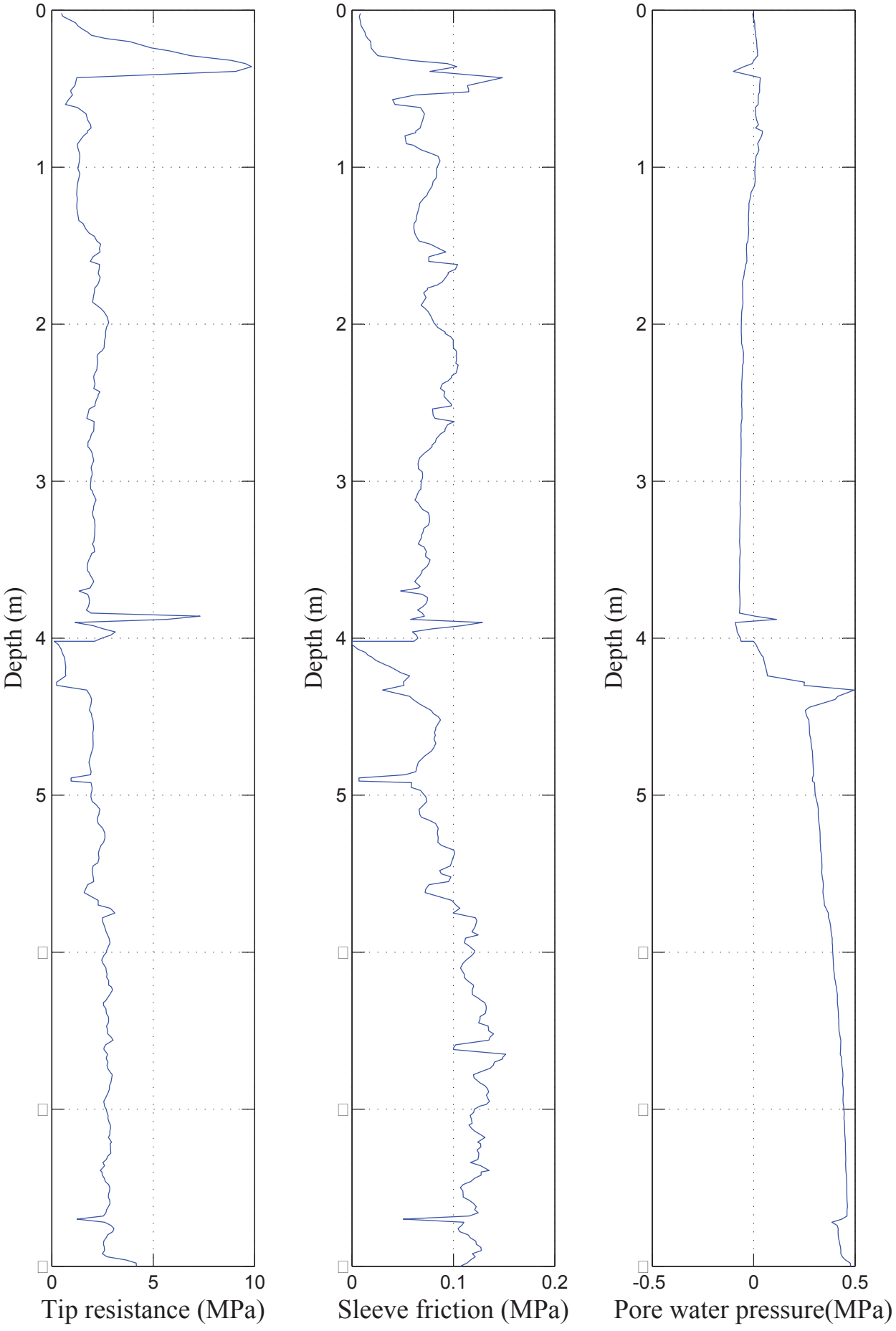
Depth (m)
0
1
2
3
4
5
0
5
10
Tip resistance (MPa)
Depth (m)
0
1
2
3
4
5
0
0.1
0.2
Sleeve friction (MPa)
Depth (m)
0
1
2
3
4
5
-0.5
0
0.5
Pore water pressure(MPa)

CPT 3

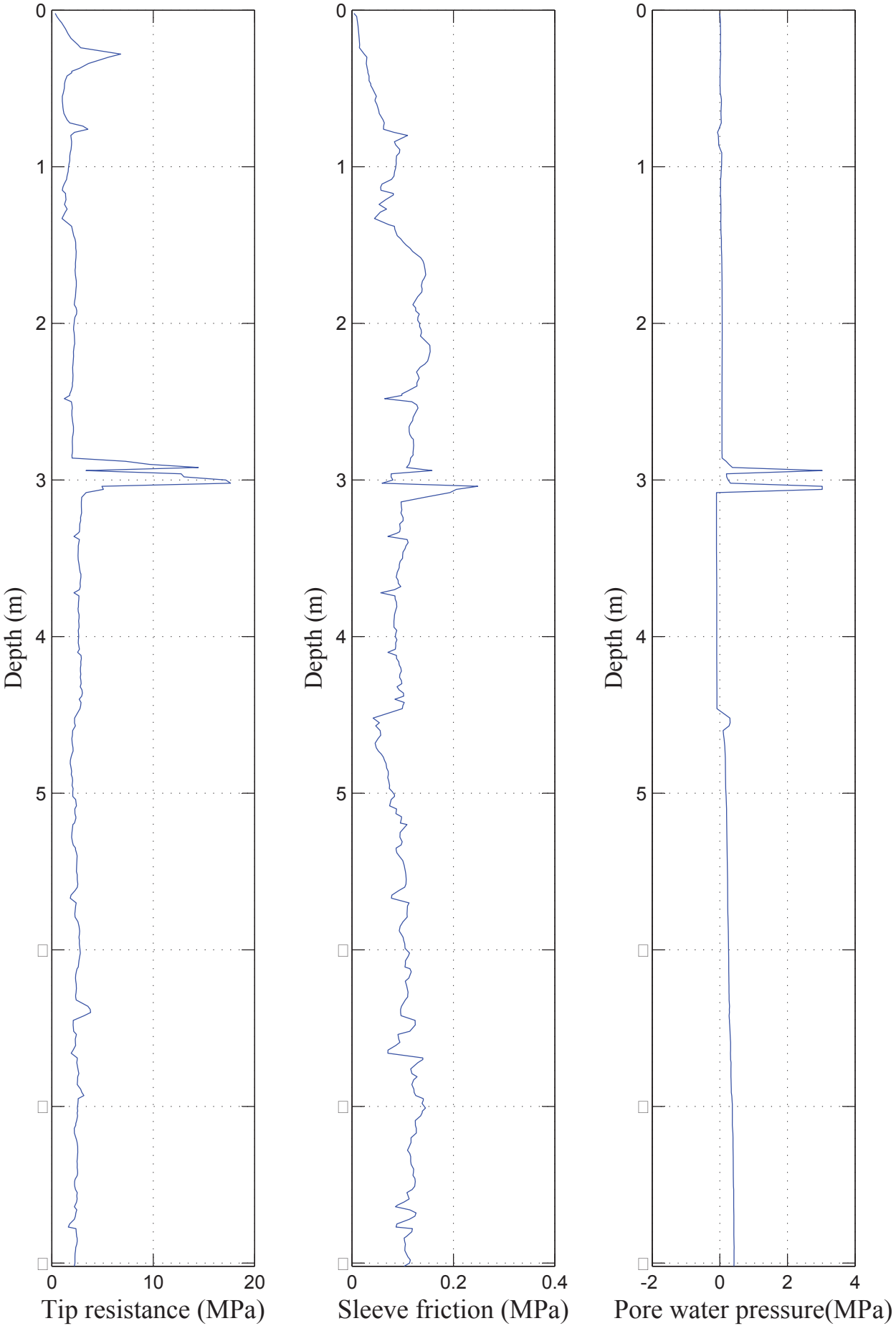
Depth (m)
0
1
2
3
4
5
0
10
20
Tip resistance (MPa)
0
0.2
0.4
Sleeve friction (MPa)
-2
0
2
4
Pore water pressure(MPa)

CPT 4

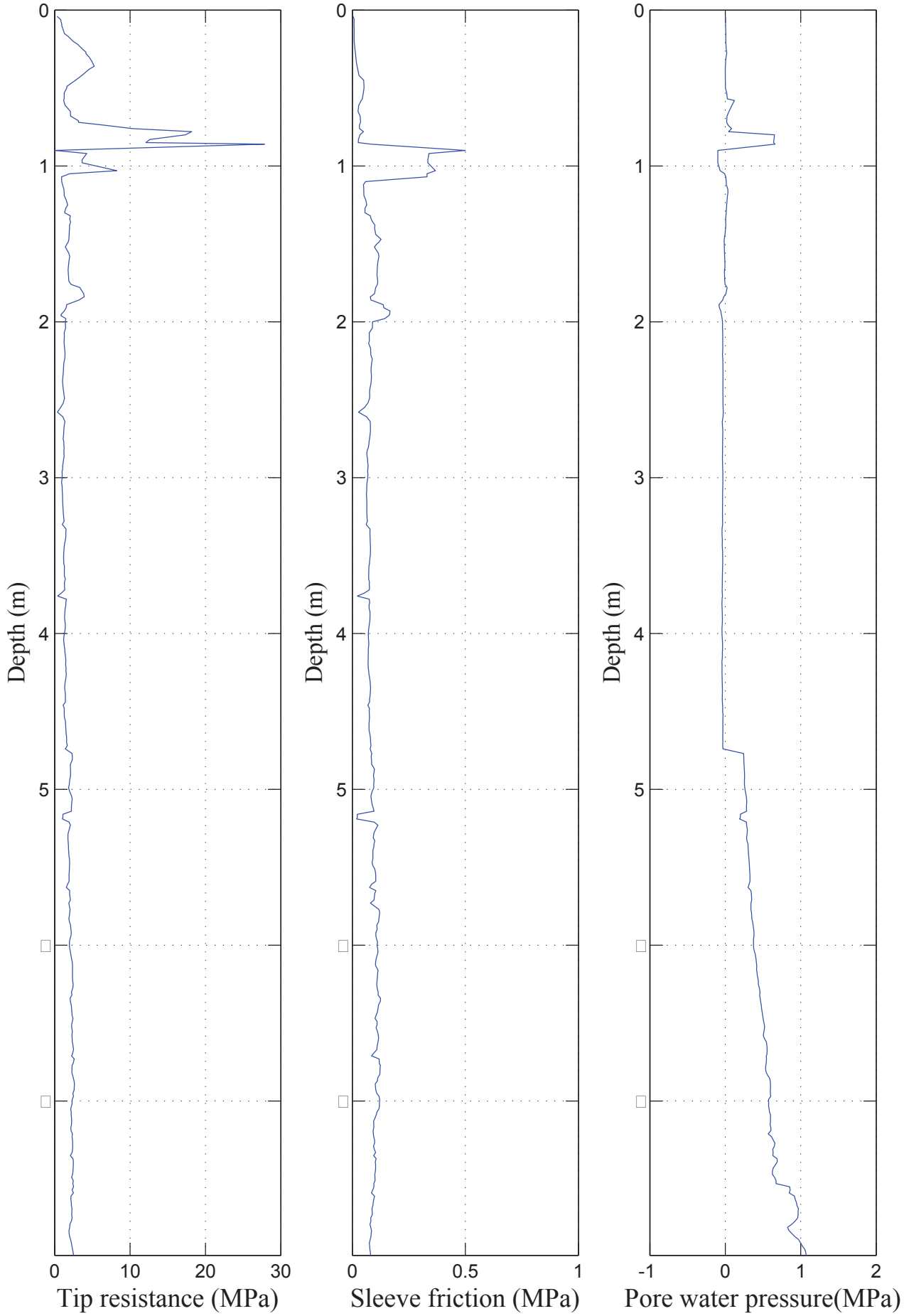
Depth (m)
0
1
2
3
4
5
0
10
20
30
Tip resistance (MPa)
Depth (m)
0
0.5
1
Sleeve friction (MPa)
Depth (m)
-1
0
1
2
Pore water pressure(MPa)

CPT 5

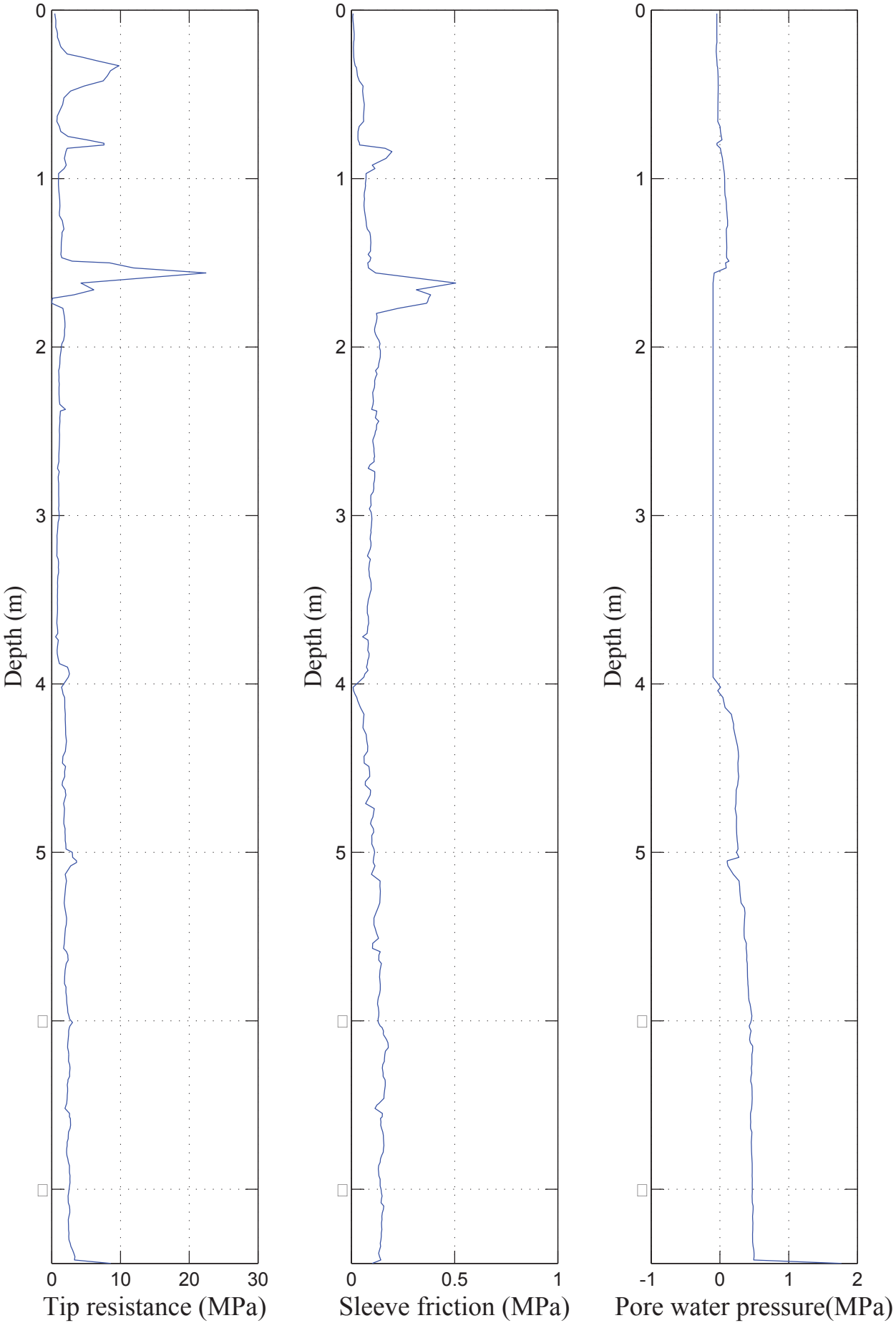
Depth (m)
0
1
2
3
4
5
0
10
20
30
Tip resistance (MPa)
0
0.5
1
Sleeve friction (MPa)
-1
0
1
2
Pore water pressure(MPa)

CPT 6

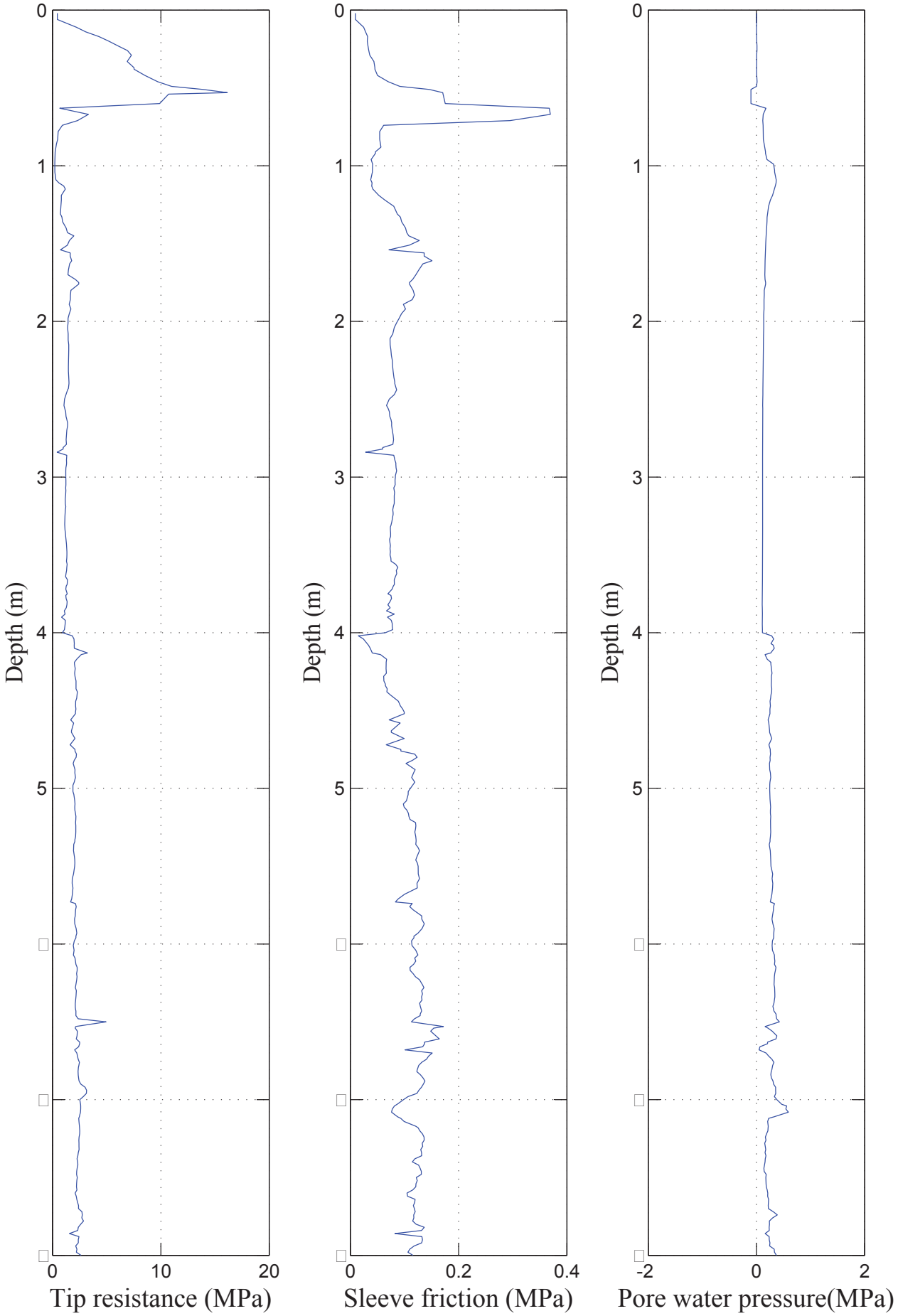
Depth (m)
0
1
2
3
4
5
0
10
20
Tip resistance (MPa)
Depth (m)
0
0.2
0.4
Sleeve friction (MPa)
Depth (m)
-2
0
2
Pore water pressure(MPa)

CPT 7

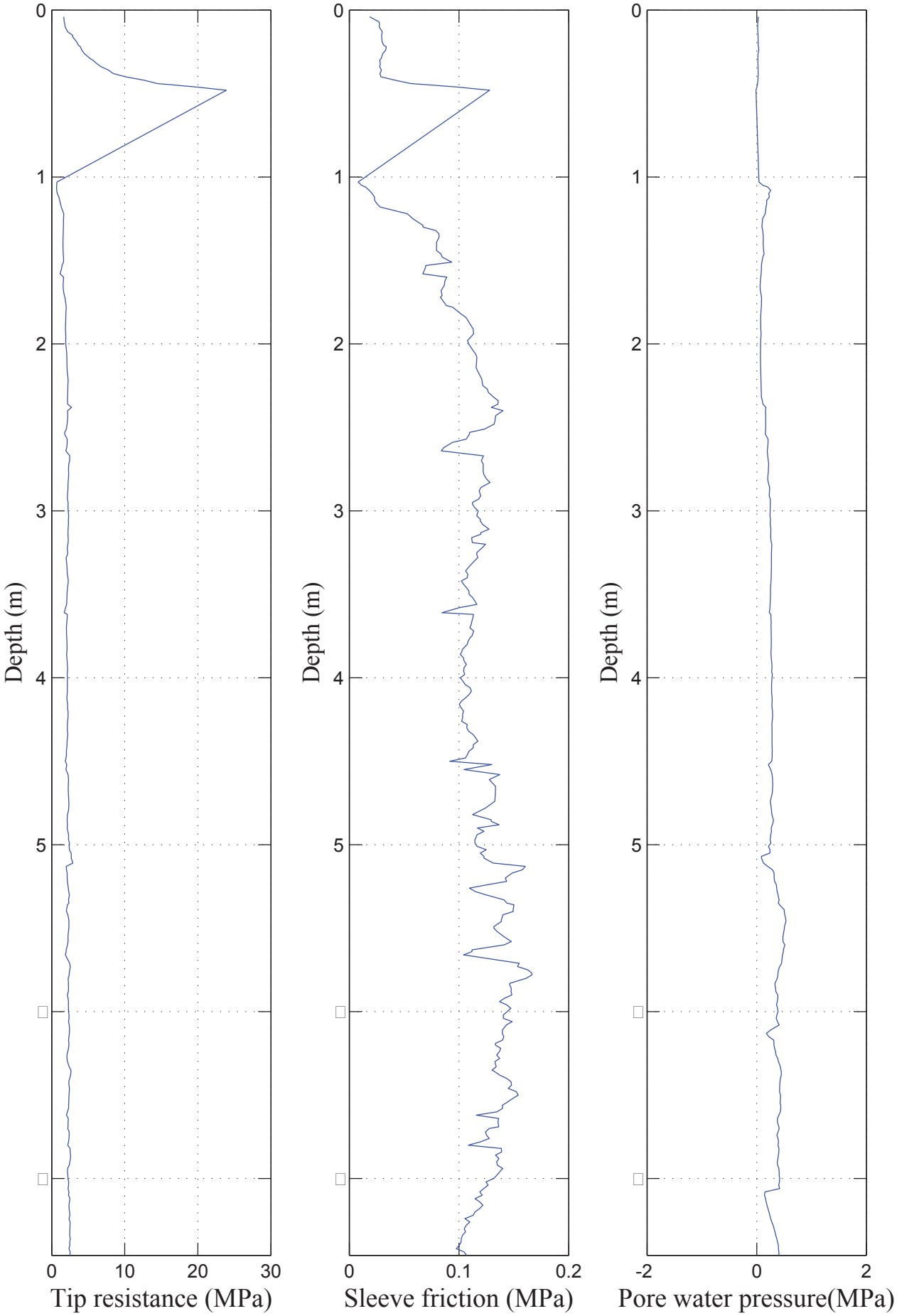
Depth (m)
0
1
2
3
4
5
0
10
20
30
Tip resistance (MPa)
0
0.1
0.2
Sleeve friction (MPa)
-2
0
2
Pore water pressure(MPa)

CPT 8

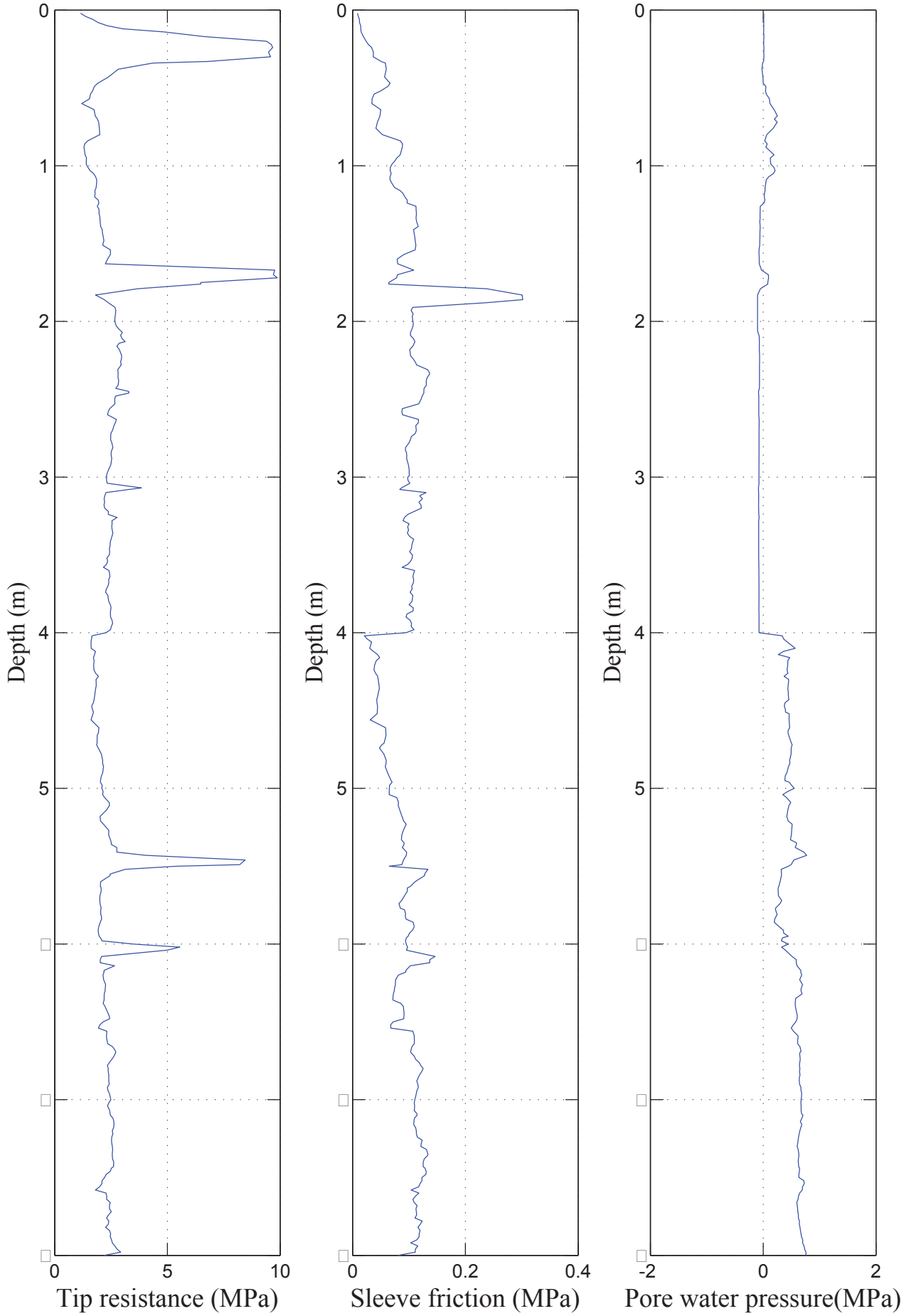
Depth (m)
0
1
2
3
4
5
0
5
10
Tip resistance (MPa)
Depth (m)
0
1
2
3
4
5
0
0.2
0.4
Sleeve friction (MPa)
Depth (m)
0
1
2
3
4
5
-2
0
2
Pore water pressure(MPa)

CPT 9

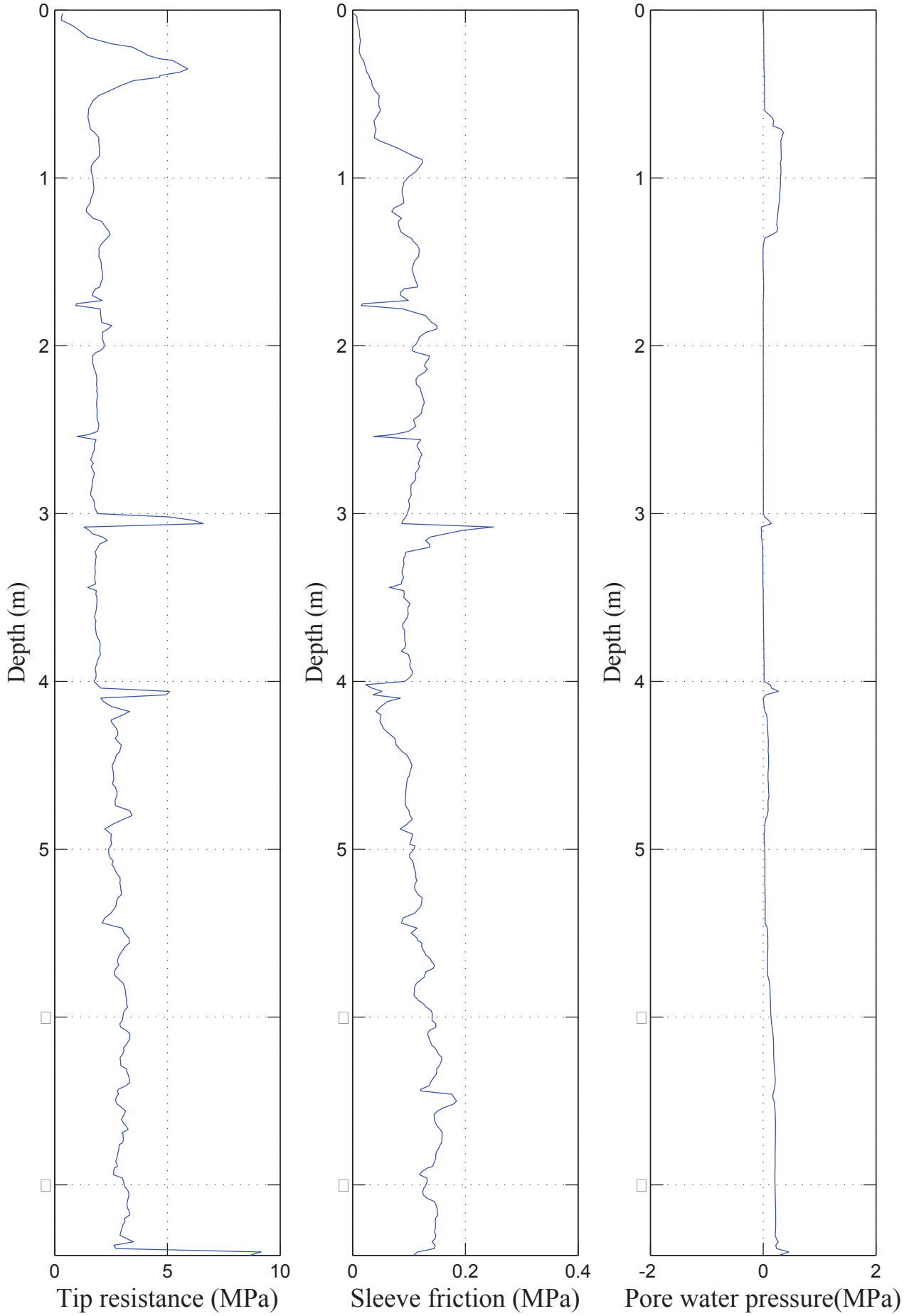
Depth (m)
0
1
2
3
4
5
0
5
10
Tip resistance (MPa)
Depth (m)
0
1
2
3
4
5
0
0.2
0.4
Sleeve friction (MPa)
Depth (m)
0
1
2
3
4
5
-2
0
2
Pore water pressure(MPa)

CPT 10

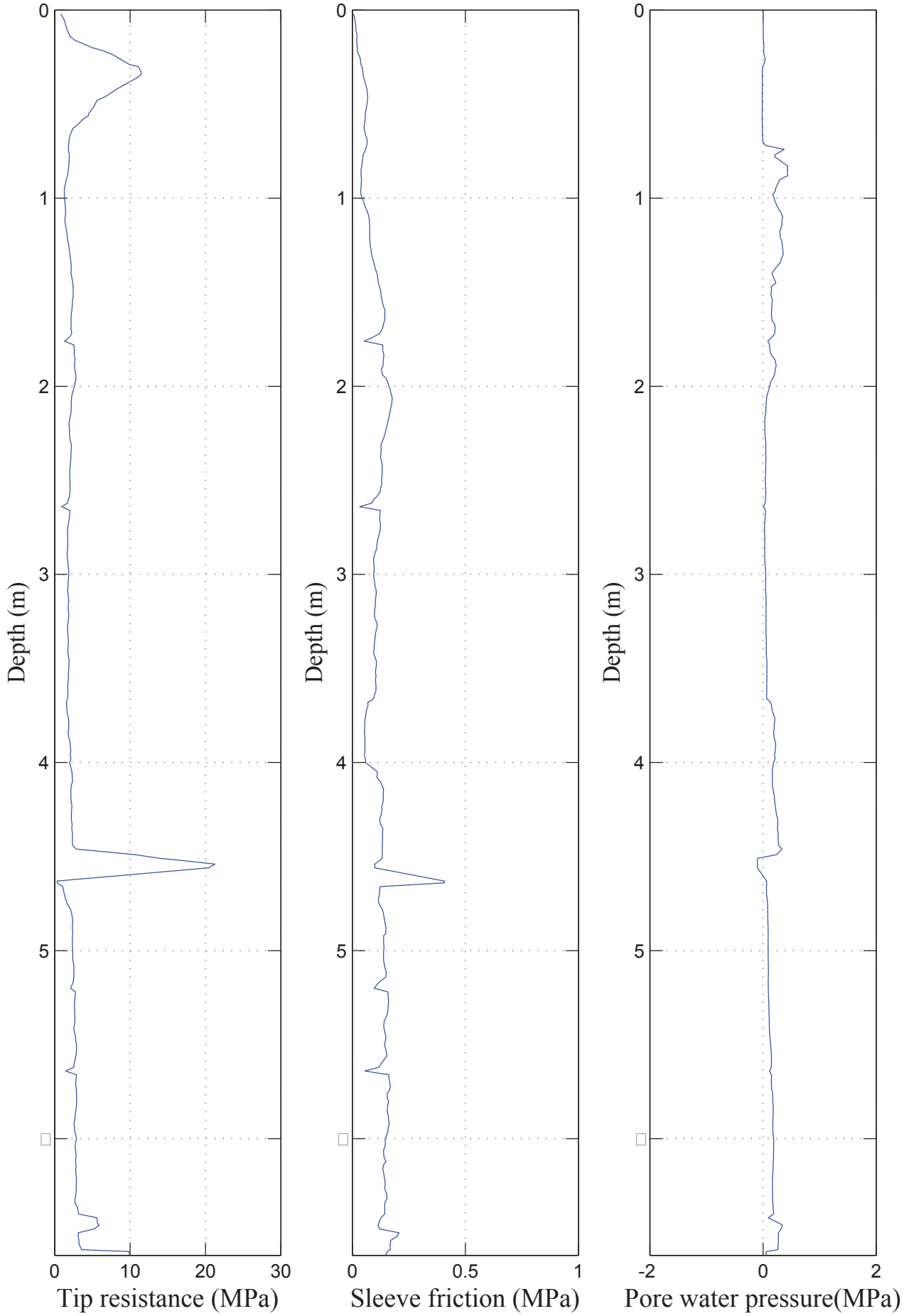
Depth (m)
0
1
2
3
4
5
0
10
20
30
Tip resistance (MPa)
0
0.5
1
Sleeve friction (MPa)
-2
0
2
Pore water pressure(MPa)

CPT 11

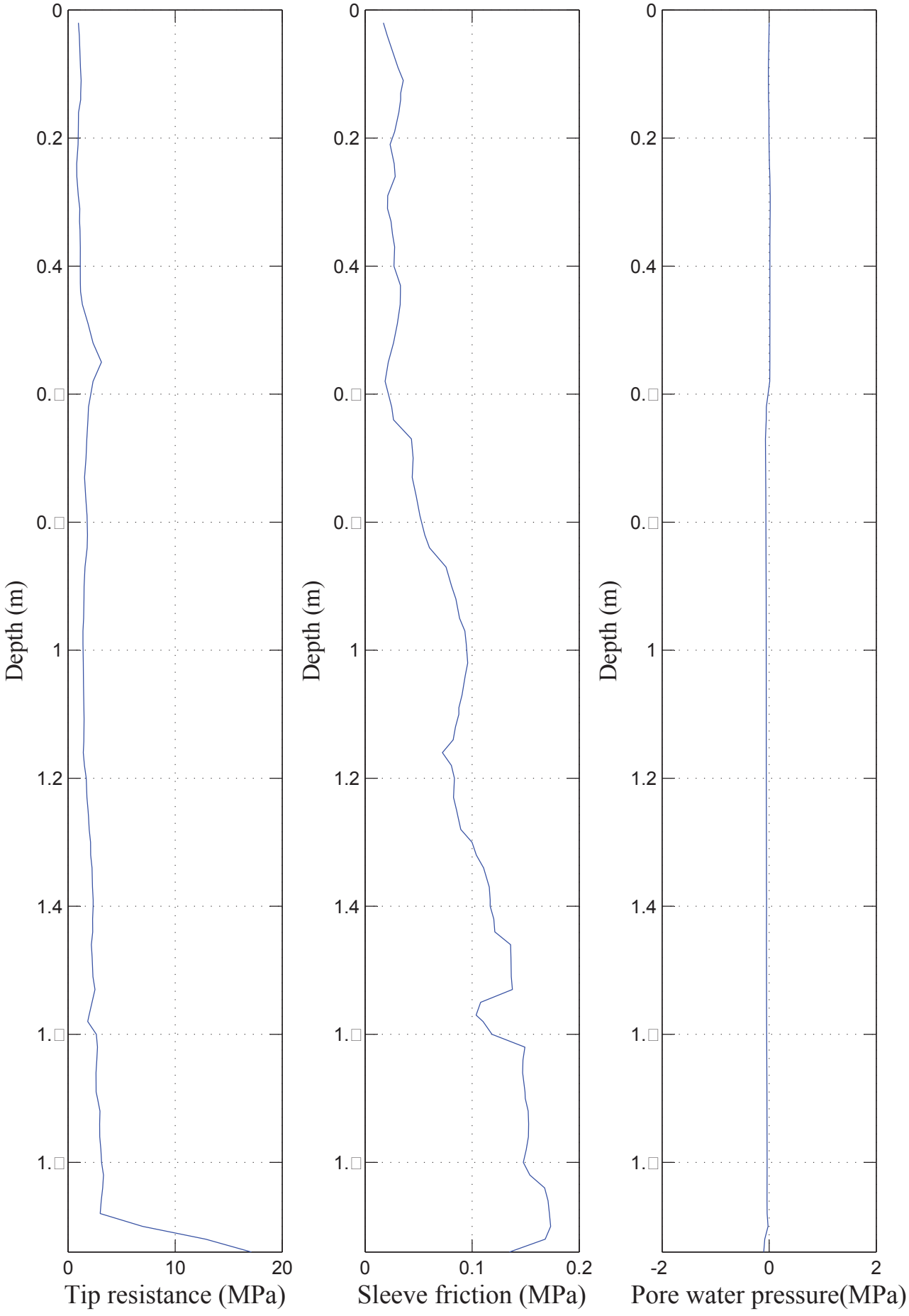
Depth (m)
0
0.2
0.4
1
1.2
1.4
0
10
20
Tip resistance (MPa)
0.1
0.2
Sleeve friction (MPa)
-2
2
Pore water pressure(MPa)

CPT 12

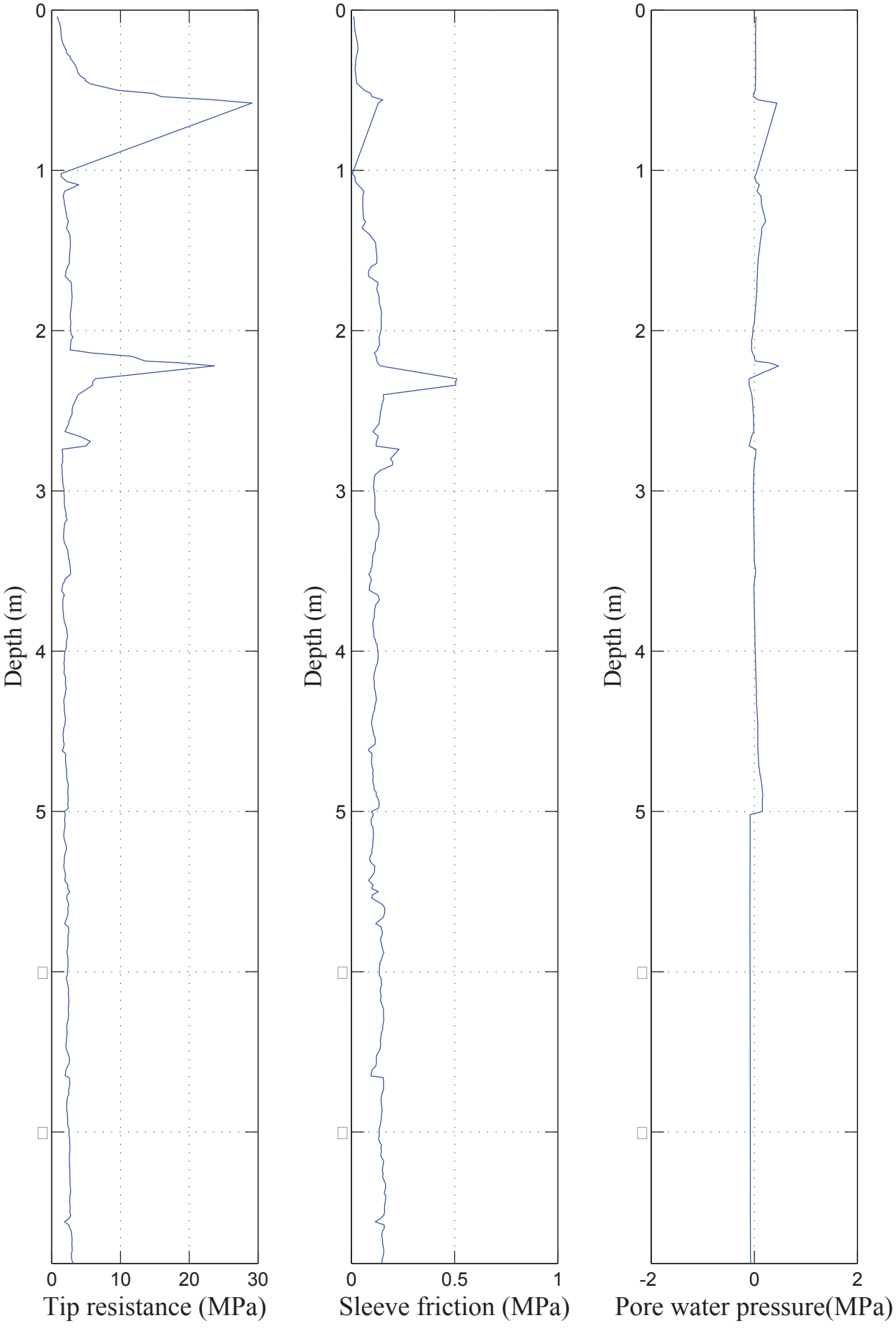
Depth (m)
0
1
2
3
4
5
0
10
20
30
Tip resistance (MPa)
0
0.5
1
Sleeve friction (MPa)
-2
0
2
Pore water pressure(MPa)

APPENDIX G: BOREHOLE PROFILES

AARHUS SITE - LIGHT HOUSE

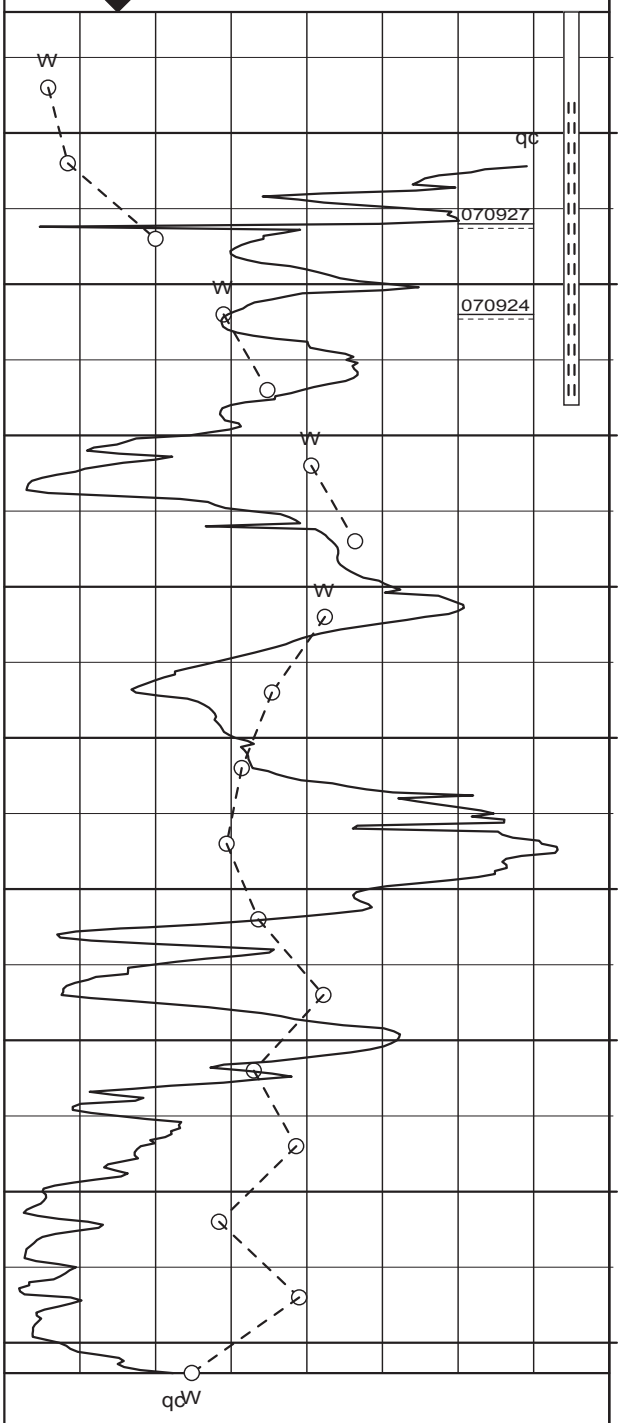

Dybde	Kote (m)	Nr.	Jordart Karakterisering	Aflejring	Alder
			ASFALT		
	1	179	FYLD: SAND, mellem, ringe sorteret, gruset, gulbrunt, khl.	Fy	Re
1		180	FYLD: SAND - " -	Fy	Re
		181	FYLD: SAND, mellem, ringe sorteret, gruset, organiskh., enk. teglstk., grålig brunt, khl.	Fy	Re
	0	182	FYLD: SAND, mellem, ringe sorteret, gruset, enk. lerklp., grålig brunt, khl.	Fy	Re
		183	FYLD: SAND - " -	Fy	Re
	-1	184	FYLD: LER, sandet, grålig brunt, khl.	Fy	Re
		185	FYLD: SAND, leret, grålig brunt, khl.	Fy	Re
	-2	186	FYLD: SAND, mellem, ringe sorteret, gruset, grålig brunt, khl.	Fy	Re
		187	FYLD: SAND - " -	Fy	Re
	-3	188	FYLD: SAND, groft, ringe sorteret, gruset, brunlig gråt, khl.	Fy	Re
		189	FYLD: SAND, mellem, ringe sorteret, gruset, brunlig gråt, khl.	Fy	Re
	-4	190	FYLD: SAND, groft, ringe sorteret, gruset, brunlig gråt, khl.	Fy	Re
		191	FYLD: SAND, leret, gråt, khl.	Fy	Re
	-5	192	FYLD: SAND, mellem, ringe sorteret, gruset, gråt, khl.	Fy	Re
		193	FYLD: SAND, mellem, ringe sorteret, gruset, leret, gråt, khl.	Fy	Re
	-6	194	FYLD: SAND, ringe sorteret, gruset, sv. leret, gråt, khl.	Fy	Re
		195	FYLD: LER, sandet, olivengråt, khl.	Fy	Re
	-7	196	FYLD: SAND, leret, olivengråt, khl.	Fy	Re

Fortsættes

○	10	20 30	W (%)
●○	100	200 300	Cv,Cvr (kN/m²)
		10	qc (MN/m²)
⊗		9	pH

Boremetode : Tørboring

X : 219068 (m) Y : 192968 (m) Plan :

Sag : 25.0705.61 Århus, Light*House

Geolog : JBM Boret af : LER/JQB Dato : 20070924 DGU-nr.: Boring : L*H7

Udarb. af : HLa Kontrol : Godkendt : Dato : Bilag : 1 S. 1 / 5

Grontmij | Carl Bro
Tlf. 98 79 98 00, Fax 98 79 98 01
Sofiendalsvej 94, 9200 Aalborg SV

Boreprofil

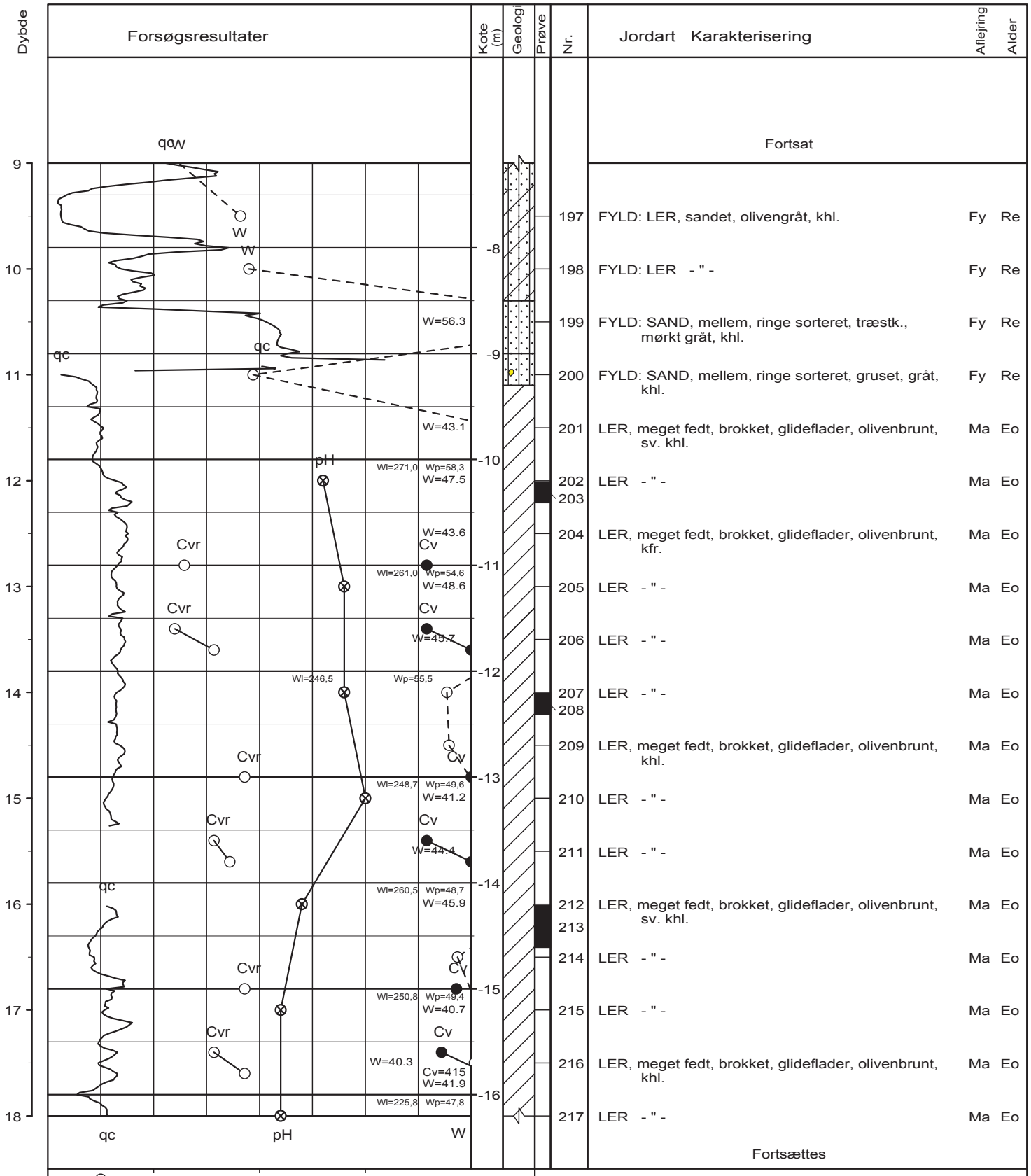

Boremetode : Tørboring

X : 219068 (m) Y : 192968 (m) Plan :

Sag : 25.0705.61 Århus, Light*House

Geolog : JBM Boret af : LER/JQB Dato : 20070924 DGU-nr.: Boring : L*H7

Udarb. af : HLa Kontrol : Godkendt : Dato : Bilag : 1 S. 2 / 5

Grontmij | Carl Bro
Tlf. 98 79 98 00, Fax 98 79 98 01
Sofiendalsvej 94, 9200 Aalborg SV

Boreprofil

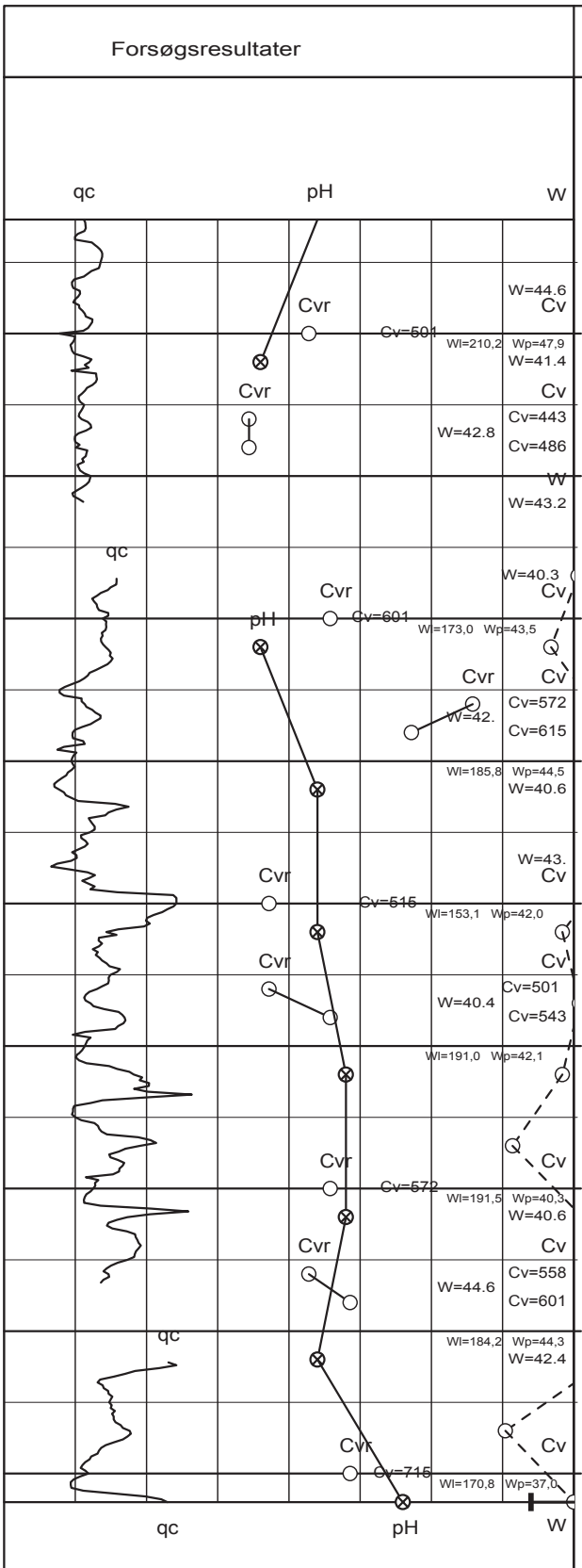

Kote (m)	Geologi	Prøve	Nr.	Jordart Karakterisering	Aflejring	Alder
				Fortsat		
			218			
			219	LER, meget fedt, brokket, glideflader, olivenbrunt, khl.	Ma	Eo
			220	LER - " -	Ma	Eo
			221	LER - " -	Ma	Eo
			222	LER - " -	Ma	Eo
			223			
			224	LER - " -	Ma	Eo
			225	LER, meget fedt, brokket, glideflader, grålig brunt, khl.	Ma	Eo
			226	LER - " -	Ma	Eo
			227	LER - " -	Ma	Eo
			228			
			229	LER - " -	Ma	Eo
			230	LER - " -	Ma	Eo
			231	LER - " -	Ma	Eo
			232	LER - " -	Ma	Eo
			233			
			234	LER - " -	Ma	Eo
			235	LER - " -	Ma	Eo
			236	LER, meget fedt, brokket, glideflader, mørkt olivenbrunt, sv. khl.	Ma	Eo
			237	LER, meget fedt, brokket, glideflader, mørkt grålig brunt, khl.	Ma	Eo
			238			
			239	LER, meget fedt, brokket, glideflader, grålig brunt, khl.	Ma	Eo
			240	LER - " -	Ma	Eo

Fortsættes

○	10	20	30 W (%)
●○	100	200	300 Cv,Cvr (kN/m²)
		10	qc (MN/m²)
⊗		9	pH

Boremetode : Tørboring

X : 219068 (m) Y : 192968 (m) Plan :

Sag : 25.0705.61 Århus, Light*House

Geolog : JBM Boret af : LER/JQB Dato : 20070924 DGU-nr.: Boring : L*H7

Udarb. af : HLa Kontrol : Godkendt : Dato : Bilag : 1 S. 3 / 5

Grontmij | Carl Bro
Tlf. 98 79 98 00, Fax 98 79 98 01
Sofiendalsvej 94, 9200 Aalborg SV

Boreprofil

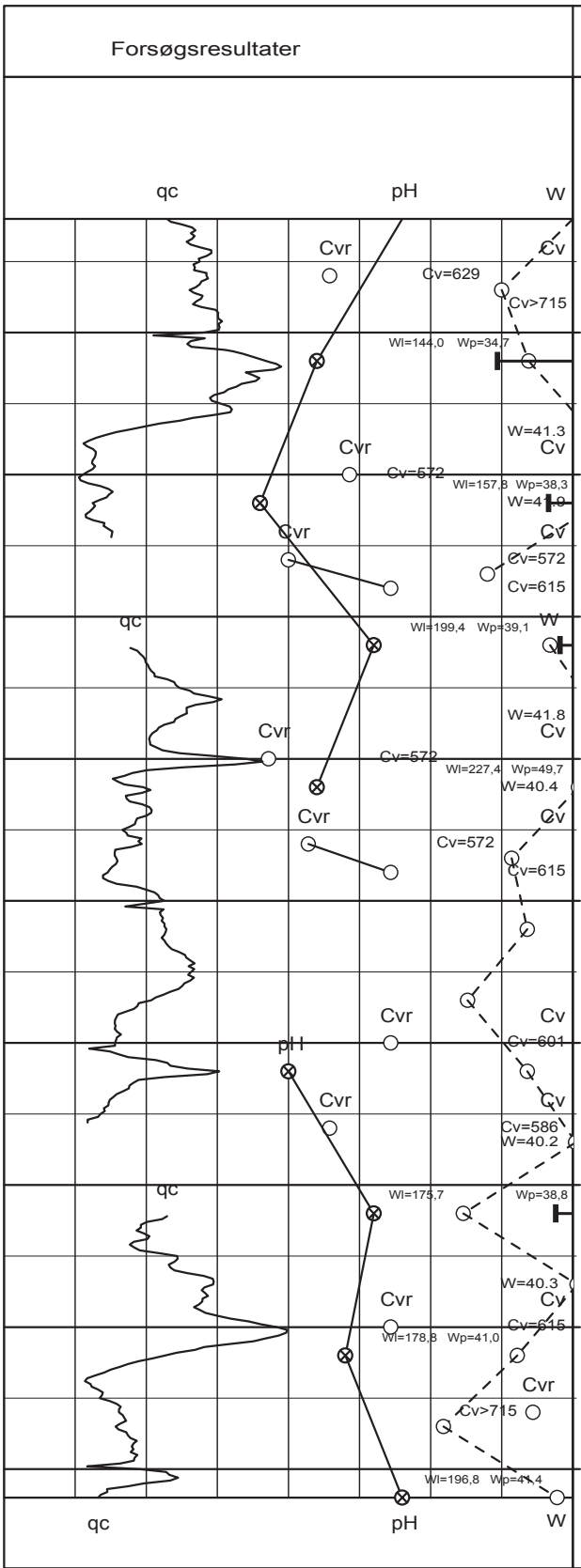

Fortsat

Nr.	Jordart Karakterisering	Aflejring	Alder
241	LER, meget fedt, brokket, glideflader, grålig brunt, khl.	Ma	Eo
242	LER - " -	Ma	Eo
243			
244	LER, meget fedt, brokket, glideflader, mørkt grålig brunt, khl.	Ma	Eo
245	LER, meget fedt, brokket, glideflader, grålig brunt, khl.	Ma	Eo
246	LER - " -	Ma	Eo
247	LER, meget fedt, brokket, glideflader, mørkt grålig brunt, khl.	Ma	Eo
248			
249	LER - " -	Ma	Eo
250	LER - " -	Ma	Eo
251	LER - " -	Ma	Eo
252	LER - " -	Ma	Eo
253			
254	LER - " -	Ma	Eo
255	LER - " -	Ma	Eo
256	LER - " -	Ma	Eo
257	LER, meget fedt, brokket, glideflader, grålig brunt, khl.	Ma	Eo
258			
259	LER, meget fedt, brokket, glideflader, mørkt grålig brunt, khl.	Ma	Eo
260	LER - " -	Ma	Eo
261	LER, meget fedt, brokket, glideflader, lyse kalkede partier, lyst olivenbrunt, khl.	Ma	Eo
262	LER, meget fedt, brokket, glideflader, grålig brunt, khl.	Ma	Eo

Fortsættes

○	10	20	30 W (%)
●○	100	200	300 Cv,Cvr (kN/m²)
		10	qc (MN/m²)
⊗		9	pH

Boremetode : Tørboring

X : 219068 (m) Y : 192968 (m) Plan :

Sag : 25.0705.61 Århus, Light*House

Geolog : JBM Boret af : LER/JQB Dato : 20070924 DGU-nr.: Boring : L*H7

Udarb. af : HLa Kontrol : Godkendt : Dato : Bilag : 1 S. 4 / 5

Grontmij | Carl Bro
Tlf. 98 79 98 00, Fax 98 79 98 01
Sofiendalsvej 94, 9200 Aalborg SV

Boreprofil

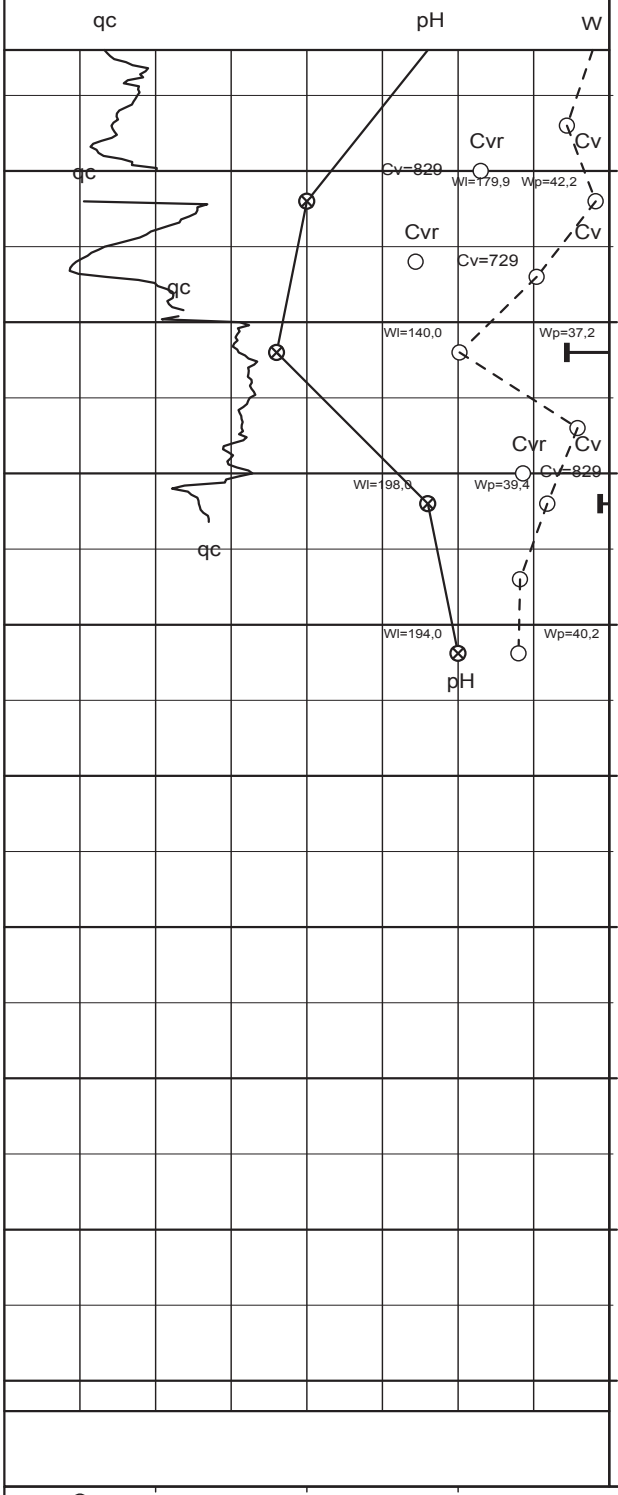

Dybde	Kote (m)	Nr.	Jordart Karakterisering	Aflejring	Alder
Forsøgsresultater			Fortsat		
36	-35	263			
		264	LER, meget fedt, brokket, glideflader, grålig brunt, khl.	Ma	Eo
37		265	LER - " -	Ma	Eo
		266	LER - " -	Ma	Eo
38	-36	267	LER, meget fedt, brokket, glideflader, lyse kalkede partier, lyst olivenbrunt, khl.	Ma	Eo
		268			
		269	LER, meget fedt, brokket, glideflader, grålig brunt, khl.	Ma	Eo
39	-37	270	LER - " -	Ma	Eo
		271	LER - " -	Ma	Eo
40	-38	272	LER - " -	Ma	Eo
41	-39				
	-40				
42					
	-41				
43					
	-42				
44					
	-43				
45					

○	10	20	30	W (%)
●○	100	200	300	Cv,Cvr (kN/m²)
		10		qc (MN/m²)
⊗		9		pH

Boremetode : Tørboring

X : 219068 (m) Y : 192968 (m) Plan :

Sag : 25.0705.61 Århus, Light*House

Geolog : JBM Boret af : LER/JQB Dato : 20070924 DGU-nr.: Boring : L*H7

Udarb. af : HLa Kontrol : Godkendt : Dato : Bilag : 1 S. 5 / 5

Grontmij | Carl Bro
Tlf. 98 79 98 00, Fax 98 79 98 01
Sofiendalsvej 94, 9200 Aalborg SV

Boreprofil

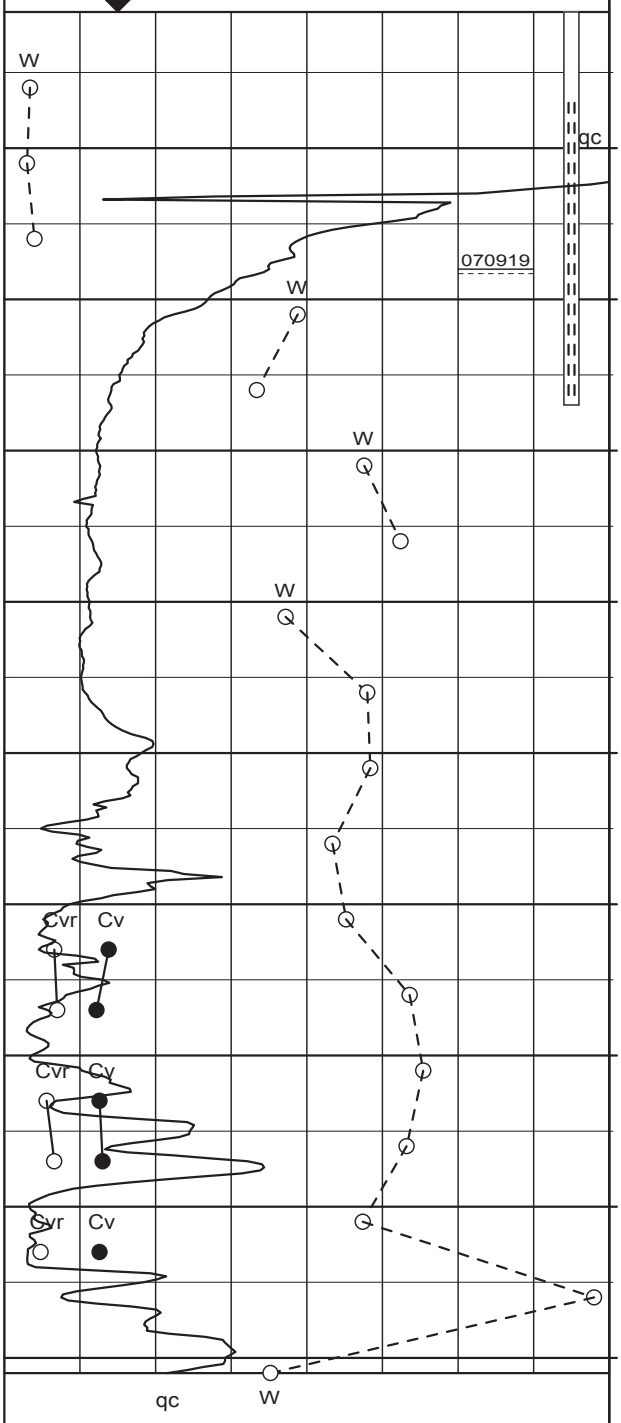

Dybde	Kote (m)	Nr.	Jordart Karakterisering	Aflejring	Alder
			ASFALT		
		85	FYLD: SAND, mellem, ringe sorteret, gruset, oliven, khl.	Fy	Re
		86	FYLD: SAND - " -	Fy	Re
		87	FYLD: SAND - " -	Fy	Re
		88	FYLD: SAND - " -	Fy	Re
		89	FYLD: SAND - " -	Fy	Re
		90	FYLD: SAND - " -	Fy	Re
		91	FYLD: SAND - " -	Fy	Re
		92	FYLD: SAND - " -	Fy	Re
		93	FYLD: SAND - " -	Fy	Re
		94	FYLD: SAND - " -	Fy	Re
		95	FYLD: SAND - " -	Fy	Re
		96	FYLD: SILT, leret, sandet, oliven, khl.	Fy	Re
		97	FYLD: SILT, leret, sandet, gråt, khl.	Fy	Re
		98	FYLD: SILT - " -	Fy	Re
		99	FYLD: SILT - " -	Fy	Re
		100	FYLD: LER, sandet, siltet, gråt, khl.	Fy	Re
		101	FYLD: SAND, mellem, ringe sorteret, gruset, siltet, leret, gråt, khl.	Fy	Re
		102	FYLD: SAND, leret, gråt, khl.	Fy	Re

Fortsættes

○	10	20	30	W (%)
●○	100	200	300	Cv,Cvr (kN/m²)
		10		qc (MN/m²)
⊗		9		pH

Boremetode : Tørboring med foring

X : 219046 (m) Y : 192911 (m) Plan :

Sag : 25.0705.61 Århus, Light*House

Geolog : JBM Boret af : LER/JQB Dato : 20070917 DGU-nr.: Boring : L*H8

Udarb. af : HLa Kontrol : Godkendt : Dato : Bilag : 2 S. 1 / 5

Grontmij | Carl Bro
Tlf. 98 79 98 00, Fax 98 79 98 01
Sofiendalsvej 94, 9200 Aalborg SV

Boreprofil

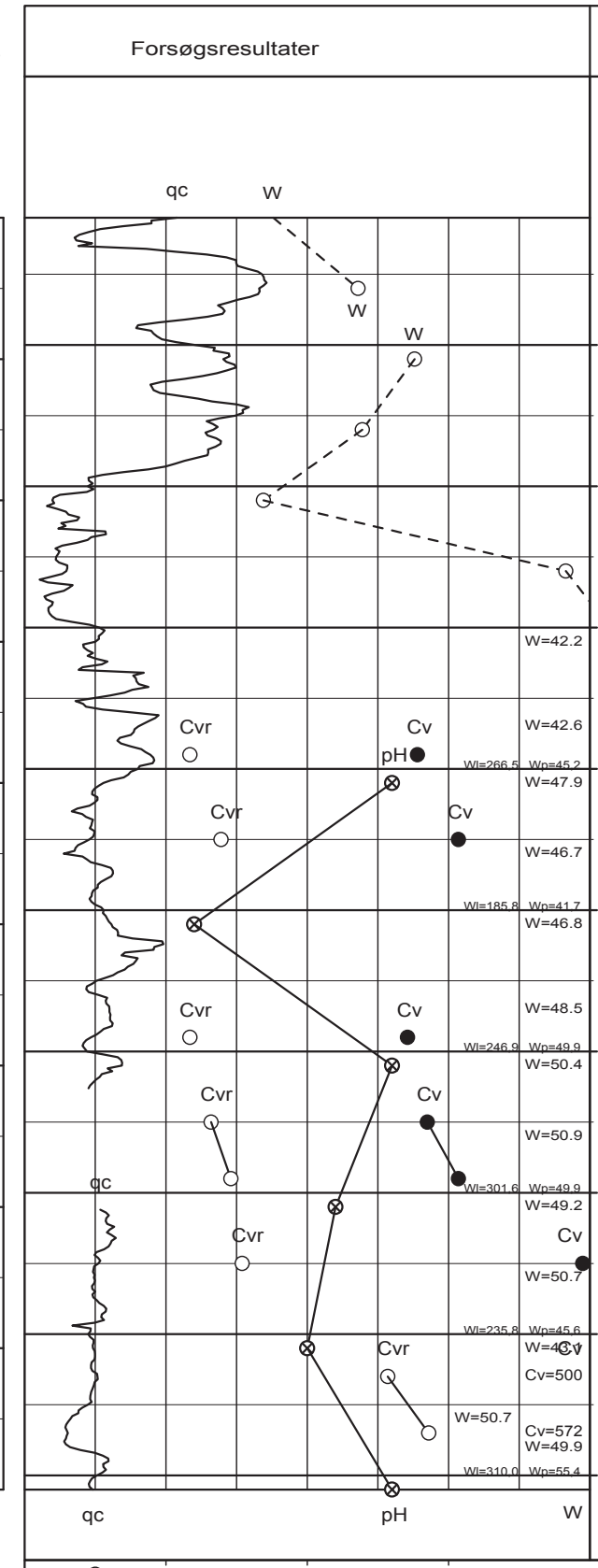

Kote (m)	Geologi	Prøve	Nr.	Jordart Karakterisering	Aflejring	Alder
				Fortsat		
-8			103	FYLD: LER, sandet, gråt, khl.	Fy	Re
			104	FYLD: SAND, leret, gråt, khl.	Fy	Re
-9			105	FYLD: SAND - " -	Fy	Re
			106	FYLD: SAND - " -	Fy	Re
			107	FYLD: LER, sandet, tertiært ler blandet med sand og GRUS, grønlig gråt, khl.	Fy?	Re?
-10			108	LER, meget fedt, brokket, lyst grønlig gråt, khl.	Ma	Eo
			109			
			110	LER, meget fedt, brokket, glideflader, olivengråt, khl.	Ma	Eo
-11			111	LER - " -	Ma	Eo
			112	LER, meget fedt, brokket, glideflader, mørkt gråt, sv. khl.	Ma	Eo
-12			113	LER, meget fedt, brokket, glideflader, olivengråt, khl.	Ma	Eo
			114			
-13			115	LER - " -	Ma	Eo
			116	LER - " -	Ma	Eo
			117	LER - " -	Ma	Eo
-14			118	LER, meget fedt, brokket, glideflader, mørkt gråt, sv. khl.	Ma	Eo
			119			
			120	LER - " -	Ma	Eo
-15			121	LER, meget fedt, brokket, glideflader, olivengråt, khl.	Ma	Eo
			122	LER, meget fedt, brokket, glideflader, mørkt gråt, sv. khl.	Ma	Eo
-16			123	LER - " -	Ma	Eo

Fortsættes

○	10	20	30 W (%)
●○	100	200	300 Cv,Cvr (kN/m²)
		10	qc (MN/m²)
⊗		9	pH

Boremetode : Tørboring med foring

X : 219046 (m) Y : 192911 (m) Plan :

Sag : 25.0705.61 Århus, Light*House

Geolog : JBM Boret af : LER/JQB Dato : 20070917 DGU-nr.: Boring : L*H8

Udarb. af : HLa Kontrol : Godkendt : Dato : Bilag : 2 S. 2 / 5

Grontmij | Carl Bro
Tlf. 98 79 98 00, Fax 98 79 98 01
Sofiendalsvej 94, 9200 Aalborg SV

Boreprofil

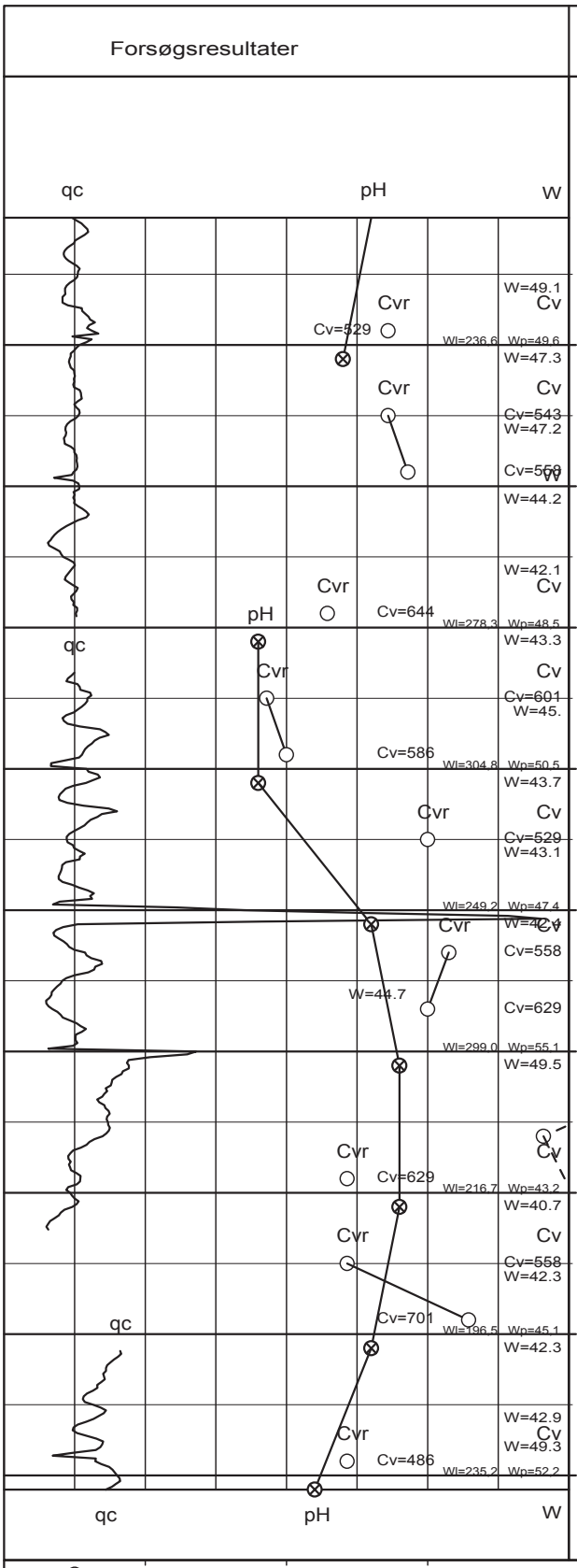

Boremetode : Tørboring med foring

X : 219046 (m) Y : 192911 (m) Plan :

Sag : 25.0705.61 Århus, Light*House

Geolog : JBM Boret af : LER/JQB Dato : 20070917 DGU-nr.: Boring : L*H8

Udarb. af : HLa Kontrol : Godkendt : Dato : Bilag : 2 S. 3 / 5

Grontmij | Carl Bro
Tlf. 98 79 98 00, Fax 98 79 98 01
Sofiendalsvej 94, 9200 Aalborg SV

Boreprofil

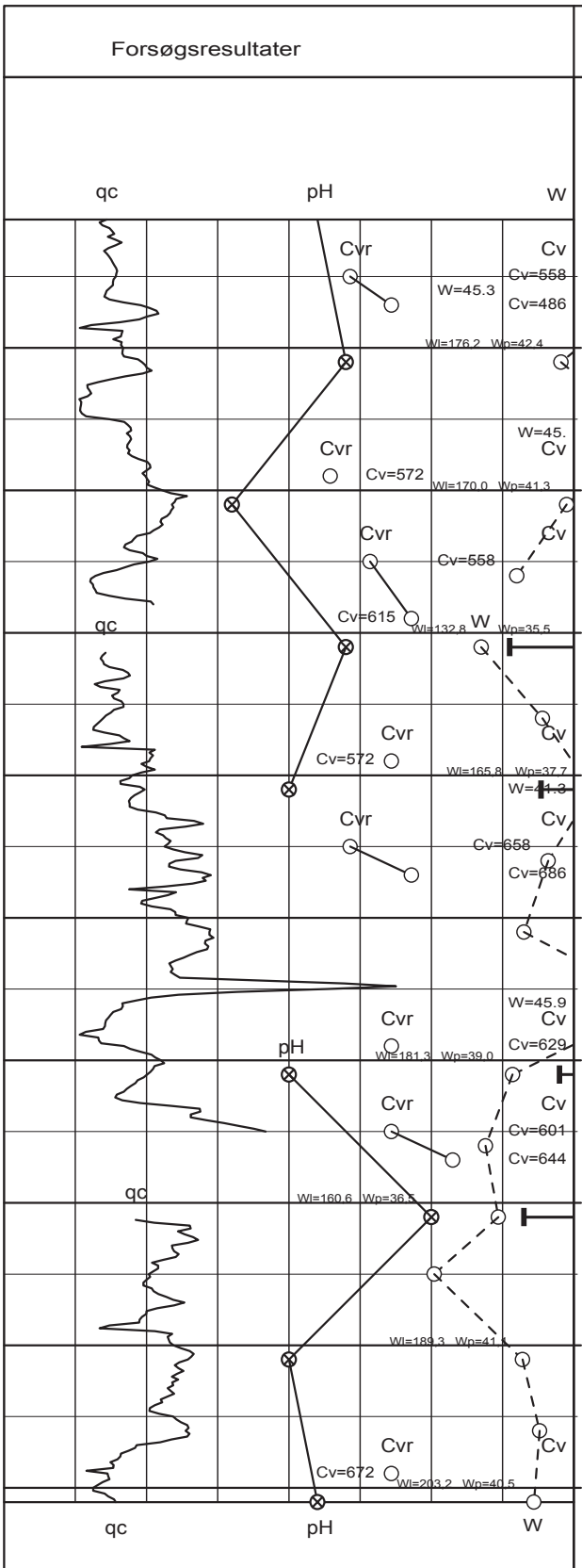

Kote (m)	Geologi	Prøve	Nr.	Jordart Karakterisering	Aflejring	Alder
				Fortsat		
-26			147	LER, meget fedt, brokket, glideflader, olivengråt, khl.	Ma	Eo
			148	LER - " -	Ma	Eo
			149			
			150	LER - " -	Ma	Eo
-27			151	LER - " -	Ma	Eo
			152	LER - " -	Ma	Eo
-28			153	LER - " -	Ma	Eo
			154			
			155	LER, meget fedt, brokket, glideflader, mørkt gråt, sv. khl.	Ma	Eo
-29			156	LER - " -	Ma	Eo
			157	LER, meget fedt, brokket, glideflader, gråt, khl.	Ma	Eo
-30			158	LER, meget fedt, glideflader, gråt, khl.	Ma	Eo
			159			
			160	LER, meget fedt, brokket, glideflader, mørkt gråt, sv. khl.	Ma	Eo
-31			161	LER, meget fedt, brokket, glideflader, gråt, khl.	Ma	Eo
			162	LER, meget fedt, glideflader, gråt, khl.	Ma	Eo
-32			163	LER - " -	Ma	Eo
			164	LER, meget fedt, brokket, glideflader, lyst gråt, st. khl.	Ma	Eo
-33			165	LER, meget fedt, brokket, glideflader, gråt, sv. khl.	Ma	Eo
			166			
			167	LER - " -	Ma	Eo
-34			168	LER - " -	Ma	Eo
				Fortsættes		

○	10	20 30	W (%)
●○	100	200 300	Cv,Cvr (kN/m²)
		10	qc (MN/m²)
⊗		9	pH

Boremetode : Tørboring med foring

X : 219046 (m) Y : 192911 (m) Plan :

Sag : 25.0705.61 Århus, Light*House

Geolog : JBM Boret af : LER/JQB Dato : 20070917 DGU-nr.: Boring : L*H8

Udarb. af : HLa Kontrol : Godkendt : Dato : Bilag : 2 S. 4 / 5

Grontmij | Carl Bro
Tlf. 98 79 98 00, Fax 98 79 98 01
Sofiendalsvej 94, 9200 Aalborg SV

Boreprofil

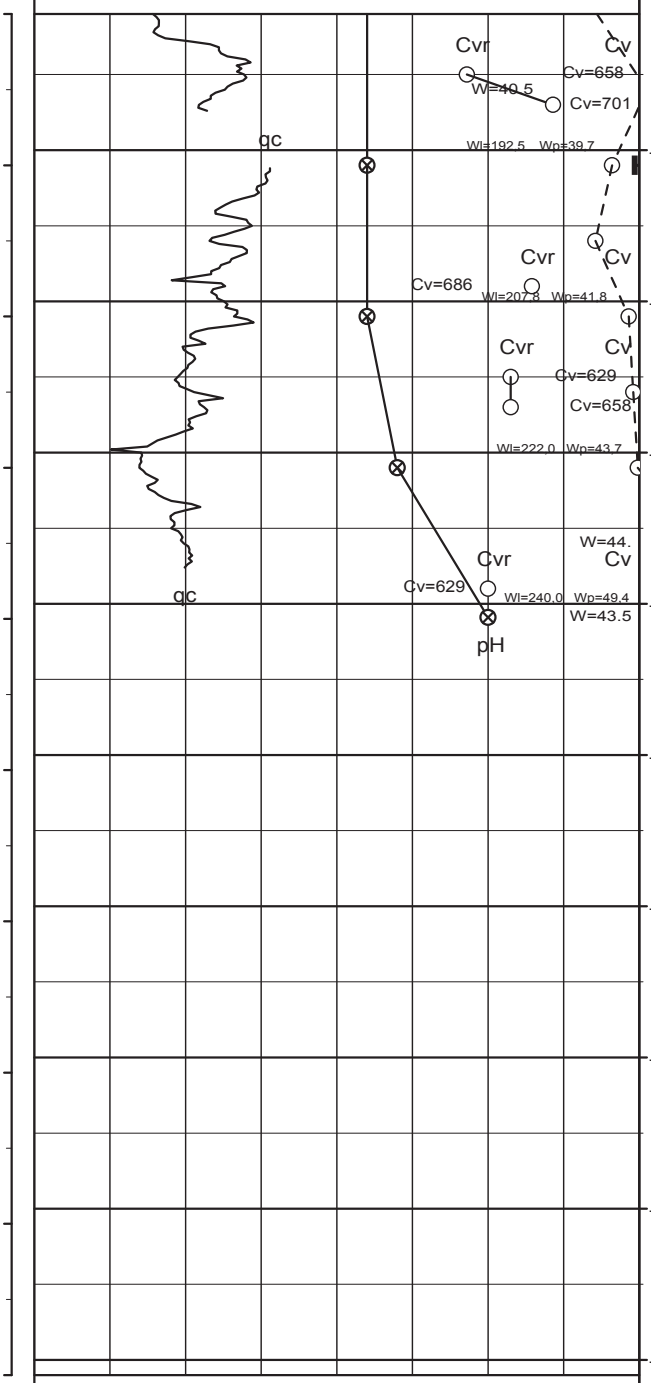

Dybde	Kote (m)	Nr.	Jordart Karakterisering	Aflejring	Alder
			Fortsat		
36					
37	-35	169	LER, meget fedt, glideflader, gråt, sv. khl.	Ma	Eo
		170	LER - " -	Ma	Eo
		171			
		172	LER, meget fedt, glideflader, gråt, khl.	Ma	Eo
38	-36	173	LER - " -	Ma	Eo
		174	LER, meget fedt, brokket, glideflader, gråt, khl.	Ma	Eo
39	-37	175	LER - " -	Ma	Eo
		176			
		177	LER, meget fedt, brokket, glideflader, mørkt gråt, khl.	Ma	Eo
40	-38	178	LER - " -	Ma	Eo
41	-39				
42	-40				
43	-41				
44	-42				
45	-43				

○	10	20	30	W (%)
●○	100	200	300	Cv,Cvr (kN/m²)
		10		qc (MN/m²)
⊗		9		pH

Boremetode : Tørboring med foring

X : 219046 (m) Y : 192911 (m) Plan :

Sag : 25.0705.61 Århus, Light*House

Geolog : JBM Boret af : LER/JQB Dato : 20070917 DGU-nr.: Boring : L*H8

Udarb. af : HLa Kontrol : Godkendt : Dato : Bilag : 2 S. 5 / 5

Grontmij | Carl Bro
Tlf. 98 79 98 00, Fax 98 79 98 01
Sofiendalsvej 94, 9200 Aalborg SV

Boreprofil

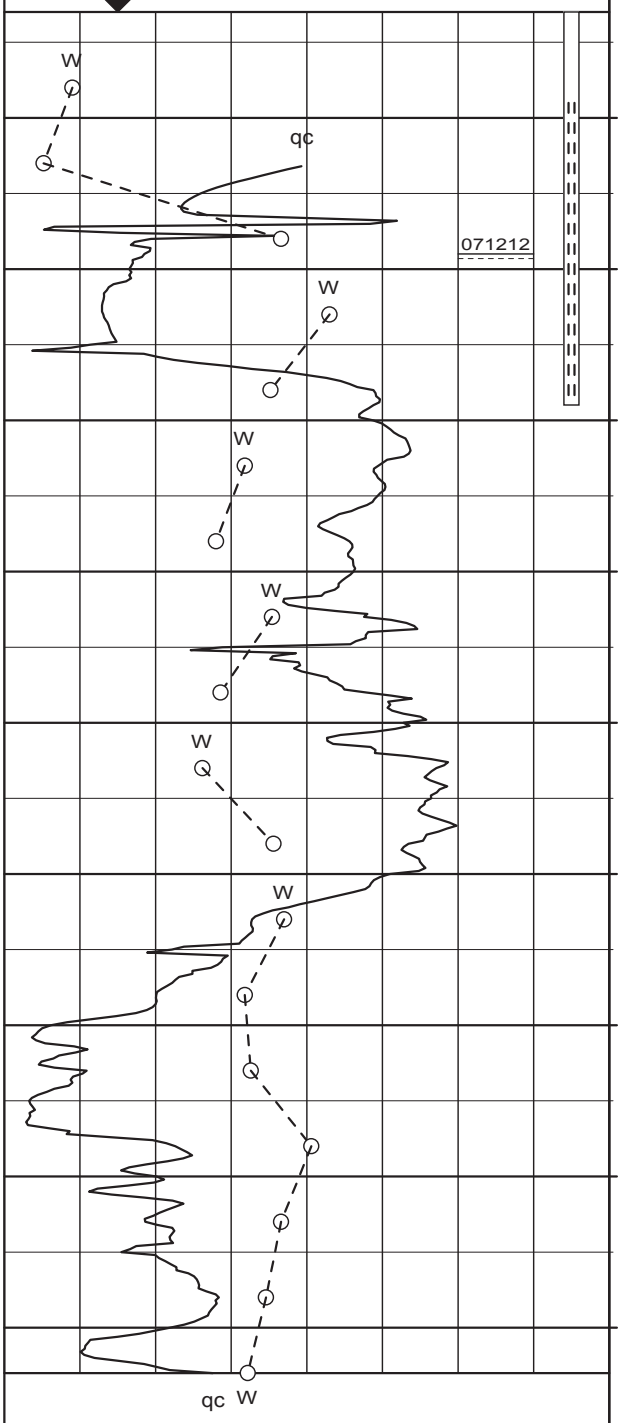

Dybde	Kote (m)	Nr.	Jordart Karakterisering	Aflejring	Alder
			ASFALT		
0	1	916	FYLD: SAND, mellem, sorteret, grålig brunt, khl.	Fy	Re
1	0	917	FYLD: SAND - " -	Fy	Re
2		918	FYLD: SAND - " -	Fy	Re
		919	FYLD: SAND - " -	Fy	Re
	-1	920	FYLD: SAND - " -	Fy	Re
3		921	FYLD: SAND, mellem, ringe sorteret, gruset, grålig brunt, khl.	Fy	Re
	-2	922	FYLD: SAND - " -	Fy	Re
4		923	FYLD: SAND - " -	Fy	Re
	-3	924	FYLD: SAND, mellem, ringe sorteret, gruset, brunlig gråt, khl.	Fy	Re
5		925	FYLD: SAND - " -	Fy	Re
	-4	926	FYLD: SAND, mellem, sorteret, gråt, khl.	Fy	Re
6		927	FYLD: SAND - " -	Fy	Re
	-5	928	FYLD: SAND - " -	Fy	Re
7		929	FYLD: SAND - " -	Fy	Re
	-6	930	FYLD: LER, sandet, gråt, khl.	Fy	Re
8		931	FYLD: SAND, sv. leret, gråt, khl.	Fy	Re
	-7	932	FYLD: SAND, mellem, sorteret, gråt, khl.	Fy	Re
9		933	FYLD: SAND, sv. leret, gråt, khl.	Fy	Re

Fortsættes

○	10	20	30	W (%)
●○	100	200	300	Cv,Cvr (kN/m²)
		10		qc (MN/m²)
⊗		9		pH

Boremetode : Tørboring med foring

X : 218995 (m) Y : 192907 (m) Plan :

Sag : 25.0705.61 Århus, Light*House

Geolog : JBM Boret af : LER/JQB Dato : 20071204 DGU-nr.: Boring : L*H9

Udarb. af : HLa Kontrol : Godkendt : Dato : Bilag : 3 S. 1 / 6

Grontmij | Carl Bro
Tlf. 98 79 98 00, Fax 98 79 98 01
Sofiendalsvej 94, 9200 Aalborg SV

Boreprofil

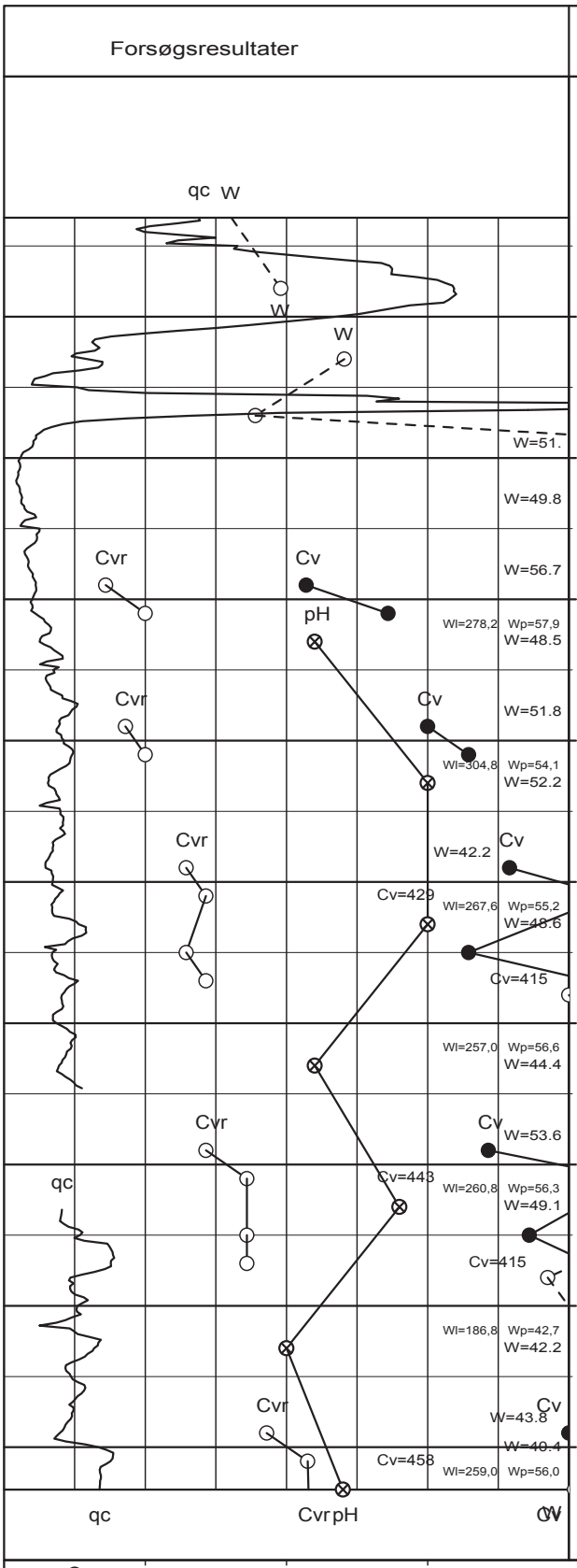

Boremetode : Tørboring med foring

X : 218995 (m) Y : 192907 (m) Plan :

Sag : 25.0705.61 Århus, Light*House

Geolog : JBM Boret af : LER/JQB Dato : 20071204 DGU-nr.: Boring : L*H9

Udarb. af : HLa Kontrol : Godkendt : Dato : Bilag : 3 S. 2 / 6

Grontmij | Carl Bro
Tlf. 98 79 98 00, Fax 98 79 98 01
Sofiendalsvej 94, 9200 Aalborg SV

Boreprofil

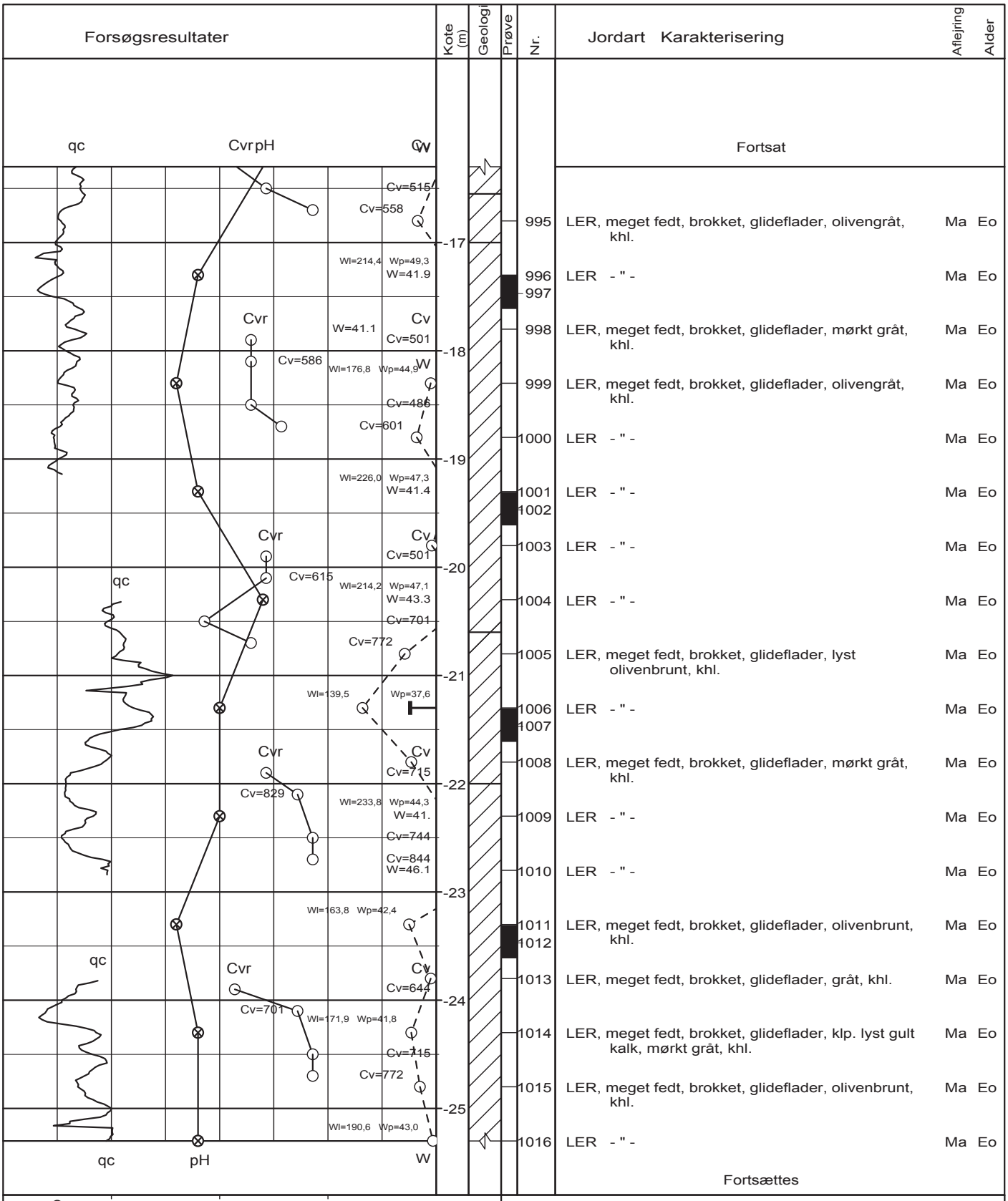

Boremetode : Tørboring med foring

X : 218995 (m) Y : 192907 (m) Plan :

Sag : 25.0705.61 Århus, Light*House

Geolog : JBM Boret af : LER/JQB Dato : 20071204 DGU-nr.: Boring : L*H9

Udarb. af : HLa Kontrol : Godkendt : Dato : Bilag : 3 S. 3 / 6

Grontmij | Carl Bro
Tlf. 98 79 98 00, Fax 98 79 98 01
Sofiendalsvej 94, 9200 Aalborg SV

Boreprofil

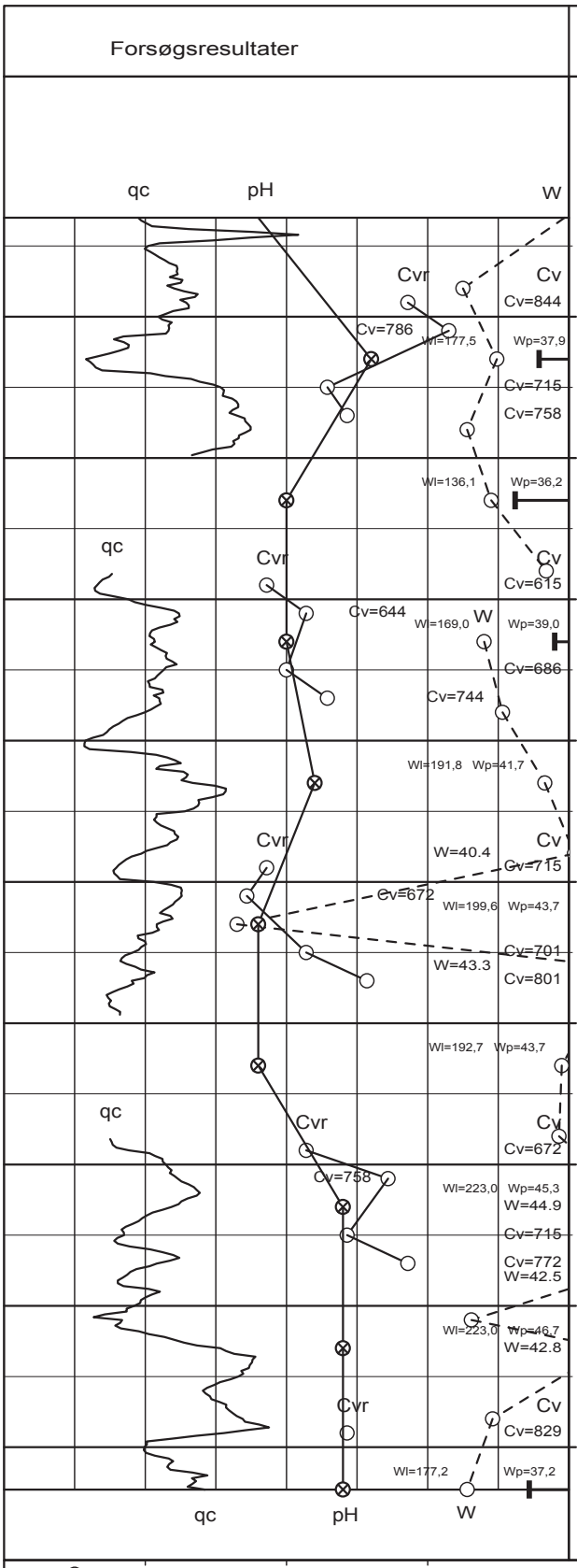

Kote (m)	Geologi	Prøve	Nr.	Jordart Karakterisering	Aflejring	Alder
				Fortsat		
			1017			
			1018	LER, meget fedt, brokket, glideflader, lyst olivengråt, khl.	Ma	Eo
			1019	LER, meget fedt, brokket, glideflader, lyst olivenbrunt, khl.	Ma	Eo
			1020	LER - " -	Ma	Eo
			1021	LER - " -	Ma	Eo
			1022			
			1023	LER, meget fedt, brokket, glideflader, meget mørkt olivengråt, khl.	Ma	Eo
			1024	LER, meget fedt, brokket, glideflader, nedknust, lyst olivengråt, khl.	Ma	Eo
			1025	LER, meget fedt, brokket, glideflader, olivenbrunt, khl.	Ma	Eo
			1026	LER - " -	Ma	Eo
			1027			
			1028	LER, meget fedt, brokket, glideflader, olivengråt, khl.	Ma	Eo
			1029	LER, meget fedt, brokket, glideflader, nedknust, mørkt olivengråt, khl.	Ma	Eo
			1030	LER, meget fedt, brokket, glideflader, nedknust, mørkt grønlig gråt, khl.	Ma	Eo
			1031	LER, meget fedt, brokket, glideflader, olivenbrunt, sv. khl.	Ma	Eo
			1032			
			1033	LER, meget fedt, brokket, glideflader, olivenbrunt, khl.	Ma	Eo
			1034	LER, meget fedt, brokket, glideflader, mørkt olivenbrunt, khl.	Ma	Eo
			1035	LER, meget fedt, brokket, glideflader, meget mørkt olivengråt, khl.	Ma	Eo
			1036	LER, meget fedt, brokket, glideflader, lyst grønlig gråt, khl.	Ma	Eo
			1037			
			1038	LER, meget fedt, brokket, glideflader, meget mørkt gråt, khl.	Ma	Eo
			1039	LER, meget fedt, brokket, glideflader, olivenbrunt, khl.	Ma	Eo
			1040	LER - " -	Ma	Eo

Fortsættes

○	10	20	30 W (%)
●○	100	200	300 Cv,Cvr (kN/m²)
		10	qc (MN/m²)
⊗		9	pH

Boremetode : Tørboring med foring

X : 218995 (m) Y : 192907 (m) Plan :

Sag : 25.0705.61 Århus, Light*House

Geolog : JBM Boret af : LER/JQB Dato : 20071204 DGU-nr.: Boring : L*H9

Udarb. af : HLa Kontrol : Godkendt : Dato : Bilag : 3 S. 4 / 6

Grontmij | Carl Bro
Tlf. 98 79 98 00, Fax 98 79 98 01
Sofiendalsvej 94, 9200 Aalborg SV

Boreprofil

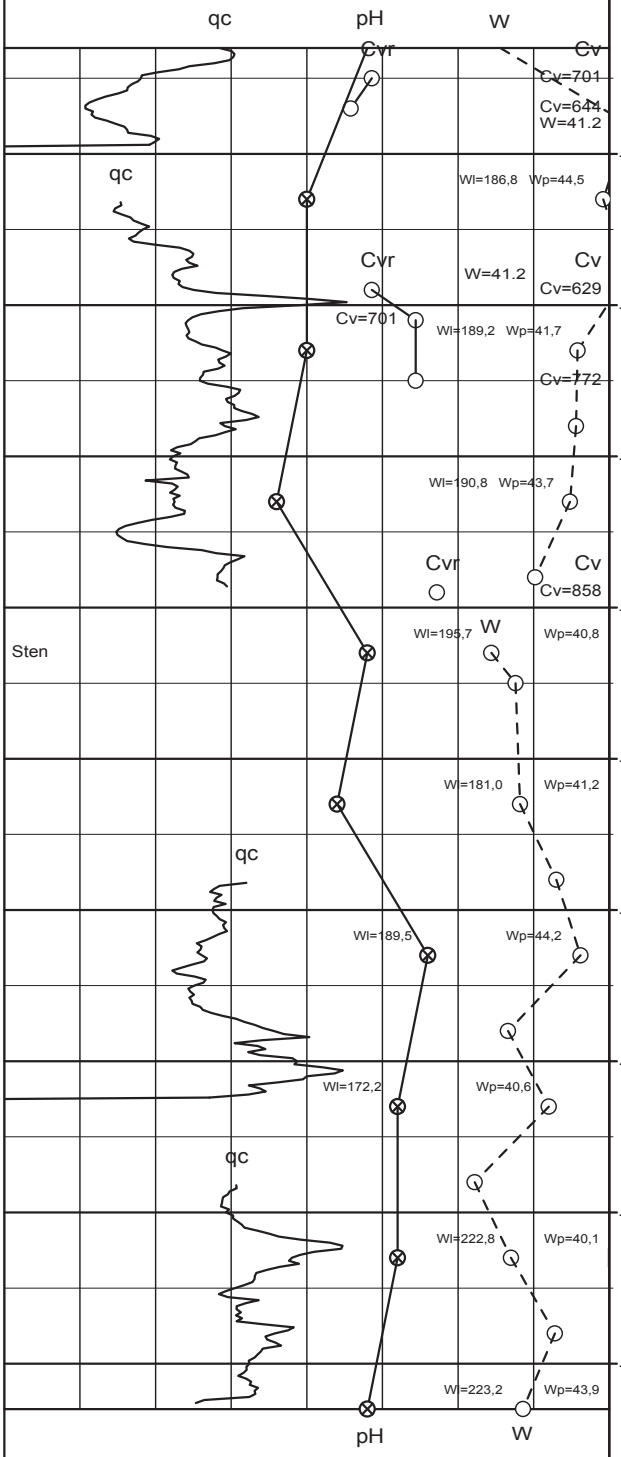

Dybde	Kote (m)	Nr.	Jordart Karakterisering	Aflejring	Alder
			Fortsat		
	-35	1041	LER, meget fedt, brokket, glideflader, mørkt olivengråt, khl.	Ma	Eo
		1042	LER - " -	Ma	Eo
		1043			
	-36	1044	LER, meget fedt, brokket, glideflader, olivenbrunt, khl.	Ma	Eo
		1045	LER, meget fedt, brokket, glideflader, nedknust, olivengråt, khl.	Ma	Eo
		1046	LER, meget fedt, brokket, glideflader, olivengråt, khl.	Ma	Eo
	-37	1047	LER, meget fedt, brokket, glideflader, mørkt olivengråt, khl.	Ma	Eo
		1048			
	-38	1049	LER, meget fedt, brokket, glideflader, olivenbrunt, khl.	Ma	Eo
		1050	LER - " -	Ma	Eo
		1051	LER - " -	Ma	Eo
	-39				
		1052	LER, meget fedt, brokket, glideflader, olivengråt, khl.	Ma	Eo
		1053			
	-40	1054	LER, meget fedt, brokket, glideflader, nedknust, olivengråt, khl.	Ma	Eo
		1055	LER - " -	Ma	Eo
		1056	LER, meget fedt, brokket, glideflader, nedknust, mørkt olivenbrunt, khl.	Ma	Eo
	-41	1057	LER, meget fedt, brokket, glideflader, olivengråt, khl.	Ma	Eo
		1058			
	-42	1059	LER, meget fedt, brokket, glideflader, olivenbrunt, khl.	Ma	Eo
		1060	LER - " -	Ma	Eo
		1061	LER - " -	Ma	Eo
	-43	1062	LER - " -	Ma	Eo
			Fortsættes		

○ 10 20 30 W (%)
●○ 100 200 300 Cv,Cvr (kN/m²)
10 qc (MN/m²)
⊗ 9 pH

Boremetode : Tørboring med foring

X : 218995 (m) Y : 192907 (m) Plan :

Sag : 25.0705.61 Århus, Light*House

Geolog : JBM Boret af : LER/JQB Dato : 20071204 DGU-nr.: Boring : L*H9

Udarb. af : HLa Kontrol : Godkendt : Dato : Bilag : 3 S. 5 / 6

Grontmij | Carl Bro
Tlf. 98 79 98 00, Fax 98 79 98 01
Sofiendalsvej 94, 9200 Aalborg SV

Boreprofil

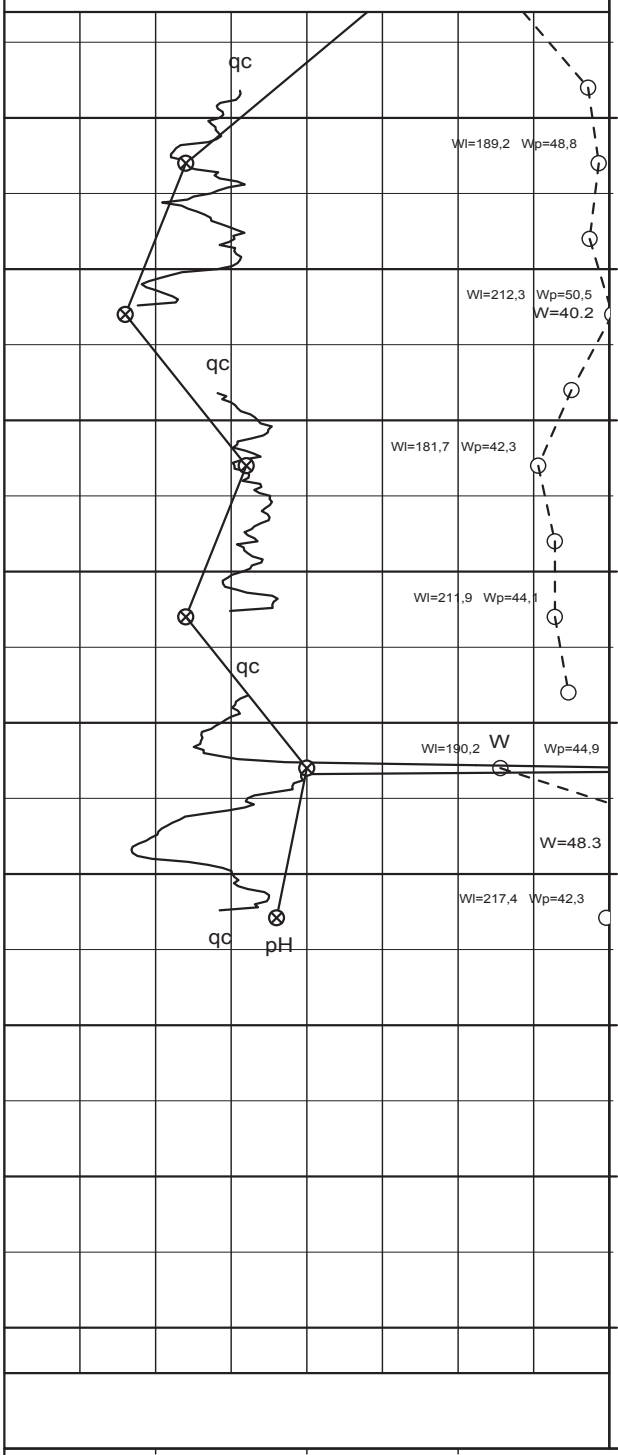

Dybde	Kote (m)	Nr.	Jordart Karakterisering	Aflejring	Alder
			Fortsat		
45	-44	1063			
		1064	LER, meget fedt, brokket, glideflader, nedknust, olivengråt, khl.	Ma	Eo
46		1065	LER, meget fedt, brokket, glideflader, nedknust, meget mørkt gråt, khl.	Ma	Eo
	-45	1066	LER, meget fedt, brokket, glideflader, nedknust, mørkt gråt, khl.	Ma	Eo
47		1067	LER, meget fedt, brokket, glideflader, meget mørkt gråt, khl.	Ma	Eo
		1068			
	-46	1069	LER, meget fedt, brokket, glideflader, nedknust, olivengråt, khl.	Ma	Eo
48		1070	LER - " -	Ma	Eo
		1071	LER, meget fedt, brokket, glideflader, olivengråt, khl.	Ma	Eo
	-47				
49		1072	LER - " -	Ma	Eo
		1073			
	-48	1074	LER, meget fedt, brokket, glideflader, nedknust, olivengråt, khl.	Ma	Eo
50		1075	LER, meget fedt, brokket, glideflader, klp. lyst gult kalk, olivengråt, khl.	Ma	Eo
		1076	LER, meget fedt, brokket, glideflader, nedknust, olivengråt, khl.	Ma	Eo
	-49				
51		1077	LER - " -	Ma	Eo
	-50				
52					
	-51				
53					
	-52				
54					

○	10	20	30	W (%)
●○	100	200	300	Cv,Cvr (kN/m²)
		10		qc (MN/m²)
⊗		9		pH

Boremetode : Tørboring med foring

X : 218995 (m) Y : 192907 (m) Plan :

Sag : 25.0705.61 Århus, Light*House

Geolog : JBM Boret af : LER/JQB Dato : 20071204 DGU-nr.: Boring : L*H9

Udarb. af : HLa Kontrol : Godkendt : Dato : Bilag : 3 S. 6 / 6

Grontmij | Carl Bro
Tlf. 98 79 98 00, Fax 98 79 98 01
Sofiendalsvej 94, 9200 Aalborg SV

Boreprofil

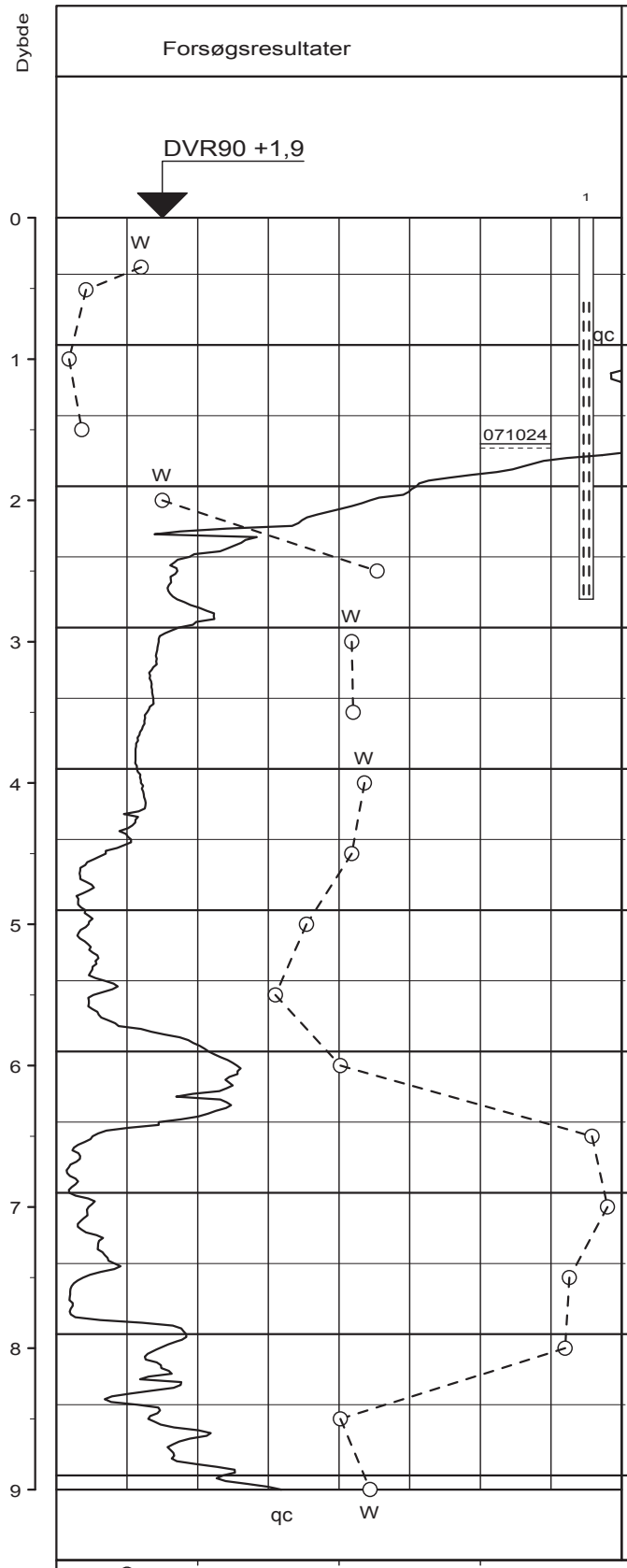

Kote (m)	Geologi	Prøve	Nr.	Jordart Karakterisering	Aflejring	Alder
				ASFALT		
			273	FYLD: SAND, groft, ringe sorteret, gruset, grålig brunt, khl.	Fy	Re
			274	FYLD: SAND, mellem, ringe sorteret, gruset, grålig brunt, khl.	Fy	Re
1			275	FYLD: SAND - " -	Fy	Re
			276	FYLD: SAND, mellem, ringe sorteret, gruset, lyst brunlig gråt, khl.	Fy	Re
0			277	FYLD: SAND, mellem, ringe sorteret, gruset, grålig brunt, khl.	Fy	Re
			278	FYLD: SAND, mellem, ringe sorteret, gruset, brunlig gråt, khl.	Fy	Re
-1			279	FYLD: SAND - " -	Fy	Re
			280	FYLD: SAND - " -	Fy	Re
-2			281	FYLD: SAND - " -	Fy	Re
			282	FYLD: SAND - " -	Fy	Re
-3			283	FYLD: LER, sandet, grålig brunt, khl.	Fy	Re
			284	FYLD: LER - " -	Fy	Re
-4			285	FYLD: SAND, mellem, ringe sorteret, gruset, grålig brunt, khl.	Fy	Re
			286	FYLD: LER, sandet, gytjeh., mørkt gråt, khl.	Fy	Re
-5			287	FYLD: LER - " -	Fy	Re
			288	FYLD: LER - " -	Fy	Re
-6			289	FYLD: LER - " -	Fy	Re
			290	FYLD: SAND, leret, gytjeh., mørkt gråt, khl.	Fy	Re
-7			291	FYLD: SAND, mellem, ringe sorteret, gruset, sv. gytjeh., mørkt gråt, khl.	Fy	Re

Fortsættes

○	10	20	30	W (%)
●○	100	200	300	Cv,Cvr (kN/m²)
		10		qc (MN/m²)
⊗		9		pH

Boremetode : Tørboring med foring

X : 218979 (m) Y : 192852 (m) Plan :

Sag : 25.0705.61 Århus, Light*House

Geolog : JBM Boret af : LER/JQB Dato : 20071024 DGU-nr.: Boring : L*H10

Udarb. af : HLa Kontrol : Godkendt : Dato : Bilag : 4 S. 1 / 5

Grontmij | Carl Bro
Tlf. 98 79 98 00, Fax 98 79 98 01
Sofiendalsvej 94, 9200 Aalborg SV

Boreprofil

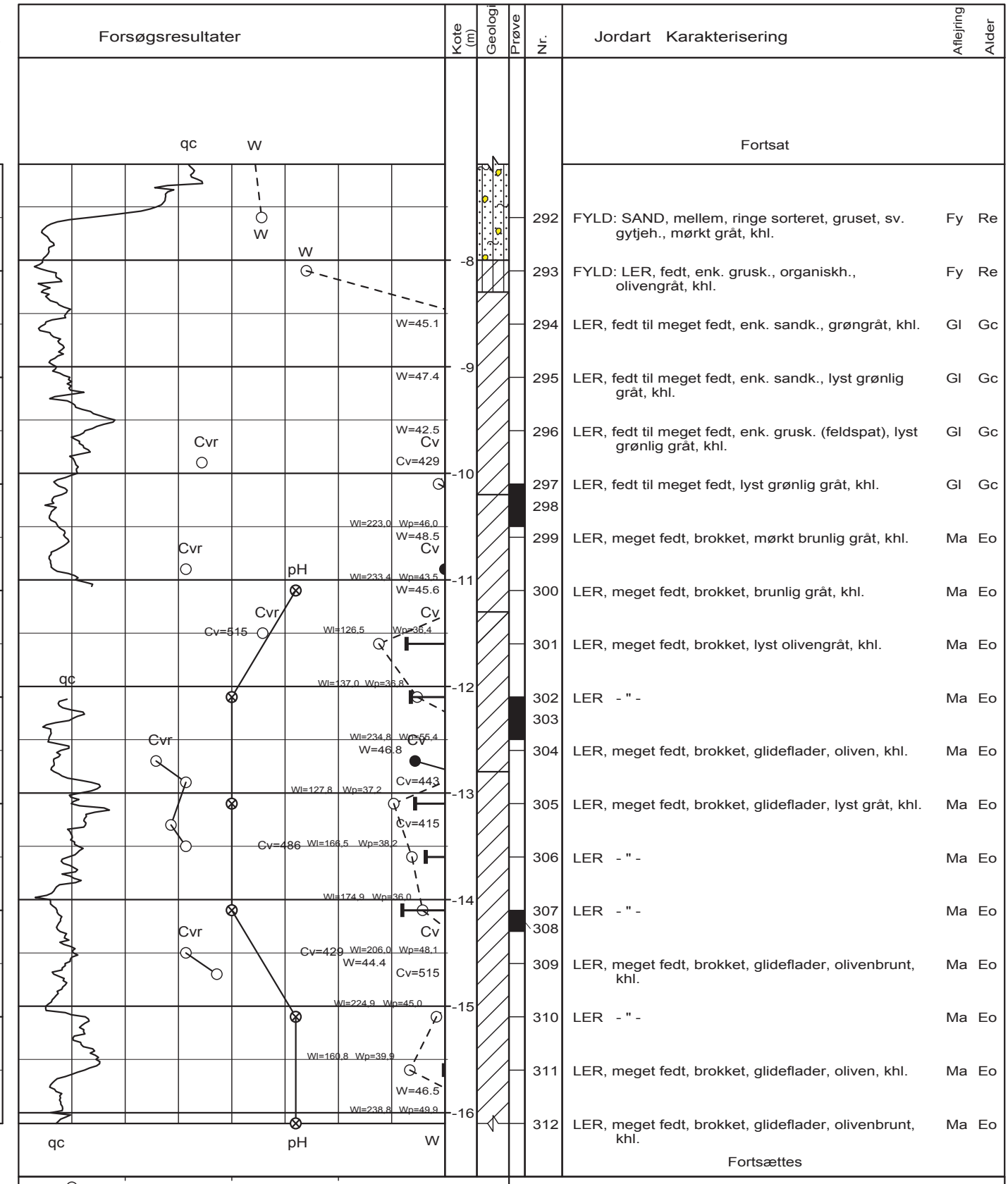

Boremetode : Tørboring med foring

X : 218979 (m) Y : 192852 (m) Plan :

Sag : 25.0705.61 Århus, Light*House

Geolog : JBM Boret af : LER/JQB Dato : 20071024 DGU-nr.: Boring : L*H10

Udarb. af : HLa Kontrol : Godkendt : Dato : Bilag : 4 S. 2 / 5

Grontmij | Carl Bro
Tlf. 98 79 98 00, Fax 98 79 98 01
Sofiendalsvej 94, 9200 Aalborg SV

Boreprofil

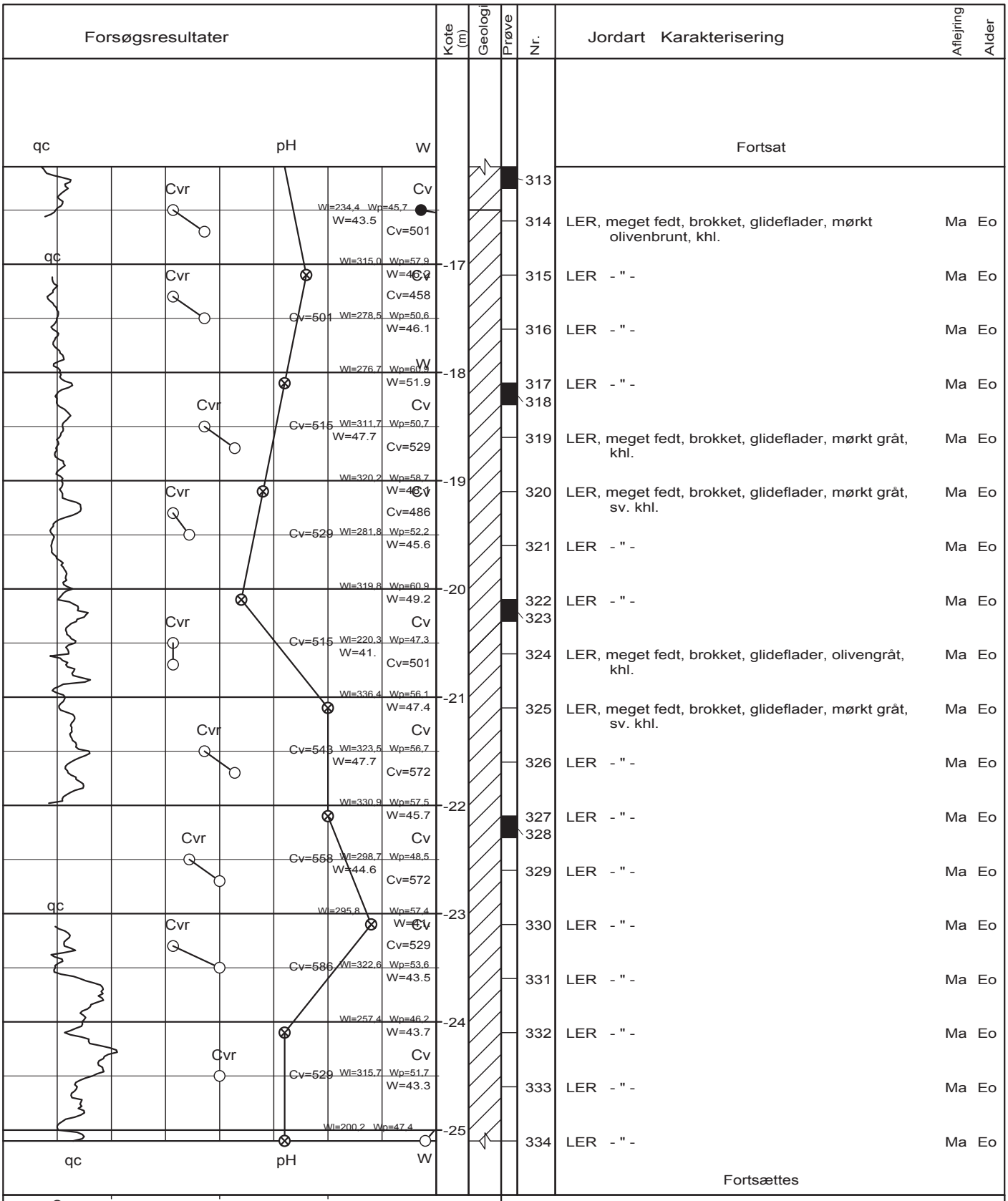

Boremetode : Tørboring med foring

X : 218979 (m) Y : 192852 (m) Plan :

Sag : 25.0705.61 Århus, Light*House

Geolog : JBM Boret af : LER/JQB Dato : 20071024 DGU-nr.: Boring : L*H10

Udarb. af : HLa Kontrol : Godkendt : Dato : Bilag : 4 S. 3 / 5

Grontmij | Carl Bro
Tlf. 98 79 98 00, Fax 98 79 98 01
Sofiendalsvej 94, 9200 Aalborg SV

Boreprofil

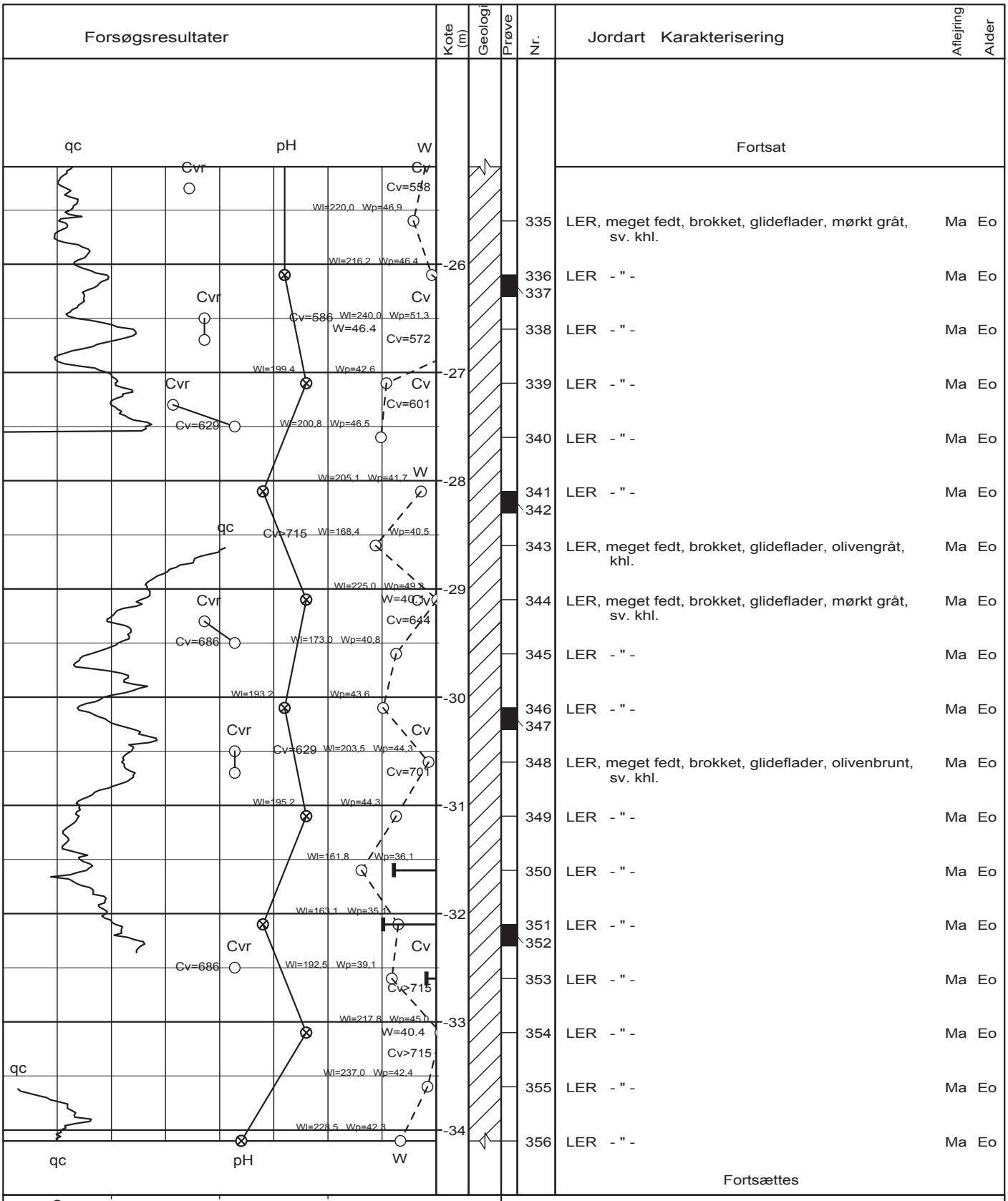

Boremetode : Tørboring med foring

X : 218979 (m) Y : 192852 (m) Plan :

Sag : 25.0705.61 Århus, Light*House

Geolog : JBM Boret af : LER/JQB Dato : 20071024 DGU-nr.: Boring : L*H10

Udarb. af : HLa Kontrol : Godkendt : Dato : Bilag : 4 S. 4 / 5

Grontmij | Carl Bro
Tlf. 98 79 98 00, Fax 98 79 98 01
Sofiendalsvej 94, 9200 Aalborg SV

Boreprofil

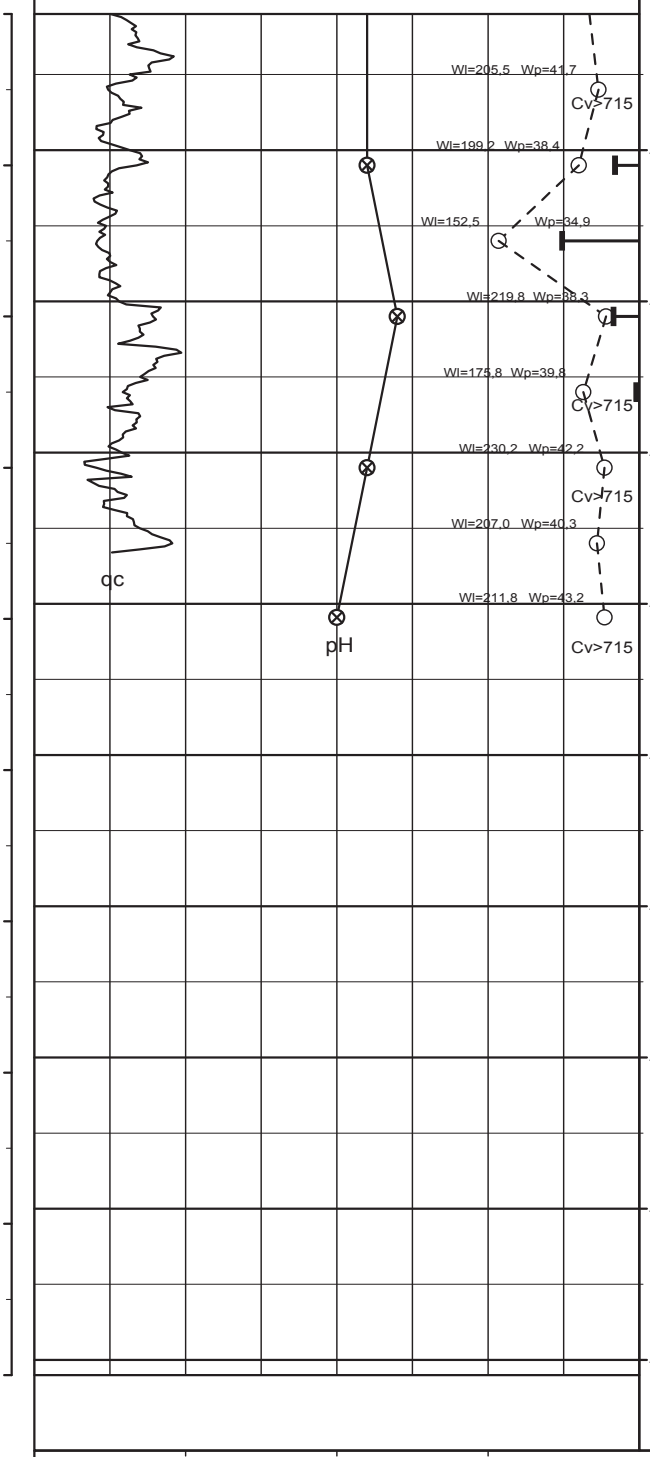

Dybde	Kote (m)	Nr.	Jordart Karakterisering	Aflejring	Alder
Forsøgsresultater			Fortsat		
36		357			
		358	LER, meget fedt, brokket, glideflader, olivenbrunt, sv. khl.	Ma	Eo
37	-35	359	LER - " -	Ma	Eo
		360	LER, meget fedt, brokket, glideflader, lyst olivenbrunt, khl.	Ma	Eo
38	-36	361	LER, meget fedt, brokket, glideflader, olivenbrunt, sv. khl.	Ma	Eo
		362			
		363	LER, meget fedt, brokket, glideflader, lyst olivenbrunt, khl.	Ma	Eo
39	-37	364	LER, meget fedt, brokket, glideflader, olivenbrunt, sv. khl.	Ma	Eo
		365	LER - " -	Ma	Eo
40	-38	366	LER - " -	Ma	Eo
41	-39				
42	-40				
43	-41				
44	-42				
45	-43				

○	10	20	30	W (%)
●○	100	200	300	Cv,Cvr (kN/m²)
		10		qc (MN/m²)
⊗		9		pH

Boremetode : Tørboring med foring

X : 218979 (m) Y : 192852 (m) Plan :

Sag : 25.0705.61 Århus, Light*House

Geolog : JBM Boret af : LER/JQB Dato : 20071024 DGU-nr.: Boring : L*H10

Udarb. af : HLa Kontrol : Godkendt : Dato : Bilag : 4 S. 5 / 5

Grontmij | Carl Bro
Tlf. 98 79 98 00, Fax 98 79 98 01
Sofiendalsvej 94, 9200 Aalborg SV

Boreprofil

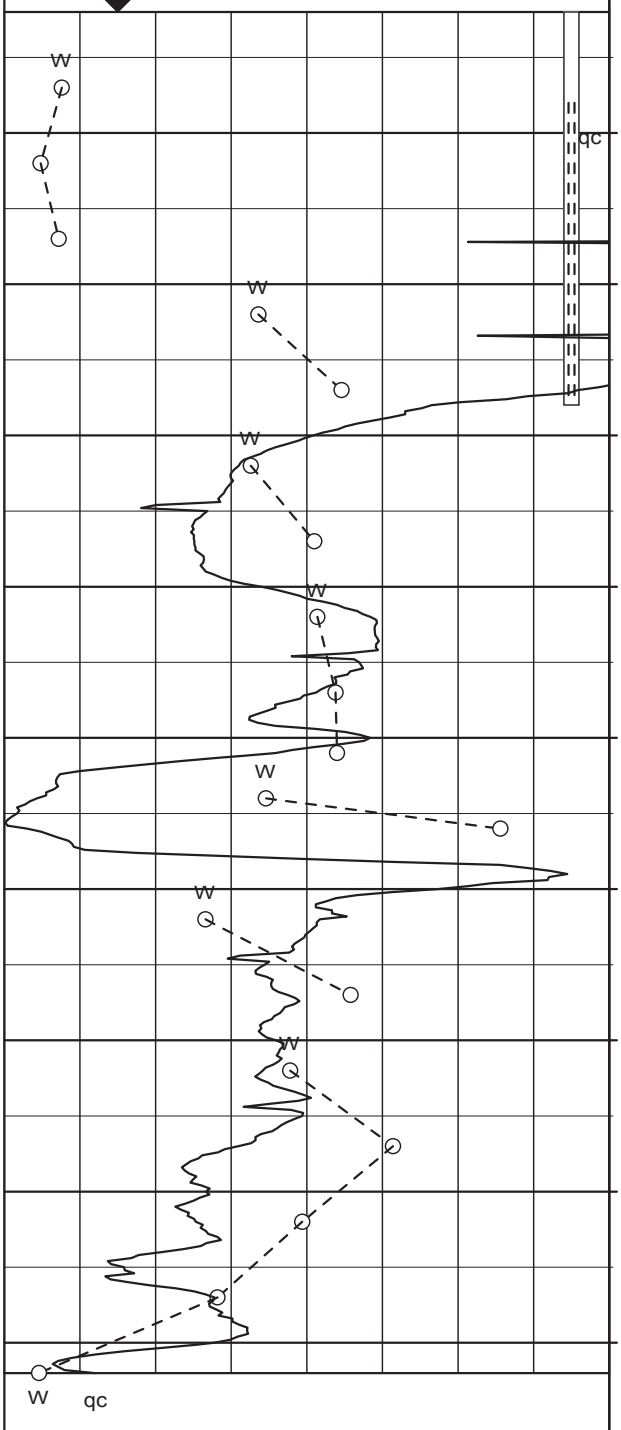

Dybde	Kote (m)	Nr.	Jordart Karakterisering	Aflejring	Alder
		A	ASFALT		
		747	FYLD: SAND, mellem, ringe sorteret, gruset, mørkt gulbrunt, khl.	Fy	Re
		748	FYLD: SAND, mellem, sorteret, grålig brunt, khl.	Fy	Re
		749	FYLD: SAND, mellem, sorteret, træstk., grålig brunt, khl.	Fy	Re
		750	FYLD: SAND, mellem, sorteret, grålig brunt, khl.	Fy	Re
		751	FYLD: SAND, mellem, sorteret, mørkt brunlig gråt, khl.	Fy	Re
		752	FYLD: SAND - " -	Fy	Re
		753	FYLD: SAND - " -	Fy	Re
		754	FYLD: SAND - " -	Fy	Re
		755	FYLD: SAND, mellem, sorteret, organiskh., mørkt gråt, khl.	Fy	Re
		756	FYLD: SAND, mellem, ringe sorteret, gruset, gråt, khl.	Fy	Re
		757	FYLD: SAND, groft, ringe sorteret, gruset, gråt, khl.	Fy	Re
		758	FYLD: SAND, fint, ringe sorteret, siltet, sv. organiskh., gråt, khl.	Fy	Re
		759	FYLD: SAND, fint sorteret, gråt, khl.	Fy	Re
		760	FYLD: SAND, mellem, sorteret, gråt, khl.	Fy	Re
		761	FYLD: SAND - " -	Fy	Re
		762	FYLD: SAND - " -	Fy	Re
		763	FYLD: SAND, mellem, ringe sorteret, gruset, gråt, khl.	Fy	Re
		764	FYLD: SAND - " -	Fy	Re
		765	FYLD: SAND, mellem, ringe sorteret, gråt, khl.	Fy	Re

Fortsættes

○	10	20	30	W (%)
●○	100	200	300	Cv,Cvr (kN/m²)
		10		qc (MN/m²)
⊗		9		pH

Boremetode : Tørboring med foring

X : 218921 (m) Y : 192840 (m) Plan :

Sag : 25.0705.61 Århus, Light*House

Geolog : JBM Boret af : LER/JQB Dato : 20071015 DGU-nr.: Boring : L*H11

Udarb. af : HLa Kontrol : Godkendt : Dato : Bilag : 5 S. 1 / 8

Grontmij | Carl Bro
Tlf. 98 79 98 00, Fax 98 79 98 01
Sofiendalsvej 94, 9200 Aalborg SV

Boreprofil

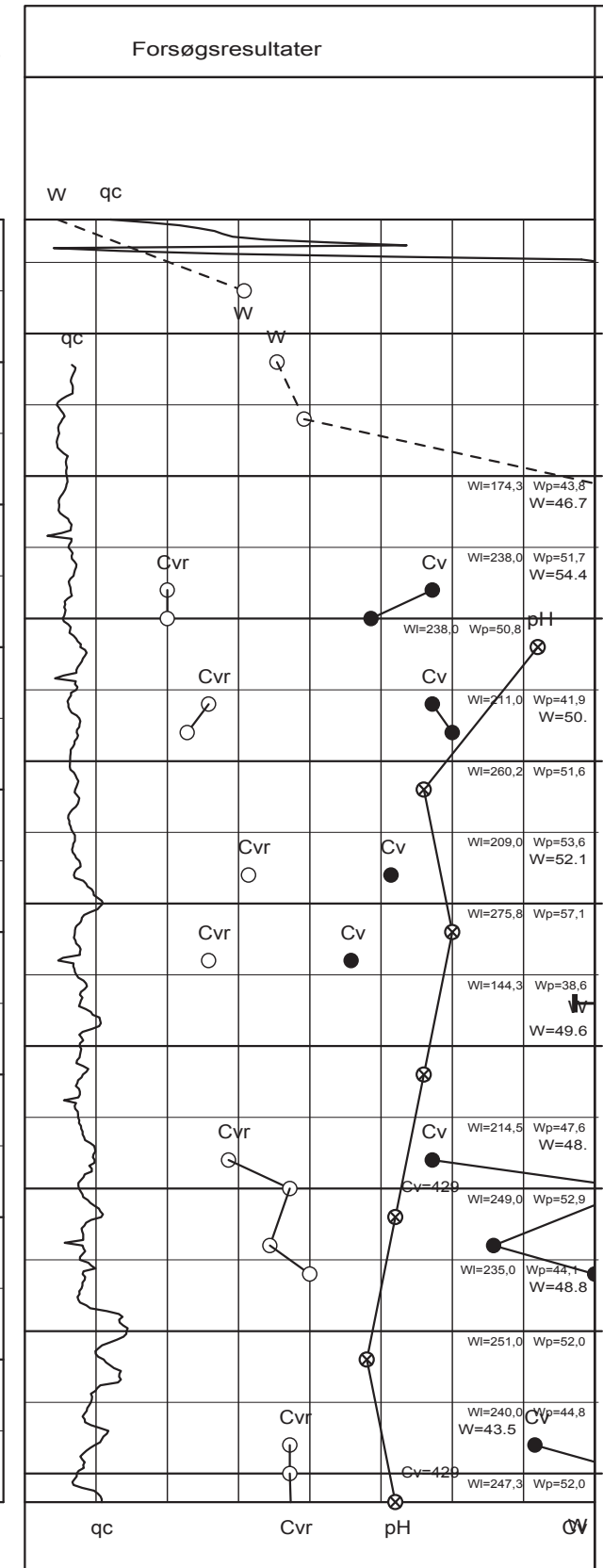

Kote (m)	Geologi	Prøve	Nr.	Jordart Karakterisering	Aflejring	Alder
				Fortsat		
-8			766	SAND og GRUS, sv. gytjeh., skalrester, gråt, khl.	Ma	Pg
			767	MORÆNELER, sandet, gråt, khl.	Gl	Gc
			768	MORÆNELER - " -	Gl	Gc
-9			769	MORÆNELER, meget fedt, st. tertiært præget, olivengråt, khl.	Gl	Gc
			770			
			771	LER, meget fedt, brokket, glideflader, grønlig gråt, khl.	Ma	Eo
-10			772	LER - " -	Ma	Eo
			773	LER - " -	Ma	Eo
-11			774	LER, meget fedt, brokket, glideflader, mørkt grønlig gråt, khl.	Ma	Eo
			775			
			776	LER - " -	Ma	Eo
-12			777	LER, meget fedt, brokket, glideflader, meget mørkt gråt, khl.	Ma	Eo
			778	LER, meget fedt, brokket, glideflader, mørkt brunlig gråt, khl.	Ma	Eo
-13			779	LER, meget fedt, brokket, glideflader, meget mørkt gråt, kfr.	Ma	Eo
			780			
			781	LER, meget fedt, brokket, glideflader, mørkt brunlig gråt, khl.	Ma	Eo
-14			782	LER, meget fedt, brokket, glideflader, meget mørkt gråt, khl.	Ma	Eo
			783	LER, meget fedt, brokket, glideflader, mørkt grønlig gråt, khl.	Ma	Eo
-15			784	LER, meget fedt, brokket, glideflader, mørkt brunlig gråt, khl.	Ma	Eo
			785			
			786	LER, meget fedt, brokket, glideflader, meget mørkt brungråt, khl.	Ma	Eo
-16			787	LER, meget fedt, brokket, glideflader, mørkt brungråt, khl.	Ma	Eo
				Fortsættes		

Boremetode : Tørboring med foring

X : 218921 (m) Y : 192840 (m) Plan :

Sag : 25.0705.61 Århus, Light*House

Geolog : JBM Boret af : LER/JQB Dato : 20071015 DGU-nr.: Boring : L*H11

Udarb. af : HLa Kontrol : Godkendt : Dato : Bilag : 5 S. 2 / 8

Grontmij | Carl Bro
Tlf. 98 79 98 00, Fax 98 79 98 01
Sofiendalsvej 94, 9200 Aalborg SV

Boreprofil

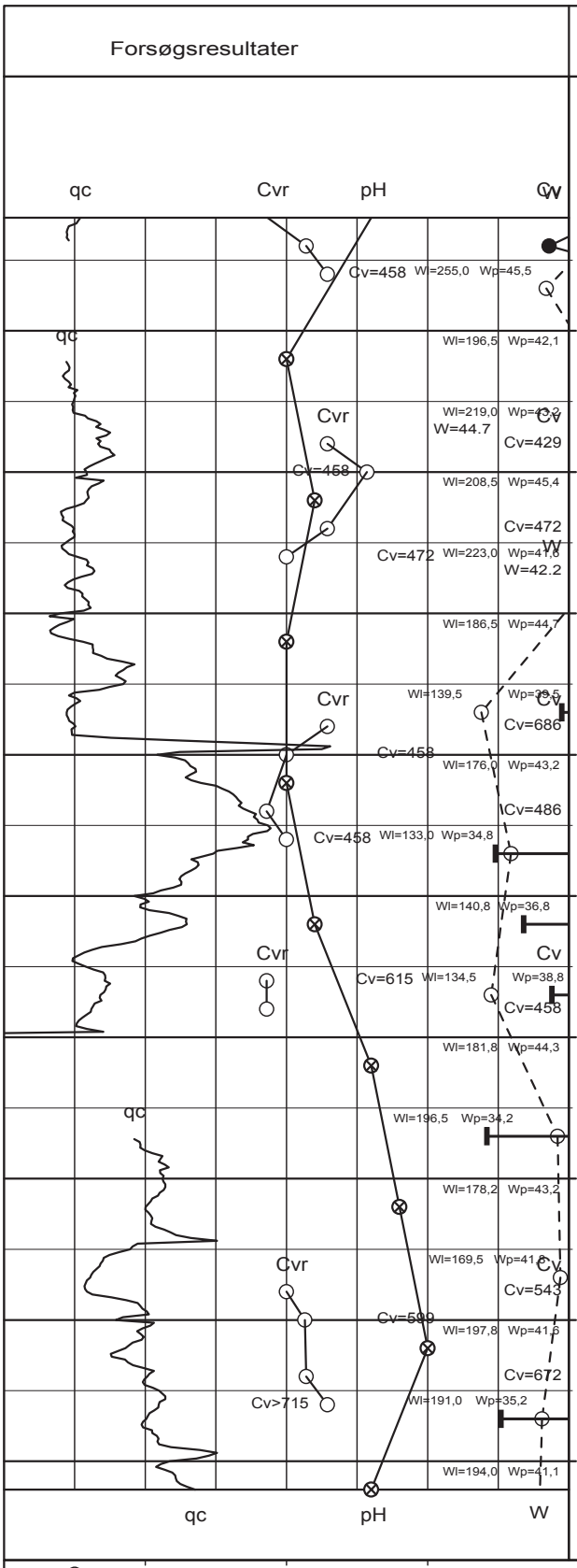

Fortsat

Nr.	Jordart Karakterisering	Aflejring	Alder
788	LER, meget fedt, brokket, glideflader, grønlig gråt, khl.	Ma	Eo
789	LER - " -	Ma	Eo
790			
791	LER - " -	Ma	Eo
792	LER - " -	Ma	Eo
793	LER, meget fedt, brokket, glideflader, mørkt gråbrunt, khl.	Ma	Eo
794	LER, meget fedt, brokket, glideflader, mørkt grålig brunt, khl.	Ma	Eo
795			
796	LER, meget fedt, brokket, glideflader, lyst brunt, khl.	Ma	Eo
797	LER, meget fedt, brokket, glideflader, grønlig gråt, khl.	Ma	Eo
798	LER, meget fedt, brokket, glideflader, lyst brunt, khl.	Ma	Eo
799	LER - " -	Ma	Eo
800			
801	LER - " -	Ma	Eo
802	LER, meget fedt, brokket, glideflader, grønlig gråt, khl.	Ma	Eo
803	LER - " -	Ma	Eo
804	LER - " -	Ma	Eo
805			
806	LER - " -	Ma	Eo
807	LER - " -	Ma	Eo
808	LER, meget fedt, brokket, glideflader, olivenbrunt, khl.	Ma	Eo
809	LER - " -	Ma	Eo

Fortsættes

○	10	20	30 W (%)
●○	100	200	300 Cv,Cvr (kN/m²)
		10	qc (MN/m²)
⊗		9	pH

Boremetode : Tørboring med foring

X : 218921 (m) Y : 192840 (m) Plan :

Sag : 25.0705.61 Århus, Light*House

Geolog : JBM Boret af : LER/JQB Dato : 20071015 DGU-nr.: Boring : L*H11

Udarb. af : HLa Kontrol : Godkendt : Dato : Bilag : 5 S. 3 / 8

Grontmij | Carl Bro
Tlf. 98 79 98 00, Fax 98 79 98 01
Sofiendalsvej 94, 9200 Aalborg SV

Boreprofil

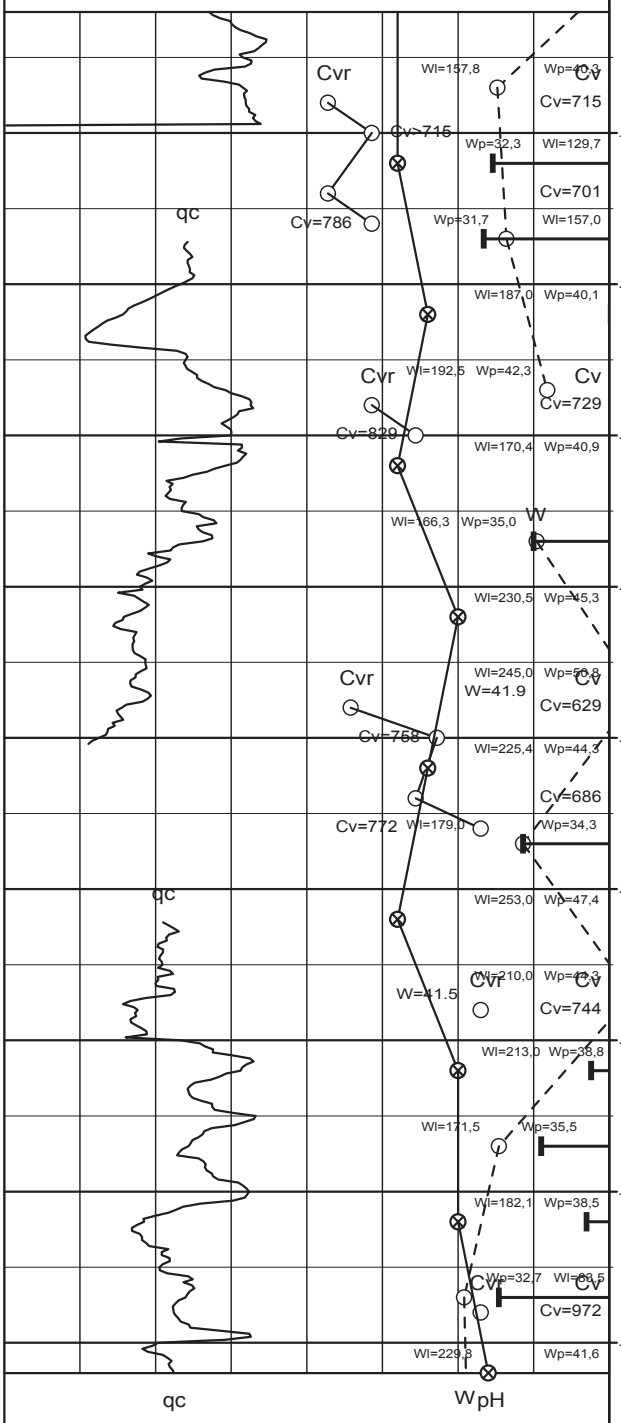

Dybde	Kote (m)	Nr.	Jordart Karakterisering	Aflejring	Alder
			Fortsat		
27	-26	810			
		811	LER, meget fedt, brokket, glideflader, lyst brunt, khl.	Ma	Eo
28		812	LER, meget fedt, brokket, glideflader, lyst olivengrået, khl.	Ma	Eo
		813	LER - " -	Ma	Eo
29	-27	814	LER, meget fedt, brokket, glideflader, olivengrået, khl.	Ma	Eo
		815			
		816	LER - " -	Ma	Eo
30	-28	817	LER - " -	Ma	Eo
		818	LER - " -	Ma	Eo
31	-29	819	LER - " -	Ma	Eo
		820			
		821	LER, meget fedt, glideflader, glaukonitk., mørkt grønlig gråt, khl.	Ma	Eo
32	-30	822	LER, meget fedt, glideflader, mørkt grønlig gråt, khl.	Ma	Eo
		823	LER, meget fedt, brokket, glideflader, olivengrået, khl.	Ma	Eo
33	-31	824	LER, meget fedt, brokket, glideflader, mørkt olivengrået, khl.	Ma	Eo
		825			
		826	LER - " -	Ma	Eo
34	-32	827	LER, meget fedt, brokket, glideflader, olivenbrunt, khl.	Ma	Eo
		828	LER - " -	Ma	Eo
35	-33	829	LER - " -	Ma	Eo
		830			
		831	LER, meget fedt, brokket, glideflader, lyst grønlig gråt, khl.	Ma	Eo
36	-34	832	LER, meget fedt, brokket, glideflader, mørkt gråt, khl.	Ma	Eo
			Fortsættes		

○	10	20 30	W (%)
●○	100	200 300	Cv,Cvr (kN/m²)
		10	qc (MN/m²)
⊗		9	pH

Boremetode : Tørboring med foring

X : 218921 (m) Y : 192840 (m) Plan :

Sag : 25.0705.61 Århus, Light*House

Geolog : JBM Boret af : LER/JQB Dato : 20071015 DGU-nr.: Boring : L*H11

Udarb. af : HLa Kontrol : Godkendt : Dato : Bilag : 5 S. 4 / 8

Grontmij | Carl Bro
Tlf. 98 79 98 00, Fax 98 79 98 01
Sofiendalsvej 94, 9200 Aalborg SV

Boreprofil

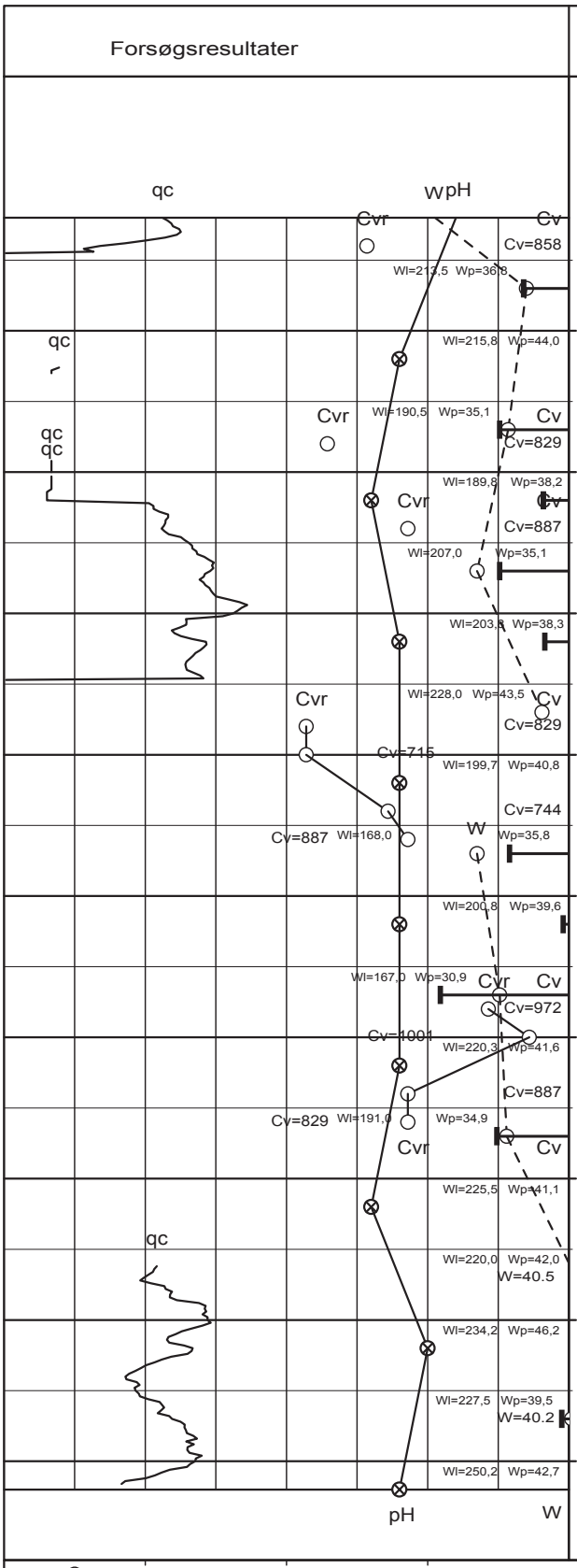

Boremetode : Tørboring med foring

X : 218921 (m) Y : 192840 (m) Plan :

Sag : 25.0705.61 Århus, Light*House

Geolog : JBM Boret af : LER/JQB Dato : 20071015 DGU-nr.: Boring : L*H11

Udarb. af : HLa Kontrol : Godkendt : Dato : Bilag : 5 S. 5 / 8

Grontmij | Carl Bro
Tlf. 98 79 98 00, Fax 98 79 98 01
Sofiendalsvej 94, 9200 Aalborg SV

Boreprofil

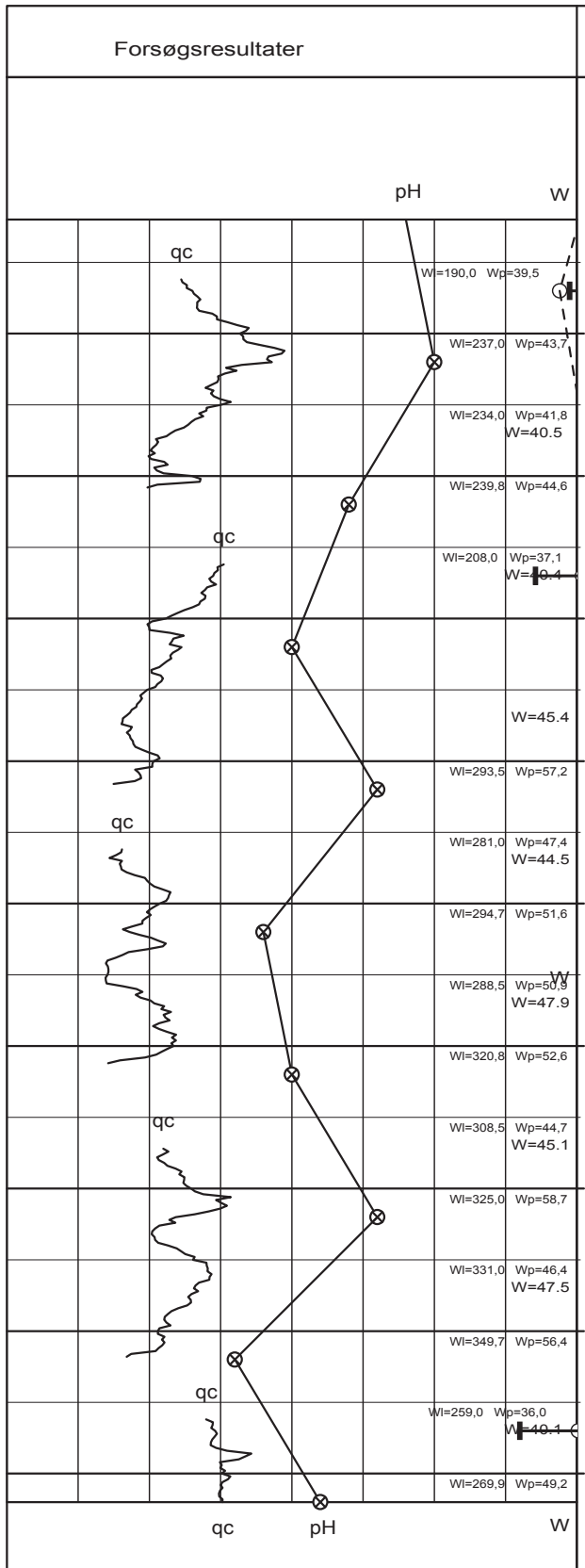

Kote (m)	Geologi	Prøve	Nr.	Jordart Karakterisering	Aflejring	Alder
				Fortsat		
			855			
			856	LER, meget fedt, brokket, glideflader, olivengråt, khl.	Ma	Eo
			857	LER - " -	Ma	Eo
			858	LER - " -	Ma	Eo
			859	LER - " -	Ma	Eo
			860			
			861	LER - " -	Ma	Eo
			862	LER - " -	Ma	Eo
			863	LER, meget fedt, brokket, glideflader, mørkt gråt, khl.	Ma	Eo
			864	LER - " -	Ma	Eo
			865			
			866	LER - " -	Ma	Eo
			867	LER - " -	Ma	Eo
			868	LER - " -	Ma	Eo
			869	LER, meget fedt, brokket, glideflader, enk. kalkkonkretioner, mørkt gråt, khl.	Ma	Eo
			870			
			871	LER, meget fedt, brokket, glideflader, mørkt olivengråt, khl.	Ma	Eo
			872	LER - " -	Ma	Eo
			873	LER - " -	Ma	Eo
			874	LER - " -	Ma	Eo
			875			
			876	LER, meget fedt, brokket, glideflader, mørkt gråt, khl.	Ma	Eo
			877	LER - " -	Ma	Eo

Fortsættes

○	10	20	30 W (%)
●○	100	200	300 Cv,Cvr (kN/m²)
		10	qc (MN/m²)
⊗		9	pH

Boremetode : Tørboring med foring

X : 218921 (m) Y : 192840 (m) Plan :

Sag : 25.0705.61 Århus, Light*House

Geolog : JBM Boret af : LER/JQB Dato : 20071015 DGU-nr.: Boring : L*H11

Udarb. af : HLa Kontrol : Godkendt : Dato : Bilag : 5 S. 6 / 8

Grontmij | Carl Bro
Tlf. 98 79 98 00, Fax 98 79 98 01
Sofiendalsvej 94, 9200 Aalborg SV

Boreprofil

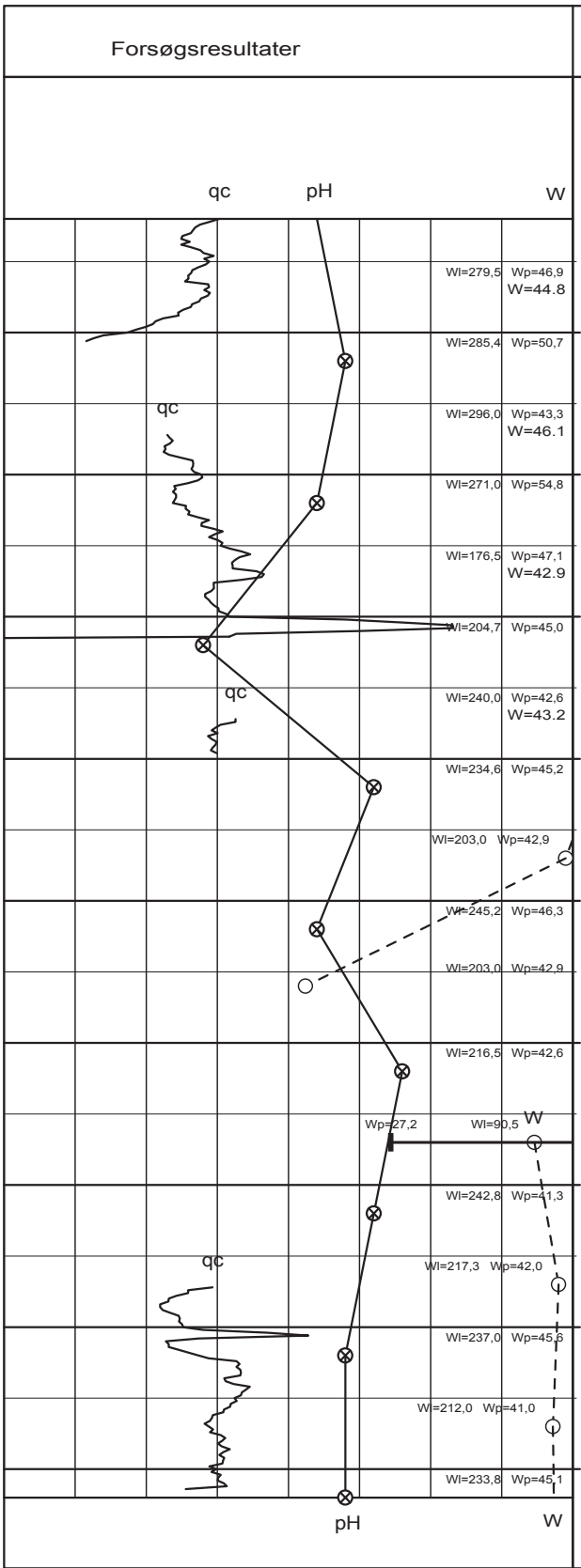

Kote (m)	Geologi	Prøve	Nr.	Jordart Karakterisering	Aflejring	Alder
				Fortsat		
-53			878	LER, meget fedt, brokket, glideflader, mørkt gråt, khl.	Ma	Eo
			879	LER - " -	Ma	Eo
			880			
-54			881	LER, meget fedt, brokket, glideflader, mørkt olivengråt, khl.	Ma	Eo
			882	LER - " -	Ma	Eo
-55			883	LER, meget fedt, brokket, glideflader, mørkt gråt, khl.	Ma	Eo
			884	LER, meget fedt, brokket, glideflader, mørkt gråt, st. khl.	Ma	Eo
			885			
-56			886	LER, meget fedt, brokket, glideflader, nedknust, mørkt gråt, khl.	Ma	Eo
			887	LER, meget fedt, brokket, glideflader, olivengråt, khl.	Ma	Eo
-57			888	LER - " -	Ma	Eo
			889	LER - " -	Ma	Eo
			890			
			891	LER, meget fedt, brokket, glideflader, store kalkkonkretioner, lyst olivengråt, st. khl.	Ma	Eo
-58			892	LER, meget fedt, brokket, glideflader, grønlig gråt, khl.	Ma	Eo
			893	LER, meget fedt, brokket, glideflader, mørkt grønlig gråt, khl.	Ma	Eo
-59			894	LER, meget fedt, brokket, glideflader, nedknust, mørkt grønlig gråt, khl.	Ma	Eo
			895			
-60			896	LER, meget fedt, brokket, glideflader, grønlig gråt, st. khl.	Ma	Eo
			897	LER - " -	Ma	Eo
			898	LER - " -	Ma	Eo
-61			899	LER, meget fedt, brokket, glideflader, grønlig gråt, kfr.	Ma	Eo
				Fortsættes		

○	10	20	30 W (%)
●○	100	200	300 Cv,Cvr (kN/m²)
		10	qc (MN/m²)
⊗		9	pH

Boremetode : Tørboring med foring

X : 218921 (m) Y : 192840 (m) Plan :

Sag : 25.0705.61 Århus, Light*House

Geolog : JBM Boret af : LER/JQB Dato : 20071015 DGU-nr.: Boring : L*H11

Udarb. af : HLa Kontrol : Godkendt : Dato : Bilag : 5 S. 7 / 8

Grontmij | Carl Bro
Tlf. 98 79 98 00, Fax 98 79 98 01
Sofiendalsvej 94, 9200 Aalborg SV

Boreprofil

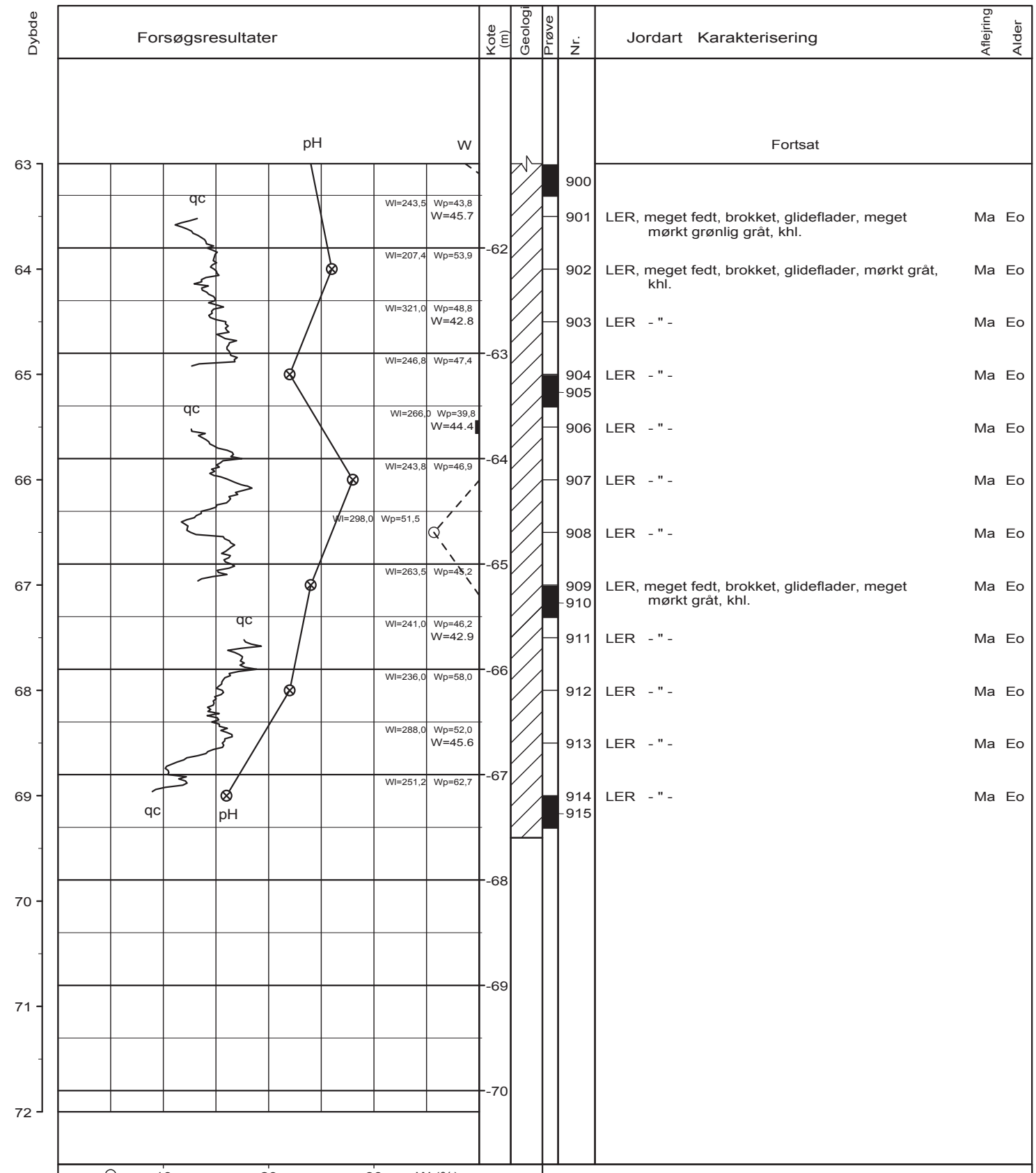

Boremetode : Tørboring med foring

X : 218921 (m) Y : 192840 (m) Plan :

Sag : 25.0705.61 Århus, Light*House

Geolog : JBM Boret af : LER/JQB Dato : 20071015 DGU-nr.: Boring : L*H11

Udarb. af : HLa Kontrol : Godkendt : Dato : Bilag : 5 S. 8 / 8

Grontmij | Carl Bro
Tlf. 98 79 98 00, Fax 98 79 98 01
Sofiendalsvej 94, 9200 Aalborg SV

Boreprofil

APPENDIX G: BOREHOLE PROFILES

AALBORG SITE - SAND

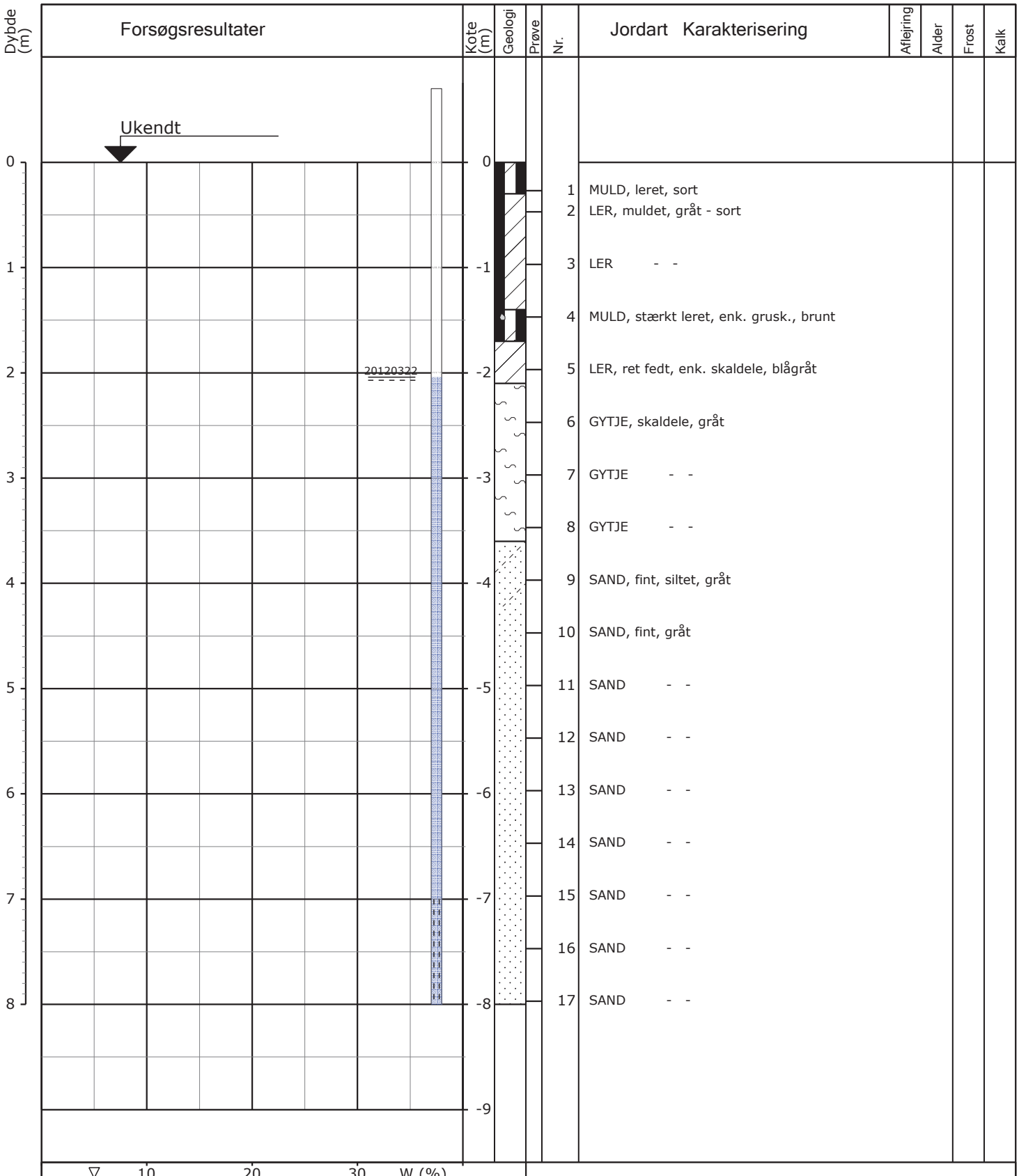

Boremetode: Tørboring med foring
Koordinatsystem: UTM32E89
X: 563436 (m) Y: 6323735 (m) Plan:

Sag: F25.1200.11 Aalborg Universitet. Havn

Boret af: Grontmij Dato: 2012.03.22 Bedømt af: DGU-Nr.: Boring: 1

Udarb. af: Kontrol: Godkendt: Dato: Bilag: S. 1/1

Boreprofil

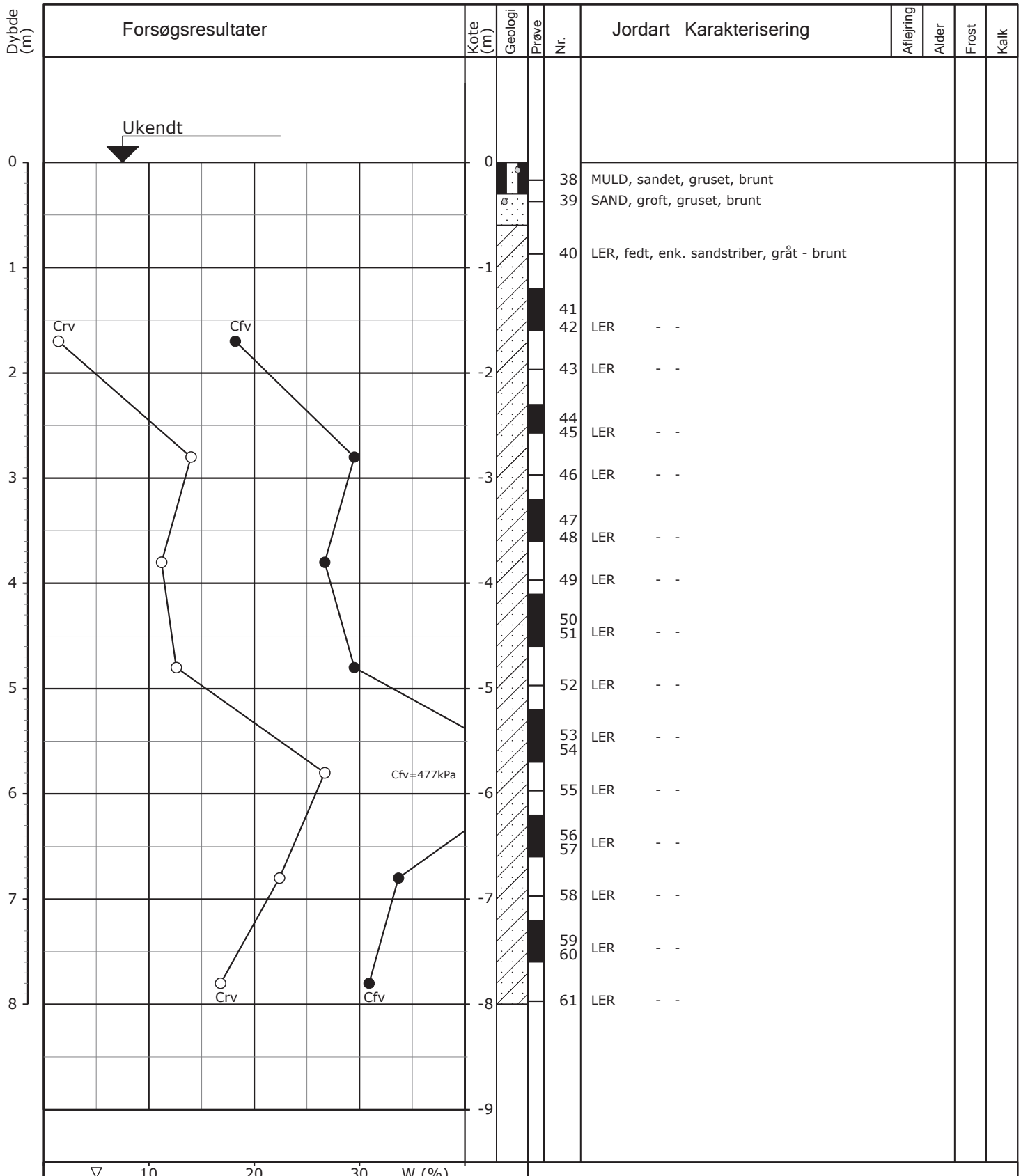

Boremetode: Tørboring med foring
Koordinatsystem: UTM32E89
Plan:

Sag: F25.1200.11 Aalborg Universitet. Havn

Boret af: Grontmij Dato: 2012.03.10 Bedømt af: DGU-Nr.: Boring: 2

Udarb. af: Kontrol: Godkendt: Dato: Bilag: S. 1/1

Boreprofil

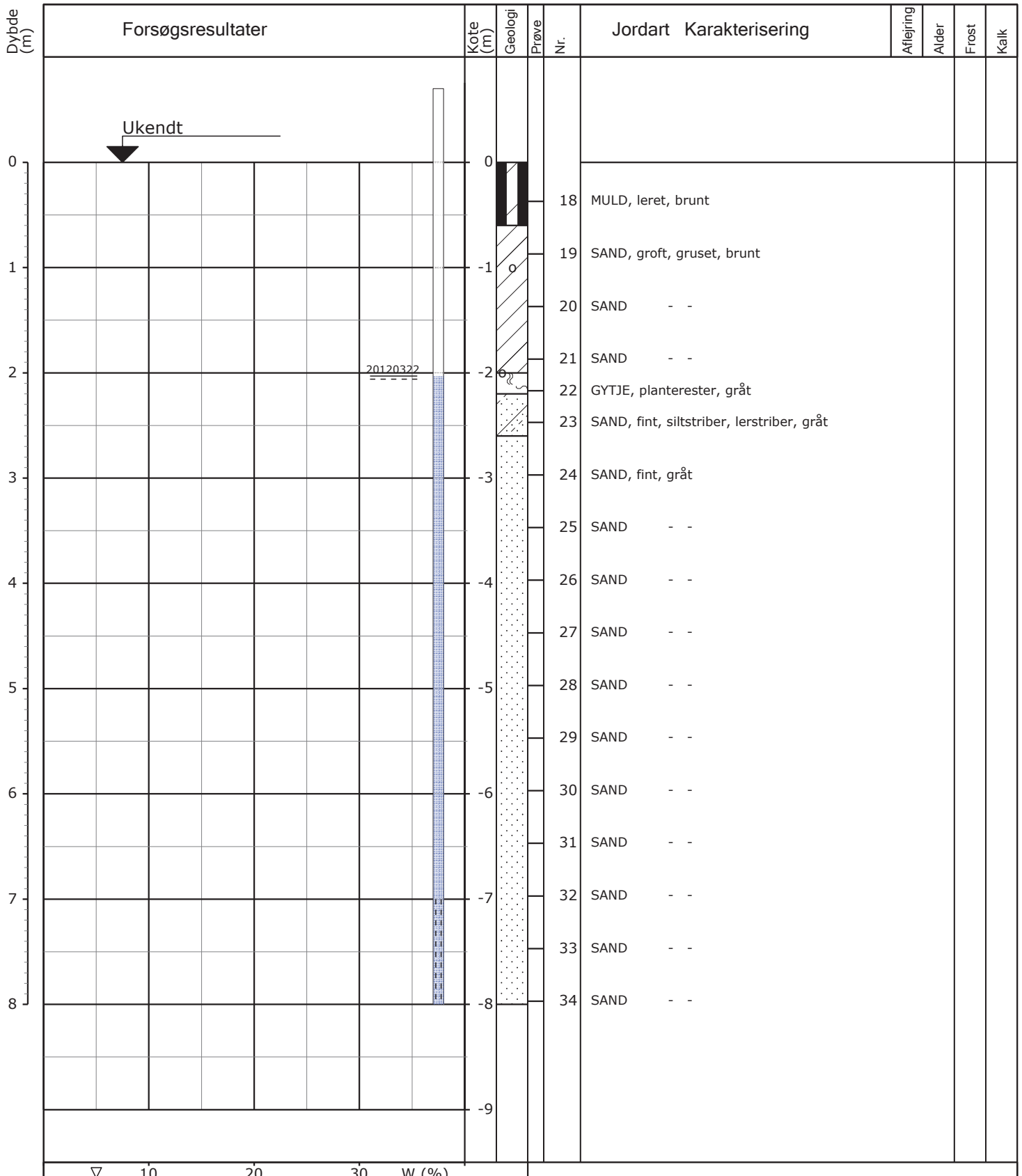

Boremetode: Tørboring med foring
Koordinatsystem: UTM32E89
X: 563408 (m) Y: 6323733 (m) Plan:

Sag: F25.1200.11 Aalborg Universitet. Havn

Boret af: Grontmij Dato: 2012.03.22 Bedømt af: DGU-Nr.: Boring: 3

Udarb. af: Kontrol: Godkendt: Dato: Bilag: S. 1/1

Boreprofil

AALBORG SITE - CLAY

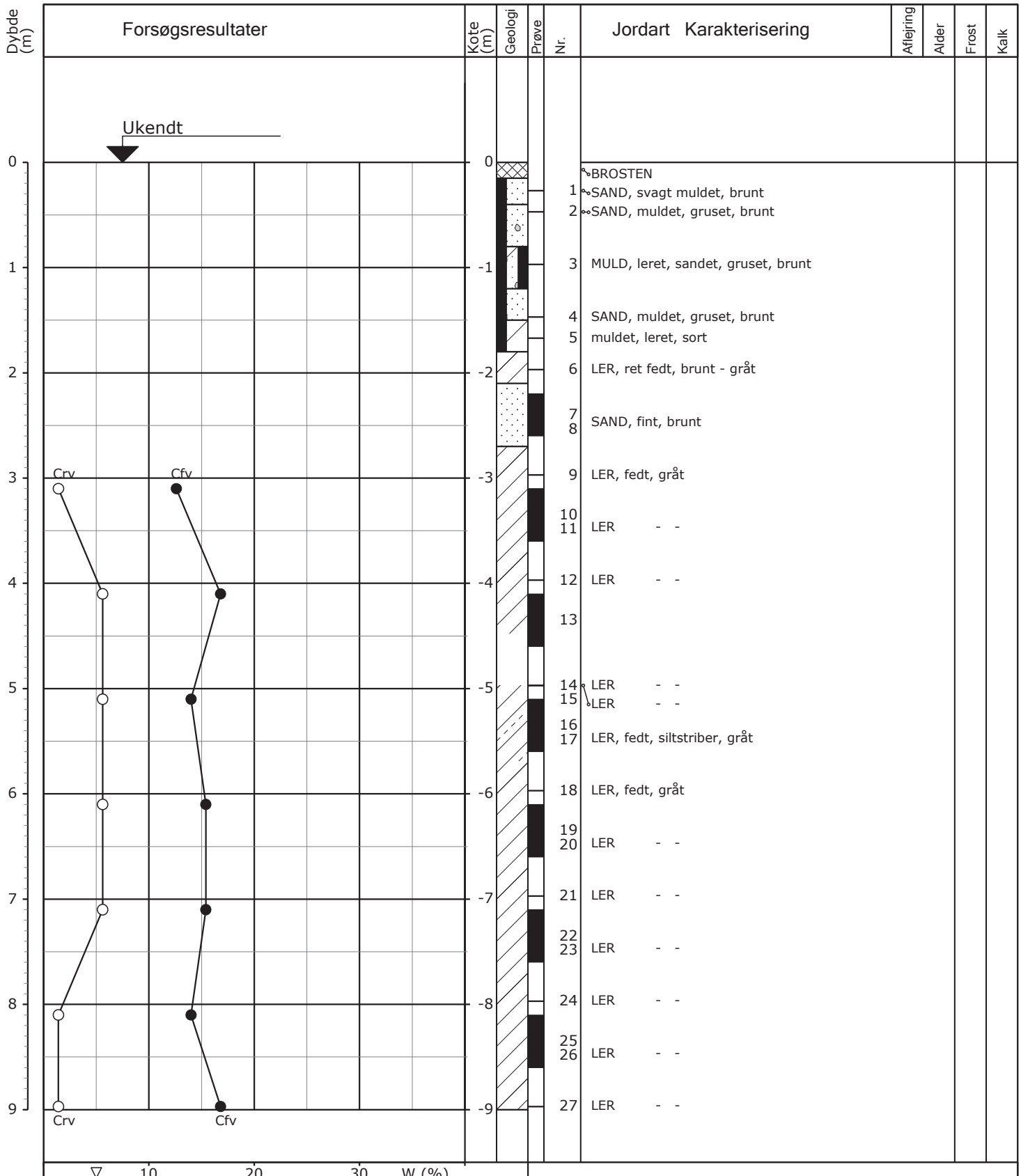

Boremetode:
Koordinatsystem: UTNM32E89
X: 555611 (m) Y: 6322334 (m) Plan:

Sag: F25.1200.11. Aalborg Universitet. Godsbanearealet

Boret af: Grontmij Dato: 2012.05.22 Bedømt af: DGU-Nr.: Boring: 1

Udarb. af: Kontrol: Godkendt: Dato: Bilag: S. 1/1

Boreprofil

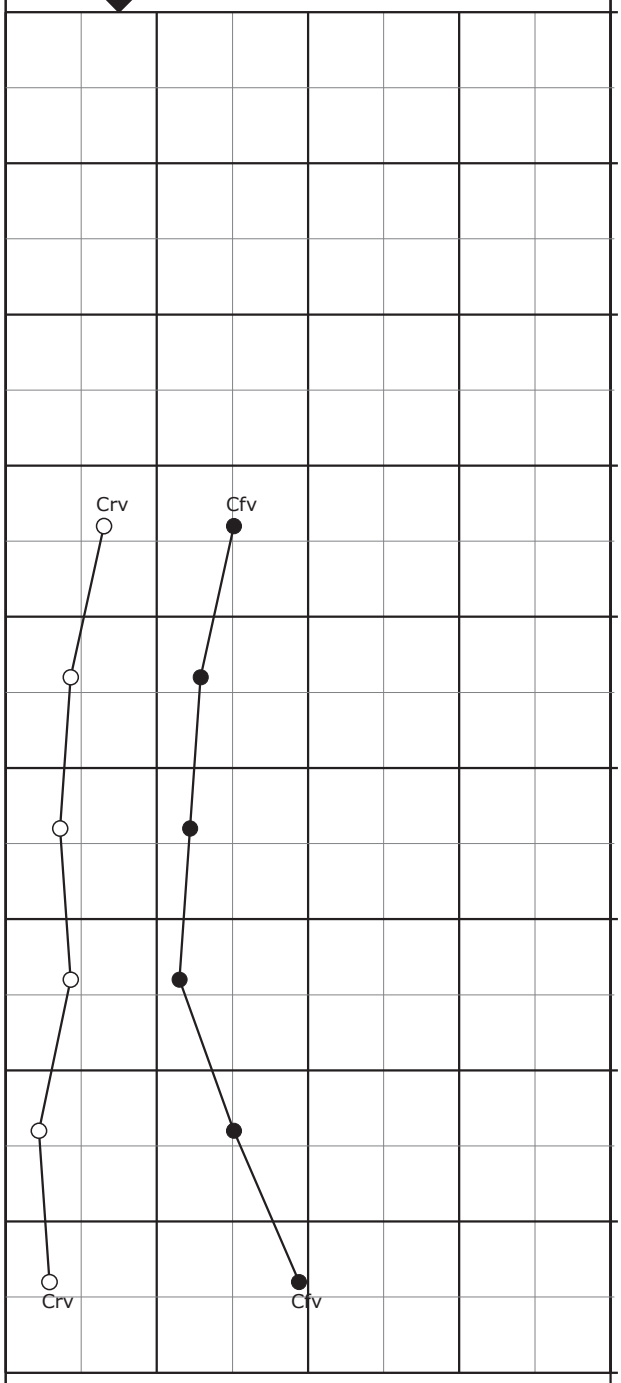

Dybde (m)	Kote (m)
0	0
1	-1
2	-2
3	-3
4	-4
5	-5
6	-6
7	-7
8	-8
9	-9

Nr.	Jordart Karakterisering	Aflejring	Alder	Frost	Kalk
27	SAND: GRUS, brunt				
28	SAND, muldet, gruset, brunt				
29	SAND, fint, enk. grusk., gulbrunt				
30	SAND - -				
31	SAND, fint - mellem, gruset, brunt				
32	SAND - -				
33	LER, fedt, enk. siltstriber, gråt				
34	LER - -				
35					
36	LER - -				
37					
38	LER - -				
39	LER - -				
40					
41	LER - -				
42	LER - -				
43					
44	LER - -				
45	LER - -				
46					
47	LER - -				
48	LER - -				
49					
50	LER - -				

▽	10	20	30	W (%)
●	100	200	300	Cfv, Crv (kPa)
×	12	16	20	γ (kN/m³)
+	2	4	6	Glr. (%)

Boremetode:
Koordinatsystem:
Plan:

Sag: F25.1200.11. Aalborg Universitet. Godsbanearealet

Boret af: Grontmij Dato: 2012.05.31 Bedømt af: DGU-Nr.: Boring: 2

Udarb. af: Kontrol: Godkendt: Dato: Bilag: S. 1/1

Boreprofil

APPENDIX H: SEISMIC ANALYSIS RESULTS

APPENDIX H: SESMIC ANALYSIS RESULTS

AALBORG SITE - SAND

Sounding 1 (Cross Correlation method)

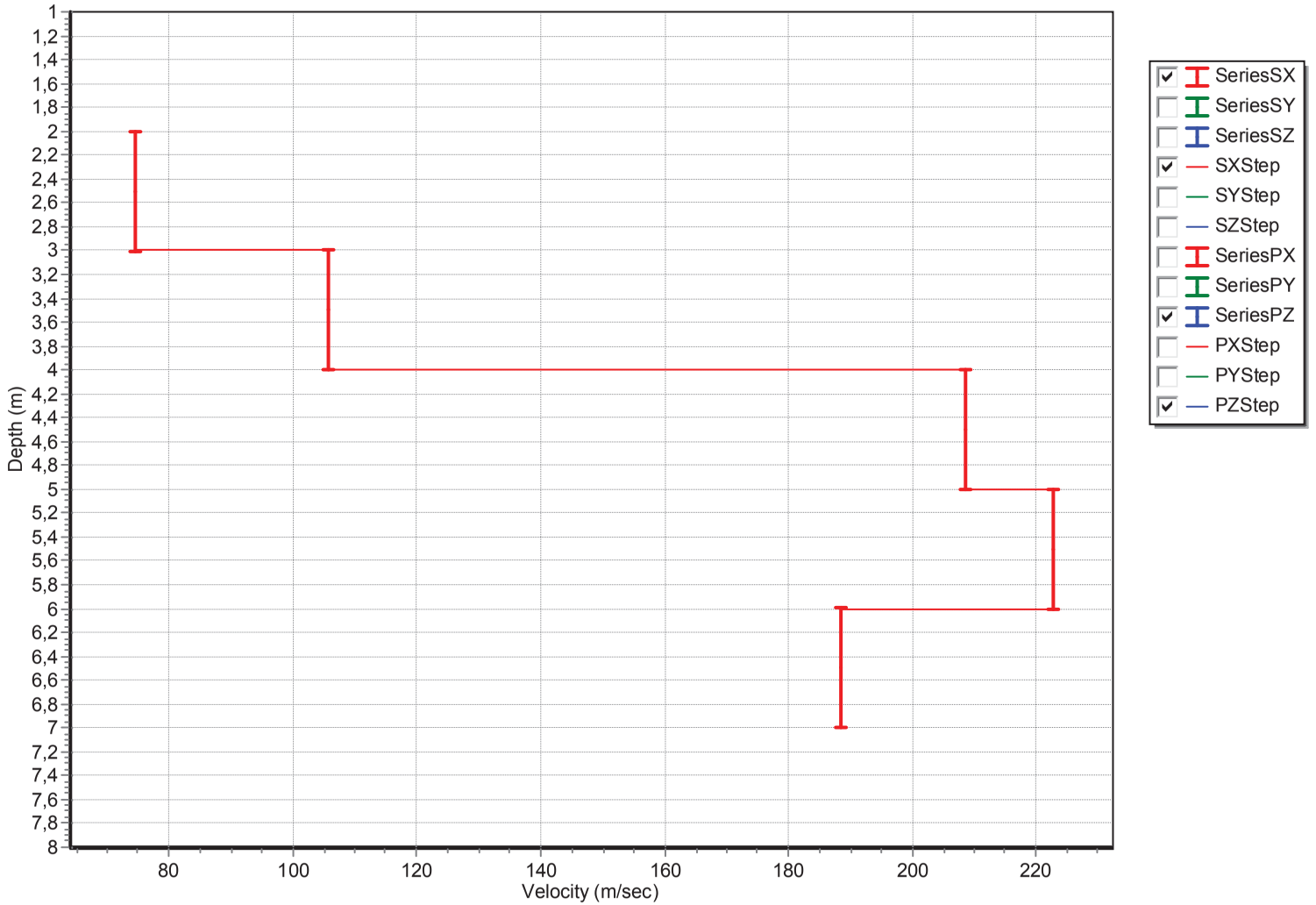

Sounding 1 (Revers Polarity method)

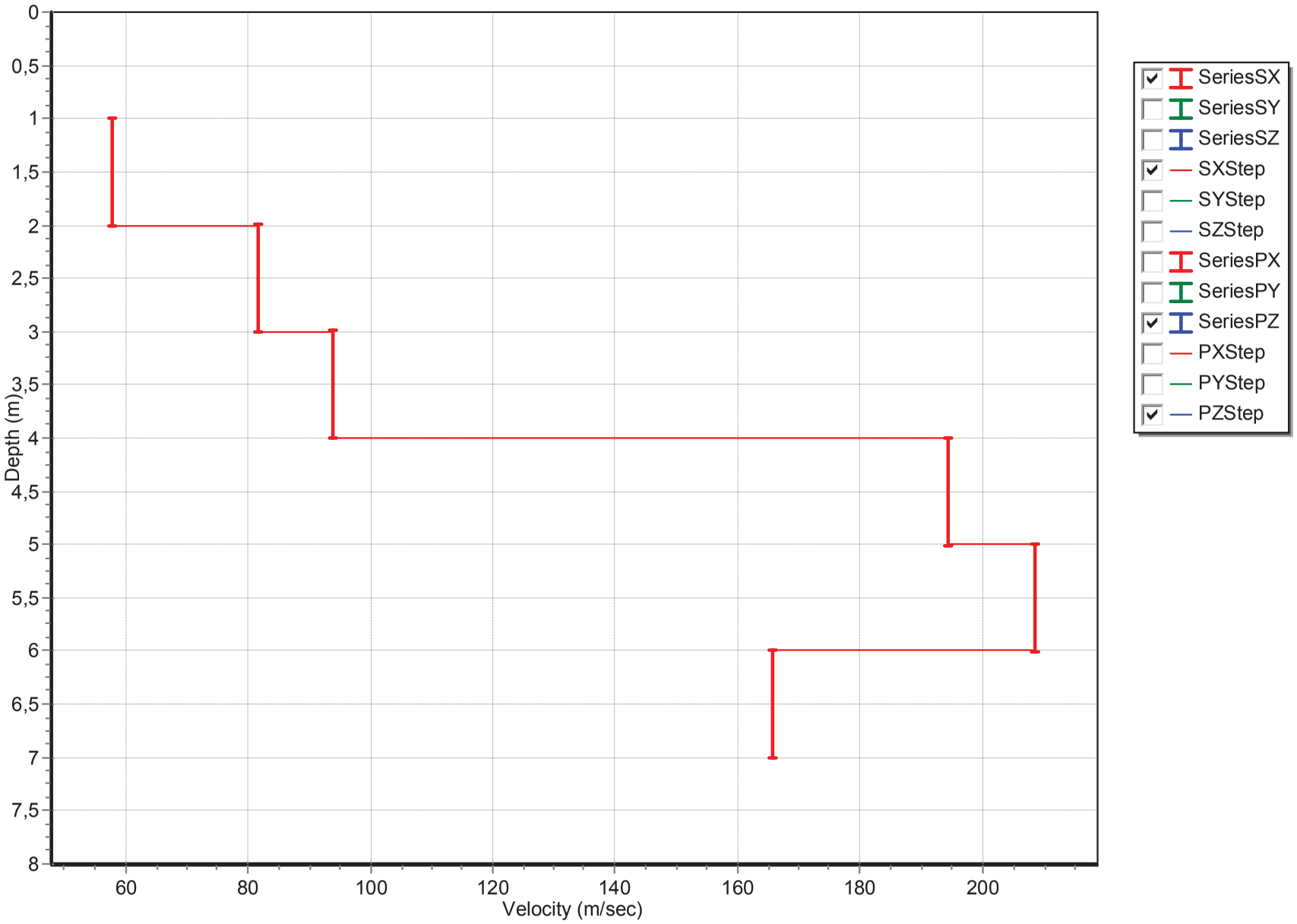

Sounding 2 (Cross Correlation method)

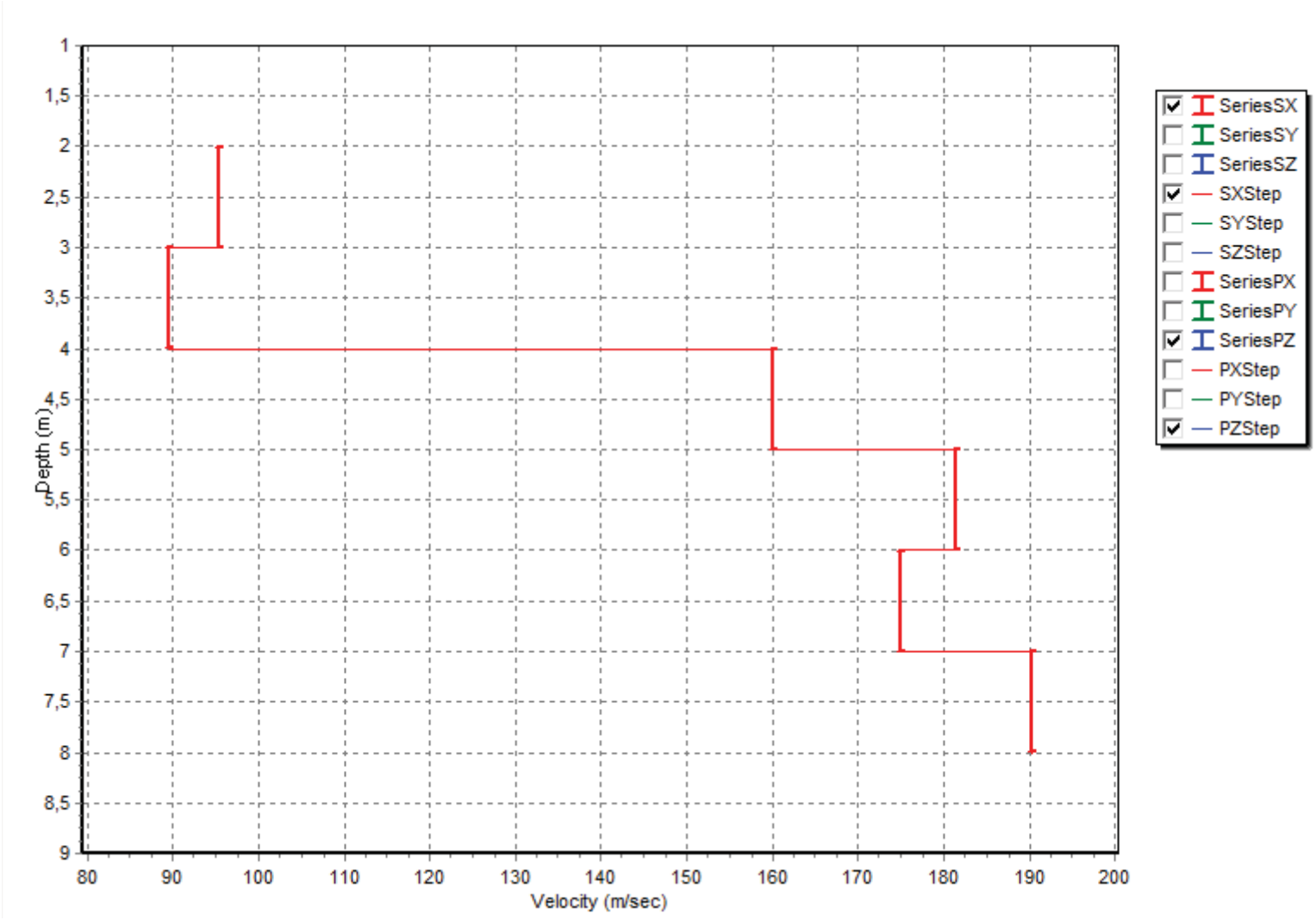

Sounding 2 (Revers Polarity method)

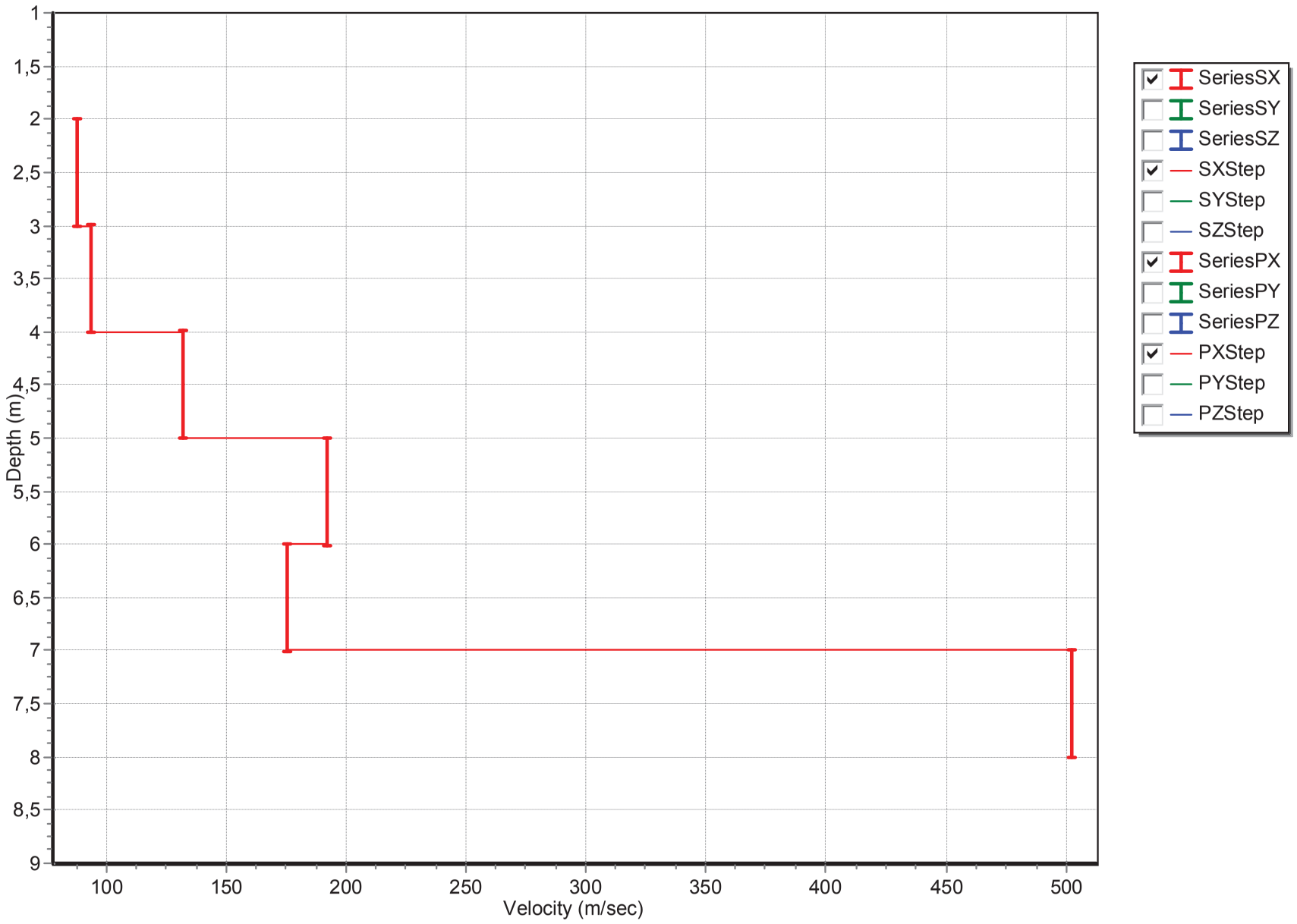

Sounding 3 (Cross correlation method)

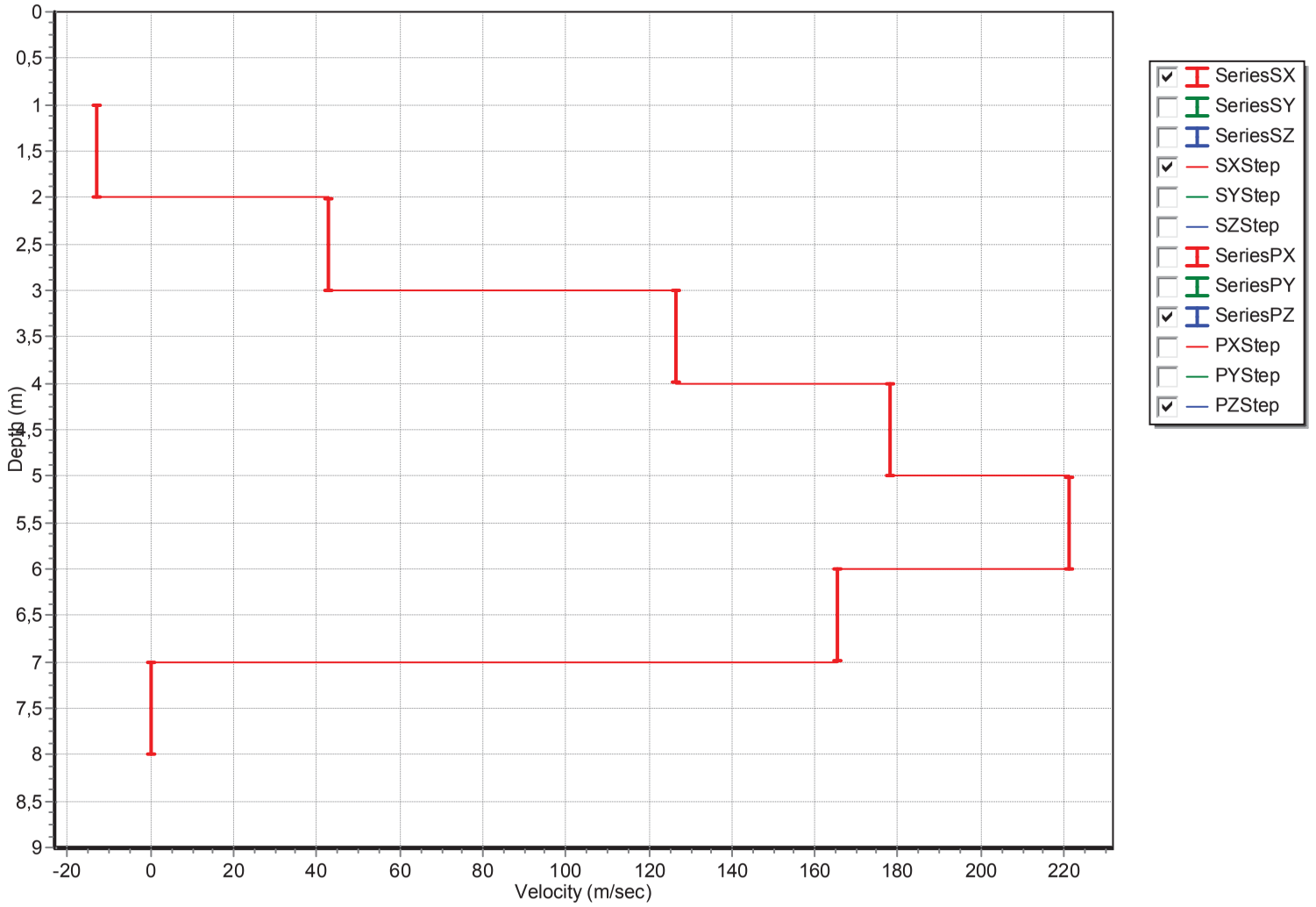

Sounding 3 (Revers Polarity method)

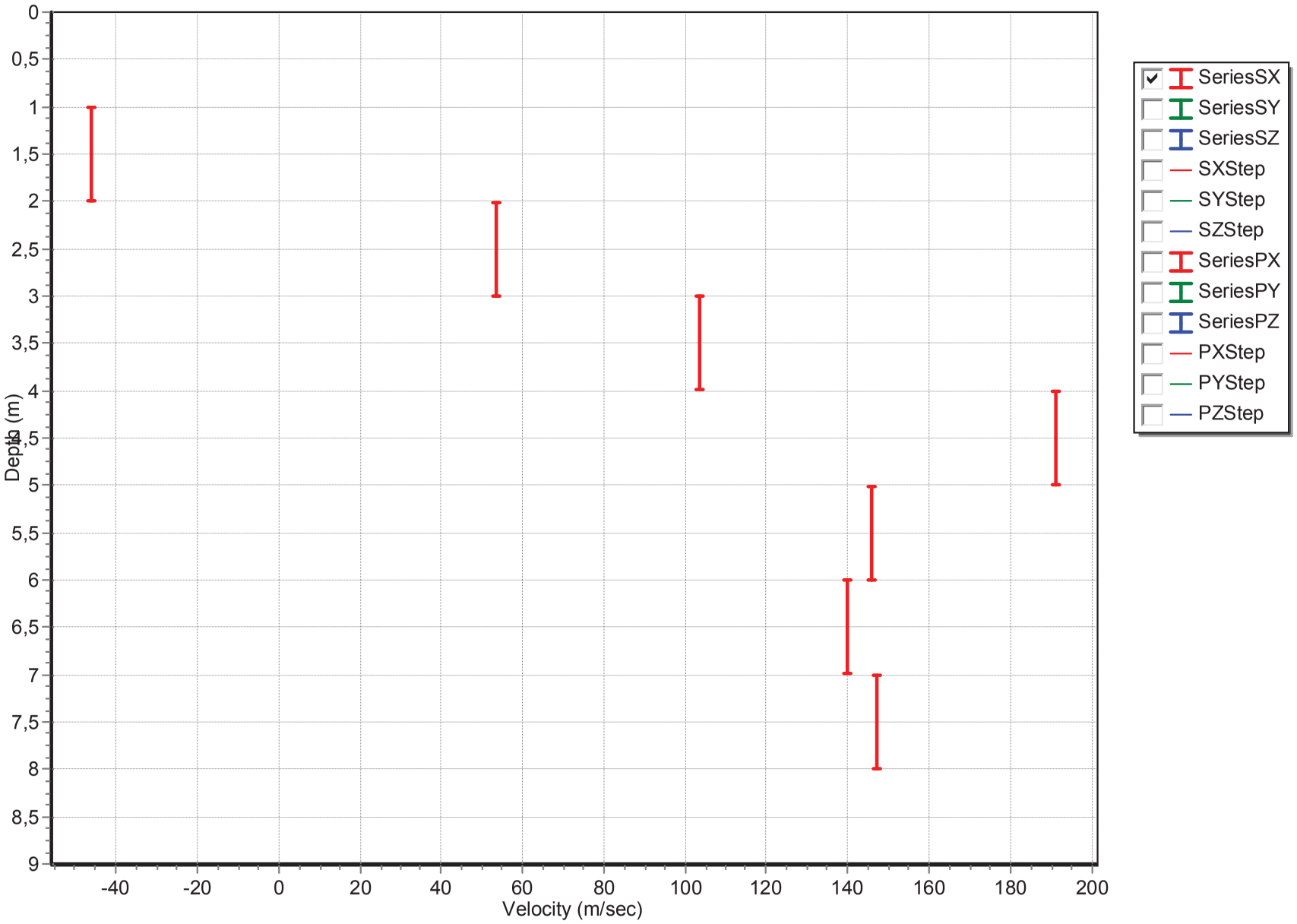

Sounding 4 (Cross correlation method)

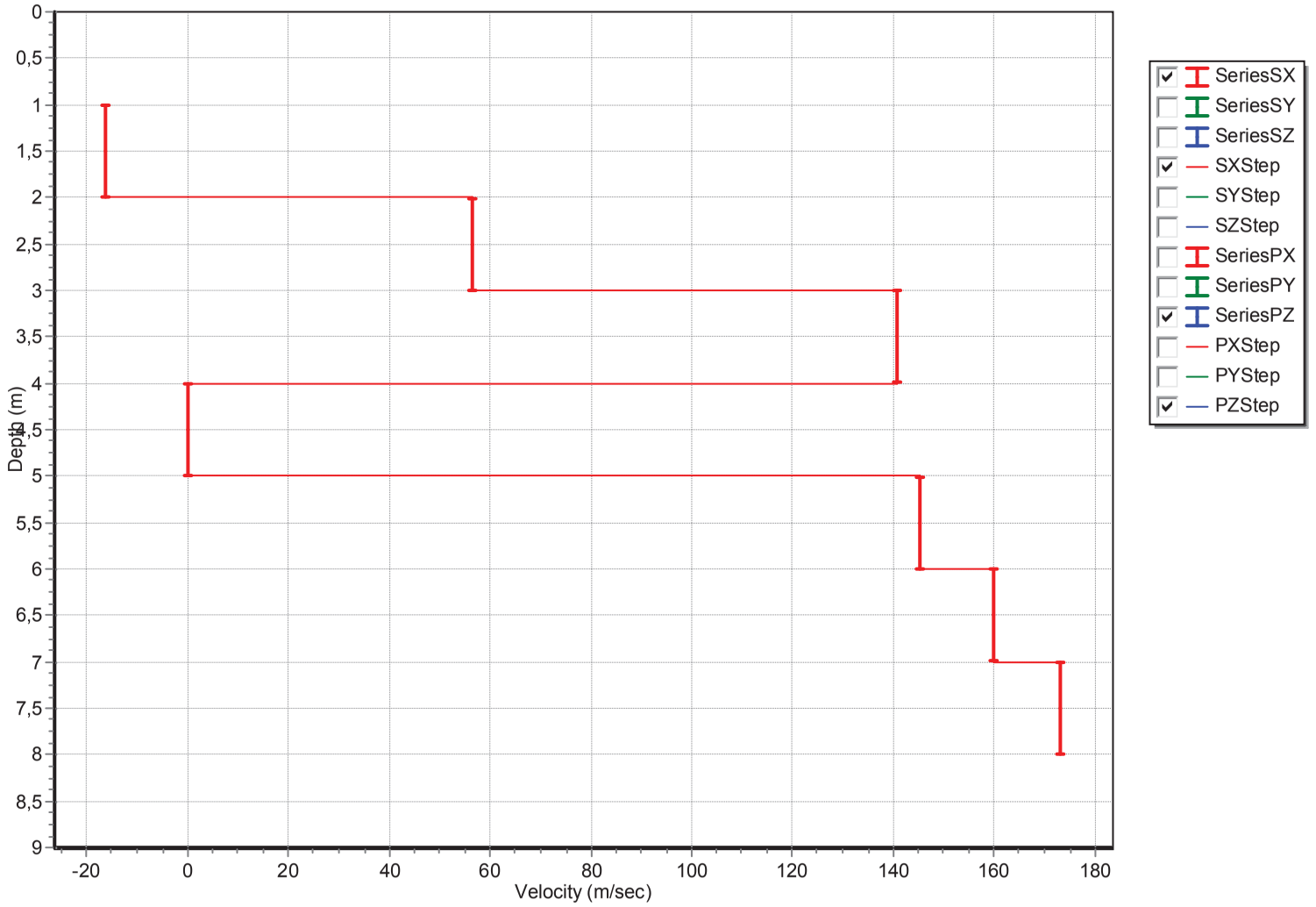

Sounding 4 (Revers Polarity method)

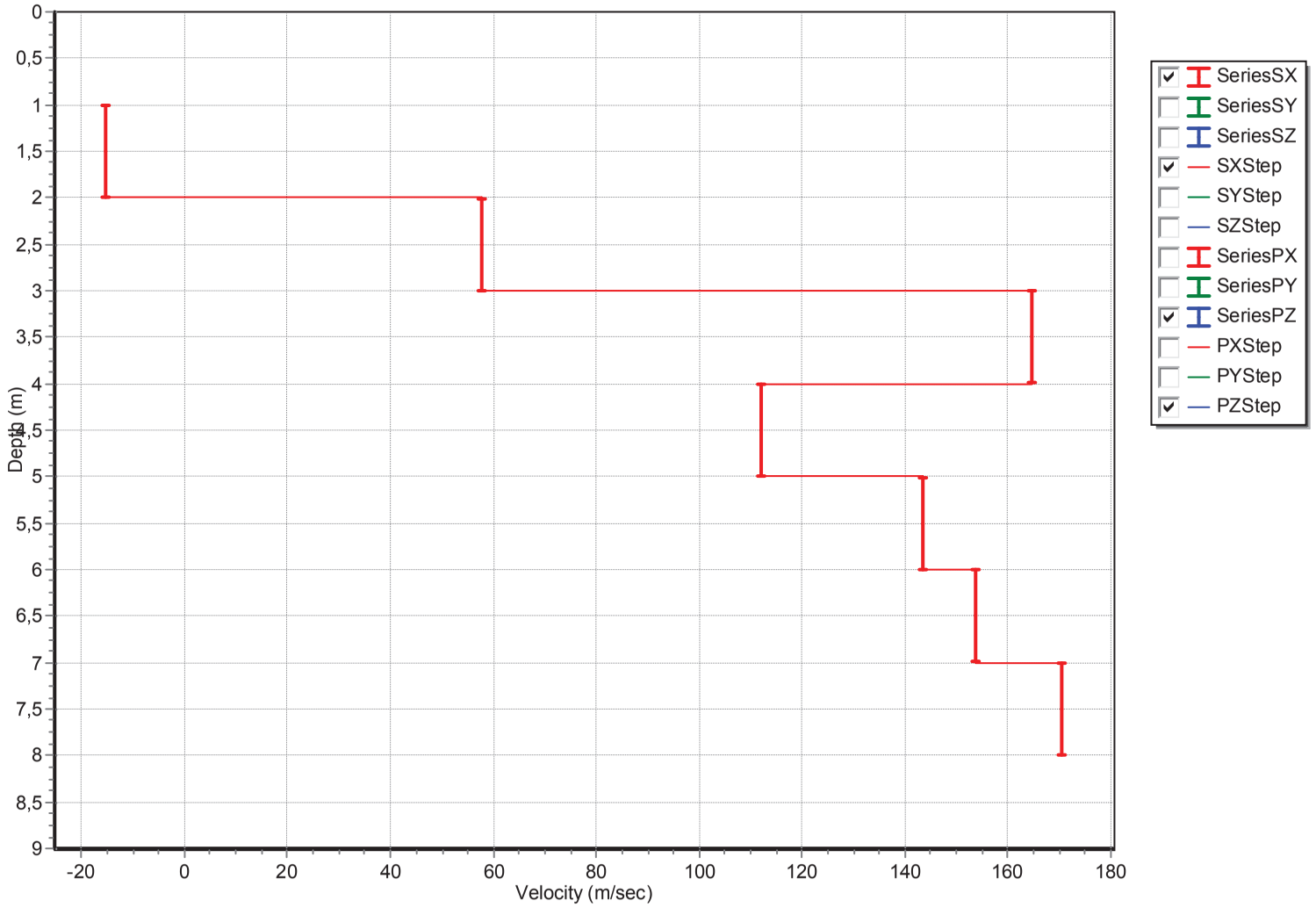

Sounding 5 (Cross Correlation method)

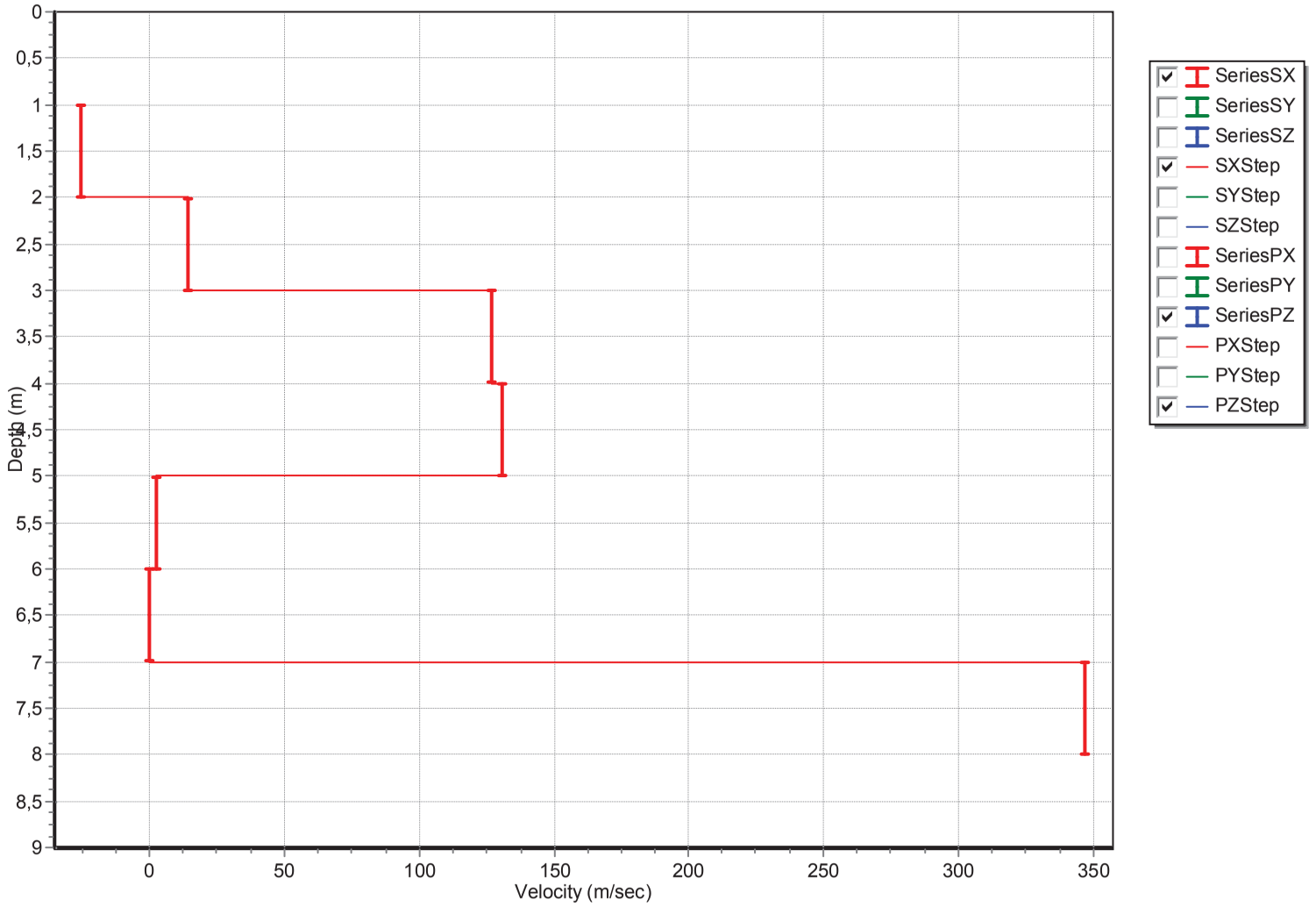

Sounding 5 (Revers Polarity method)

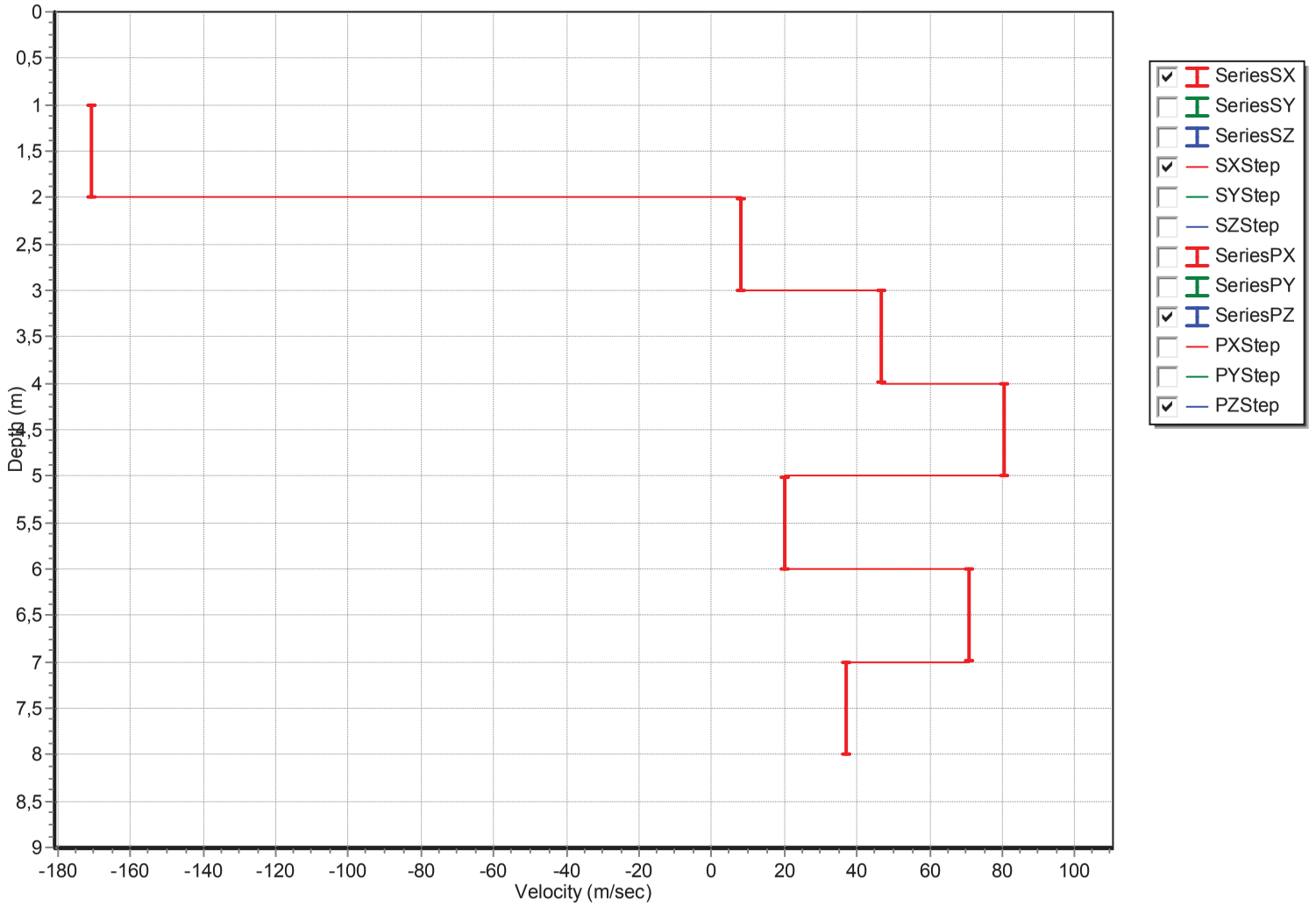

Sounding 6 (Cross Correlation method)

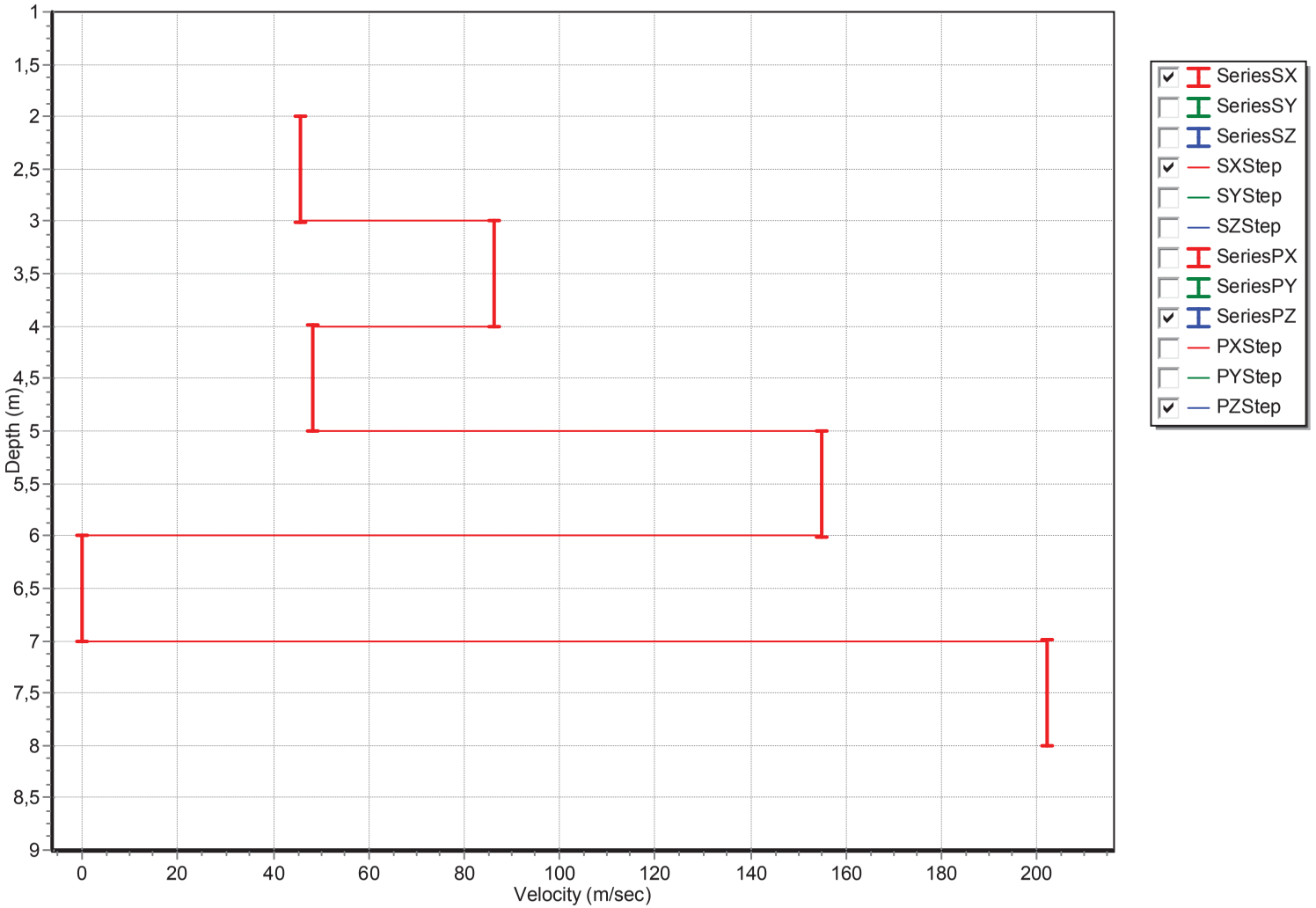

Sounding 6 (Revers Polarity method)

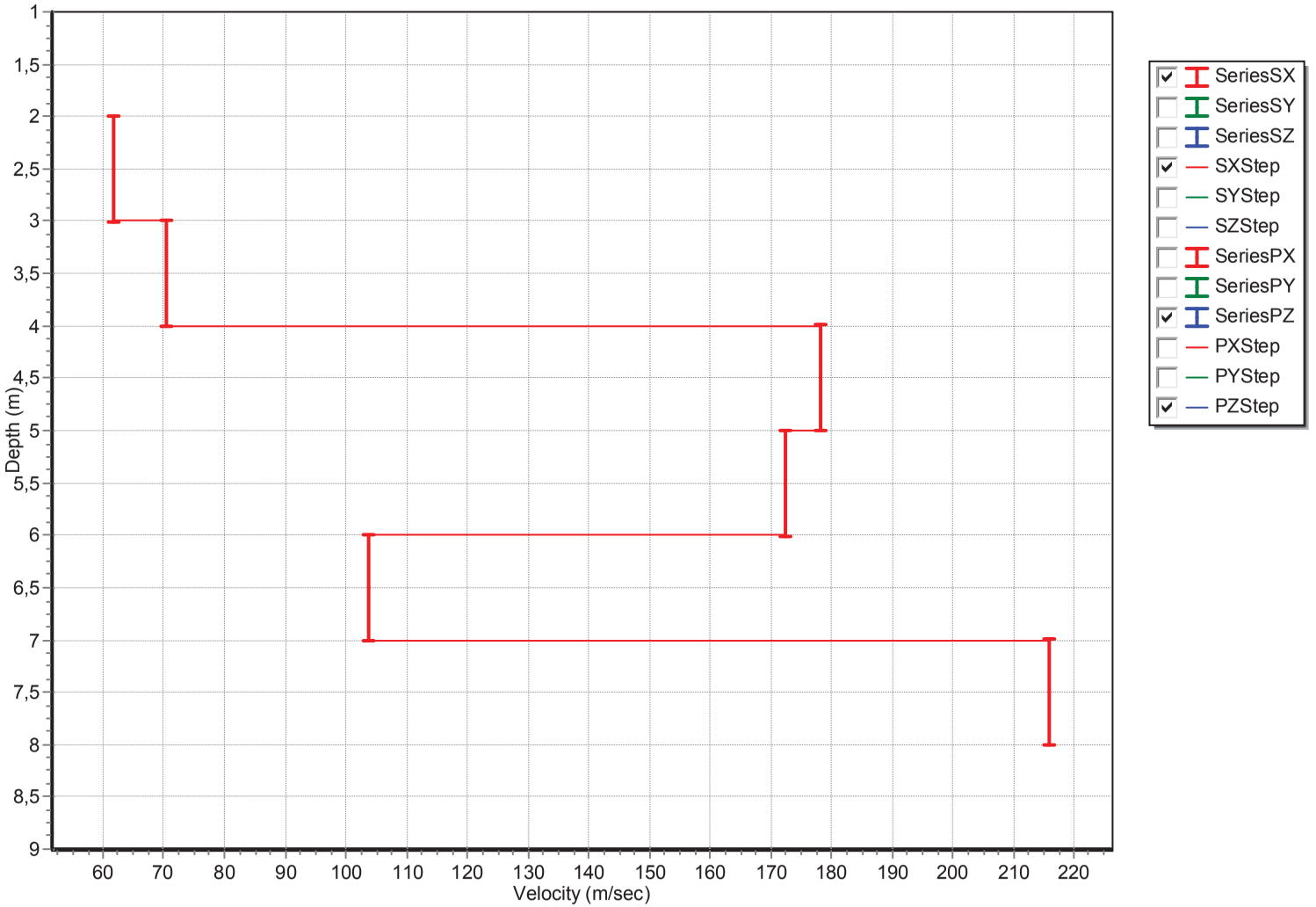

Sounding 7 (Cross Correlation method)

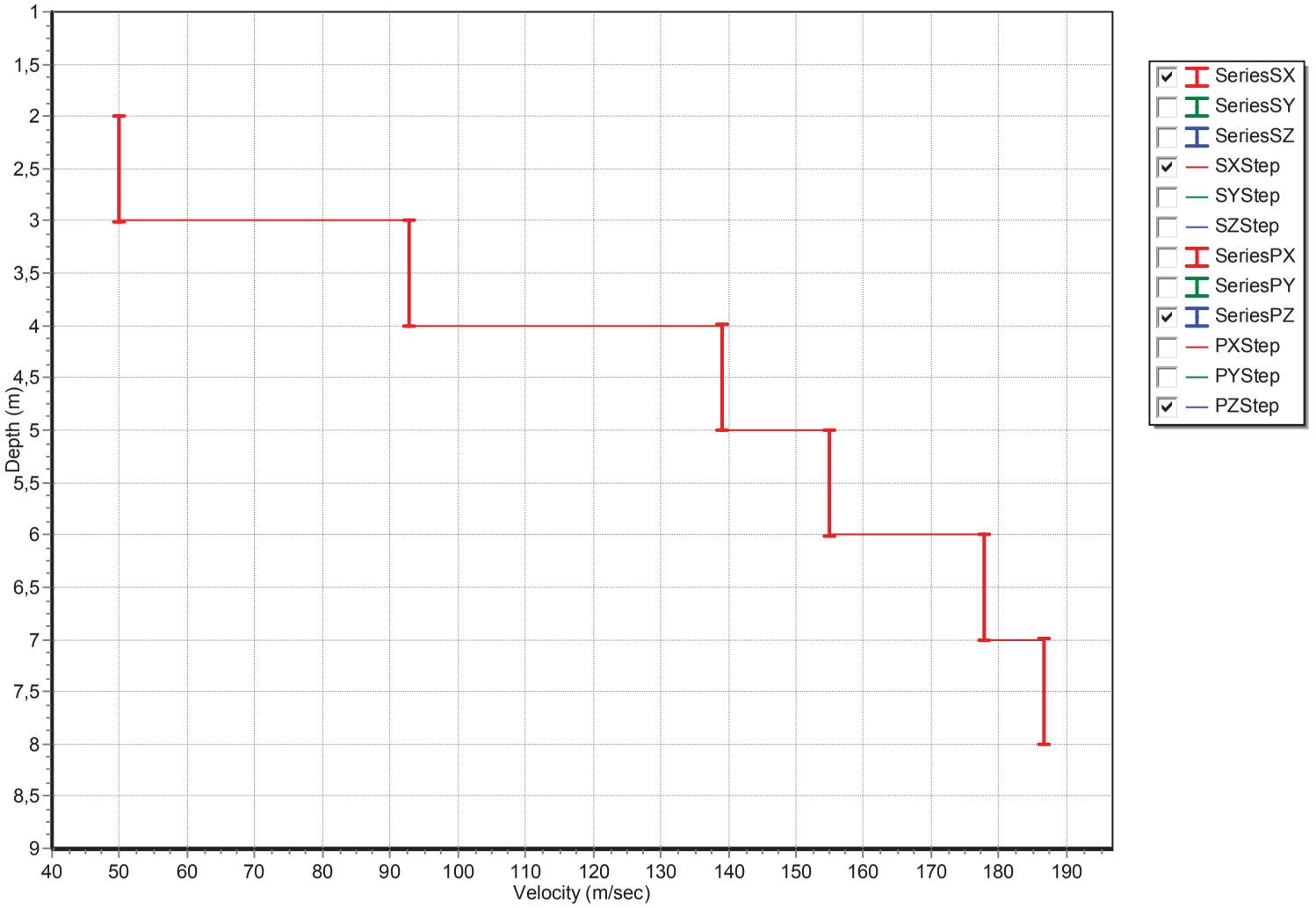

Sounding 7 (Revers Polarity method)

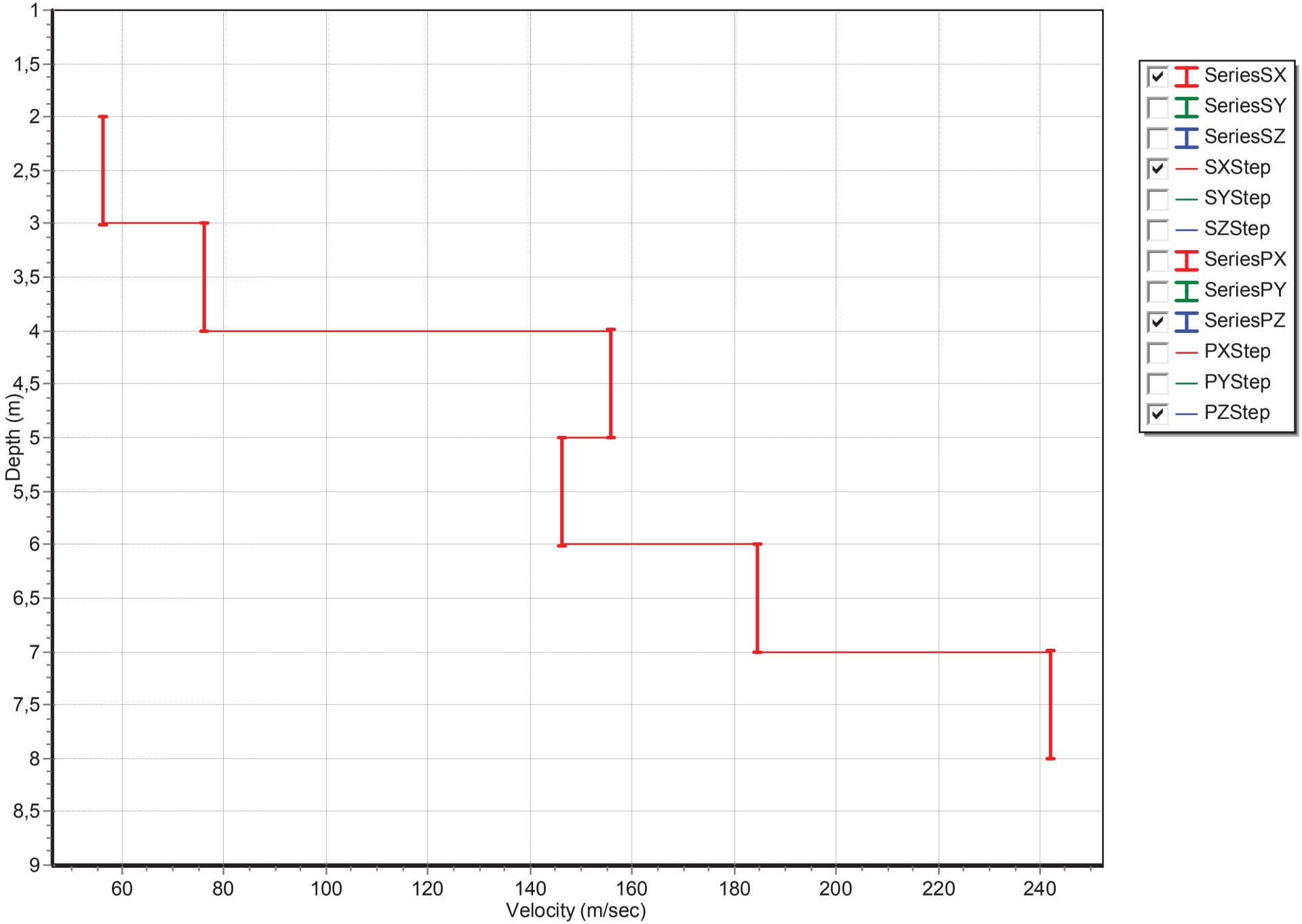

Sounding 8 (Cross Correlation method)

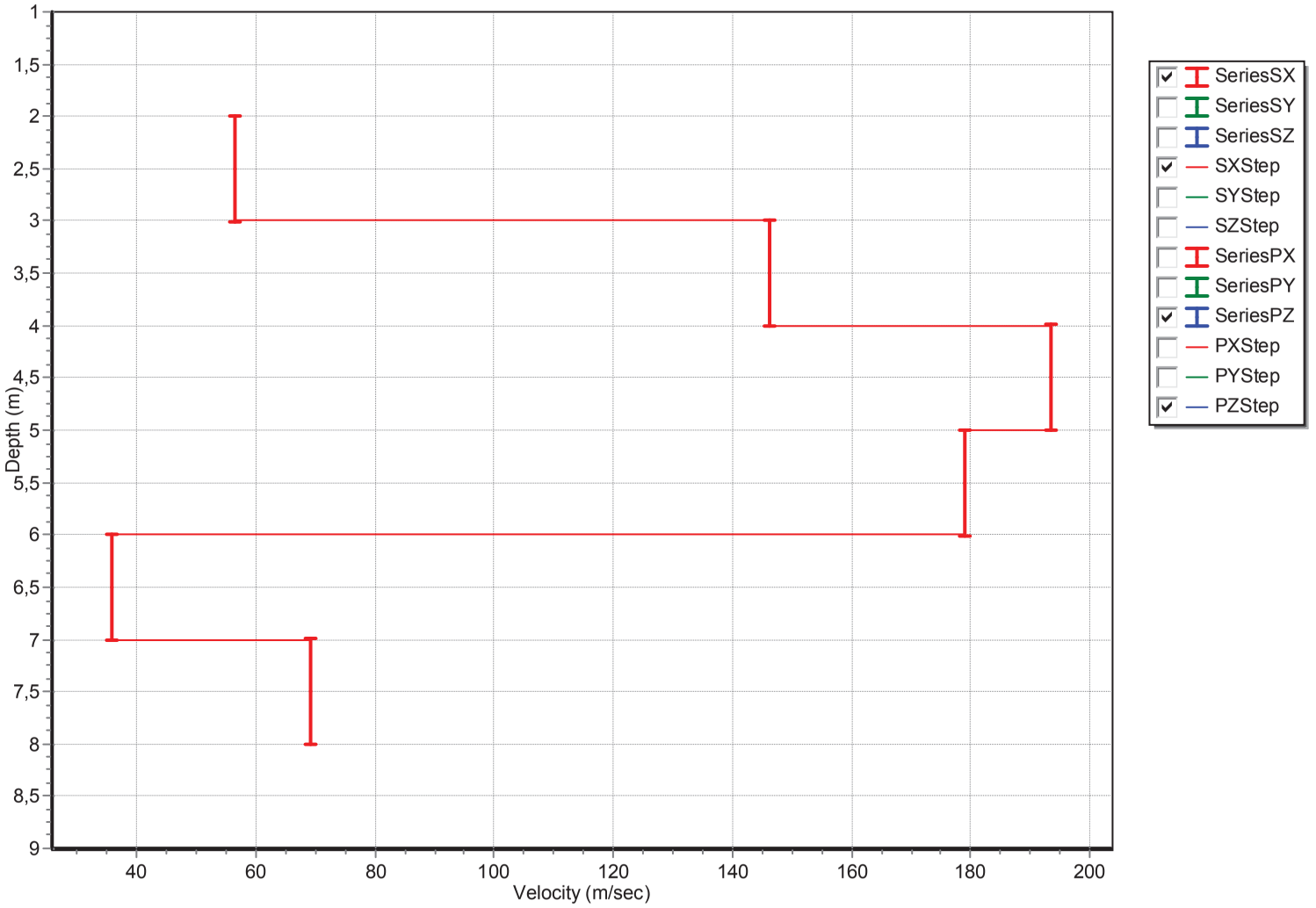

Sounding 8 (Revers Polarity method)

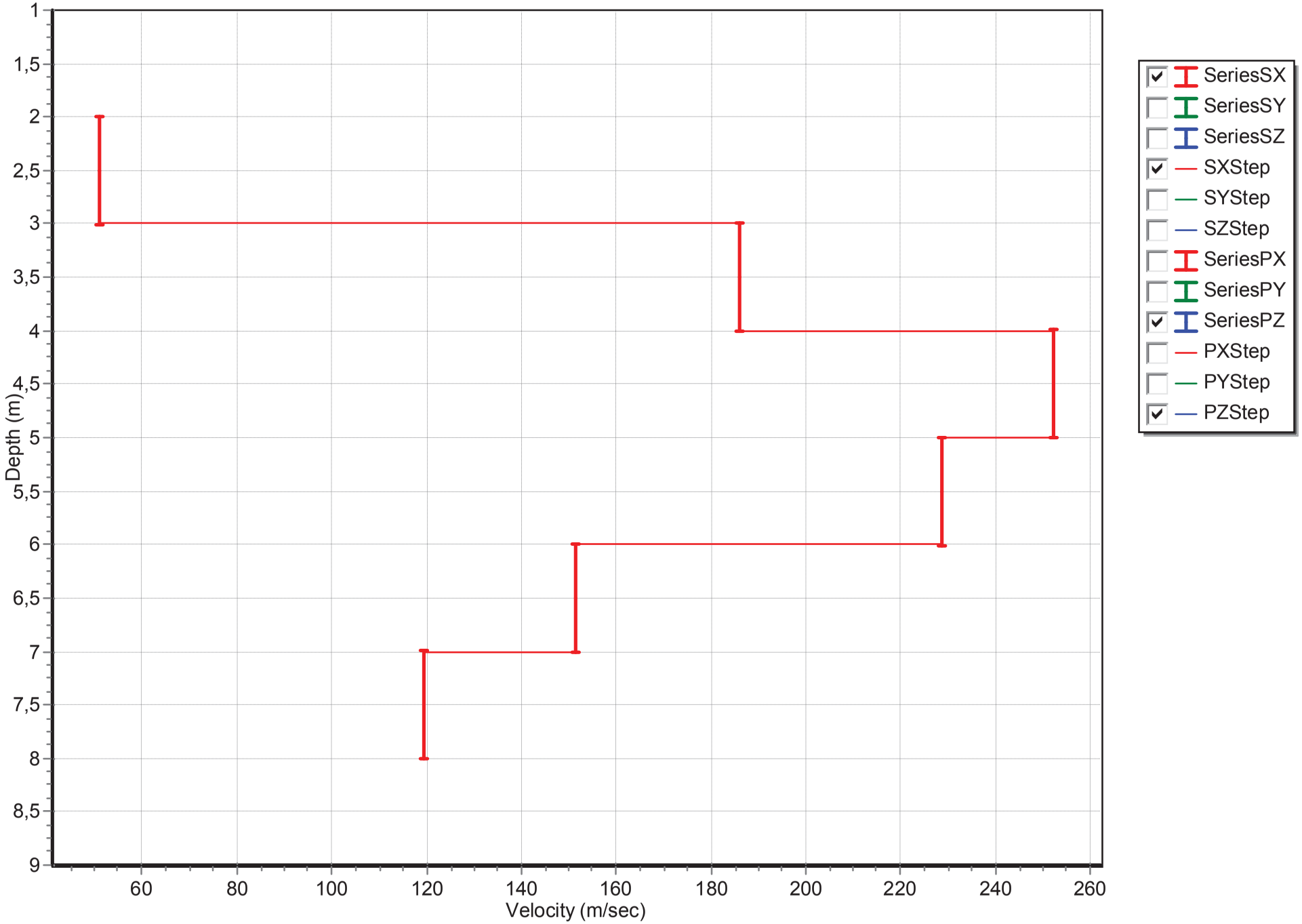

Sounding 9 (Cross correlation method)

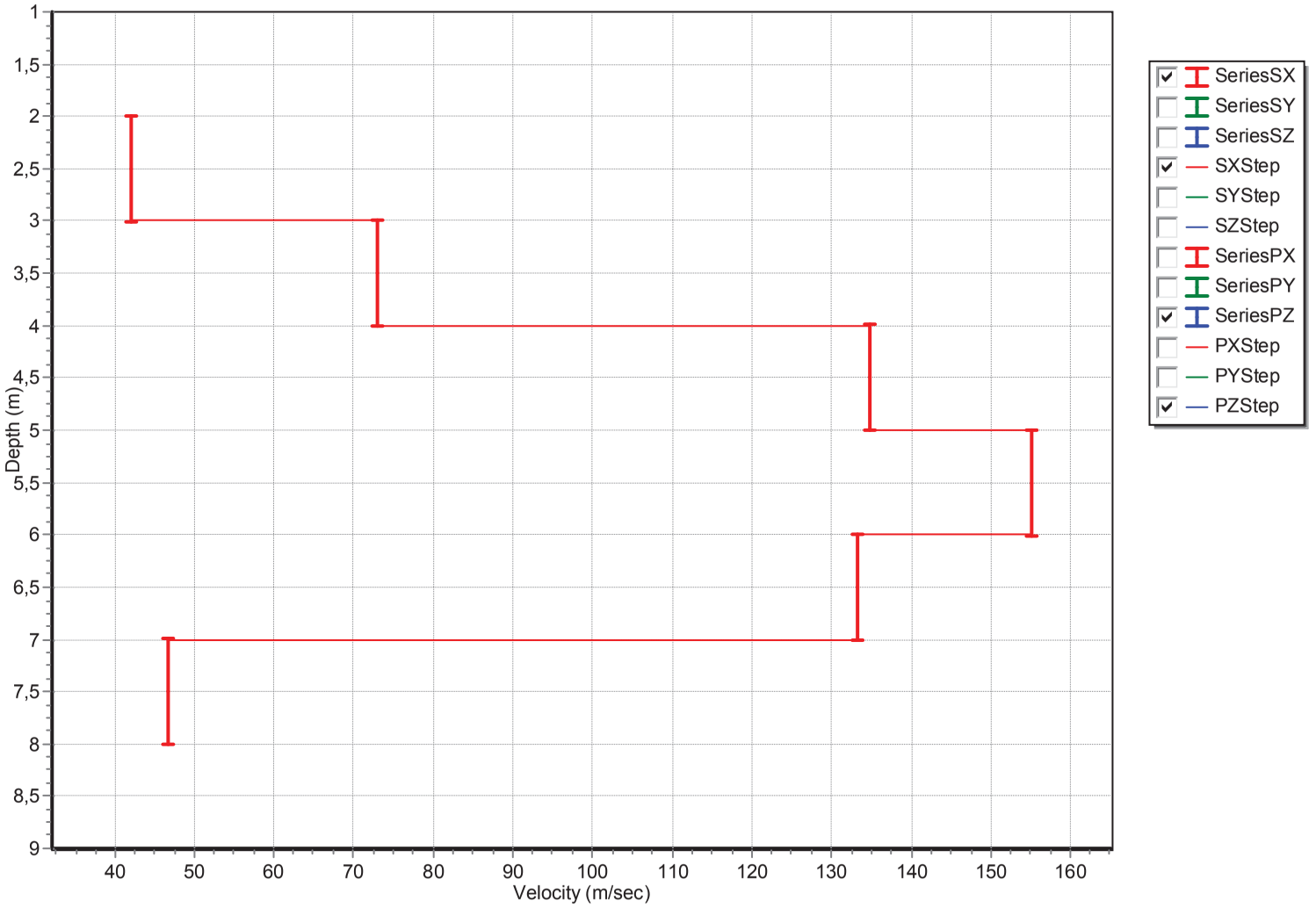

Sounding 9 (Revers Polarity method)

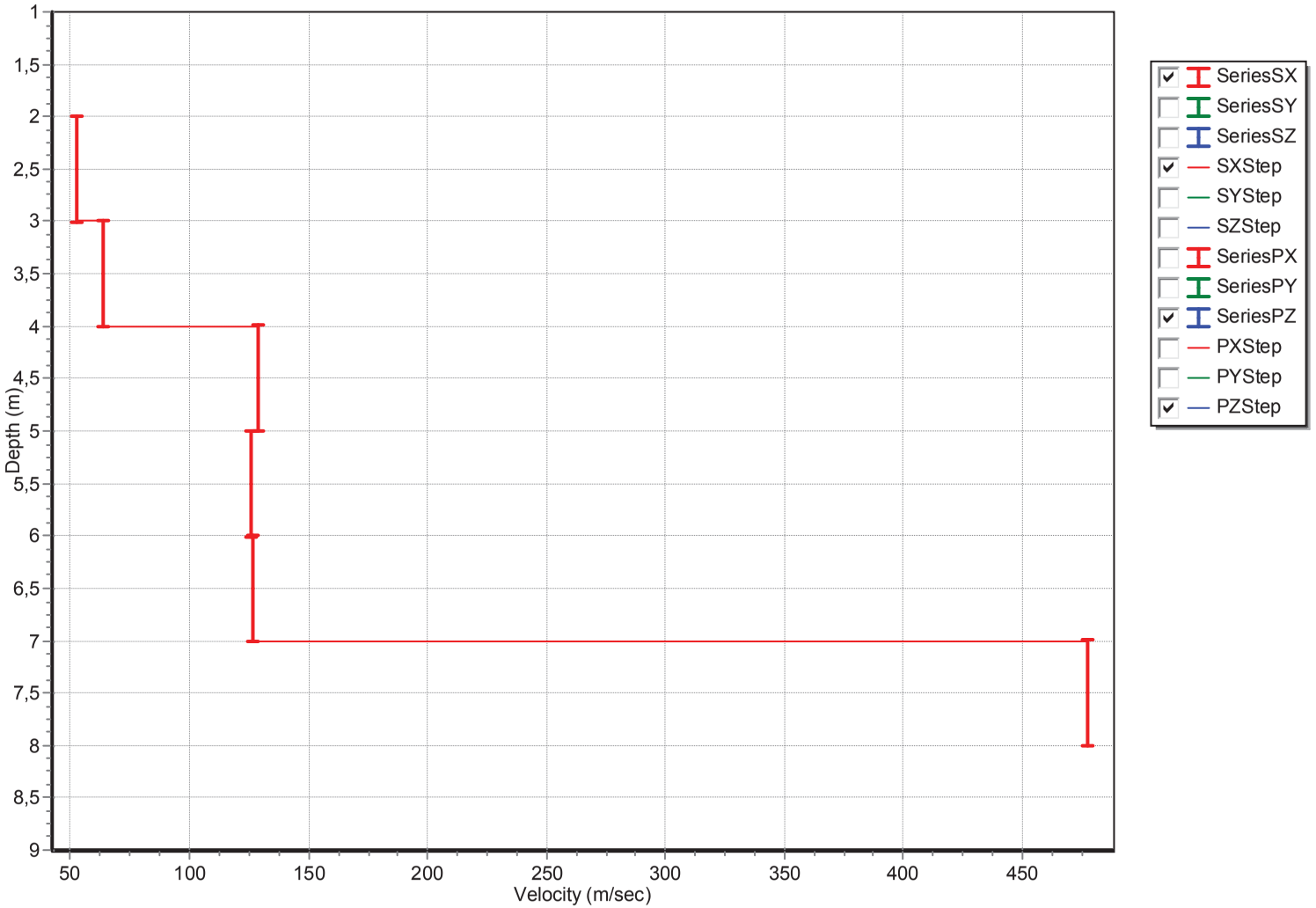

APPENDIX H: SESMIC ANALYSIS RESULTS

AALBORG SITE - CLAY

Sounding 1(Cross Correlation method)

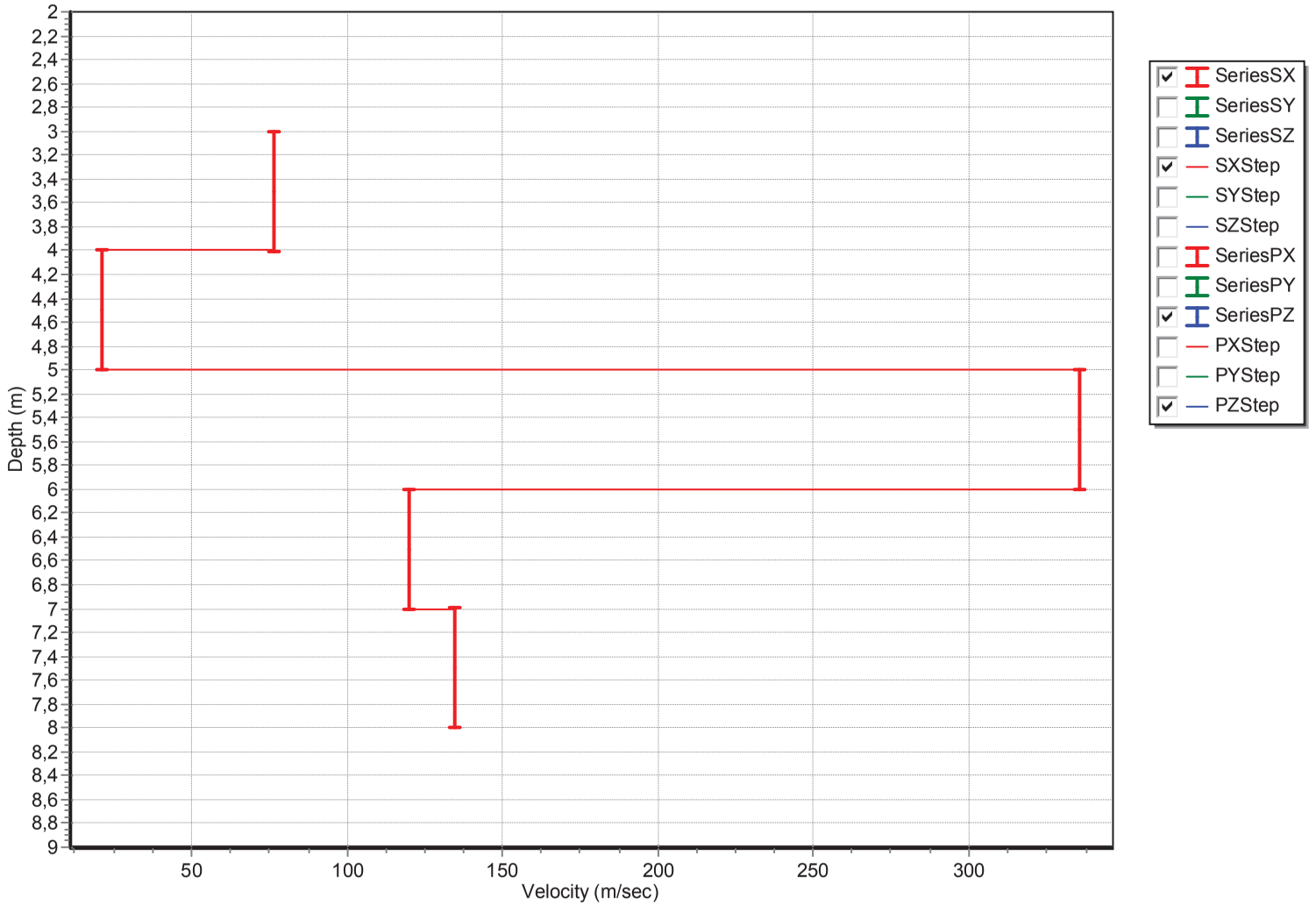

Sounding 1 (Revers Polarity method)

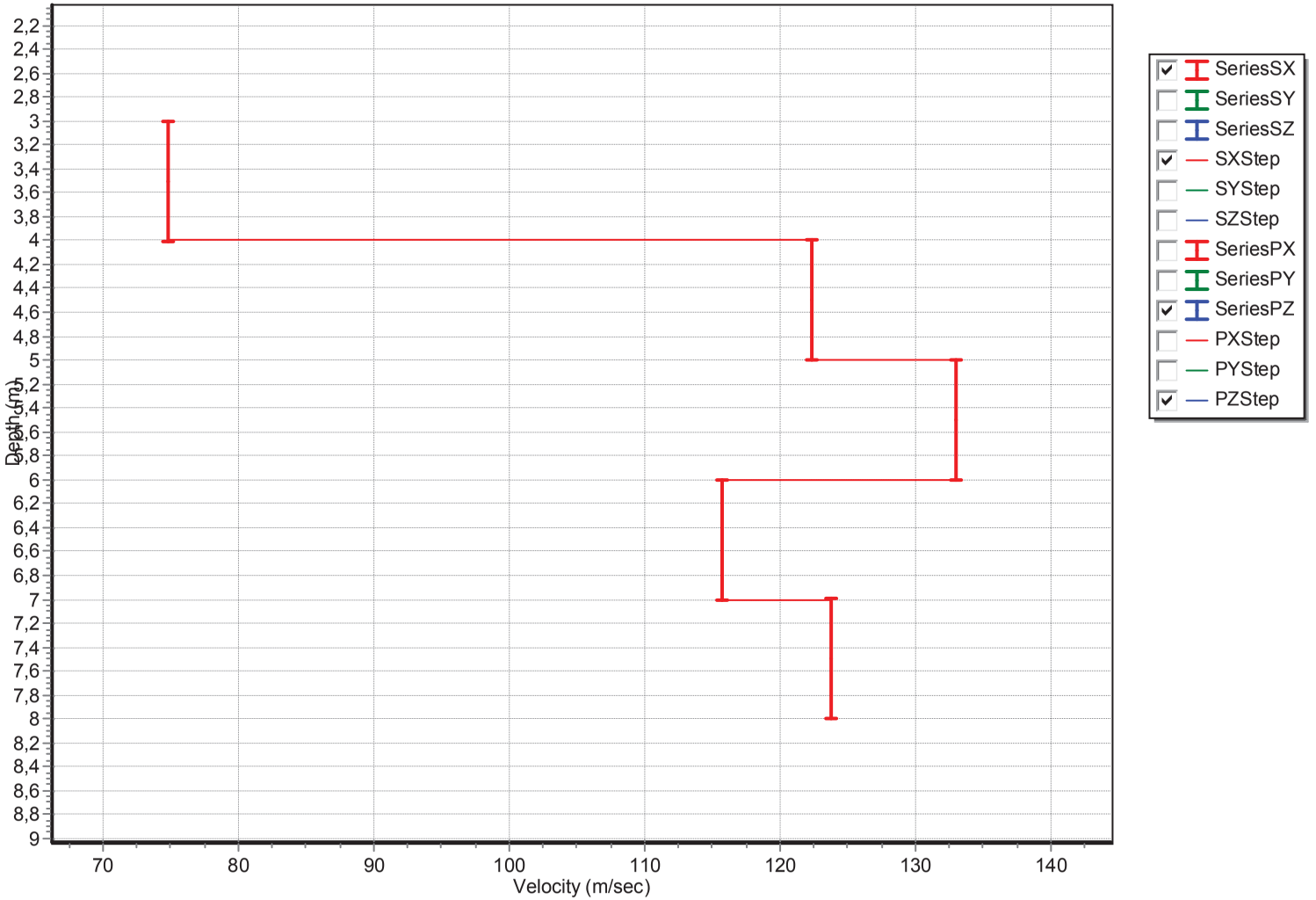

Sounding 2 (Cross Correlation method)

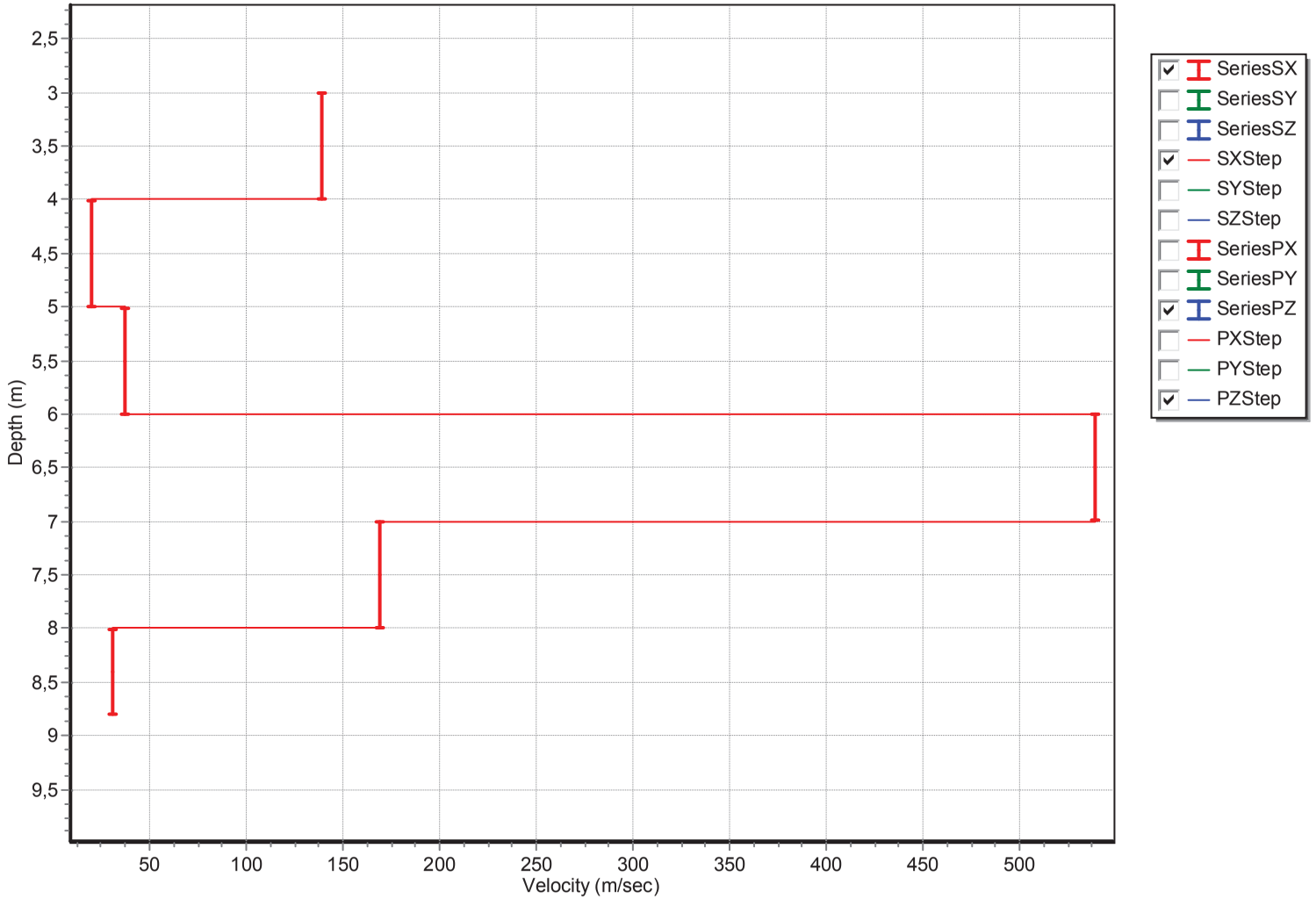

Sounding 2 (Reverse Polarity method)

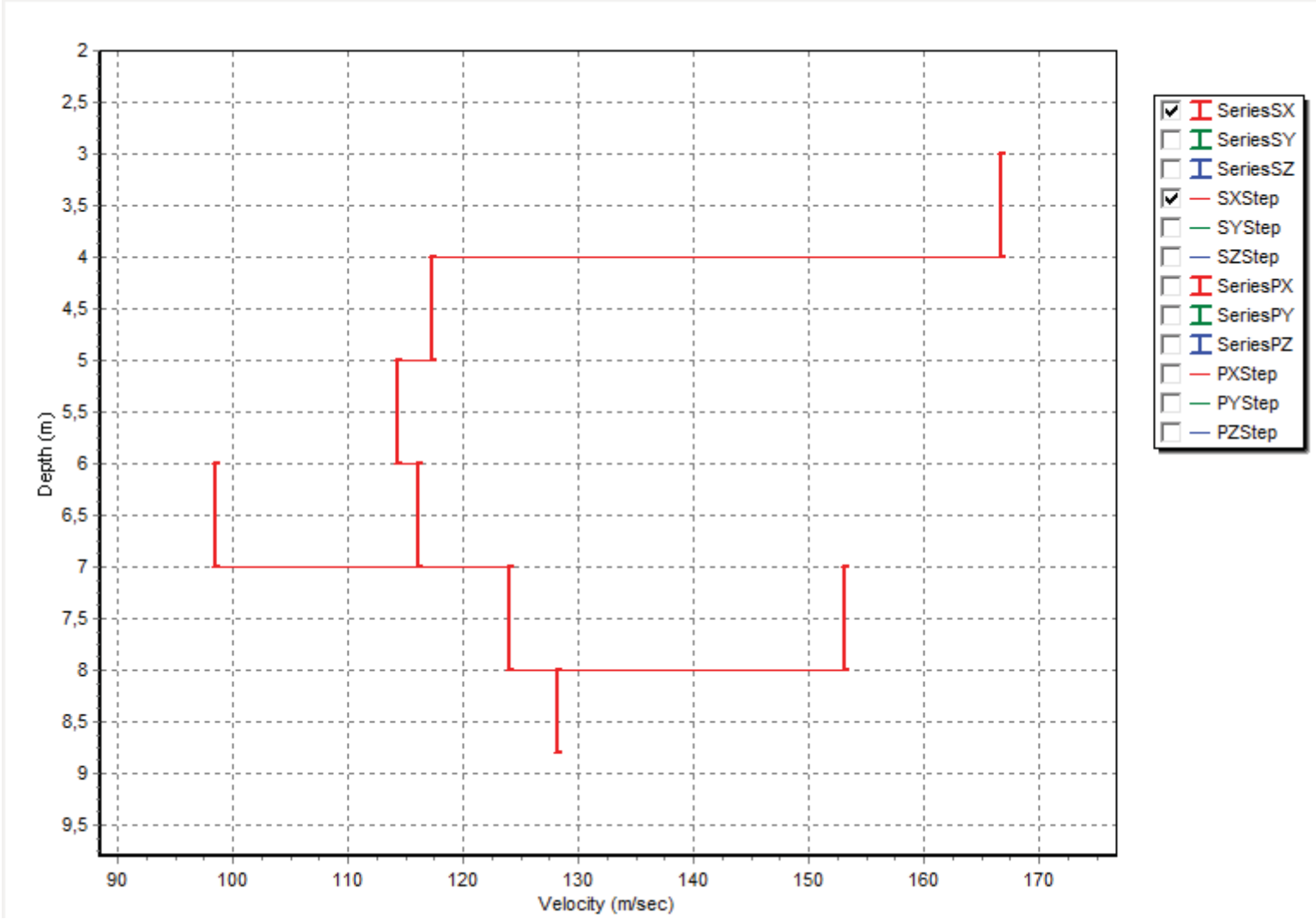

Sounding 3 (Cross Correlation method)

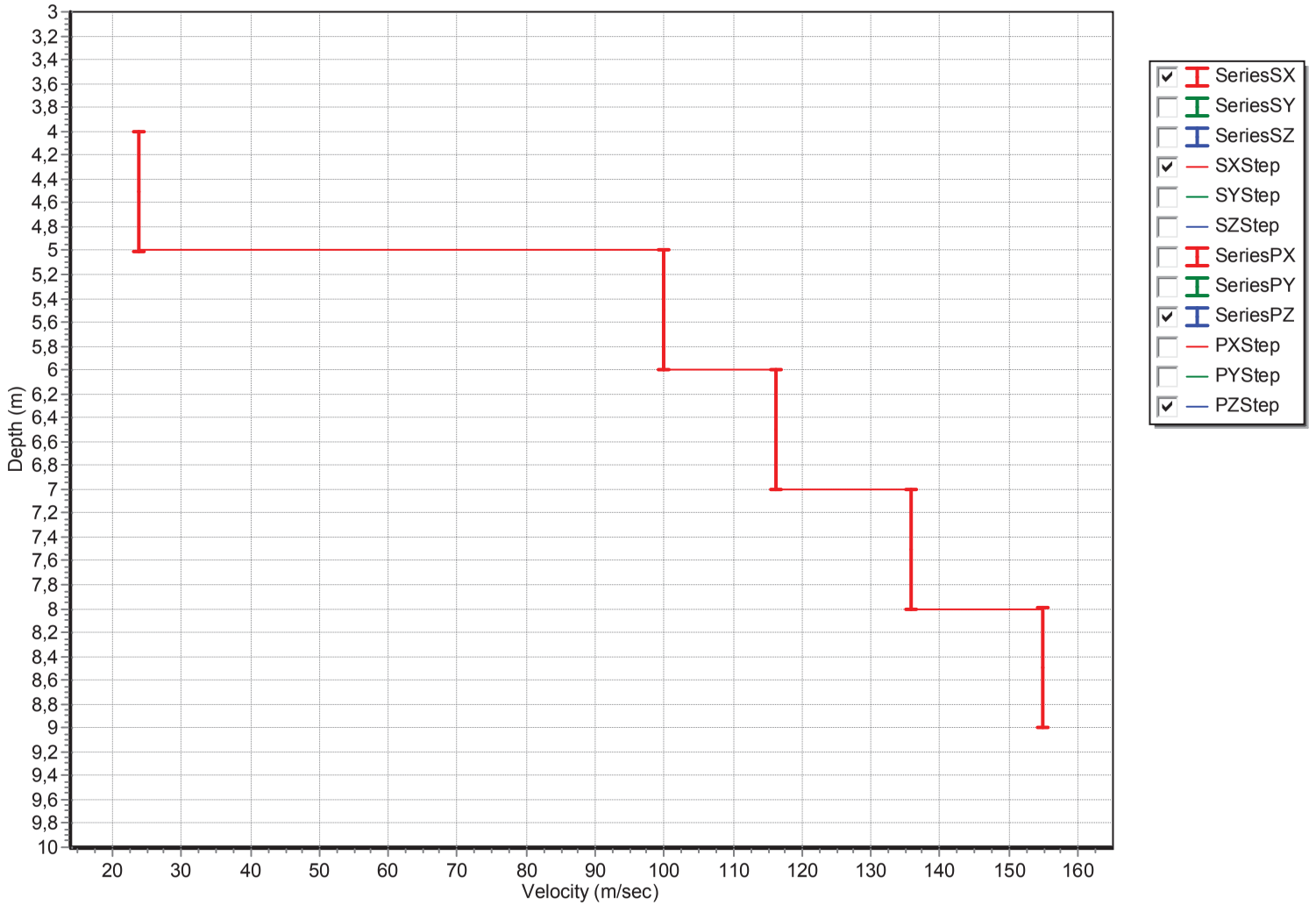

Sounding 3 (Revers Polarity method)

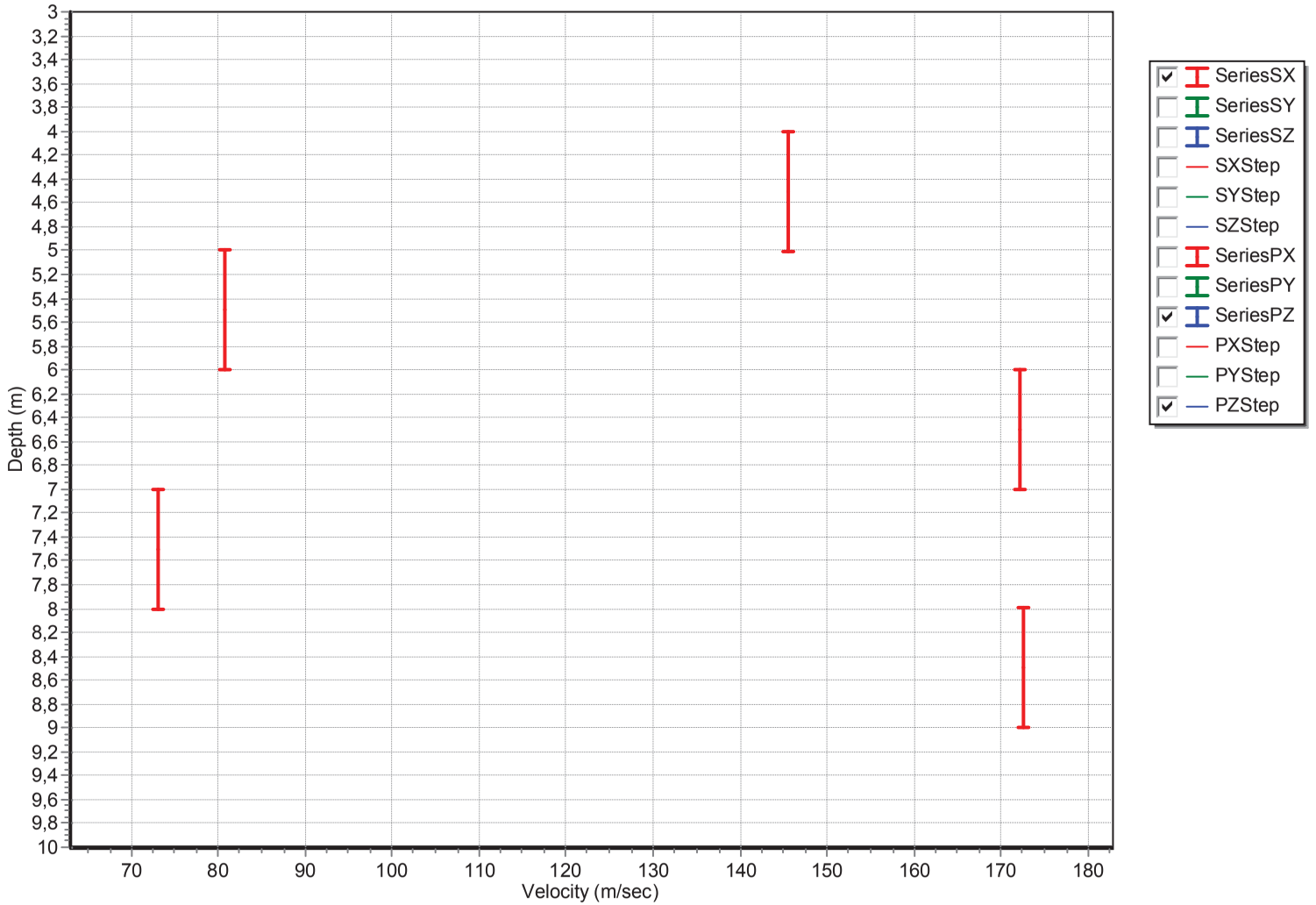

Sounding 4 (Cross Correlation method)

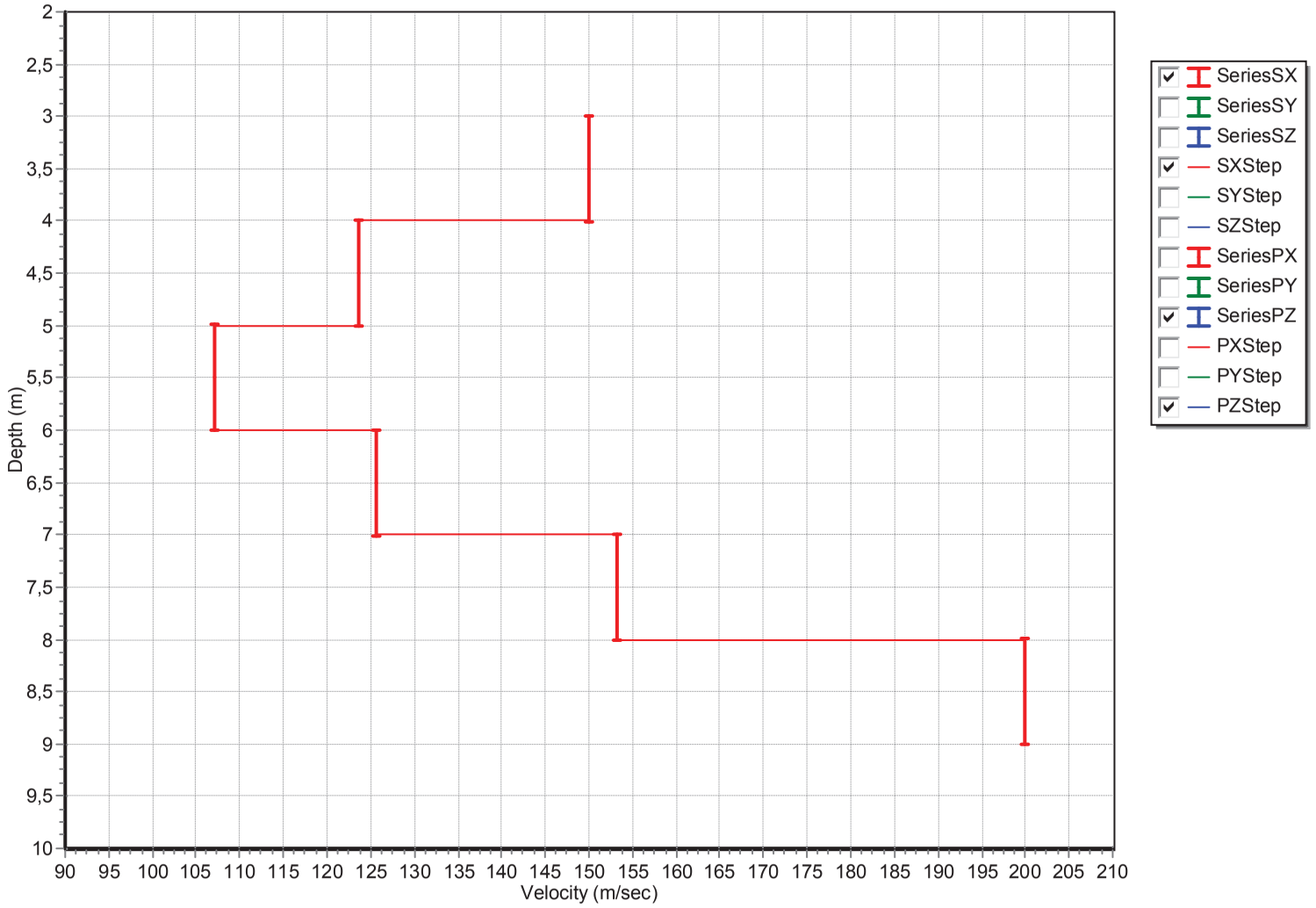

Sounding 4 (Reverse Polarity method)

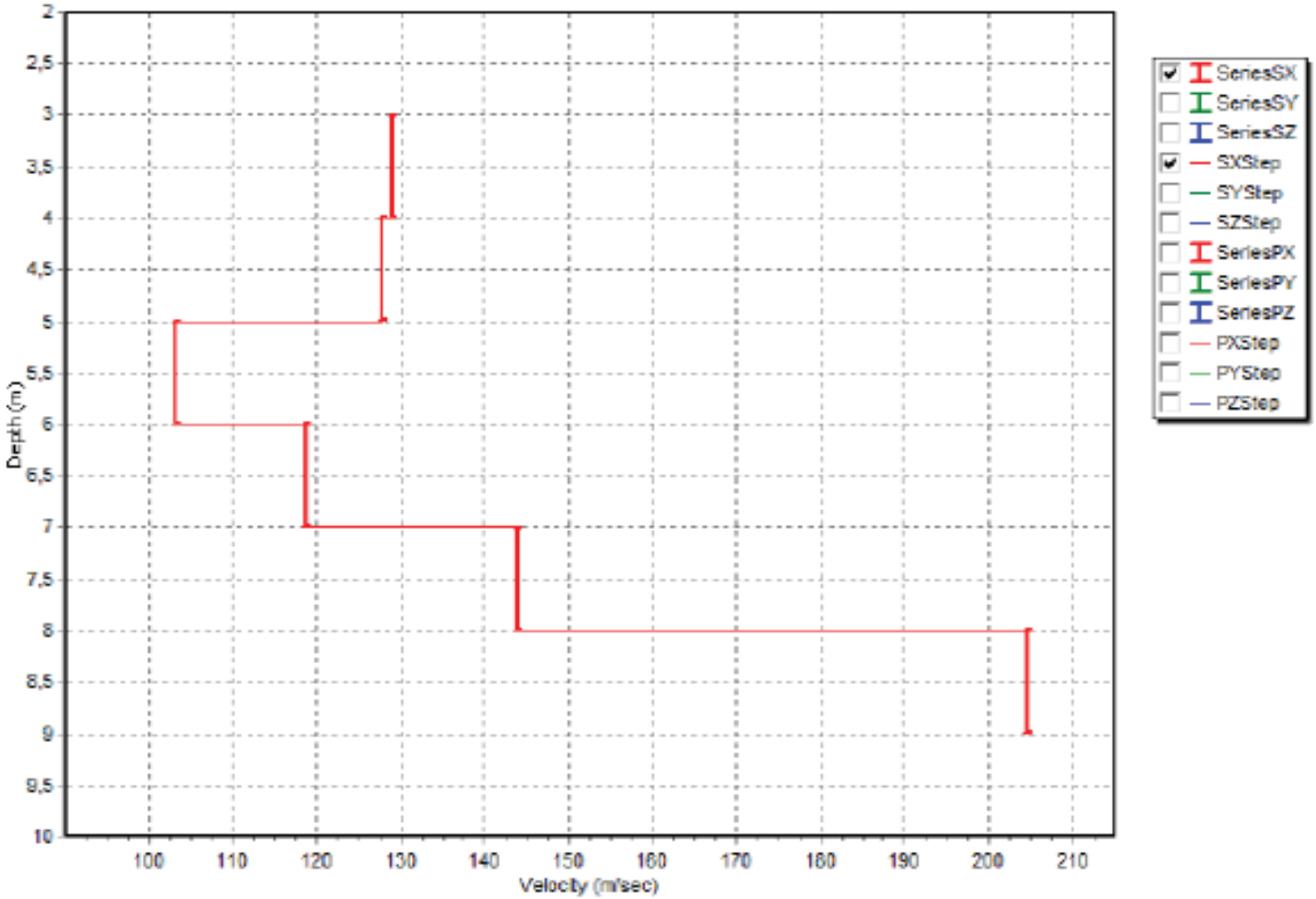

Sounding 5 (Cross Correlation method)

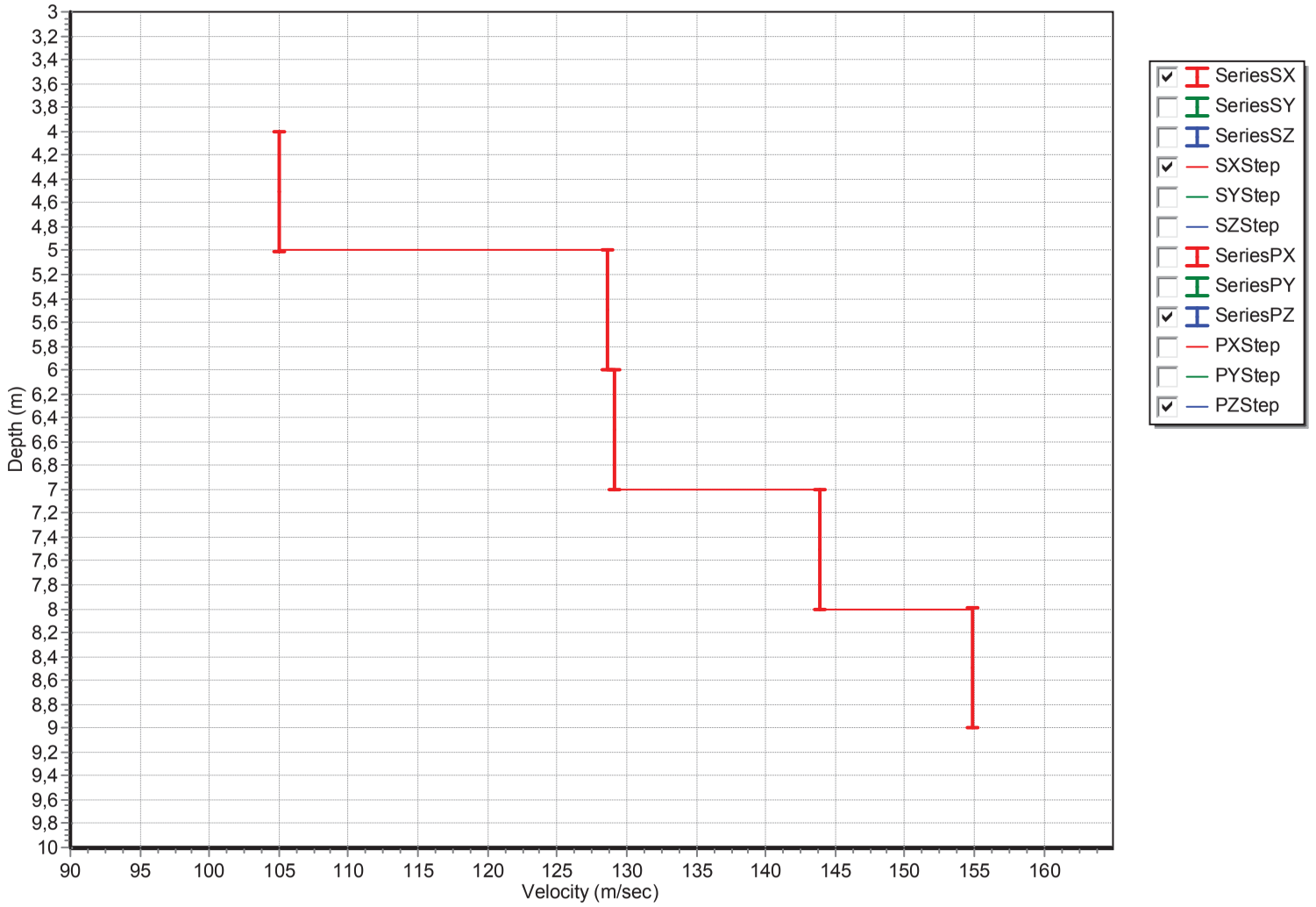

Sounding 5 (Revers Polarity method)